

ISTANBUL TECHNICAL UNIVERSITY ★ GRADUATE SCHOOL OF SCIENCE
ENGINEERING AND TECHNOLOGY

**PRODUCTION AND CHARACTERIZATION OF
POLY(ACRYLONITRILE-co-BUTYL ACRYLATE)/POLYPYRROLE
COMPOSITES AND NANOPARTICLES**

Ph.D. THESIS

Cem ÜNSAL

Department of Textile Engineering

Textile Engineering Graduate Programme

MAY 2014

ISTANBUL TECHNICAL UNIVERSITY ★ GRADUATE SCHOOL OF SCIENCE
ENGINEERING AND TECHNOLOGY

**PRODUCTION AND CHARACTERIZATION OF
POLY(ACRYLONITRILE-co-BUTYL ACRYLATE)/POLYPYRROLE
COMPOSITES AND NANOPARTICLES**

Ph.D. THESIS

**Cem ÜNSAL
(503052802)**

Department of Textile Engineering

Textile Engineering Graduate Programme

**Thesis Advisor: Prof. Dr. Fatma KALAOĞLU
Thesis Co-advisor: Prof. Dr. A. Sezai SARAÇ**

MAY 2014

İSTANBUL TEKNİK ÜNİVERSİTESİ ★ FEN BİLİMLERİ ENSTİTÜSÜ

**POLİ(AKRİLONİTRİL-ko-BÜTİL AKRİLAT)/POLİPİROL KOMPOZİTLERİN
VE NANOPARTİKÜLLERİN ÜRETİMİ VE KARAKTERİZASYONU**

DOKTORA TEZİ

**Cem ÜNSAL
(503052802)**

Tekstil Mühendisliği Anabilim Dalı

Tekstil Mühendisliği Lisansüstü Programı

**Tez Danışmanı: Prof. Dr. Fatma KALAOĞLU
Eş Danışman: Prof. Dr. A. Sezai SARAÇ**

MAYIS 2014

Cem ÜNSAL, a Ph.D. student of ITU **Graduate School of Science Engineering and Technology** student ID 503052802, successfully defended the **thesis** entitled “**Production and Characterization of Poly(Acrylonitrile-co-Butyl acrylate) /Polypyrrole Composites and Nanoparticles**”, which he prepared after fulfilling the requirements specified in the associated legislations, before the jury whose signatures are below.

Thesis Advisor : **Prof. Dr. Fatma KALAOĞLU**

İstanbul Technical University

Co-advisor : **Prof. Dr. Abdülkadir Sezai SARAÇ**

İstanbul Technical University

Jury Members : **Prof. Dr. Hale Canbaz KARAKAŞ**

İstanbul Technical University

Prof. Dr. Nuray UÇAR

Istanbul Technical University

Prof. Dr. Merih SARIŞIK

Dokuz Eylül University

Prof. Dr. Ziya ÖZEK

Namık Kemal University

Assoc. Prof. Dr. Aysun CİRELİ

Dokuz Eylül University

Date of Submission : 11 April 2014

Date of Defense : 22 May 2014

To my mum and dad,

FOREWORD

First of all, I send my best regards and thanks to my dear mum who was always just like a genuine angel to me, to my dad who never forgot supporting me, and to my brothers for their honest brotherhood and finest support all the time, and to whole our family for their love, understanding and continuous support by all meanings since the beginning.

Then, I would love to thank my advisor Prof.Dr. Fatma KALAOĞLU for her understanding and unbeatable belief in me, and especially I would love to thank my second advisor Prof.Dr. A. Sezai SARAÇ for his scientifically enlightening and fully support which is so hard-to-describe-by-any words indeed, and my teacher Prof.Dr. Hale Canbaz KARAKAŞ, for her enrouting ideas and positive character. It was really impossible to achieve anything without their fully support and coaching while all the stages of this study.

And of course, i cannot deny the psychological support of all my good friends, i never forget their role in forming my today; thus, i send my sincere thanks, my best wishes and the best luck to all of them. And, thanks go also to the friends which are ex-/existent- members of Electropol-Nanotech Research Group, for their honesty, and their friendly support. The existence of such fellow colleagues was really an important factor not to feel lonely while trying to have achievement.

Thanks; to my family, to my advisors, to my teachers from Istanbul Technical University, to the members of the jury commitee, to all my good friends and to all of the good people and fair colleagues those showed even only a few traces of support.

May God be with all of you,

April 2014

Cem ÜNSAL
(Textile Eng.&Res.Scientist)

TABLE OF CONTENTS

	<u>Page</u>
FOREWORD	ix
TABLE OF CONTENTS	xi
ABBREVIATIONS	xv
LIST OF TABLES	xvii
LIST OF FIGURES	xix
SUMMARY	xxiii
ÖZET	xxv
1. INTRODUCTION	1
1.1 Purpose of Thesis	2
1.2 Literature Review	3
2. THEORETICAL PART	5
2.1 Polymers.....	5
2.1.1 Classification of polymers	6
2.1.1.1 Origin	7
2.1.1.2 Thermal response	7
2.1.1.3 Formation mode.....	8
2.1.1.4 Line structure.....	10
2.1.1.5 Application and physical properties	11
2.1.1.6 Tacticity	13
2.1.1.7 Crystallinity	16
2.1.1.8 Polarity	17
2.1.2 Production of polymers.....	21
2.1.3 Modification of polymers.....	22
2.1.4 Processing the polymers	24
2.2 Polyacrylates.....	26
2.3 Polyacrylonitrile	32
2.3.1 Uses of Polyacrylonitrile.....	35
2.3.2 Production of Polyacrylonitrile	38
2.3.2.1 Acrylonitrile	38
2.3.2.2 Polyacrylonitrile	38
2.3.2.3 Polyacrylonitrile-based copolymers	39
2.4 Butyl Acrylate	41
2.5 Conductive Polymers	42
2.6 Pyrrole and Polypyrrole	59
2.6.1 Polymerization of Pyrrole	62
2.6.1.1 Electropolymerization of Pyrrole	62
2.6.1.2 Chemical polymerization of Pyrrole	65
2.6.2 Processability of Polypyrrole	67
2.6.2.1 Solutions of Polypyrrole	67
2.6.2.2 Chemical preparation of Polypyrrole composites	67
2.6.3 Copolymers and graft copolymers of Polypyrrole	68

2.6.4 Electrochemically synthesis of Polypyrrole	69
2.6.5 Polypyrrole studies on textiles	69
2.7 Electrospinning	71
2.8 Emulsion Polymerization.....	74
3. EXPERIMENTAL PART	77
3.1 Materials	77
3.2 Analyses and Instruments	77
3.2.1 Spectroscopic analyses	77
3.2.1.1 ATR-FTIR analysis	77
3.2.1.2 Uv-Vis analysis	78
3.2.1.3 EIS analysis.....	78
3.2.1.4 Broad-band dielectric spectrometry	79
3.2.2 Morphological analyses.....	80
3.2.2.1 SEM analysis.....	80
3.2.2.2 AFM analysis	81
3.2.3 Dynamic Mechanical Analysis	82
3.3 Synthesis of Polyacrylonitrile (PAN)	83
3.3.1 Bulk polymerization of Acrylonitrile (AN).....	83
3.3.1.1 Materials	83
3.3.1.2 Polymerization procedure of Acrylonitrile	83
3.3.2 Emulsion polymerization of AN	84
3.3.2.1 Materials	84
3.3.2.2 Polymerization procedure	85
3.4 Synthesis of Polybutyl acrylate (PBuA)	85
3.4.1 Materials	85
3.4.2 Polymerization process of BuA	85
3.5 Synthesis of P(AN-co-BuA) Copolymer	85
3.6 Thin Film Production.....	86
3.6.1 Materials	87
3.6.2 Procedure	87
3.7 Electrospun-Nanofiber Production.....	87
3.7.1 Materials	87
3.7.2 Procedure	87
3.8 Matrix polymerization of Pyrrole.....	88
3.8.1 Composite-thin-film production	88
3.8.1.1 Synthesis of the polymeric matrix	89
3.8.1.2 Preparation of composite thin films	90
3.8.2 Composite-electrospun-nanofiber production	90
3.9 Production of Composite Core-Shell Nanoparticles	91
3.9.1 Synthesis of P(AN-co-BuA) nanoparticles.....	93
3.9.2 Synthesis of P(AN-co-BuA)/PPy core/shell nanoparticles	95
3.10 Production of Electrospun Nanomats	96
3.11 Solvent Effect on Electrical Conductivity of Composites	97
4. RESULTS AND DISCUSSION.....	99
4.1 Characterization of Synthesized Polymers	99
4.2 Characterization of Copolymeric Films.....	101
4.2.1 FTIR spectroscopy	103
4.2.2 DMA analysis	104
4.2.3 Thermal gravimetric analysis (TGA)	105
4.3 Characterization of Composite Films	108

4.3.1 FTIR spectroscopy.....	108
4.3.2 DMA characterization.....	110
4.3.3 Morphological characterization.....	111
4.3.4 Impedance spectroscopy	113
4.4 Nanofiber Characterization	117
4.5 Characterization of Composite Nanomats.....	134
4.6 Characterization of Core-Shell Nanoparticles.....	137
4.6.2 Particle size analysis of P(AN-co-BuA) and PPy/P(AN-co-BuA) NP ...	144
4.6.3 Atomic Force Microscope (AFM) analysis of nanoparticles	144
4.6.4 ATR-FTIR characterization of nanoparticles.....	146
4.6.6 Thin-films of CSNP and their EIS characterization	150
5. CONCLUSIONS	159
CURRICULUM VITAE.....	183

ABBREVIATIONS

AN	: Acrylonitrile
BuA	: Butyl acrylate
-co-	: Copolymer
CP	: Conductive polymer
Py	: Pyrrole
PAN	: Polyacrylonitrile
PBuA	: Polybutyl acrylate
P(AN-co-BuA)	: Acrylonitrile-Butyl acrylate copolymer
PPy	: Polypyrrole
PhPy	: N-Phenylpyrrole
n-MPy	: N-Methylpyrrole
EDOT	: -3, -4, Ethylene dioxi-thiophene
PEDOT	: Poly(-3, -4, ethylene dioxi-thiophene)
CAN	: Cerium (IV) Ammonium Nitrate
KPS	: Potassium persulphate
APS	: Ammonium peroxodisulphate
SEM	: Scanning Electron Microscope
TEM	: Transmission Electron Microscope
DMA	: Dynamic Mechanical Analyzer
AFM	: Atomic Force Microscope
NMR	: Nuclear Magnetic Resonance
GPC	: Gas Permeation Chromatography
ATR-FTIR	: Attenuated total reflectance - Fourier transform infrared spectroscopy
UV-Vis	: Ultra-violet Visible Spectrophotometry
DMF	: Dimethylformamide
DMSO	: Dimethylsulphoxide
cm	: centimeter
mm	: millimeter
µm	: micron / micrometer
nm	: nanometer
ml	: milliliter
µl	: microliter
g	: gram
M	: molarity / molar concentration
NP	: nanoparticle
CS	: core/shell
CSNP	: core/shell nanoparticle
ITO-PET	: Indium tin oxide coated Polyethyleneterephthalate substrate
EIS	: Electrochemical Impedance Spectroscopy

LIST OF TABLES

	<u>Page</u>
Table 2.1 : Classification types of polymers.	7
Table 2.2 : Some addition polymers.	9
Table 2.3 : Some condensation polymers.....	10
Table 2.4 : Some of elastomers.....	12
Table 2.5 : Some polymers used to make fibres.....	14
Table 2.6 : Additives used to enhance the properties of polymers.	24
Table 2.7 : Methods of processing the polymers.	25
Table 2.8 : Glass-transition temperatures (T _g) of some polyacrylates.	31
Table 2.9 : Properties of Polyacrylonitrile (PAN).	32
Table 2.10 : Annual production of Acrylonitrile.	37
Table 2.11 : The applications of conductive polymers.	52
Table 3.1 : Ingredients and their amounts in reaction medium.	84
Table 3.2 : Electrospinning parameters used to produce nanofibers.	88
Table 3.3 : Compositions of electrospinning solutions.....	90
Table 3.4 : The total monomer, AN, BuA, SDBS and APS composition in feed.	94
Table 4.1 : Electrospinning parameters and resultant average fiber diameters.	134
Table 4.2 : P(AN-co-BuA) and PPy/P(AN-co-BuA) nanoparticle sizes estimated from SEM images.	141
Table 4.3 : P(AN-co-BuA) and PPy/P(AN-co-BuA) CSNP sizes measured by particle size analyzer via light-scattering.	145
Table 4.4 : Absorbance peaks regarding to PPy, PAN and P BuA of CSNP thin films.	157

LIST OF FIGURES

	<u>Page</u>
Figure 2.1 : Polymer chain of Polyacrylonitrile.	5
Figure 2.2 : Polymer chain of Poly(Butyl acrylate).....	6
Figure 2.3 : Polymerization of Vinyl chloride to form Polyvinylchloride (PVC).....	8
Figure 2.4 : Polymerization of Polyamide 6.6.....	10
Figure 2.5 : Structure of a linear polymer.	11
Figure 2.6 : Structure of a branched polymer.....	11
Figure 2.7 : Structure of a cross-linked polymer.	11
Figure 2.8 : After stretching to make a fiber, the crystalline regions are aligned along the axis of the fiber, and this adds strength to it.	13
Figure 2.9 : Propylene molecule.....	13
Figure 2.10 : Isotactic Polypropene.	15
Figure 2.11 : Syndiotactic Polypropene.	15
Figure 2.12 : Atactic Polypropene.	15
Figure 2.13 : Crystalline and amorphous regions in a polymer structure.	16
Figure 2.14 : Polyacrylonitrile homopolymer.	18
Figure 2.15 : Styrene-Butadiene-Styrene (SBS) polymer.....	19
Figure 2.16 : Representative chemical structure of ABS polymer.	19
Figure 2.17 : Structures of different types of copolymer.	20
Figure 2.18 : Different types of copolymer have different properties and end-uses.	20
Figure 2.19 : Free radical polymerization of low density polyethylene (LDPE).	22
Figure 2.20 : A mechanism for the free radical polymerization of Vinyl chloride to Poly(Vinyl chloride) (PVC).....	23
Figure 2.21 : A protective shirt which is made of Polypropanoate(acrylic), Aramid and Polyamide fibers' mixture.	23
Figure 2.22 : Some monomers to synthesize polyacrylates.	26
Figure 2.23 : General formula of acrylates.	28
Figure 2.24 : Polyacrylonitrile's repeating unit.....	32
Figure 2.25 : The copolymer of AN and MA is a wool substitute and is often mixed with wool itself for heavier fabrics, used in pullovers and jumpers and in suits.....	36
Figure 2.26 : The high heels are made from a blend of ABS and a Polyamide which is very strong.....	36
Figure 2.27 : Global consumption of Acrylonitrile by end use in year of 2013.	37
Figure 2.28 : Reaction to produce Acrylonitrile (AN) monomer.	38
Figure 2.29 : The soft tops for high quality cars are produced from almost pure homopolymer of PAN.	38
Figure 2.30 : Acrylonitrile-Vinyl acetate copolymer.....	39
Figure 2.31 : Acrylonitrile-Methyl acrylate copolymer.....	39
Figure 2.32 : Acrylonitrile-Methyl methacrylate copolymer.	39
Figure 2.33 : Skeletal formula of Butyl acrylate and its basic properties.	41
Figure 2.34 : "sigma" (σ) and "pi" (π) bonds in Polyacetylene molecular chain.	44

Figure 2.35 : Structural schemes of (a) Diamond, (b) Graphite, and (c) Polyacetylene.....	45
Figure 2.36 : Acetylene’s polymerization.	46
Figure 2.37 : Some of the p-doped conductive polymers.	47
Figure 2.38 : The most stable of p-doped polymers is Polypyrrole (PPy).	47
Figure 2.39 : Reduction-oxidation of PPy.	47
Figure 2.40 : Electron-conducting polymers.	48
Figure 2.41 : Doping process of Polyacetylene with Iodine.	48
Figure 2.42 : The conductivity levels of various materials.	49
Figure 2.43 : The effect of temperature change on conductive polymer.....	50
Figure 2.44 : Insertion of a “spacer” to separate the donor and acceptor (functionalized chain ends).	54
Figure 2.45 : Application of Polyacetylene to a glucose sensor.	56
Figure 2.46 : An application of laser scribed graphene ultracapacitor.....	57
Figure 2.47 : Proposed use of paired bimorph actuators as micro-electrochemical tweezers.....	58
Figure 2.48 : Pyrrole.....	59
Figure 2.49 : Formula of Polypyrrole.....	60
Figure 2.50 : Oxidative polymerization of Pyrrole to Polypyrrole.	61
Figure 2.51 : Chemical structures of PPy in neutral aromatic and quinoid forms and in oxidized polaron and bipolaron forms.	62
Figure 2.52 : Electropolymerization mechanism of Pyrrole.....	63
Figure 2.53 : Schematic of electrospinning setup and process.	73
Figure 2.54 : Schematic view of emulsion polymerization.	75
Figure 3.1 : Parstat 2263 Electrochemical Analyser.	79
Figure 3.2 : Novocontrol BDS-40 Broadband Dielectric/Impedance Spectrometer.	80
Figure 3.3 : SEC SEN-3000M Mini-SEM instrument.	81
Figure 3.4 : FEI - Quanta FEG 250 instrument.....	81
Figure 3.5 : Nanosurf Easy Scan 2 AFM-STM instrument.	82
Figure 3.6 : TA Instruments DMA Q800 Dinamic Mechanical Analyzer.	83
Figure 3.7 : Polymerization scheme of AN with Oxalic Acid-CAN couple.	84
Figure 3.8 : Synthesized P(AN-co-BuA) random copolymer structure and interactions between molecules of copolymer matrix, PPy and DMF. .	91
Figure 3.9 : Monomers used in synthesis of Poly(AN-co-BuA) template nanoparticles.	95
Figure 3.10 : P(AN-co-BuA) structure.....	95
Figure 3.11 : Tentative mechanism of studied core-shell formation.....	96
Figure 4.1 : ATR-FTIR spectra of synthesized PAN polymer.	99
Figure 4.2 : ATR-FTIR spectra of synthesized AN-BuA copolymers.....	100
Figure 4.3 : Absorbance ratios of characteristic peaks in copolymer (related to AN feed rates)	101
Figure 4.4 : The morphological change of polymeric film surfaces with increasing BuA mol% amount in copolymer structure (a: 100% PAN film, b: 95/5 AN/BuA, c: 90/10 AN/BuA, d: 80/20 AN/BuA, e: 67/33 AN/BuA).	102
Figure 4.5 : ATR-FTIR spectra of the films made by solution casting from AN-BuA copolymers.....	103
Figure 4.6 : Stress-Strain Curves of 95/5, 90/10, 80/20 and 67/33 AN/BuA mol% fed Copolymeric Films (C1 : 95/5, C2 : 90/10, C3 : 80/20, C4 : 67/33).	104

Figure 4.7 : Storage Modulus, Loss Modulus and Tan Delta Curves of Copolymeric Films according to Multifrequency-strain Test Results (DMA1 : 95/5, DMA2 : 90/10, DMA3 : 80/20, DMA4 : 67/33 AN/BuA).	105
Figure 4.8 : Decomposition analysis of 100% PAN film.	106
Figure 4.9 : Decomposition analysis of 95/5 mol% AN/BuA copolymeric film. ...	106
Figure 4.10 : Decomposition analysis of 90/10 mol% AN/BuA copolymeric film.	107
Figure 4.11 : Decomposition analysis of 85/15 mol% AN/BuA copolymeric film.	107
Figure 4.12 : Decomposition analysis of 90/10 mol% AN/BuA + 200Py copolymeric film by TGA.....	108
Figure 4.13 : The changes of characteristic peaks' ratios of copolymer matrix and PPy related to Py contents.	109
Figure 4.14 : ATR-FTIR spectra comparison graph of composite thin films with various Py contents (a: 0 μ l, b: 100 μ l, c: 200 μ l, d: 300 μ l).	110
Figure 4.15 : Stress / Strain curves of composite thin films with various Py contents.	111
Figure 4.16 : SEM image of composite thin film with no Py added (X3000 magnification).	112
Figure 4.17 : SEM image of composite thin film with 300 μ l Py added (X3000 magnification).	112
Figure 4.18 : Variation of dielectric constants of the composite thin films with 0, 100, 200, and 300 μ l Py (INSET: Extended view of the curves).....	113
Figure 4.19 : Conductivity curves of composite thin films (INSET: Extended view of the curves).....	114
Figure 4.20 : Impedance curves of composite thin films (INSET: Extended view of the curves).....	115
Figure 4.21 : 2-Y graphical view of relation between Py contents, breakdown stresses, and conductivity values (at 10 ⁷ Hz) of composite thin films.	116
Figure 4.22 : SEM pictures and average diameter analyses of co-1 nanofibers.	118
Figure 4.23 : SEM pictures and average diameter analyses of co-2 nanofibers.	119
Figure 4.24 : SEM pictures and average diameter analyses of co-3 nanofibers.	120
Figure 4.25 : SEM pictures and average diameter analyses of co-4 nanofibers.	121
Figure 4.26 : SEM pictures and average diameter analyses of coPy-1 nanofibers.	123
Figure 4.27 : SEM pictures and average diameter analyses of coPy-2 nanofibers.	124
Figure 4.28 : SEM pictures and average diameter analyses of coPy-3 nanofibers.	125
Figure 4.29 : SEM pictures and average diameter analyses of coPy-4 nanofibers.	127
Figure 4.30 : SEM pictures and average diameter analyses of coPy-5 nanofibers.	128
Figure 4.31 : SEM pictures and average diameter analyses of coPy-6 nanofibers.	129
Figure 4.32 : SEM pictures and average diameter analyses of coPy-7 nanofibers.	131
Figure 4.33 : SEM pictures and average diameter analyses of coPy-8 nanofibers.	132
Figure 4.34 : SEM pictures and average diameter analyses of coPy-9 nanofibers.	133
Figure 4.35a : Color change of nanomats due to changing Polypyrrole content. ...	135
Figure 4.35b : Optical characterizations of nanomats (picture on the left is the photo view, and the picture on the right is the light-microscope view of 150x magnification).	135
Figure 4.36 : SEM view of a produced nanomat sample.	136
Figure 4.37 : ATR-FTIR spectra of 40, 80, 120, 160, and 200 μ l Py polymerized nanomats.	137

Figure 4.38 : P(AN-co-BuA) nanoparticles.	138
Figure 4.39 : P(AN-co-BuA)/PPy core/shell nanoparticles (15 microliters Py).	139
Figure 4.40 : P(AN-co-BuA)/PPy core/shell nanoparticles (40 microliters Py).	140
Figure 4.41 : P(AN-co-BuA)/PPy core/shell Nanoparticles (120 microliters Py)..	142
Figure 4.42 : P(AN-co-BuA)/PPy core/shell Nanoparticles (240 microliters Py)..	143
Figure 4.43 : The colour change of CSNP emulsions by increasing PPy content. .	144
Figure 4.44 : The surface topographies of (a) polymer template and (b) CSNPs. ...	146
Figure 4.45 : ATR-FTIR spectra of nanoparticles and core-shell nanoparticles. ...	147
Figure 4.46 : The change in ratio of PPy/PAN characteristic peaks by initial Py amount.	148
Figure 4.47 : UV-Visible spectrum of P(AN-co-BuA) and PPy/P(AN-co-BuA) nanoparticles in distilled water medium (emulsion/water 1/1000 dilution).	149
Figure 4.48 : UV-Visible spectrum of PPy/P(AN-co-BuA) nanoparticles in DMF solvent (0.001 g of particules / 10 ml DMF).	150
Figure 4.49 : Preparation stages of thin-films and the resultant samples.	151
Figure 4.50 : The morphology change on surfaces of CSNPs' thin-films (a: thin-film obtained from 20 μ l Py polymerized CSNPs, b: thin-film obtained from 40 μ l Py polymerized CSNPs).	152
Figure 4.51 : Nyquist plots' comparison on EIS (analyses were performed in 10 ml 0,1 M NaClO ₄ /H ₂ O).	153
Figure 4.52 : Bode Phase plots' comparison on EIS (analyses were performed in 10 ml 0,1 M NaClO ₄ /H ₂ O).	153
Figure 4.53 : Bode Magnitude plots' comparison on EIS (analyses were performed in 10 ml 0,1 M NaClO ₄ /H ₂ O).	154
Figure 4.54 : Admittance curves' comparison on EIS (analyses were performed in 10 ml 0,1 M NaClO ₄ /H ₂ O).	154
Figure 4.55 : FTIR spectra of CSNP thin-films between 3800-2000 cm ⁻¹ band. ...	155
Figure 4.56 : FTIR spectra of CSNP thin-films between 4000-650 cm ⁻¹ band.	156
Figure 4.57 : PPy FTIR absorbance peaks – admittance maximums correlation. ..	157

PRODUCTION AND CHARACTERIZATION OF POLY(ACRYLONITRILE-co-BUTYL ACRYLATE)/POLYPYRROLE COMPOSITES AND NANOPARTICLES

SUMMARY

In this study, it was aimed to produce a new –Acrylonitrile(AN) based copolymer and to use it to produce various electrical conductive/semi-conductive composites for different applications which compensate lacks of mechanical behavior and processability of electroactive polymers, while keeping their electroactivity behavior as good as possible in the composite structure.

First, it was achieved to synthesize Polyacrylonitrile (PAN) homopolymer via Bulk Polymerization method; by using Acrylonitrile as monomer, and Cerium (IV) Ammonium Nitrate (CAN) as initiator, in aqueous medium, at 60°C temperature, for 3 hours. The conversion was over 95%. The resulting polymer was precipitated, washed, and dried, and obtained in powder form. And, optical (taking photo images, conventional-light-microscopic) and spectroscopic (analyses on ATR-FTIR spectrometer and UV-Vis spectrophotometer) analyses were achieved on this synthesized polymer.

As the second stage of this study, Butyl acrylate (BuA) was chosen as a co-monomer to pair AN monomer. In order to better learn this monomer, BuA was polymerized as alone and in the presence of AN as well. Then the same optical and spectroscopic characterizations were performed on both polymers as it was done for PAN in previous step. The P BuA homopolymer was obtained in latex form as reported in literature, and its disadvantages/superiorities were observed.

In the third part, P(AN-co-BuA) copolymer was synthesized from its monomers, with different molar ratios, by using CAN as initiator, at 60°C temperature, for 3 hours in aqueous medium. The conversion was over 90% for all 5 different molar ratios of synthesized copolymers. High conversion was obtained, but the copolymeric product was hardly soluble in most of the organic solvents which makes more difficult to prepare films from solution. Various methods were tried to solve it; such as, different temperatures, different ambient pressures, different organic solvents and their mixtures at various volume ratios, etc. For this reason, minimum amount of BuA was used ($\leq 5\%$), while trying to solve it in a high polar organic solvent such as Dimethylformamide (DMF) at a temperature higher than 100-110°C, at least for a few hours.

Increasing the solubility therefore the processability of the copolymer was possible by synthesizing it via emulsion polymerization method, using a free radical initiator (Potassium persulphate –KPS-, or Ammonium persulphate –APS-), at 70°C, in again aqueous medium with Sodium dodecylbenzenesulfonate (SDBS) as surfactant, for 5 hours. The resultant copolymers were in powder form, easy to process, and they showed the similar characteristics with previously synthesized copolymers in

spectroscopic analyses; as both were copolymers of AN-BuA, but just were synthesized via different polymerization methods. Synthesized copolymers were quite soluble in DMF, and the films showed obvious changes in their morphological, spectroscopic, mechanical and thermal properties with changing BuA monomer amount in copolymer.

As the fourth stage of study, to prepare composites of Polypyrrole (PPy) in P(AN-co-BuA) matrix, PPy was synthesized in polymer matrix by redox polymerization of Pyrrole (Py). By casting the resultant solutions in different molar ratios of Py on to the smooth glass cells, its films were obtained; by casting the same solvents onto the spin-coater device, the thin-films (thinner than 10 microns) were obtained; and by applying these solvents in an injection pump (just like in extruder system) of an electrospinning device, the micro/nano-fibers of these electrical (semi)conductive composites were obtained. For the characterization of samples, following techniques were used: morphological (light microscopy, scanning electron microscopy (SEM), atomic force microscopy (AFM)); mechanical (dynamic mechanical analyses); spectroscopic (via analyses on ATR-FTIR spectrometer, UV-Vis spectrophotometer, electrical impedance spectroscopy –EIS-); and the dielectrical behavior (solid dielectric broad-band spectroscopy) analyses; so to characterize all the products and correlate and/or compare them with each other.

In the last part, (AN-co-BuA) polymeric nanoparticles were synthesized by micro-emulsion polymerization method, to use as template for producing PPy/P(AN-co-BuA) core-shell nanoparticles via polymerizing different amounts of Py monomer in the same medium without any precipitation nor adding any extra initiator to reaction medium at room temperature. With such a cost-effective method, composite core-shell nanoparticles were produced and their particle-sizes were analysed by two different methods i.e. Light-Scattering and image analyzing techniques, and also other various analyses such as ATR-FTIR spectroscopy, UV-Vis spectrophotometer, SEM, AFM, Electrical Impedance Spectroscopy (EIS) were performed on their prepared samples, to enlighten their morphological, spectroscopic and electrical properties.

POLİ(AKRİLONİTRİL-ko-BÜTİL AKRİLAT)/POLİPİROL KOMPOZİTLERİN VE NANOPARTİKÜLLERİN ÜRETİMİ VE KARAKTERİZASYONU

ÖZET

Bu çalışmada, yeni bir Akrilonitril esaslı kopolimer sentezi, ve iletken polimer içeren kompozit nanoyapıların sentezi amaçlanmıştır. Öncelikle homopolimerler sentezlenmiş ve ayrıca bu monomerleri içeren Poli(Akrilonitril-ko-Bütül akrilat) [P(AN-ko-BuA)] kopolimeri elde edilmiştir. Polimerizasyon verimi, karakterizasyonu, yükseltgen ve çözücü gibi parameterelerin polimerizasyon verimine etkisi incelenmiş ve optimize edilmiş, ve elde edilen kopolimer DMF içerisinde çözülerek çözeltilerinden polimerik ince filmeler elde edilerek bu filmlerin Dinamik Mekanik Analiz (DMA) , ATR-FTIR spektroskopisi, SEM görüntü analizi ve Atomik Güç Mikroskopu (AFM) analizleri gerçekleştirilmiştir. Ayrıca kopolimer sentezinde emülsiyon polimerizasyonu yöntemi kullanılmış, bu yolla, ve su ortamında CAN gibi molekül zincirleri arası kuvvetli çapraz-bağ oluşturan serbest-radikal başlatıcısı ve Potasyum persülfat (KPS) veya Amonyum persülfat (APS) gibi başlatıcılar ve sodyumdodesilbenzensülfonat (aktif madde) kullanılmıştır, bu yolla polimerin çözünürlüğü ve dolayısıyla işlenebilirliği önemli derecede artırılmıştır. Elde edilen kopolimer, DMF gibi bir organik çözücüde rahatça çözünebilir hale getirilmiş, ve böylece kolaylıkla film, ince-film, nanolifler elde edilebilmiştir. Bu tez çalışmasında ayrıca, yeni sentezlenen kopolimerler DMF/DMSO gibi bir organik çözücüde çözülerek, CAN başlatıcısı kullanılarak polimer matrisinde elektroaktif polimer olan PPy büyütülmüş ve elektrik iletken / yarı iletken kompozit polimerik filmler üretilmiştir. Yine aynı yöntemle elde edilen farklı içeriklerdeki kompozit çözeltilerinden spin-coating, daldırma, damlatma ve elektro-eğirme yöntemleriyle ince film (10 mikrondan daha ince filmler), nanoelyaf, nano-dokusuz-yüzey, vs. gibi çeşitli ürünler elde edilmiştir. Farklı üretim parametreleriyle ile oynanarak ürün özellikleri (optik mikroskop, dinamik mekanik analiz cihazında yapılan sabit sıcaklıkta / değişen sıcaklıktaki dayanım testleri, morfolojik (Atomik Güç Mikroskopu) analizleri, ve spektroskopik (ATR-FTIR ve UV-Vis Spektrofotometre) analizleri yapılmıştır.

İlk olarak, yağın polimerizasyonu yöntemi ile Poliakrilonitril (PAN) homopolimeri sentezlenmiş, polimerizasyon su ortamında Seryum (IV) Amonyum Nitrat (CAN) başlatıcısı kullanılarak, 60 derece sıcaklıkta 3 saat boyunca gerçekleştirilmiştir. Polimerizasyon verimi %95'in üzerinde olmuştur. Oluşan polimer çöktürülmüş, yıkanmış, kurutulmuş ve toz halinde elde edilmiştir. Ardından, sentezlenen polimer üzerinde optik (dijital fotoğrafı, ışık mikroskopu analizi) ve spektroskopik (ATR-FTIR spektrometre ve UV-Visible spektrofotometre) analizler gerçekleştirilmiştir.

Çalışmanın ikinci aşamasında, AN monomerine eşlik ederek kopolimer oluşturacak ikincil monomer olarak Bütül akrilat (BuA) seçilmiştir. BuA monomerinin özelliklerini belirlemek ve üretilmesi hedeflenen kopolimere ne gibi avantaj/dezavantajlar katacağını görebilmek amacıyla, çalışmanın ilk aşamasında

PAN sentezinde kullanılan polimerizasyon yöntemi ve reçetesi aynı şekilde Polibütül akrilat (PBuA) eldesinde de kullanılmıştır. Sentezlenen PBuA homopolimeri, literatürde sentezlenen homopolimerlerle uyumlu karakteristik özelliklerde olmuş, ve bu homopolimer üzerinde PAN'ın karakterizasyonundakiyle aynı görsel ve spektroskopik analizler gerçekleştirilmiş ve eksiklikleri / üstünlükleri gözlenmiştir.

Çalışmanın üçüncü aşamasında, AN ve BuA monomerlerini beraber farklı monomer %mol oranlarında ve yine su ortamında CAN başlatıcısını kullanarak 60°C sıcaklıkta polimerleştirmek, ve böylece Poli(Akrilonitril-ko-Bütül akrilat) [P(AN-ko-BuA)] kopolimerini elde etmek amaçlanmıştır. Polimerizasyon verimi 5 farklı monomer %mol oranında olan kopolimerlerin tümü için %90'ın üzerinde olmuştur. Kopolimer yapısında BuA monomerinin miktarı arttıkça, polimer rengi PAN'ın karakteristik pudra-beyaz yapısından farklılaşarak krem-sarı renk ve lateks formuna doğru bir değişim göstermiştir. Polimerizasyon verimi iyi seviyelerde gerçekleşmiş, kopolimerin fiziksel görünüşü ve yapısı monomer içerikleriyle korelasyon sergilemiş, ancak elde edilen kopolimerik malzeme şaşırtıcı şekilde düşük işlenebilirliğe sahip çıkmıştır. Polimeri herhangi bir organik çözücüde çözmek ve böylece film, ince film, ve/veya lif elde etmek zorlaşmıştır. Sentezlenen kopolimerin işlenebilirliğini artırmak için, farklı sıcaklıklarda, farklı basınç seviyelerinde, farklı organik çözücüler ve onların çeşitli hacim oranlarındaki karışımlarında çözmeye çalışmak gibi çeşitli yöntemler denenmiştir. Tüm bu çözüm denemeleri göstermiştir ki, başlatıcı olarak CAN kullanıldığı durumda, kopolimer sentezindeki BuA monomer oranının %molce 5 ve daha az tutulması, ve kopolimerin yüksek polariteye sahip Dimetilformamid (DMF) gibi bir organik çözücü içerisinde 100-110°C sıcaklığın üzerinde ve en az birkaç saat boyunca manyetik karıştırma ile çözünmesi, bir sonraki aşamada kompozit ürünlerin eldesi için tek çözümdür. Bu şekilde elde edilen kopolimer/DMF çözeltilerinden polimerik filmler ve ince filmler yapılmış, dinamik mekanik analiz, ATR-FTIR spektroskopisi, SEM görüntü analizi ve Atomik Güç Mikroskopu (AFM) analizleri gerçekleştirilmiştir.

Kopolimer sentezinde emülsiyon polimerizasyonu yönteminin, ve su ortamında CAN gibi molekül zincirleri arası kuvvetli çapraz-bağ oluşturan serbest-radikal başlatıcısı olan Potasyum persülfat (KPS) veya Amonyum persülfat (APS)'in 70 derece sıcaklıkta, 5 saat boyunca ve Sodyum dodesilbensülfonat gibi etkili bir yüzey aktif madde, polimerin çözünürlüğünü ve dolayısıyla işlenebilirliğini çok önemli derecede artırmıştır. Elde edilen kopolimer, toz formunda, çözünürlüğü/işlenebilirliği çok yüksek; DMF gibi bir organik çözücüde hemen her oranda rahatça çözünebilen, ve böylece kolaylıkla film, ince-film, nanolifler elde edilmiş ve bunların birbirleriyle ve öncülleriyle karşılaştırmaları yapılmıştır. Polimer yapısında değişen BuA monomeri miktarıyla orantılı olarak, polimerik kompozit ürünlerin morfolojik, spektroskopik, mekanik ve termal özelliklerinde değişimler meydana gözlenmiştir.

Bu tez çalışmasının dördüncü bölümünde, yeni sentezlenen kopolimerleri ve PAN'ı polimer matrisi olarak kullanılmış; ve bu polimerler DMF/DMSO gibi bir organik çözücüde çözülerek, CAN başlatıcısı kullanılarak polimer matrisinde elektroaktif polimer olan PPy sentezlenmiş, elde edilen farklı PPy içeriğine sahip kompozit çözeltilerinden elektrik iletken / yarı iletken kompozit polimerik filmler ; spin-coating, daldırma, damlatma, ve elektro-eğirme yöntemleriyle ince film (10 mikrondan daha ince filmler); ve elektro-eğirme yöntemiyle nanoelyaf, nano-dokusuz-yüzey, gibi çeşitli ürünler elde edilmiştir. Farklı üretim parametreleriyle ile oynanarak ürünlerde ortaya çıkan değişimler ve bu değişimlerin olası nedenleri

çeşitli optik (dijital fotografi analizleri, ışık mikroskopisi), mekanik (dinamik mekanik analiz cihazında yapılan sabit sıcaklıkta / değişen sıcaklıktaki dayanım testleri), morfolojik (Taramalı Elektron Mikroskobu ve Atomik Güç Mikroskobu analizleri) ve spektroskopik (ATR-FTIR spektrometre ve UV-Vis Spektrofotometre) analizler yardımıyla aydınlatılmaya çalışılmıştır.

Son bölümde, kompozit öz-kabuk nanopartikül yapıları da ayrıca üretilmiş, ve (AN-ko-BuA) polimerinin nanopartikülleri mikro-emülsiyon metodu ile sentezlenip, aynı emülsiyon ortamında oda sıcaklığında Py monomeri polimerleştirilmiş ve ürün olarak PPy/P(AN-ko-BuA) öz-kabuk nanopartikül yapıları elde edilmiştir. Böylece, pratik ve düşük maliyetli, tek-adımlı bir işlem sonucu elde edilen kompozit öz-kabuk nanopartikül yapılarının, partikül büyüklüğü analizleri yapılmış, ayrıca spektroskopik, morfolojik ve elektriksel özellikleri incelenmiştir.

1. INTRODUCTION

There has been always an interest on upgrading the existent materials or creating new ones to satisfy specific needs of different purposes in all industrial areas including textile, chemistry, material, mechanical and medical technologies and sciences. After machinery revolution, industries needed better materials to produce more efficient products which can better serve to the end-use, thus, the scientists studied and made researches to make them possible. The high speed of technological improvements is supported by new scientific researches, and researchers are tending to answer the existing needs of daily life, and/or to create new ones day by day. And the textile industry is one of those fields which are still in need of answer many of problems while production stage or even while designing.

In electronics, it is essential to control the move of electrons in appropriate material, thus to make it possible giving activation to the system, or to take response from the system by this way. In an electronic system, the faster the interaction between the components, the lower the response times and the better the achievement of the desired process. Because the limit of conductivity is theoretically already known and practically almost reached, last years it is more desired to improve different aspects of the systems to obtain superior products such as lighter in weight, softer in touch, ergonomic in design and shape, etc., while keeping their performance at same or even better levels. In this journey of creating new products and improving our daily-life comfort, it is essential to make everything more efficient; not only faster and smarter, but also better in energy consumption, cheaper in cost, and more capable with multi-functions for actual needs. While metals are suitable for their stability and electrical conductivity properties, because their resulting products are with limited performance/weight ratios, and because ergonomics and economics are today's new but far more important aspects to take into account in everyday life, the new materials have been researched instead of metals, to satisfy the higher needs of today and the future. For instance, the machines and the electronic devices left their durable but heavy and expensive metal cases to the lighter, cheaper, but even more durable

composites, and their inside metal components to the smaller, lighter, and more efficient as energy-consumption which are better to satisfy the needs of increasing population so the increasing need of energy-saving in today's world. But those needs of improvements are not only because of ergonomic or economic worries, but also because of the need for replacing the steady nature of traditional life-style with the mobility of modern life-style. And the mobility requires easy-to-carry products which are compact in form, efficient while working, and lower while consuming. To obtain all those properties at once in one body, apparently polymers are the only alternative to be used as raw-material of today's and also future's consumer products.

The textile industry is maybe the only one which has begun taking place in our lives since the first humans, it also had some changes because of militaristic needs, but kept seeking more comfort of humans, and because of today's mobility and ergonomics, it is also changing as application areas from the conventional fibers, yarns, fabrics, garments; to the special and functional composite products of the future. These new products are sometimes simply a mixture of multiple electronic/electrochemical devices with conventional textile body, and sometimes not only modified by some electronic attachments, but completely a new embodiment of new compounds such as electrical conductive polymers, phase-changing materials, antimicrobial, self-cleaning multifunctional technical textiles.

1.1 Purpose of Thesis

Because of their nature, conductive polymers are hard-to-process and –to-turn into the products which could be easily handled by users. Thus, it is necessary to enhance their properties by supporting their structure with other elements such as polymeric matrixes, metal dopes, supporting layers, interacting surfactants/solvents, etc.

In this study, it is aimed to produce a new electrically conductive copolymeric composite system which is better in various characteristics such as mechanical behavior and morphological properties, and to obtain its composite products in different forms for different potential purposes of end-use.

1.2 Literature Review

In recent years, many scientists aimed to produce advanced materials for textile structures to enhance mainly their electromagnetic shielding, antimicrobial, auto-climation, etc. characteristics [1-20].

In order to obtain a better biopolymeric surface for cellular growth, in order to add functionality to modern smart textile materials, or, in order to create a better interaction between electronic devices and human behaviors; the electroactive polymers took great interest. Some researchers aimed to enlighten the mechanism of various polymerization methods such as emulsion, miniemulsion, microemulsion, surfactant-free emulsion, chemical oxidative and electrochemical polymerization; while some other researchers studied in practical way and tried simply blending the conventional polymers with electroactive polymers, so observing and analyzing the changes in the composite structure. Some researchers followed the way to build chemical interactions between different monomers and so synthesizing new compounds and products by electrochemical and/or chemical polymerization methods and analyzing them for different purposes of usage. Most of the recent studies focused on trying to create metal/polymer, metaloxide/polymer, ceramic/polymer, polymer/polymer, polymer/metal core-shell nanocomposites via various types of recipes and methods. and it was also used creating new applicational areas for existing polymeric materials, such as preparing biocompatible or bioactive polymers to use with a 3-D printer to shape biopolymeric-electropolymeric composite nano-frames to make an artificial organ from stem-cells by growing them on those frames [226-316].

2. THEORETICAL PART

2.1 Polymers

Polymers are large molecules. The chemical properties of polymers do not so differ from their simple molecules', for instance, if the polymer contains a carbon-nitrogen triple bond ($\text{—C}\equiv\text{N}$) as in Polyacrylonitrile (PAN) (Figure 2.1), it gives similar interactions (for instance, electron accepts) with other molecules such as organic solvents, just like its monomer (acrylonitrile) does [21-26].

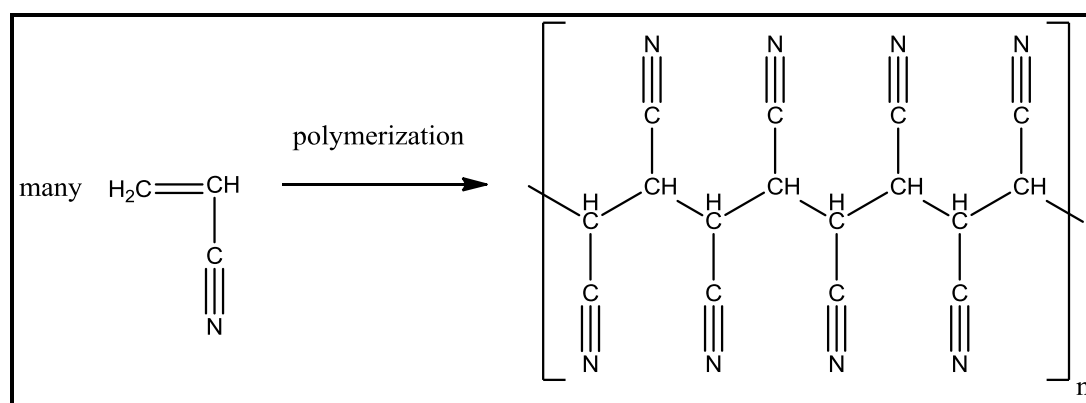


Figure 2.1 : Polymer chain of Polyacrylonitrile.

If the polymer contains carbon-oxygen double bond ($\text{C}=\text{O}$) as it is in Poly(butyl acrylate) (PBUA), it will react with catalysts to give hydrogenation reactions, as its monomer, Butyl acrylate (BuA) does (Figure 2.2).

While the chemical properties do not show a big difference, the physical properties differ more between small molecules and bigger ones; because of their larger molecular structure which means more and stronger intermolecular forces, they show higher melting points, flexibility, hardness, etc. as characteristics.

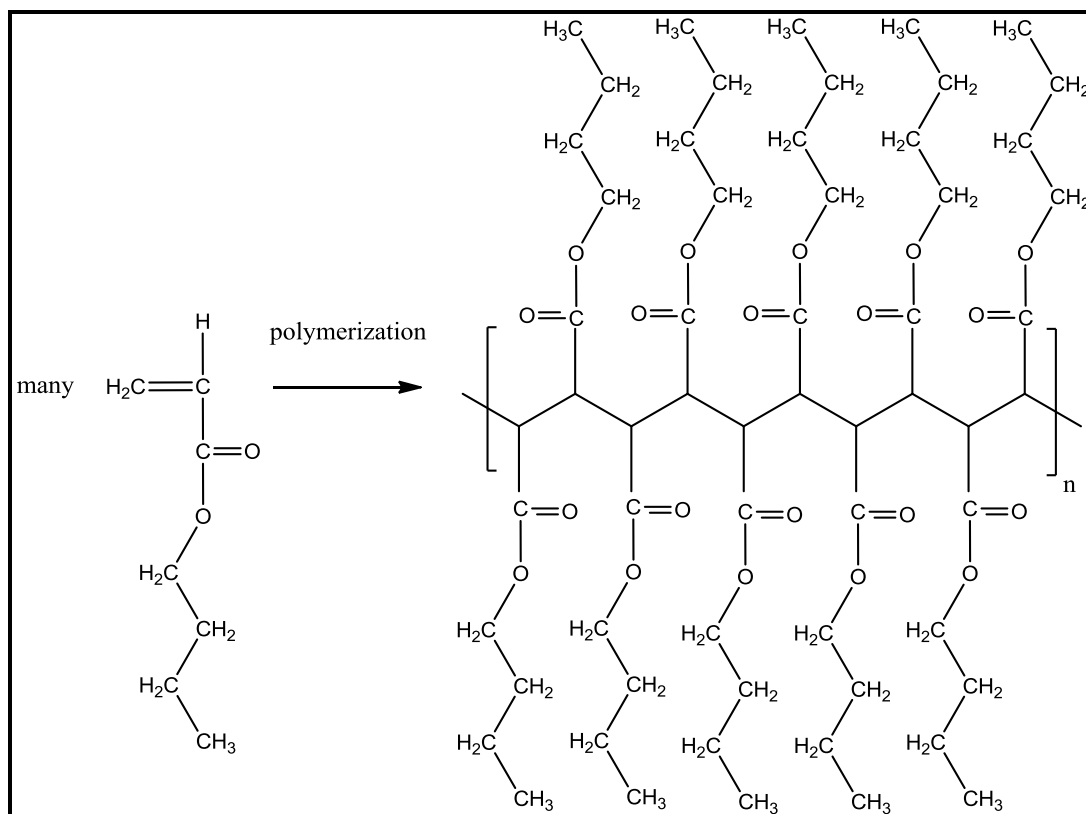


Figure 2.2 : Polymer chain of Poly(Butyl acrylate).

Most of today's polymers were found in last century, and they are synthetic copies of natural polymers such as proteins, cellulose, and starch. Every year, millions of tones polymers are produced, and they exist as many forms of products in almost all areas of our lives directly or indirectly. Polymers are mostly used in their fiber form, and some others are shaped into various forms to satisfy our needs, which are called as "plastics". Plastics indeed opened a new age in history of mankind, because it was such a revolutionary step to find a material which could be produced and modified into the required shapes and colors and properties.

2.1.1 Classification of polymers

Polymer is a generic name given to a vast number of materials of high molecular weight. These materials exist in countless form and numbers because of very large number and type of atoms present in their molecule. Polymer can have different chemical structure, physical properties, mechanical behavior, thermal characteristics, etc., and on the basis of these properties polymer can be classified in different ways, which are summarized in Table 2.1 [21,22,36,37,72,216].

Table 2.1 : Classification types of polymers.

Classification Type	Polymer Type
Origin	Natural, Semi-synthetic, Synthetic
Thermal Response	Thermoplastic, Thermoset
Formation Mode	Addition, Condensation
Line Structure	Linear, Branched, Cross-linked
Application and Physical Properties	Rubber (elastomers), Plastic, Fiber
Tacticity	Isotactic, Syndiotactic, Atactic
Crystallinity	Non-crystalline (amorphous), Semi-Crystalline, Crystalline
Chain Polarity	Polar, Nonpolar
Polymer composition	Homopolymer, Copolymer

2.1.1.1 Origin

On the basis of their occurrence in nature, polymers have been classified in three types:

- a. Natural polymer:** The polymers, which occur in nature are called natural polymer also known as biopolymers. Examples of such polymers are natural rubber, natural silk, cellulose, starch, proteins, etc.
- b. Semi synthetic polymer:** They are the chemically modified natural polymers such as hydrogenated, natural rubber, cellulosic, cellulose nitrate, methyl cellulose, etc.
- c. Synthetic polymer:** The polymer which has been synthesized in the laboratory is known as synthetic polymer. These are also known as manmade polymers. Examples of such polymers are polyacrylonitrile, polyacrylates, polyvinyl alcohol, polyethylene, polystyrene, polysulfone, etc.

2.1.1.2 Thermal response

On the basis of thermal response, polymers can be classified into two groups [36]:

- a. Thermoplastic polymer:** Thermoplastic polymers do not contain covalent bonding between their individual molecules, but only intermolecular bonds hold them together. Such polymers can be softened or plasticized repeatedly on application of thermal energy, without much change in properties if treated with certain precautions, and they can be molded into the desired shape again and again

by reheating and remolding. Example of such polymers are polyolefins, nylons, linear polyesters and polyethers, PVC, sealing wax, etc (Table 2.2).

b. Thermoset polymer: Some polymers undergo certain chemical changes on heating and convert themselves into an infusible mass that consists of a three dimensional big complex structure and behaves like a single molecule because its molecular chains strongly fixed to each other by covalent bonds. Thermoset polymers can be molded by heat and pressure, but after once molded into a shape, they cannot be remolded, so they permanently keep their shape after a required amount of pressure and temperature effect. The curing or setting process involves chemical reaction leading to further growth and cross linking of the polymer chain molecules and producing giant molecules. For example, Phenolic resins (Phenol formaldehyde resins - PF), urea, epoxy resins, diene rubbers, etc. are such thermoset polymers.

2.1.1.3 Formation mode

a. Addition polymer: Addition polymers are formed from olefinic, diolefinic, vinyl and related monomers. They are formed from simple addition of monomer molecules to each other in a quick succession by a chain mechanism. This process is called addition polymerization. In addition polymerization, the polymer consists of a repeating monomer unit, and as result of polymerization process, any side products do not occur. Addition polymers have the same empirical formula with their monomer unit, but only with a higher molecular mass. Examples of such polymers are polyethylene, polypropylene, polystyrene (Table2.2). Addition polymerization of Vinyl chloride (chloroethene) to form Polyvinylchloride (PVC) is shown in Figure 2.4 as example [21]:

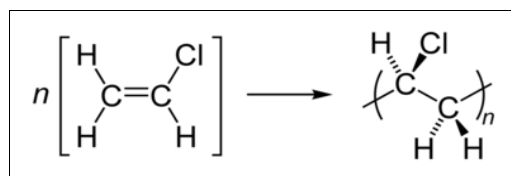


Figure 2.3 : Polymerization of Vinyl chloride to form Polyvinylchloride (PVC).

Table 2.2 : Some addition polymers.

Monomer	Formula	Polymer	Trivial name	Structure
Ethene	$H_2C=CH_2$	LDPE Low density poly(ethene)	low density polythene	$-CH_2-CH_2-CH_2-CH_2-$
Chloroethene	$H_2C=CHCl$	Poly(chloroethene)	polyvinyl chlorine, PVC	$-CH_2-\overset{Cl}{\underset{ }{CH}}-CH_2-\overset{Cl}{\underset{ }{CH}}-$
Propene	$H_2C=CH-CH_3$	Poly(propene)	polypropylene	$-CH_2-\overset{CH_3}{\underset{ }{CH}}-CH_2-\overset{CH_3}{\underset{ }{CH}}-$
Propenenitrile	$H_2C=CH-CN$	Poly(propenenitrile)	polyacrylonitrile	$-CH_2-\overset{CN}{\underset{ }{CH}}-CH_2-\overset{CN}{\underset{ }{CH}}-$
Methyl 2-methyl propenoate	$H_2C=C(\overset{CO_2CH_3}{ })-CH_3$	Poly(methyl 2-methylpropenoate)	polymethyl methacrylate	$-CH_2-\overset{CO_2CH_3}{\underset{CH_3}{ }{C}}-CH_2-\overset{CO_2CH_3}{\underset{CH_3}{ }{C}}-$
Phenylethene	$H_2C=CH-\text{C}_6\text{H}_5$	Poly(phenylethene)	polystyrene	$-CH_2-\overset{\text{C}_6\text{H}_5}{\underset{ }{CH}}-CH_2-\overset{\text{C}_6\text{H}_5}{\underset{ }{CH}}-$
Tetra fluoroethene	$F_2C=CF_2$	Poly(tetrafluoroethene) (PTFE)	Poly tetrafluoroethylene PTFE	$-CF_2-CF_2-CF_2-CF_2-$

b. Condensation polymer: They are formed from intermolecular reactions between bifunctional or polyfunctional monomer molecules having reactive functional groups such as -OH, -COOH, -NH₂, -NCO, etc. In condensation polymerization, the polymerization process of monomer/s takes place, meanwhile the elimination process of small molecular side products such as ammonia, water, etc. occurs (Table 2.3). A good example is the polymerization of Polyamide 6,6, (or Nylon 6.6), where two different monomers are used to produce the resultant polymer, but the process gives water as the side product [22,37].

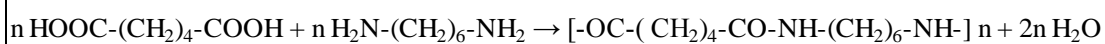
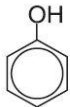
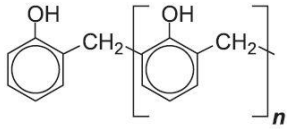


Figure 2.4 : Polymerization of Polyamide 6.6.

Another type of condensation polymer is said to be formed if the polymer chain contains (rather than attached to the branches of chain) a functional group such as an amide, ester, or urethane (Table 2.3).

Table 2.3 : Some condensation polymers.

Polymer	Monomer	Formula
Polyesters	$\text{HO}-(\text{CH}_2)_x-\text{C} \begin{array}{l} \text{O} \\ // \\ \text{OH} \end{array}$	$[(\text{CH}_2)_x-\text{C} \begin{array}{l} \text{O} \\ // \\ \text{O} \end{array}]_n$
Polyamides	$\begin{array}{c} \text{H} \quad \quad \quad \text{H} \\ \quad \quad \quad \\ \text{N}-(\text{CH}_2)_x-\text{N} \\ \quad \quad \quad \\ \text{H} \quad \quad \quad \text{H} \\ \text{O} \quad \quad \quad \text{O} \\ // \quad \quad // \\ \text{C}-(\text{CH}_2)_y-\text{C} \\ \quad \quad \quad \\ \text{HO} \quad \quad \quad \text{OH} \end{array}$	$[\text{NH}-(\text{CH}_2)_x-\text{NH}-\text{C} \begin{array}{l} \text{O} \\ // \\ \text{O} \end{array}(\text{CH}_2)_y-\text{C} \begin{array}{l} \text{O} \\ // \\ \text{O} \end{array}]_n$
Phenol-methanal plastics	 CH_2O	
Polyurethanes	$\text{HO}-\text{R}^1-\text{OH}$ $\text{O}=\text{C}=\text{N}-\text{R}^2-\text{N}=\text{C}=\text{O}$	$[\text{R}^1-\text{O}-\text{C} \begin{array}{l} \text{O} \\ // \\ \text{O} \end{array}-\text{NH}-\text{R}^2-\text{NH}-\text{C} \begin{array}{l} \text{O} \\ // \\ \text{O} \end{array}-\text{O}]_n$

2.1.1.4 Line structure

On the basis of structure, polymers are of three types [72]:

a. Linear polymer: If the monomer units are joined in a linear fashion, polymer is named as linear polymer.

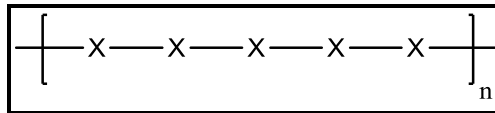


Figure 2.5 : Structure of a linear polymer.

b. Branched polymer: When monomer units are joined in a branched manner, it is called branched polymer.

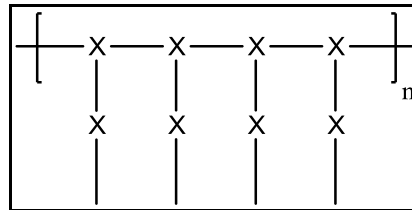


Figure 2.6 : Structure of a branched polymer.

c. Cross-linked polymer: A polymer is said to be a cross-linked polymer, if the monomer units are joined together in a chain fashion.

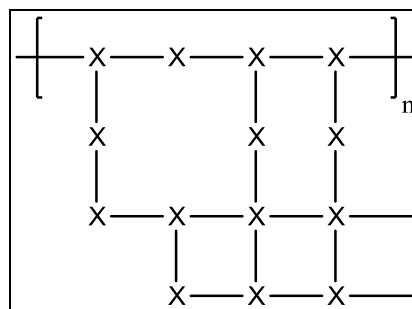


Figure 2.7 : Structure of a cross-linked polymer.

2.1.1.5 Application and physical properties

Depending on its ultimate form and use a polymer can be classified as [37]:

a. Rubber (Elastomers): Rubber is high molecular weight polymer with long flexible chains and weak intermolecular forces. Elastomers are amorphous solids which show elastic behavior (Table 2.3). Such polymers contain coiled molecular chains which can be stretched out by applied force, but recoil and spring back to their original shape when stretching force is released. They exhibit tensile strength in the range of 2-20 MPa and elongation at break ranging between 300-1000 %. Examples are natural and synthetic rubber.

Table 2.4 : Some of elastomers.

Polymer	Formula
Polybutadiene	$\left[\text{CH}_2 - \text{CH} = \text{CH} - \text{CH}_2 \right]_n$
Polyurethanes	$\left[\text{R}^1 - \text{O} - \overset{\text{O}}{\parallel}{\text{C}} - \text{NH} - \text{R}^2 - \text{NH} - \overset{\text{O}}{\parallel}{\text{C}} - \text{O} \right]_n$
ABS (Acrylonitrile butadiene styrene)	$\left[\text{CH}_2 - \text{CH} = \text{CH} - \text{CH}_2 \right]_a \left[\text{CH}_2 - \text{CH}_2 - \underset{\begin{array}{c} \\ \text{CH}_2 \\ \\ \text{CHCN} \\ \\ \text{---} \end{array}}{\text{CH}} - \text{CH}_2 \right]_b \left[\text{CH}_2 - \underset{\begin{array}{c} \\ \text{C}_6\text{H}_5 \end{array}}{\text{CH}} \right]_c$
Silicones	$\left[\begin{array}{c} \text{R} \\ \\ \text{---O---Si---} \\ \\ \text{R} \end{array} \right]_n$

b. Plastics: Plastics are relatively tough substances with high molecular weight that can be molded with (or without) the application of heat. These are usually much stronger than rubbers. They exhibit tensile strength ranging between 25-100 MPa and elongation at break ranging usually from 20 to 200% or even higher. The examples of plastics are, polyethylene, polypropylene, PVC, polystyrene, etc [36,37].

c. Fibers: Fibers are long-chain polymers characterized by highly crystalline regions resulting mainly from secondary forces. They have a much lower elasticity than plastics and elastomers. They also have high tensile strength ranging between 150-1050 MPa. Fibers are light weight, and they possess moisture absorption properties. They are thin threads which are produced by extruding a polymer melt/solution through a die in which there are many small holes called as spinnerette, and consists of dozens/hundreds of polymer molecular chains along their axis. The polymer examples for most widely used to produce fibers are; the polyamides (nylon fibers), the polyesters (for example, terylene), the polypropylenes, and the polyacrylics (acrylic fibers) (Table 2.5).

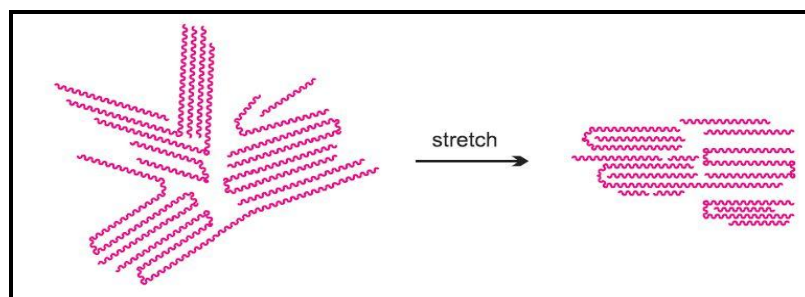


Figure 2.8 : After stretching to make a fiber, the crystalline regions are aligned along the axis of the fiber, and this adds strength to it.

When extruded and stretched out, the polymer molecules become aligned in the direction of the fiber axis, and, any tendency to return to a random orientation is prevented by the strong intermolecular forces between molecular chains along the axis. Fibers can be twisted into threads (yarns), and then they can be woven/knitted into cloth, or they can be embedded into a plastic as nonwoven to give it much greater strength (Table 2.5).

2.1.1.6 Tacticity

Tacticity may be defined as the geometric arrangement (orientation) of the characteristic group of monomer unit with respect to the main chain (backbone) of the polymers [37,42]. A good example is Polypropylene (PP) for a polymer with a side chain (Figure 2.9).

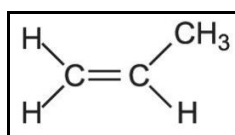


Figure 2.9 : Propylene molecule.

The propene molecule is asymmetrical, and when it is polymerized, it can form three basic structures dependent on the position of the methyl groups; two of them are stereoregular (isotactic and syndiotactic) and the third structure does not have a regular distribution and it is named as atactic (Figure 2.12). Thus, on the basis of structural arrangement, polymers may be classified into three groups; isotactic, syndiotactic, and atactic.

Table 2.5 : Some polymers used to make fibres.

Polymer	Formula
Polyamide 6	$\left[\text{NH}-(\text{CH}_2)_5-\overset{\text{O}}{\parallel}{\text{C}} \right]_n$
Polyamide 6,6	$\left[\underset{\text{H}}{\text{N}}-(\text{CH}_2)_6-\underset{\text{H}}{\text{N}}-\overset{\text{O}}{\parallel}{\text{C}}-(\text{CH}_2)_4-\overset{\text{O}}{\parallel}{\text{C}} \right]_n$
The polyester (terylene) formed from the dimethyl ester of 1,4-benzenedicarboxylic acid and ethane-1,2-diol	$\left[\text{O}-\overset{\text{O}}{\parallel}{\text{C}}-\text{C}_6\text{H}_4-\overset{\text{O}}{\parallel}{\text{C}}-\text{O}-(\text{CH}_2)_2 \right]_n$
Polyacrylonitrile	$\left[\text{CH}_2-\underset{\text{CN}}{\text{CH}} \right]_n$
Polyethylene	$\left[\text{CH}_2-\text{CH}_2 \right]_n$
Polypropylene	$\left[\text{CH}_2-\underset{\text{CH}_3}{\text{CH}} \right]_n$
Poly(vinyl chloride)	$\left[\text{CH}_2-\underset{\text{Cl}}{\text{CH}} \right]_n$
Poly(tetrafluoroethene)	$\left[\text{CF}_2-\text{CF}_2 \right]_n$

a. Isotactic polymer: It is the type of polymer in which the characteristic group are arranged on the same side of the main chain. The one-sided structure of isotactic Polypropylene causes the molecules to form helices. This regular form of polymer structure causes the molecules to crystalize to a hard, relatively rigid material, which in its pure form melts at 167 °C.

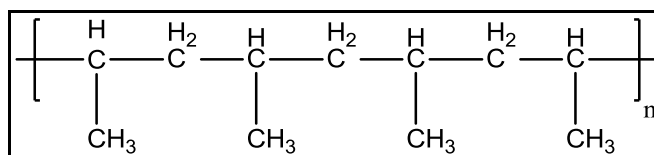


Figure 2.10 : Isotactic Polypropene.

b. Syndiotactic polymer: A polymer is said to be syndiotactic if the side group (characteristic group) are arranged in an alternate fashion. The syndiotactic polymer also shows crystalline character, because of its regular structure.

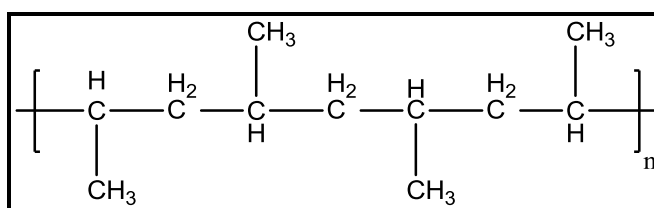


Figure 2.11 : Syndiotactic Polypropene.

c. Atactic polymer: A polymer is termed as atactic, if the characteristic groups (side group) are arranged in irregular fashion (randomness) around the main chain. Such a polymer has proper strength and more elasticity [42].

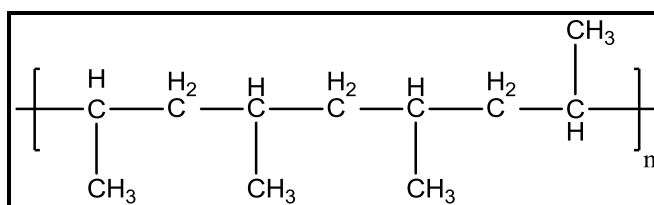


Figure 2.12 : Atactic Polypropene.

The atactic polymer contains fully random molecular structure, so it does not have crystallinity, but it is amorphous. High molecular mass atactic PP is a good example to such a polymer, and it is a rubber-like material. Commercial PP contains predominantly isotactic polymer, but also 1-5wt% atactic polymer. This is because of the commercial reasons which require affinity and shape-molding of amorphous structure, and also thermal and mechanical resistance govern from crystalline parts.

Stereoregular polymers can be produced by using Ziegler-Natta or metallocene catalysts while synthesis.

2.1.1.7 Crystallinity

a. Crystalline polymer: When the polymer chains pack in regular form in a polymer structure, which are called as crystalline regions, the intermolecular forces which exist in and between molecular chains are stronger. A good example of this situation is HDPE (High Density Polyethylene). When HDPE polymer is subjected to the required amount of heat, its temperature comes up to a point – melt transition temperature (T_m) – which is an important term about a polymer's characteristic property, so it melts and loses the crystallinity of its structure. This temperature does not give a sharp peak on heat flow – temperature curve. The polymer is crystalline below T_m , and amorphous above.

b. Non-crystalline (amorphous) polymer: On the other hand, some polymers are hard and amorphous, they do not have crystalline regions, for example, Polymethylmethacrylate (PMMA). Such polymers have another characteristic transition point as temperature, which is termed as – glass transition point (T_g) - , where below this temperature they are hard and resistant to mechanical effects, while above this point they become softer and foldable. Using this characteristic, to give shape to a polymeric construction or to change the mechanical behavior of a polymeric compound is possible, and such processes are called as heat-processing, for example; annealing.

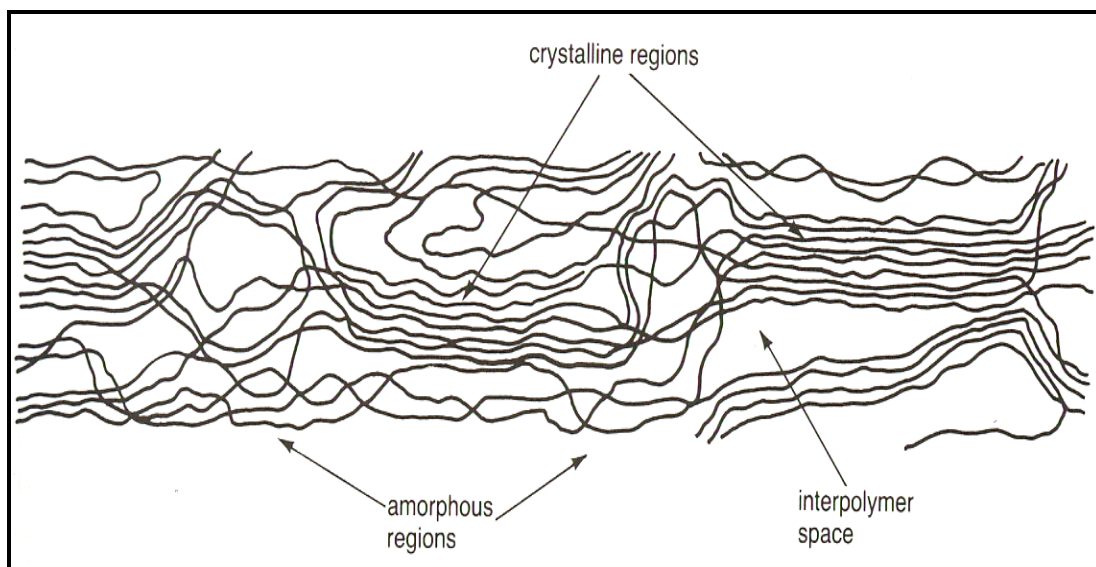


Figure 2.13 : Crystalline and amorphous regions in a polymer structure.

2.1.1.8 Polarity

A molecule is a group of atoms connected by covalent bonds. Chemical reactions are required to form or break covalent bonds. Weaker attractions often form between molecules of a polymer chain, encouraging them to stick together in groups. The weaker attractions are called secondary bonds or intermolecular forces. These can be overcome by adding heat or dissolving in a liquid. The functional groups on a polymer determine the types of polarity and strength of its secondary bonds[36,37,42].

a. Polar polymer: The valence electrons moving around a molecule may not be symmetrically distributed. The nonmetallic elements closest to the right top corner of the periodic table - nitrogen, oxygen, fluorine and chlorine - tend to shift shared electrons away from carbon and hydrogen. When there is a functional group with one of those elements, it has a slight negative charge and the rest of the molecule (carbon and hydrogen) is slightly positive. The molecule is polarized (or polar, for short). Its positive sections are attracted to negative sections of neighboring polymers.

Poly(ethylene terephthalate) or PET, a polymer used to make bottles for carbonated beverages, has oxygen-containing functional groups that make it polar. Protein and cellulose chains are also polar.

Positive and negative charges can be localized on a covalent molecule since they have no path for conduction of electrons. The carbon atoms in the backbone always follow the octet rule with four covalent bonds, so can't pass extra electrons along the chain. If polymer fibers are rubbed together they can build up a static electricity charge.

b. Nonpolar polymer: As valence electrons move around the nuclei in a nonpolar polymer, like polyethylene or polyfluoroethylene, they can become temporarily imbalanced. For a brief moment of time one part of a molecule would be negative, another part positive; it is temporarily polar. These occasional imbalances are enough to allow nonpolar molecules to attract each other, but the interaction is much weaker than that observed for polar polymers.

Polyfluoroethylene is nonpolar (not polar) because it is completely covered with fluorine atoms; there is no exposed positive section to interact with a neighboring molecule's negative section.

2.1.1.9 Polymer composition

Polymers are classified into two main groups as homopolymers and copolymers, regarding to the types of monomers to produce it, which are one type of monomer, or two or more types of monomers (Table 2.2) [36].

a. Homopolymer: If a polymer consists of one type of monomer, then it is called as homopolymer. Polyacrylonitrile (PAN) homopolymer is shown in Figure 2.14.

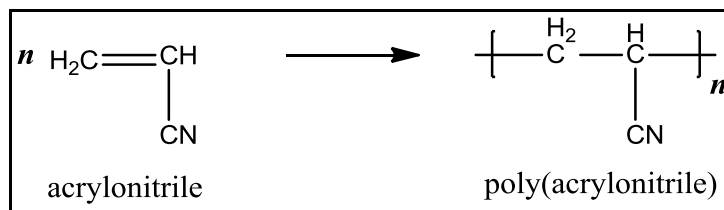


Figure 2.14 : Polyacrylonitrile homopolymer.

b. Copolymer: There are several copolymer types regarding to the coordination of their monomers; “alternating copolymer”, “random copolymer”, “block copolymer” and “graft copolymer”. Alternating and random copolymers are produced when two or more monomers are mixed and polymerized together. Depending on the reactivities of the monomers, they may form polymers with different arrangements of their monomer units (Figure 2.18).

Styrene-Butadiene-Styrene (SBS) is an example of block copolymer. SBS is so named with S referring to Styrene and B for Butadiene. To produce SBS, first, Styrene monomer is polymerized; Butadiene monomer is then added into the polymerization medium and it adds onto both reactive ends of the polystyrene molecules to form SBS polymer, which can be shown as in Figure 2.15.

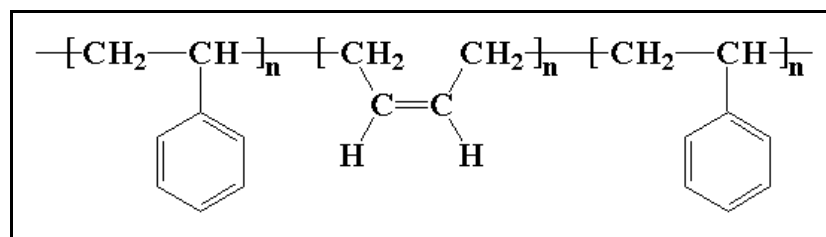


Figure 2.15 : Styrene-Butadiene-Styrene (SBS) polymer.

Another copolymer type is graft copolymer. A typical example of such copolymer is Acrylonitrile-Butadiene-Styrene (ABS). The backbone of polymer form from styrene and butadiene monomers; acrylonitrile monomer is then added to the polymerization medium and forms a grafted side chain onto this backbone. The nitrile adds to the double bond on the butadiene unit, shown as in Figure 2.16.

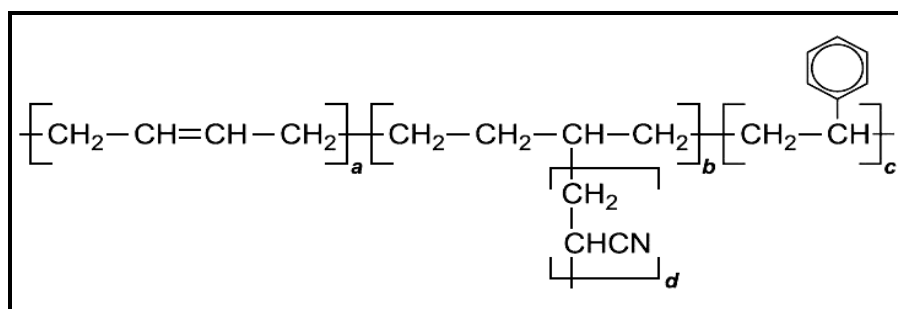


Figure 2.16 : Representative chemical structure of ABS polymer.

Being in copolymer form gives better properties to the polymers compared to their homopolymeric precursors. Copolymers are more capable and better in their characteristics, because they have the properties of the constituent polymers and thus can be produced for specific end-uses. The overall character of a copolymer is dependent on its comonomers, but also the ratios of monomers in which they were as amount in copolymer structure. For example, well known PAN and PS polymers are brittle in their homopolymer form, but when they are copolymerized with butadiene or alkyl acrylates such methyl or butyl acrylate, the comonomer gives the resultant polymer resilience and strength. In such a copolymer form PS is known as High Impact Polystyrene (HIPS), and it is now more durable, so can receive impacts without failure [36,42].

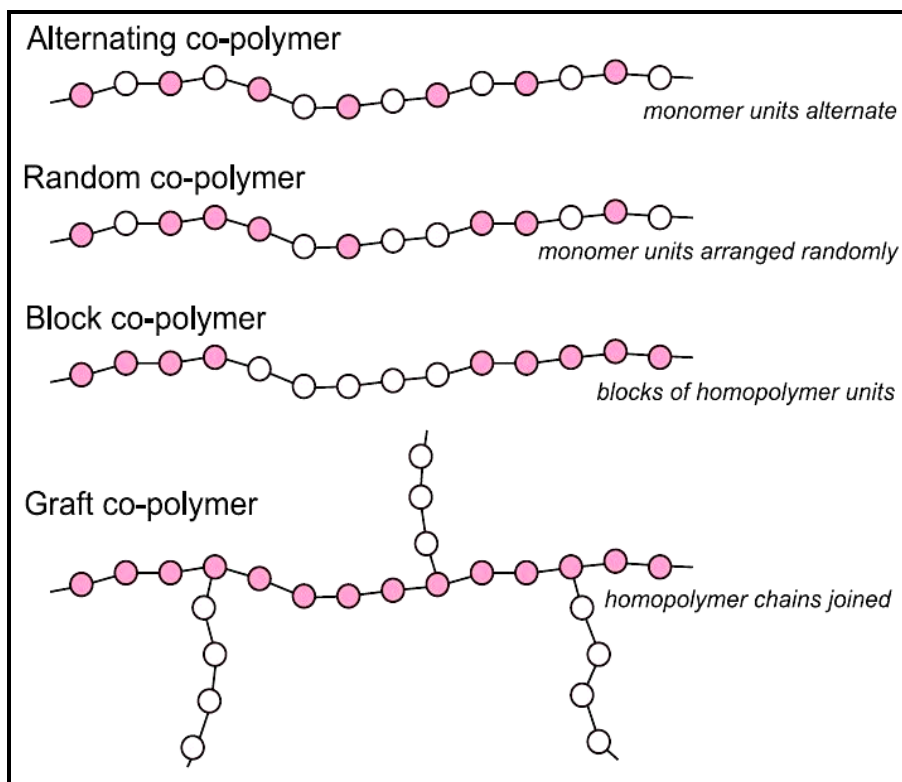


Figure 2.17 : Structures of different types of copolymer.

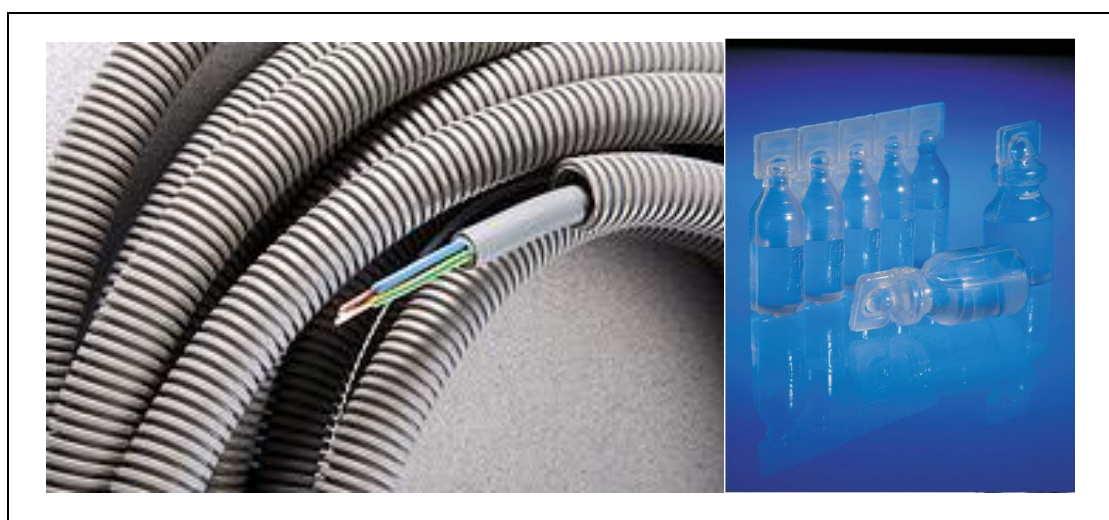


Figure 2.18 : Different types of copolymer have different properties and end-uses.

In Fig 2.18, on the right, the medical vials are made of a “random copolymer” of ethylene and propylene that give a flexible and clear material. And, on the left, the covering of the cable is a block copolymer of the two alkenes, giving a very tough material with rubber-like properties.

2.1.2 Production of polymers

Polymers can be characterized by polymerization methods mainly in two groups as addition and condensation polymers [44].

Most of the addition polymers are conventionally produced by using Ziegler-Natta catalysts, which are organometallic compounds. Those catalysts were developed by Karl Ziegler and Giulio Natta, so they were termed by these chemists' surnames, since their achievement was awarded also with 1963 Nobel Prize. Other addition polymers are generally produced by using free radical initiators, which catalyze the reaction while synthesis. Most of the condensation polymers also require catalysts while their synthesis process.

Almost all the polymers and all of the addition polymers (Table 2.1), are synthesized using radical initiators which act as catalyst. The polymerization of Vinyl chloride is an example of such a reaction as it is shown in Figure 2.21, and here the polymerization process starts by heating the reaction medium with inclusion of an initiator such as peroxide (R-O-O-R), and results by formation of PVC.

The free radical polymerization of Ethene results a polymer with lower density and softening point, compared to the PE synthesized using a Ziegler-Natta catalyst or a metallic oxide, as it was mentioned above. Such produced Low Density Polyethylene (LDPE) has side chains in its polymeric structure, because while polymerization process, the radicals do not react only with Ethene monomer molecules by addition, but they also react with polymer molecules and follows a process named as hydrogen abstraction. The polymer radical can also abstract a hydrogen atom from its own chain, so this procedure goes on and results a complex and random structure of molecular chains in polymer body, which means amorphous structure, so lower melting and/or softening point, lower density, and lower mechanical and chemical resistance.

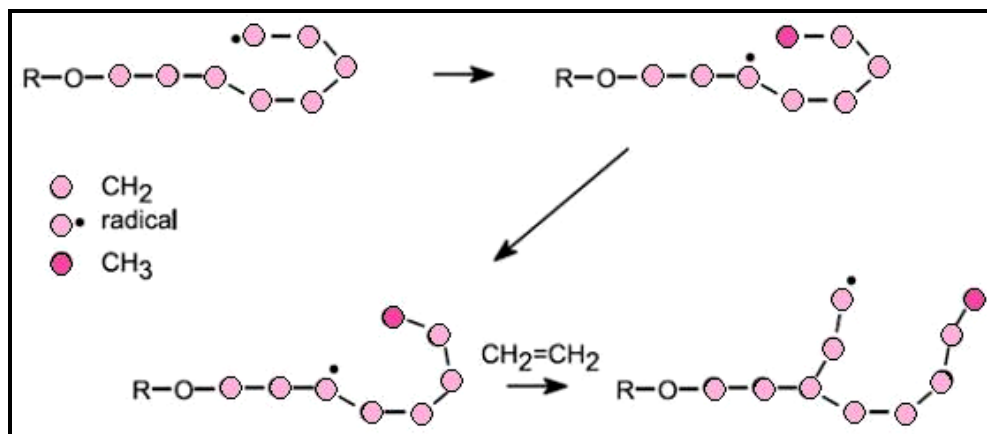


Figure 2.19 : Free radical polymerization of low density polyethylene (LDPE).

Both of these reactions (Figure 2.19 and 2.20) lead to side chains therefore the molecules of the polymer cannot pack together in a regular way. The polymer thus has a lower melting point and lower density.

2.1.3 Modification of polymers

The properties of many polymers can be modified by changing their composition. In industry, the most commonly used polymer is maybe PVC. This polymer can be made into either rigid or flexible form by using some additives, which are listed in Table 2.6.

Mixing the polymers which individually have different properties, is another method to obtain specific properties for an end-use [36,37,42,72,75,84]. For example, the shirt shown in Figure 2.21 is produced from a mixture of Polyacrylate (acrylic), aramide, and polyamide fibers, which gives protection against chemical and thermal affects, but still is comfortable to wear.

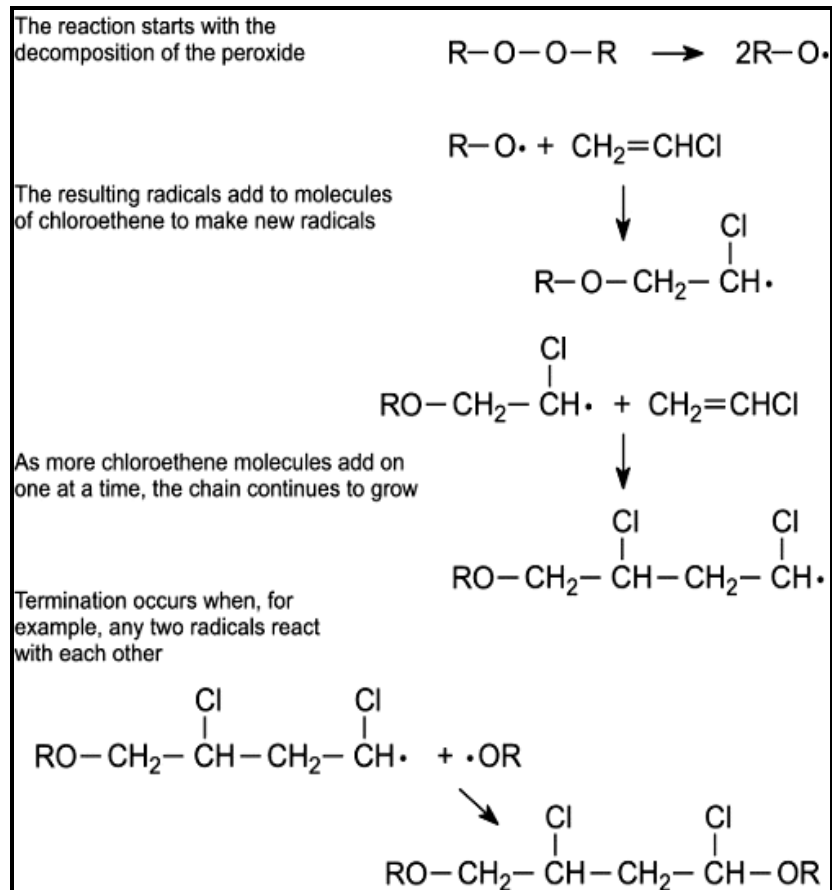


Figure 2.20 : A mechanism for the free radical polymerization of Vinyl chloride to Poly(Vinyl chloride) (PVC).



Figure 2.21 : A protective shirt which is made of Polypropanoate(acrylic), Aramid and Polyamide fibers' mixture.

Table 2.6 : Additives used to enhance the properties of polymers.

Additive	Examples	Function
Plasticiser	e.g. esters of benzene-1,2-dicarboxylic acid	Acts as a lubricant for polymer chains. Large amounts give a flexible product, low quantities produce a rigid one.
Stabiliser	e.g. lead carbonate (<1%), lead phosphate or, for non-toxic requirements, mixtures of metal octadecanoates and epoxidized oil	Prevents decomposition of polymer. Without a stabiliser, poly(chloroethene), for example, decomposes on heating to give a brittle product and hydrogen chloride. Some plastics become coloured (yellowing) when exposed to long periods of sunlight.
Extender	Chlorinated hydrocarbons	Extends the effect of the plasticiser, but generally cannot plasticise alone. They are cheaper than plasticisers, so help reduce costs.
Fillers	Chalk, glass fibre	Tailor the plastic for special requirements, or make it cheaper.
Miscellaneous	Flame retardants, UV stabilisers, antistatics, processing aids, pigments	Impart specially required properties to the plastic for the manufacturing process or for end-use.

2.1.4 Processing the polymers

To obtain useful products for specific end-uses requires some thermal and/or mechanical processes are applied on the polymeric materials [23,25,216]. Some of the processing methods are listed in Table 2.7.

Table 2.7 : Methods of processing the polymers.

Process	Application
Compression moulding	Usually for thermosets - powder moulded under heat and pressure.
Injection moulding	Usually for thermoplastics - molten plastics injected into a mould under pressure. The mould surface detail can be accurately reproduced. Very widely used.
Rotational moulding	Usually for thermoplastics. The powder is heated in a closed mould which is rotated, fairly slowly, simultaneously about two axes. Surface detail is poor but this method can be used to make large hollow articles.
Reaction injection moulding	Usually for thermosets, polymerization takes place in the mould thereby producing the finished article directly from a resin.
Extrusion	Usually for thermoplastics - the molten plastics are fed by a screw through a die, which for sheet or film, for instance, is a slit. Various extensions to the process are possible - e.g. a tube may be inflated by air whilst still hot to produce a tubular film (for bags, etc.), or short lengths of hot extruded tube can be inflated in moulds to form bottles.
Calendering	Usually for thermoplastics - molten plastics squeezed between hot rollers to form foil and sheet.
Thermoforming	Heat-softened thermoplastic sheet is drawn into or over a mould. If a vacuum is used to 'suck' the sheet into a mould, the process is known as vacuum forming. This process is used for a variety of articles, ranging from chocolate box liners to acrylic baths.

2.2 Polyacrylates

Acrylate polymers are a group of polymers which could be termed generally as plastics. They are known with their elasticity, resilience, and transparency. They are commonly termed also as polyacrylates, or acrylics.

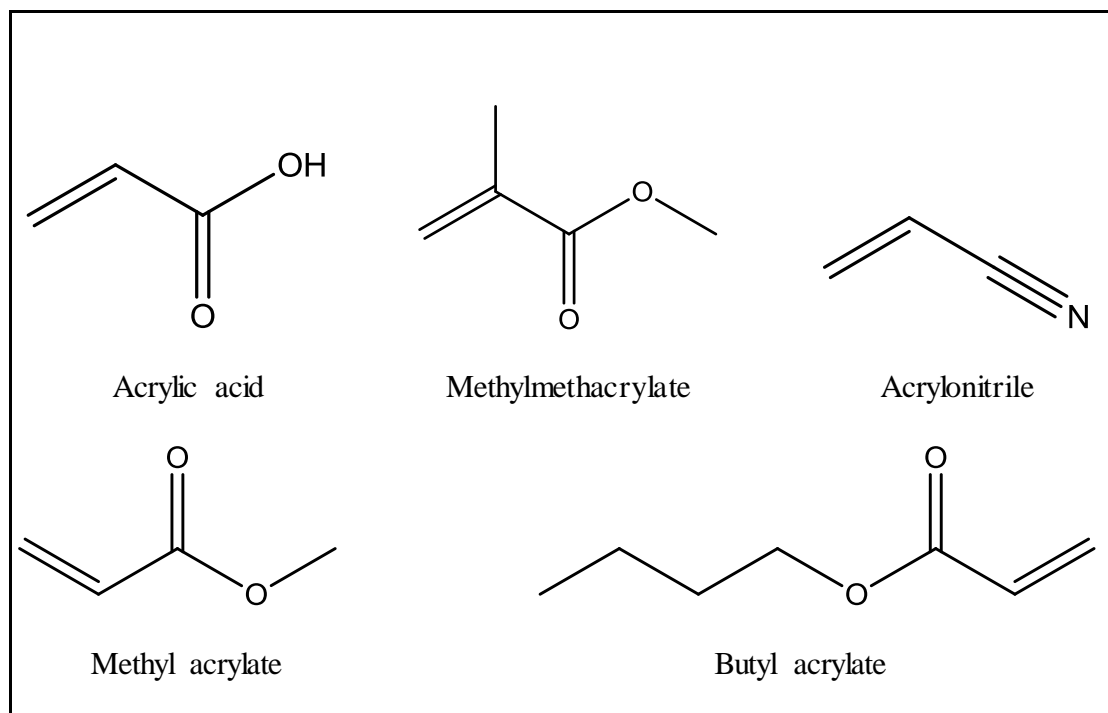


Figure 2.22 : Some monomers to synthesize polyacrylates.

Acrylate monomers which form polyacrylates are based on the structure of acrylic acid, which consists of a vinyl group and a carboxylic acid terminus. Most of the typical acrylate monomers are acrylic acid derivatives. For instance, methyl methacrylate contains methyl groups in place of both vinyl hydrogen and carboxylic acid hydrogen; and acrylonitrile contains a nitrile group instead of the carboxylic acid group (Figure 2.22).

Some other acrylate monomers are; Methyl acrylate, Ethyl acrylate, Butyl acrylate, 2-Ethylhexyl acrylate, Trimethylolpropane triacrylate, 2-Chloroethyl vinyl ether, Methacrylates, Hydroxyethyl methacrylate, and Butyl methacrylate.

An elastomer is a material that can be repeatedly stretched at least to double times of its original length at room temperature. Acrylics elastomers are useful and therefore used to enhance the mechanical and chemical resistance of many products. An

acrylic elastomer is a type of synthetic rubber that contains an acrylic acid alkylester (methyl, ethyl, or butyl ester) as main component. Acrylic elastomers show high resistance to heat and oil. They can endure a temperature of 170 ~ 180 °C under dry heat or in oil. Lack of a double bond gives acrylic rubber also the characteristics of good weatherability and ozone resistance.

There are mainly two types of acrylic elastomers; old type and new type. Old types include ACM (copolymer of acrylic acid ester and 2-chloroethyl vinyl ether) containing chlorine and ANM (copolymer of acrylic acid ester and acrylonitrile) without chloride. Both these copolymers have poor processability and similar physical structure; but ANM has a better water resistance than ACM. The characteristics of these materials are good, but because of their high prices, demand is not so high. New type acrylic rubber has an unclear chemical composition, although it does not contain any chlorine. Its processability has been improved, and most of cohesiveness as well as staining problems have been solved.

Despite of their resistance to heat, the cold resistance is not that good. The saturation point is -15 °C for the old type rubber and about -30 °C for the new type rubber. Vulcanization is a chemical process to convert natural rubber or its synthetic imitations into more durable materials via the addition of sulfur or some other curatives or accelerators. These additives modify the polymer by forming cross-links (bridges) between individual polymer chains. Vulcanized materials are less sticky and have superior mechanical properties. The standard vulcanization method for the old type rubber is amine vulcanization; in this process approximately 5% halogen compound containing acrylate rubber is processed with triethylene tetramine. To minimize permanent deformation, it requires curing for 24 hours under 150 °C temperature (Amine vulcanization of ethyl polyacrylate, Hansen, J.E., et al., U.S. patent, september 1948). On the other hand, for the new type, the press curing time and follow-up vulcanization time are significantly reduced by combining metal soap and sulfur. It has no special characteristics. The rebound resilience and abrasion resistance of the new type are poor, and even its electrical characteristics are considerably poor compared with acrylonitrile-butadiene rubber and butyl rubber. The vulcanized acrylate rubber materials are used mainly for oil seals and packagings related to automobiles.

Most of acrylic polymers find various uses in industry. Polymethyl methacrylate (PMMA) is an acrylate polymer familiar to consumers with its clear break resistant glassy end products or sheetings sold in hardware stores as acrylic glass or under the trade name of Plexiglas. Water-borne coatings, which are water dispersions of polyacrylates are used as binder for outdoor and indoor latex house paints which uses water as solvent to disperse resin. Acrylic paints are well known as artist paints. Acrylic fibers are main materials used for textiles and concrete-reinforcing applications. Sodium polyacrylate water-soluble thickeners, a polymer for the production of the Super Absorbent Polymer (SAP) used in disposable diapers due to its high absorbency per unit mass (a SAP may absorb 500 times its weight (from 30–60 times its own volume) and can become up to 99.9% liquid). Acrylic resin as pressure-sensitive adhesive, a glue product with its well known generic name of “super glue” is a formulation of cyanoacrylate. PVAc copolymer emulsion is used as an adhesive of vinyl acetate (VAc) and acrylic acid (AA), and Polyacrylamide copolymer is used as flocculation agent in water treatment.

The polyacrylates are highly heat and oil resistant polymers. Some of the application areas of acrylate and methacrylate esters are, to obtain polymers for textiles, latex paints, surgical cements and dental resins.

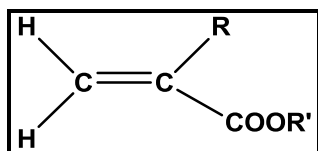


Figure 2.23 : General formula of acrylates.

Acrylates contain Hydrogen (H), and methacrylates contain CH₃ in place of R, in their molecular structure (Figure 2.23). The substituents R' can vary from n-alkyl chains to more complicated functional groups [26].

Adhesives: Acrylate polymers and copolymers are frequently used in construction of adhesives and pressure-sensitive adhesives.

Chemical Intermediates: Acrylates are widely used as molecular building blocks, or intermediates due to their chemical structures and useful chemical functionalities.

Coatings: Acrylates are used as monomers in the production of textile copolymers, adhesive resins, and surface coatings. They are widely used in water-based coatings. Some are used in paints, leather finishing, and paper coatings.

Leather: Acrylic copolymers are used as film coatings and leather finishes, particularly nubuck and suede.

Plasticizers: A balance of properties including molecular mobility, resin viscosity, solubility, hydrophobicity, thermal stability and low toxicity are critical for selecting a material for use as a plasticizer.

Plastics: Acrylate monomers and copolymers are used in the manufacture of plastics.

Textiles: Acrylate monomers and copolymers are used in the manufacture of both woven and non-woven textiles.

Water Treatment: Methyl Acrylate is used to produce dimethylaminoethylacrylate (DMAEA), which is used as a monomer to make flocculants for water treatment. Sodium acrylate (the sodium salt of glacial acrylic acid) is copolymerized with acrylamide to make an anionic copolymer (a-PAA), which is also used as a flocculant in water treatment.

Esters of general acrylates are crystalline solids at ambient temperatures, then form liquid at slightly higher temperatures. They are ready easily to polymerize and copolymerize, therefore frequently employed in copolymers to obtain alkali-soluble polymers. The acids of acrylates are water-soluble. For example, methacrylic acid is more soluble in esters, and to some extent in styrene; because of its angular methyl group; which makes it more useful in copolymerization process, especially if it is water-based [27].

The first report of a polymeric acrylic ester was published in 1877 by Fittig and Paul [28] and in 1880 by Fittig and Engelhorn [29] and by Kahlbaum [30], who observed the polymerization reaction of both methyl acrylates and methacrylates. But, it was a chance to O. Röhm [6] in 1901 to recognize the technical potential of the acrylic polymers. After continuing his work, he got a U.S. patent on the sulfur-vulcanization of acrylates in 1914 [31]. Then in 1924, Barker and Skinner [32] researched and

published the details of the polymerization of methyl and ethyl methacrylates. In 1927

[33], based on the extensive work of Röhm, the first industrial production of polymeric acrylic esters was started by the Röhm & Haas Company in Darmstadt, Germany (since 1971, Röhm GmbH, Darmstadt). After 1934, the Röhm & Haas Co. in Darmstadt was able to produce an organic glass (Plexiglas) by a cast polymerization process of methyl methacrylate [34]. Soon after, Imperial Chemical Industries (ICI, England), Röhm & Haas Co. (United States), and Du Pont de Nemours followed in the production of such acrylic glasses [35].

Acrylic polymers has a first-time usage as an interlining for automobile windshields, but poly(methyl methacrylate) sheet (commercial name Plexiglas, Lucite) soon became the main usage area of acrylic plastics. Poly(methyl methacrylate), chemical Formula with $[-\text{CH}_2-\text{CH}(\text{CH}_3)\text{COOCH}_3-]$, has a light transmittancy of about 92% and has good weathering resistance. It is widely used in aircraft wind shields, bathtubs [36], electron beam or ion beam resistance of them is important in the manufacture of microelectronics such as chips [37,38]. Poly(methyl methacrylate) is used as an automobile lacquer and polyacrylonitrile, $(-\text{CH}_2-\text{CHCN}-)_n$, is used as a fiber. Poly(ethyl acrylate), $(-\text{CH}_2-\text{CHCOOC}_2\text{H}_5-)_n$, is more flexible and has a lower softening temperature than PMMA. Poly(hydroxyethyl methacrylate), is used for contact lenses, and poly(butyl methacrylate) is used as an additive in lubricating oils [36].

The glass transition temperatures of acrylate polymers are generally below room temperature. This means that these polymers are usually soft and rubbery. Solubility in oils and hydrocarbons increases with increasing length of the side group, while polymers become harder, tougher, and more rigid as the size of the ester group decreases. Polyacrylates have been used in finishes and textile sizing and in the production of pressure-sensitive adhesives. Poly(methyl acrylate) is used in fiber modification, poly(ethyl acrylate) in fiber modification and in coatings, and poly(butyl acrylate) and poly(2-ethylhexyl acrylate) are used in paints and adhesive formulation [216]. Whilst esters of acrylic acid give soft and flexible polymers, except for those with long alkyl chains, methyl methacrylate polymerizes to an extremely hard polymers. The polymers in this series become softer with increasing

alkyl chain lengths up to C₁₂. The highest alkyl chain acrylics in both series tend to give side chain crystallization.

Table 2.8 : Glass-transition temperatures (T_g) of some polyacrylates. [216]

R (radical group)	T _g (°C)
Methyl	3
Ethyl	-20
n-Propyl	-44
n-Butyl	-56

The methacrylic ester series closely parallels the acrylics, but boiling points tend to be somewhat higher, especially with the short chain esters. Methyl methacrylate is by far the most freely available and least costly of the monomers of the series. As an alternative to the simple alkyl esters, several alkoxyethyl acrylates are available commercially, e.g. ethoxyethyl methacrylate $\text{CH}_3\text{C}(\text{CH}_3)\text{COOC}_2\text{H}_4\text{OC}_2\text{H}_5$ and the corresponding acrylate. The ether oxygen which interrupts the chain tends to promote rather more flexibility than a simple carbon atom.

Some technical perfluorinated alkyl acrylates are as following they include N-ethylperfluorooctanesulfonamido)ethyl acrylate $\text{C}_n\text{F}_{2n+1}\text{SO}_2\text{N}(\text{C}_2\text{H}_5)\text{-CH}_2\text{O-C(O)-CH=CH}_2$ (n approximately 7.5, fluorine content 51.7 %), the corresponding methacrylate and the corresponding butyl derivatives. The ethyl derivatives are waxy solids, the ethyl acrylate and the corresponding methacrylate derivative having a melting range of 27–42 °C. The butyl acrylic derivative is a liquid, freezing at -10 °C. Butyl acrylate/Methyl methacrylates (BA/MMA), emulsion copolymers are versatile materials extensively used as adhesives (BA homopolymers and BA rich copolymers) and coatings (BA/MMA 50/50 wt/wt copolymers). In spite of their commercial importance, only a few literature reports dealing with the microstructural properties of BA/MMA emulsion copolymers have been published [39].

Polyacrylate elastomers can be prepared by the water emulsion system, suspension system, solvent solution method, or even the mass (bulk homogenous)

polymerization process. Most are made by the water emulsion (latex) or the suspension method. Peroxides or persulfate initiated free radical systems are most commonly used in the presence of heat. Polymerization is usually taken to completion. Coagulation is best with salts, followed by water washing and drying with hot air, vacuum, or extrusion [40].

2.3 Polyacrylonitrile

Poly(propenenitrile), usually known as Polyacrylonitrile, is manufactured from propene via propenenitrile (acrylonitrile). It is very widely used in copolymers, particularly in fabrics and when materials need to be made hard and shock proof.

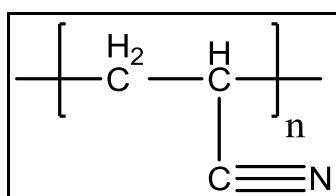


Figure 2.24 : Polyacrylonitrile's repeating unit.

Polyacrylonitrile (PAN) is a vinyl polymerization product of Acrylonitrile (AN) monomer.

Table 2.9 : Properties of Polyacrylonitrile (PAN).

IUPAC Name	poly(1-acrylonitrile)	
Chemical Properties	Empirical Formula	(C ₃ H ₃ N) _x
	Molar Mass	53.0626 g/mol
		C 67.91%, H 5.7%, N 26.4%
Physical Properties	Glass Transition Temperature	~95 °C
	Fusion Temperature	322 °C
	Solubility Parameters	26.09 MPa ^{1/2} (25 °C)
		25.6 to 31.5 J ^{1/2} cm ^{-3/2}
	Density	1.15 g/cm ⁻³
Electronic Properties	Dielectric Constant	5.5 (1 kHz, 25°C)
		4.2 (1 MHz, 25°C)

PAN has taken an increasing interest from the researchers of all kinds of scientific areas because of its superior properties and common usage in many textile and engineering applications. Although it has high stability and color fastness, it is still needed to be strengthened to be used as an efficient functional compound. In textile industry, as long as weaving and knitting machines reached higher working speeds, the higher stress resistance became a more critical requirement for raw materials which were taken under process to turn them into the yarns, fabrics, garments, and all the other kinds of products.

Here in this study, we have chosen PAN as base polymer because of its higher performance/price ratio, its mechanical and chemical stability, and its ease of polymerization and modification.

Polyacrylonitrile (PAN) is a synthetic, semicrystalline organic polymer resin, with the linear formula $(C_3H_3N)_n$. Though it is thermoplastic, it does not melt under normal conditions. It degrades before melting. It melts above 300 °C if the heating rates are 50 degrees per minute or above [197]. Almost all polyacrylonitrile resins are copolymers made from mixtures of monomers with acrylonitrile as the main component. It is a versatile polymer used to produce large variety of products including ultra filtration membranes, hollow fibers for reverse osmosis, fibers for textiles, oxidized PAN fibers. PAN fibers are the chemical precursor of high-quality carbon fiber. PAN is first thermally oxidized in air at 230 degrees to form an oxidized PAN fiber and then carbonized above 1000 degrees in inert atmosphere to make carbon fibers found in plenty of both high-tech and common daily applications such as civil and military aircraft primary and secondary structures, missiles, solid propellant rocket motors, pressure vessels, fishing rods, tennis rackets, badminton rackets & high-tech bicycles. It is a component repeat unit in several important copolymers, such as styrene-acrylonitrile (SAN) and acrylonitrile butadiene styrene (ABS) plastic.

All commercial methods of production of PAN are based on free radical polymerization of Acrylonitrile (AN). Most of the cases, small amount of other vinyl comonomers are also used (1-10%) along with AN depending on the final application [198]. Anionic polymerization also can be used for synthesizing PAN.

For textile applications, molecular weight in the range of 40,000 to 70,000 is used. For producing carbon fiber higher molecular weight is desired.

In the production of carbon fibers containing 600 tex (6k) PAN tow, the linear density of filaments is 0.12 tex and the filament diameter is 11.6 μm which produces a carbon fiber that has the filament strength of 417 kgf/mm^2 and binder content of 38.6%. This data is demonstrated in the Indexes for Experimental Batches of PAN Precursor and Carbon Fibers Made from It table.

Homopolymers of polyacrylonitrile have been used as fibers in hot gas filtration systems, outdoor awnings, sails for yachts, and fiber-reinforced concrete. Copolymers containing polyacrylonitrile are often used as fibers to make knitted clothing like socks and sweaters, as well as outdoor products like tents and similar items. If the label of a piece of clothing says "acrylic", then it is made out of some copolymer of polyacrylonitrile. It was made into spun fiber at DuPont in 1941 and marketed under the name of Orlon. Acrylonitrile is commonly employed as a comonomer with styrene, e.g. acrylonitrile, styrene and acrylate plastics.

PAN absorbs many metal ions and aids the application of absorption materials. Polymers containing amidoxime groups can be used for the treatment of metals because of the polymers' complex-forming capabilities with metal ions [199].

PAN has properties involving low density, thermal stability, high strength and modulus of elasticity. These unique properties have made PAN an essential polymer in high tech.

Its high tensile strength and tensile modulus are established by fiber sizing, coatings, production processes, and PAN's fiber chemistry. Its mechanical properties derived are important in composite structures for military and commercial aircraft [200, 201].

Polyacrylonitrile is used as the precursor for 90% of carbon fiber production [202]. Approximately 20-25% of Boeing and Airbus wide-body airframes are carbon fibers. However, applications are limited by PAN's high price of around \$15/lb, by end of year 2013.

In 2013, researches announced a structural PAN nanofiber that is both strong and tough. Strength refers to a material's ability to carry a load, while toughness is the

amount of energy needed to break it. The researchers used a technique called electrospinning (applying high voltage to a solution until a small jet of liquid ejects). Making the nanofiber thinner made it both stronger and tougher [203, 204].

Electrospun PAN has different effects on the properties of the nanofibers. Depending on the ionic and nonionic surfactants added to the PAN during processing, the properties can be enhanced. With the presence of the anionic surfactant sodium dodecyl sulfate (SDS) during electro spinning, for example, the electron emission from PAN are enhanced [205].

High tacticity PAN has been made with the addition of AlCl_3 . Molecular weight and tacticity have been changed in PAN through atom transfer radical polymerization with the presence of AlCl_3 . This addition of AlCl_3 improved the PAN's isotacticity and narrowed its polydispersity [206].

2.3.1 Uses of Polyacrylonitrile

PAN itself is a very harsh fibre, rather like horse hair. An almost pure homopolymer is used when a very tough fabric is needed, for example for awnings, a soft top of a car or in brake linings. It is even used to reinforce concrete and in road construction. However, the vast majority of the polymer is copolymerized. Although these copolymers often contain more than 85% of acrylonitrile units, they are much softer. The fibres formed from them are known as “acrylic” fibers [41].

Two of the most used acrylic fibres are formed from the copolymerization of Acrylonitrile (AN) with Ethenyl ethanoate (Vinyl acetate - VAc); and, AN with Methyl propenoate (Methyl acrylate - MA). The former is often mixed with cotton fibres to produce a light fabric, used in women's clothes. The latter is often used with wool (Figure 2.25).

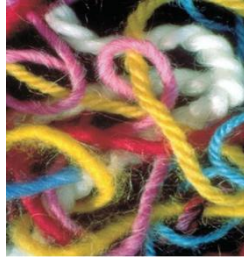


Figure 2.25 : The copolymer of AN and MA is a wool substitute and is often mixed with wool itself for heavier fabrics, used in pullovers and jumpers and in suits.

The copolymers with phenylethene (styrene) known as SAN and with butadiene and phenylethene, known as ABS, are plastics which are very strong and able to withstand shocks.



Figure 2.26 : The high heels are made from a blend of ABS and a Polyamide which is very strong.

The copolymers with phenylethene (styrene) known as SAN and with butadiene and phenylethene, known as ABS, are plastics which are very strong and able to withstand mechanical shocks.

Other copolymers of AN include those when the comonomer is methyl 2-methylpropenoate (methyl methacrylate) and with 1,1-dichloroethene.

With 1,1-dichloroethene as the co-monomer, a block copolymer is formed which is fire-resistant and is often used in children's clothing.

An increasing use of PAN copolymers is in producing carbon fibres. If fibres of the polymer are heated under strictly controlled conditions the resulting fibres have remarkable strength [41].

Table 2.10 : Annual production of Acrylonitrile.

World	5.9 million tonnes
Europe	1.8 million tonnes
US	1.2 million tonnes

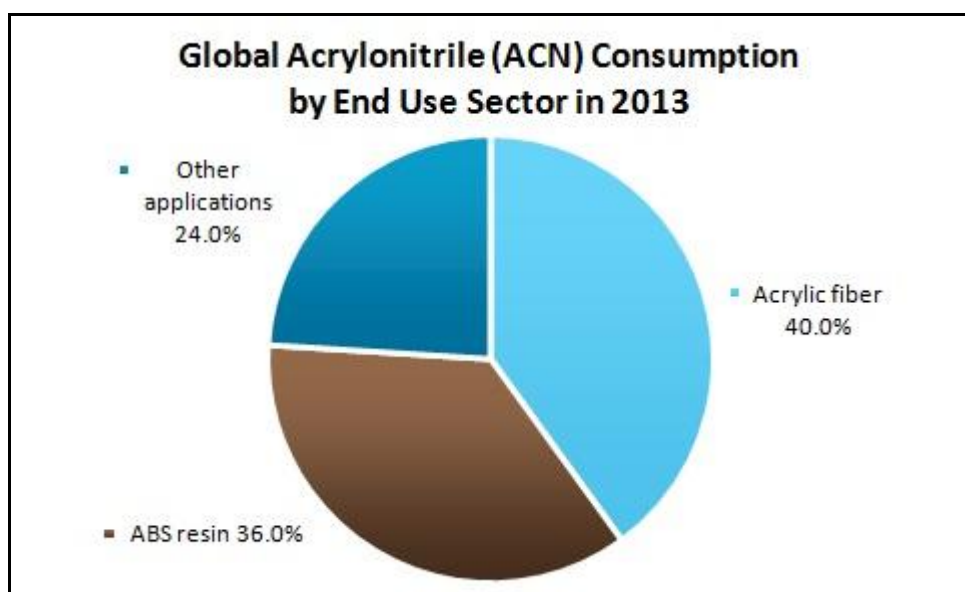


Figure 2.27 : Global consumption of Acrylonitrile by end use in year of 2013.

Acrylonitrile is used in production of acrylic fibres, acrylonitrile-butadiene-styrene (ABS), styrene-acrylonitrile (SAN) and nitrile-butadiene-rubber (NBR). Today capacity utilization rate stands at near 85%, but is expected to grow and reach 91% by 2017. In the near future new capacities are expected to be added in China, Iran and Saudi Arabia. By adding new ACN plants China aims to become more self-sufficient and less dependent on import [214].

Global acrylonitrile market is expected to grow at 4% per year, driven mainly by ABS resins. Asia Pacific will still be the leader in acrylonitrile consumption with growth rate of ~5%, while Europe and North America will show more moderate growth.

2.3.2 Production of Polyacrylonitrile

2.3.2.1 Acrylonitrile

Acrylonitrile (propenoane), the monomer, is produced from propene. The alkene is mixed with ammonia and oxygen (from air) (1:1:2 volume ratio) and passed over a mixture of bismuth(III) and molybdenum(VI) oxides:

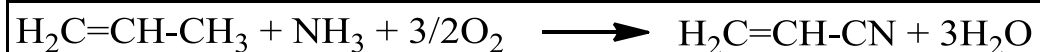


Figure 2.28 : Reaction to produce Acrylonitrile (AN) monomer.

As it is a very exothermic reaction, and the temperature must be controlled at 237 °C, a fluidized bed reactor is used. A small amount of hydrogen cyanide (3-6%) is also formed, which can be used in the manufacture of methyl methacrylate. The process has been modified, in Japan, to use propane as the feedstock. It will become particularly important if propane becomes much cheaper than propene. The catalyst used is based on vanadium(V) and antimony(III) oxides [34,41].

2.3.2.2 Polyacrylonitrile

The polymer is manufactured by radical polymerization initiated by either a peroxide or by a mixture of potassium peroxydisulfate, $\text{K}_2\text{S}_2\text{O}_8$ and a reducing agent such as potassium hydrogensulfite, KHSO_3 . About equal amounts of the stereoregular polymer, isotactic and syndiotactic, are produced. The polymerization is either in solution or as a slurry [36,41].



Figure 2.29 : The soft tops for high quality cars are produced from almost pure homopolymer of PAN.

2.3.2.3 Polyacrylonitrile-based copolymers

Polymerization takes place as for the homopolymer, a radical polymerization. The two monomers are mixed prior to addition of the initiator. When, ethenyl ethanoate is used as the copolymer, polymerization is initiated with small amounts of potassium hydrogensulfite and potassium peroxydisulfate incorporated into the copolymer, giving it sites which can bind to colorants and make them with better fastness. Alternatively, a small amount of a third monomer containing, for example a sulfonic acid group, serves the same purpose [35-37].

The copolymer contains a more or less regular alternation of the individual monomers, an example of an alternating copolymer [41].

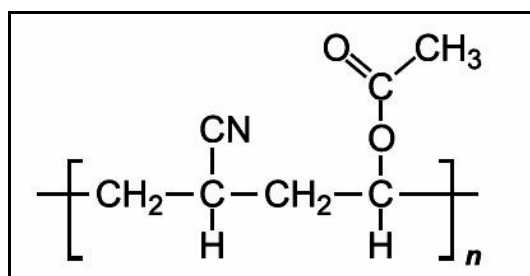


Figure 2.30 : Acrylonitrile-Vinyl acetate copolymer.

Similar procedures are used when other comonomers are used. With Methyl acrylate and Methyl methacrylate, block copolymers are produced [42]:

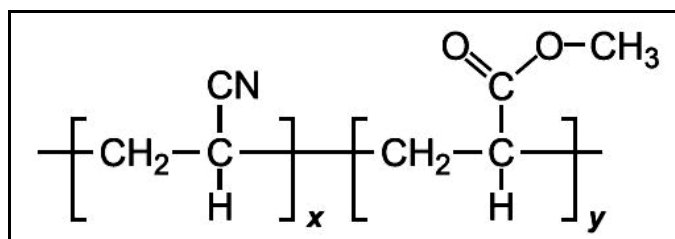


Figure 2.31 : Acrylonitrile-Methyl acrylate copolymer.

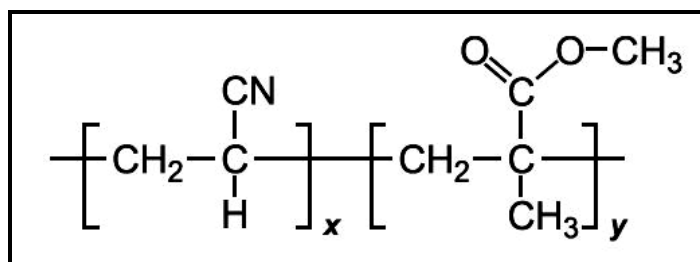


Figure 2.32 : Acrylonitrile-Methyl methacrylate copolymer.

An alternating polymer is produced with 1,1-dichloroethene as the comonomer.

Polyacrylonitrile (PAN) and copolymers of PAN have been widely studied for almost a century for commercial/technological exploitations. PAN may be crosslinked, but also may exist without crosslinking. Crosslinking of PAN will impart some of its important physical properties, such as insolubility and resistance to swelling in common organic solvents. Recently, considerable efforts have been devoted to its processing and fiber forming technologies. Among the various precursors for producing carbon nanofibers (CNFs), PAN is the most commonly used polymer, mainly due to its high carbon yield (up to 56%), flexibility for tailoring the structure of the final CNF products and the ease of obtaining stabilized products due to the formation of a ladder structure via nitrile polymerization [43-47].

Even though acrylonitrile (AN) was known as far back as 1893, but PAN, because of difficulties in dissolving it for spinning, no progress was made in converting into a usable fiber until 1925. Acrylonitrile monomer was also useful as a copolymer with styrene, especially in a terpolymer with styrene and butadiene, known as ABS rubber. The homopolymer of PAN was developed for manufacturing of fibers in 1940, after a suitable solvent was discovered by DuPont. PAN is soluble in polar solvents like DMF, DMSO, DMAc, Dimethylsulfone, Tetramethylsulfide and aqueous solutions of Ethylene carbonate, as well as some mineral salts. PAN forms saturated solution with 25% dissolved in DMF at 50°C, which is high solubility compared to other solvents [22]. PAN and its copolymers are predominantly white powders up to 250°C, at which point they become darker due to degradation. Having a relatively high T_g, these polymers have low thermal plasticity and cannot be used as a plastic material. The high crystalline melting point (317°C) of PAN, its limited solubility in certain solvents coupled with superior mechanical properties of its fibers is due to intermolecular forces between the polymer chains. Appreciable electrostatic forces occur between the dipoles of adjacent CN groups and this intramolecular interaction restricts the bond rotation, leading to a stiffer chain [48].

PAN-based CNFs are seemingly a new class of materials used in a wide array of applications including filtration barriers, material reinforcements, garments, insulators, medical and energy storage devices, and many more. However, their unique properties make them perfect modern materials of choice across many

disciplines covering engineering, medicine, and biology. The accelerating technologies of producing PAN-based nanofibers have now matured enough to overcome the drawbacks of low production rate of few grams per hour in laboratory environments to large industrial scale production. Nanofiber membranes comprising sheets of randomly oriented nanofibers show an extremely effective removal method with a high rejection rate of airborne particles by both physical trapping and adsorption. It is anticipated that the future will witness many more applications of PAN-based nanofibers in a wide variety of scientific disciplines. [49]

2.4 Butyl Acrylate

The acrylates are clear, colorless, volatile liquid with a slight solubility in water and complete solubility in alcohols, ethers and many organic solvents[315]. Methacrylate esters are used to make polymers for textiles, latex paints, surgical cements and dental resins. It can be used as a copolymer in the process of polymerization of polyanionic cellulose (PAC) polymers, to reduce the glass transition temperature of the PAC polymers. Its linear formula is $\text{CH}_2=\text{CHCOO}(\text{CH}_2)_3\text{CH}_3$. It has boiling point $147\text{ }^\circ\text{C}$ at 760 mmHg and have melting point about $-64\text{ }^\circ\text{C}$. Although the monomer can be polymerized under the influence of heat, light, ionic or high energy mechanisms, free radical initiation is the most commonly used method of polymerization. The skeletal formula of Butyl acrylate is shown in Figure 2.33.

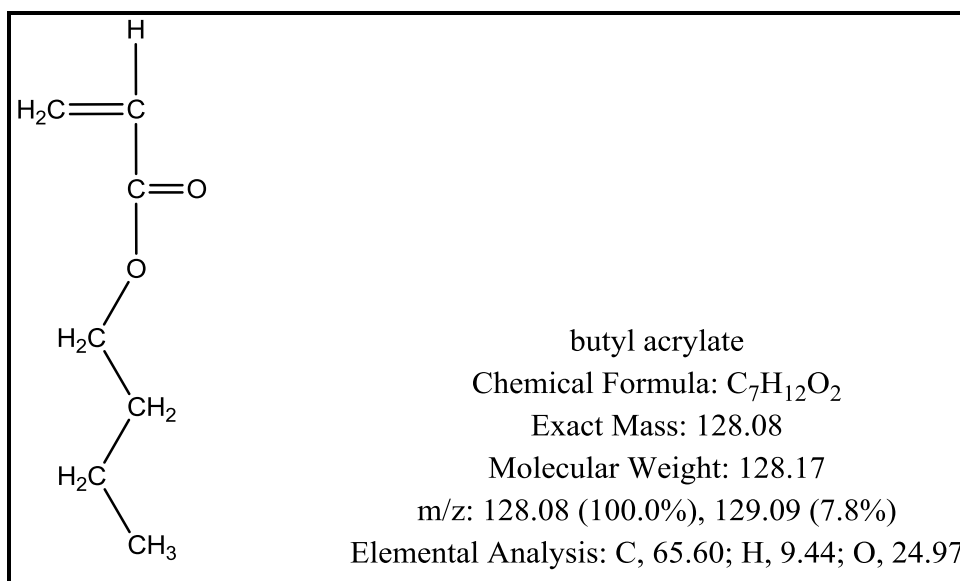


Figure 2.33 : Skeletal formula of Butyl acrylate and its basic properties.

It exists in forms of butyl acrylate copolymer and homopolymer. Since the bulk polymer is very soft, sticky hair serious state colorless transparent rubber material. The glass transition temperature is -55°C . $1.08\text{g}/\text{cm}^3$ density. Refractive index of 1.474. 2000% elongation. Low intensity. similar to the solubility of polypropylene. Commonly used for acrylate rubber substrate. Emulsion polymers and polymer solution for the general copolymer. Using butyl acrylate as the main component of the copolymer emulsion, as a good "soft monomer" component, results a film which is soft, feels good, better resistance to cold. Applicable to make fabric and leather processing agent. Butyl acrylate is a volatile chemical compound classified as a butyl ester. It has a strong characteristic odor and is used in the preparation soft base acrylic polymers. The product is highly demanded for making different industrial products. Moreover, this chemical compound is a flammable, water insoluble, colorless liquid and possess the property to mix with most organic solvents. Butyl acrylate is used in the production of coatings, elastomers, adhesives, thickeners, amphoteric surfactants, fibers, plastics, textiles and inks.. Butyl acrylate is also used in chemical synthesis. When used in latex paint formulations acrylic polymers have good water resistance, low temperature flexibility and excellent weathering and sunlight resistance [315].

2.5 Conductive Polymers

Materials can be classified into two main groups regarding to their behavior about electron move through them; insulator materials and conductive materials. While the insulators do not let electron transfer through their body, the conductive materials behave vice versa. Conductivity equation is simply described by Ohm's Law as $V = IR$. Where R is the resistance, I the current and V the voltage present in the material. The conductivity of a material depends on the number and the mobility of its charge carriers (number of electrons). In a metal it is assumed that all the outer electrons are free to carry charge and the impedance to flow of charge is mainly due to the electrons bumping into each other. If an electron moves toward neighbor electrons, they move away, and this creates a chain of interactions propagating through the material. Insulators however have tightly bound electrons, therefore nearly no electron flow occurs, and as consequence they show high resistance to charge flow. In shorter terms, for the conductivity, the free electrons are needed [52].

Most the polymers are good insulators by their nature, as they do not have free valance electrons as in metals, so they were all known as insulators. The discovery that the conductivity of conjugated organic polymers can be controlled through oxidation or reduction led to materials combining the electronic properties of metals with the weight and density of plastics. For this reason, such materials have been studied extensively and their importance recognized with the awarding of the 2000 Nobel Prize in chemistry to Alan Heeger, Alan MacDiarmid, and Hideki Shirakawa for their polyacetylene work beginning in the 1970s. While these studies produced the most dramatic results, investigations of electrically conductive conjugated polymers date back to the early 1960s, particularly with the work of Donald Weiss on polypyrrole, as well as that of René Buvet and Marcel Jozefowicz on polyaniline. The discovery of conductive polymers was a unique and incredible discovery which showed a possible substitute for metallic conductors and semiconductors. Although conducting polymers have been known for at least 25 years (reports on the synthesis date back to the last century), the date was only in the early 1990s, that a tidal wave of renewed and amplified interest in these materials has catalysed many new developments, both on a fundamental level as well as from the manufacturing side. In particular, the discovery of light-emitting polymers in 1990, in the Cavendish Laboratory at Cambridge University, was a major if not the turning point in the fortunes of plasronics, i.e. the use of polymeric materials as substitute for metal and their derivatives in electronic devices [217].

The efforts forhaving a tailor-made polymer in respect of its electrical, mechanical, optical and thermal properties have been pursued by several research groups. But still, serious problems like oxidative stability and device lifetimes have to be overcome.

There are mainly two conditions for a polymer to become conductive;

a. The first condition is that the polymer has to have alternating single and double bonds, called conjugated double bonds. In conjugation mechanism, the bonds between the carbon atoms alternately distributes as single and double bonds. Each bond contains a “sigma” (σ) bond which forms a strong chemical bond. In addition, every double bond contains a weaker “pi” (π) bond [54].

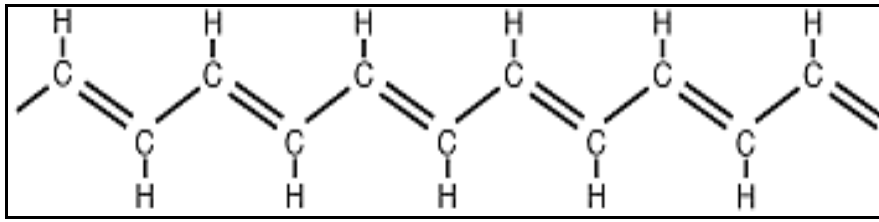
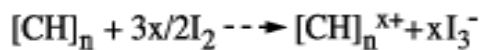


Figure 2.34 : “sigma” (σ) and “pi” (π) bonds in Polyacetylene molecular chain.

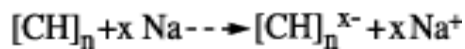
b. The second condition is that the plastic has to be disturbed - either by removing electrons from (oxidation), or inserting them into (reduction), the material. This process is known as “Doping”.

There are two types of doping:

- Oxidation with halogen (or p-doping).



- Reduction with alkali metal (called n-doping).



Conductive polymers can be classified into three main groups according to their conducting mechanisms [51]:

a. Electron-conducting polymers

b. Proton-conducting polymers

c. Ion-conducting polymers

All these types of conductive polymers found a wide-range use in many applications such as optical, i.e. electrochromic film applications for automobile glasses, conductive compounds for optical devices; electronic, i.e. batteries, displays, plastic wires, optical signal processing, data storage, solar energy conversion; chemical, i.e. anti-corrosion coatings, antistatic agents, gas-sensors; mechanical, i.e., conductive adhesives, micro/nano actuators, molecular robotic devices; biological, biocompatible and/or bioactive polymeric frames for cellular immobilization/growth,

robotic body implants; and textiles, electromagnetic shielding applications, antistatic cloths, sensor-integrated smart-textile applications.

Three simple carbon compounds are diamond, graphite and polyacetylene. They may be regarded as three- two- and one-dimensional forms of carbon materials. Diamond, which contains only σ bonds, is an insulator and its high symmetry gives it isotropic properties. Graphite and acetylene both have mobile π electrons and are, when doped, highly anisotropic metallic conductors.

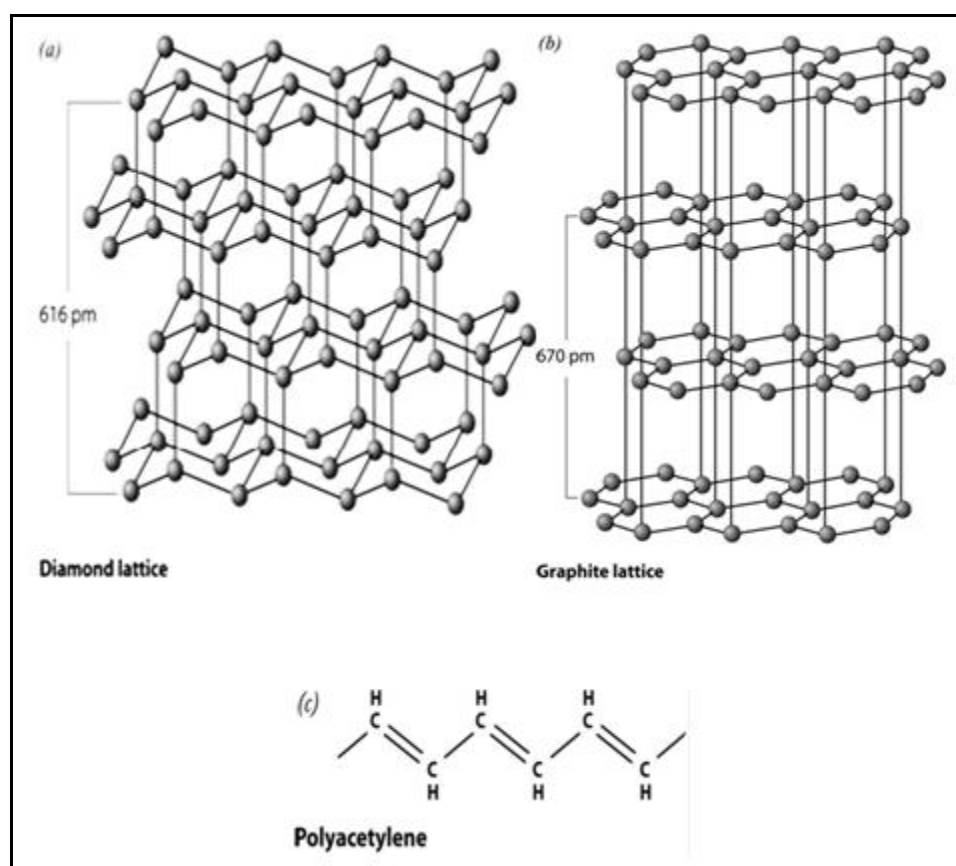


Figure 2.35 : Structural schemes of (a) Diamond, (b) Graphite, and (c) Polyacetylene.

Polymers are molecules that form long chains, repeating themselves. In becoming electrically conductive, a polymer has to imitate a metal, which means, its electrons need to be free to move and not bound to the atoms [53]. Polyacetylene is the simplest possible conjugated polymer. It is obtained by polymerization of acetylene, simply shown in Figure 2.36.

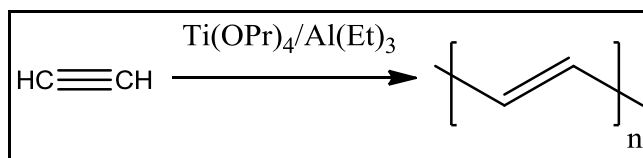


Figure 2.36 : Acetylene's polymerization.

Ionic electroactive polymers (EAP) are conductive polymers that feature a conjugated backbone (they include a backbone that has an alternating series of single and double carbon-carbon bonds, and sometimes carbon-nitrogen bonds, i.e. π -conjugation) and have the ability to increase the electrical conductivity under oxidation or reduction. For polymers allows freedom of movement of electrons, therefore allowing the polymers to become conductive. The pi-conjugated polymers are converted into electrically conducting materials by oxidation (p-doping) or reduction (n-doping).

The volume of these polymers changes dramatically through redox reactions at corresponding electrodes through exchanges of ions with an electrolyte. The EAP-containing active region contracts or expands in response to the flow of ions out of, or into, the same. These exchanges occur with small applied voltages and voltage variation can be used to control actuation speeds in a electro-mechanical device with a built-in EAP actuator [1-16,63,82,284].

The main examples of p-doped conductive polymers include, but are not limited to, polypyrroles, polyanilines, polythiophenes, polyethylenedioxythiophenes, poly(p-phenylenes), poly(p-phenylene vinylene)s, polysulfones, polypyridines, polyquinoxalines, polyanthraquinones, poly(N-vinylcarbazole)s and polyacetylenes, with the most common being polythiophenes, polyanilines, and polypyrroles [241-250]. Some of the structures are shown in Figure 2.37.

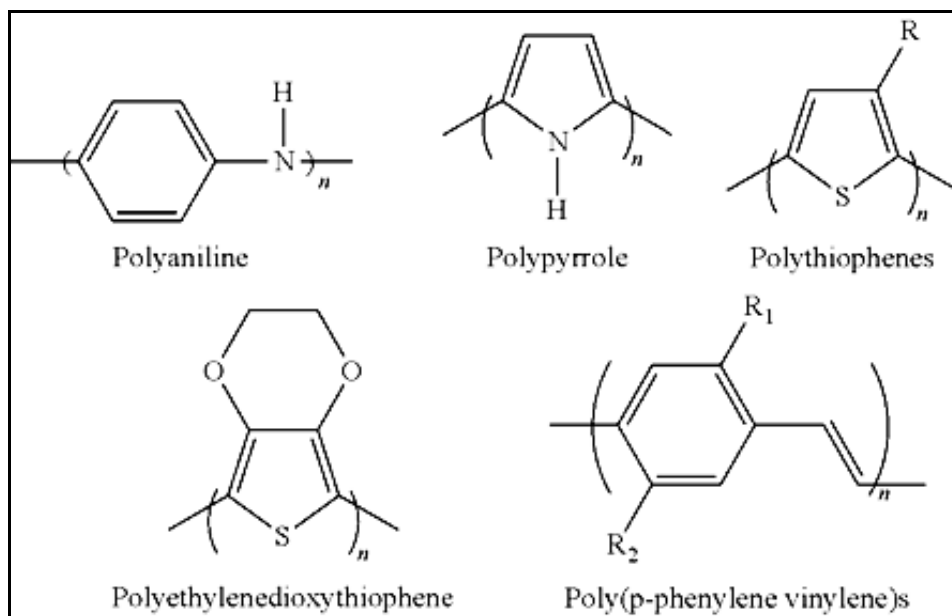


Figure 2.37 : Some of the p-doped conductive polymers.

Polypyrrole, shown in more detail below, is one of the most stable of these polymers under physiological conditions:

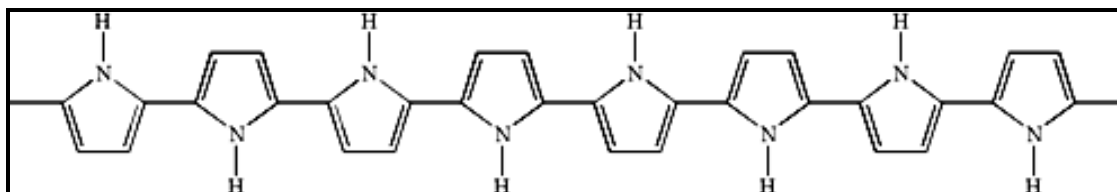


Figure 2.38 : The most stable of p-doped polymers is Polypyrrole (PPy).

The behavior of conjugated polymers is dramatically altered with the addition of charge transfer agents (dopants). These materials can be oxidized to a p-type doped material by doping with an anionic dopant species or reducible to an n-type doped material by doping with a cationic dopant species. Generally, polymers such as PPy are partially oxidized to produce p-doped materials:

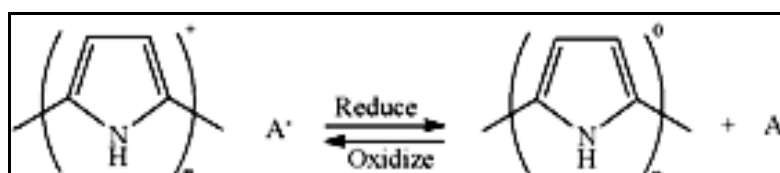


Figure 2.39 : Reduction-oxidation of PPy.

Dopants have an effect on this oxidation-reduction scenario (Figure 2.39), and convert semi-conducting polymers to conducting versions close to metallic

conductivity in many instances. Such oxidation and reduction are believed to lead to a charge imbalance that, in turn, results in a flow of ions into or out of the material. These ions typically enter/exit the material from/into an ionically conductive electrolyte medium associated with the EAP.

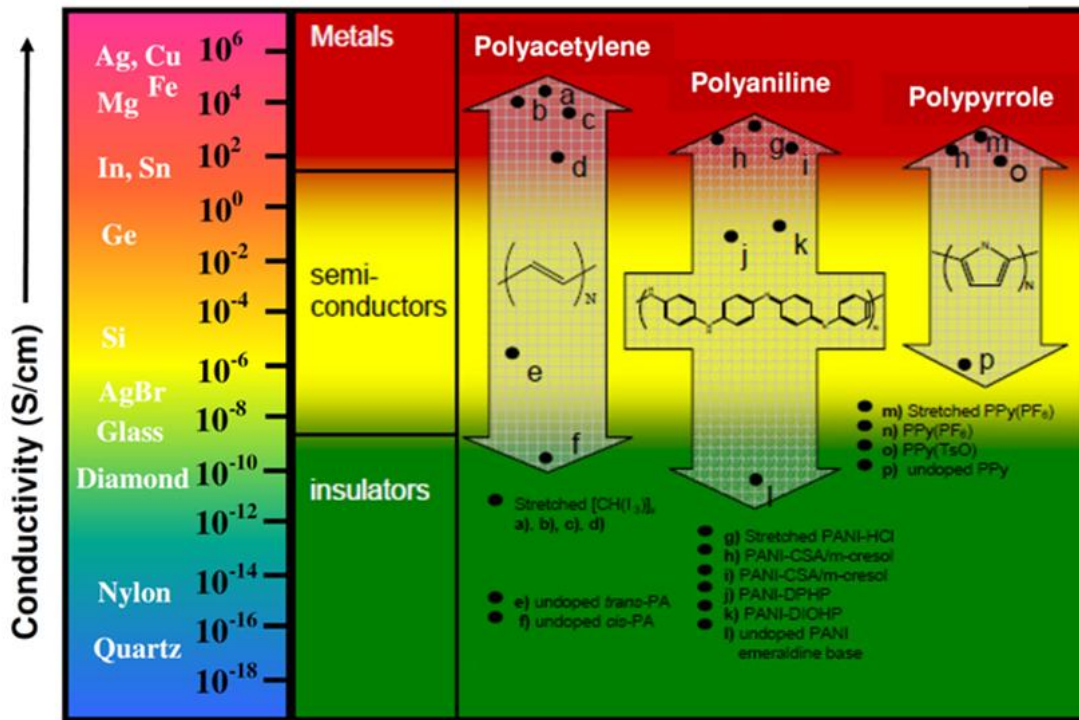


Figure 2.40 : Electron-conducting polymers.

The halogen doping process transforms polyacetylene to a good conductor. Oxidation with iodine causes the electrons to be jerked out of the polymer, leaving "holes" in the form of positive charges that can move along the chain (Fig 2.41).

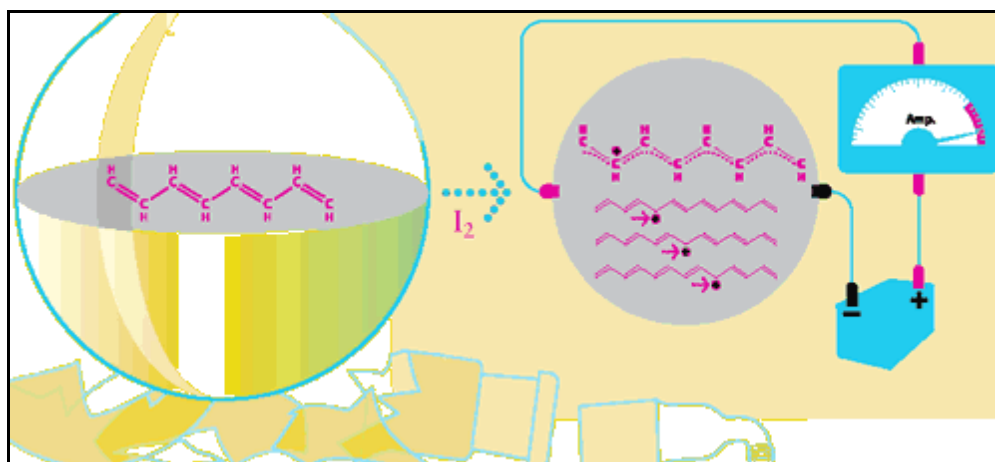


Figure 2.41 : Doping process of Polyacetylene with Iodine.

The iodine molecule attracts an electron from the polyacetylene chain and becomes I_3^- . The polyacetylene molecule, now positively charged, is termed a radical cation, or “polaron”. The lonely electron of the double bond, from which an electron was removed, can move easily. As a consequence, the double bond successively moves along the molecule. The positive charge, on the other hand, is fixed by electrostatic attraction to the iodide ion, which does not move so readily [55-57].

For a better molecular performance, the doping process is an important necessity. For example, doped polyacetylene is comparable to good conductors such as copper and silver, whereas in its original form it is a semiconductor.

Figure 2.40 and 2.42 show the conductivity levels of conductive polymers compared to those of other materials, from quartz (insulator) to copper (conductor) [317]. Polymers may also have conductivities corresponding to those of semiconductors.

Factors that effect the conductivity of polymers are; density of charge carriers, mobility of charge carriers, the direction, the presence of doping materials (additives that facilitate the polymer conductivity), and the temperature.

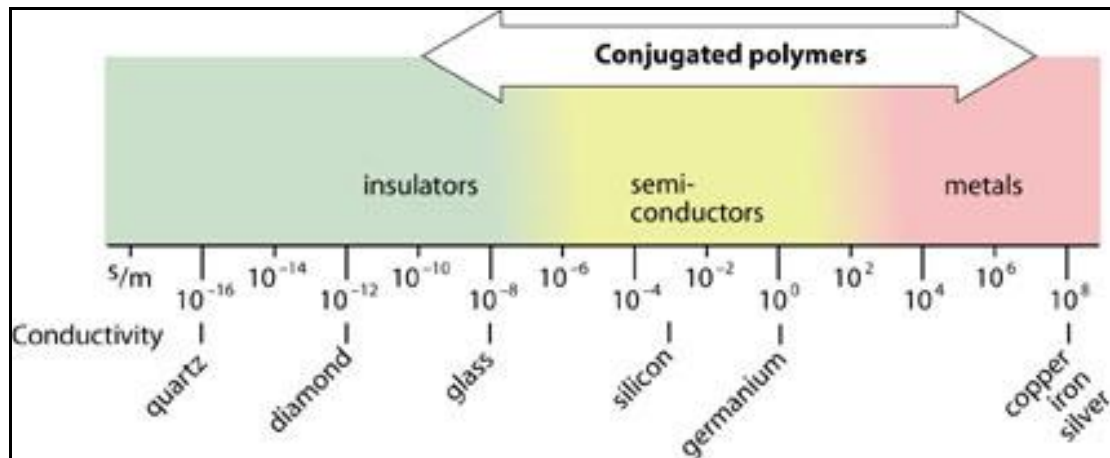


Figure 2.42 : The conductivity levels of various materials.

The conductivity of conductive polymers decreases with falling temperature in contrast to the conductivities of typical metals, e.g. silver, which increase with falling temperature [58].

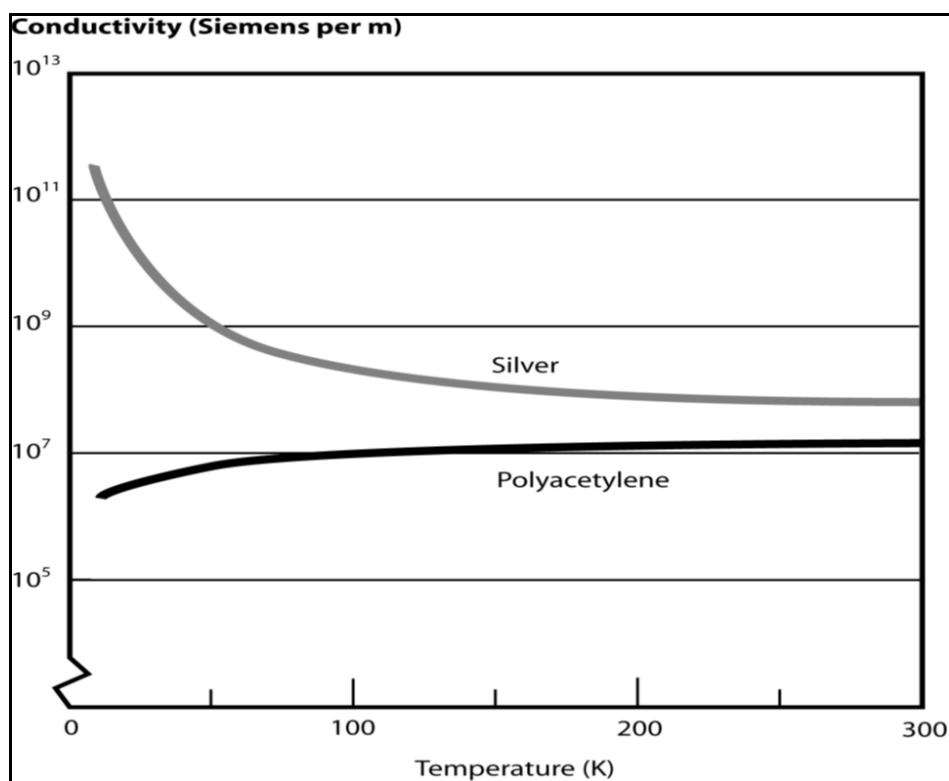


Figure 2.43 : The effect of temperature change on conductive polymer.

A main aspect in this relatively new but large literature is to obtain films of conductive polymers. Generally, potentiostatic conditions are recommended to obtain thin films, while galvanostatic conditions are recommended to obtain thick films. The electrochemical technique has received wider attention both because of the simplicity and the added advantage of obtaining a conductive polymer being simultaneously doped. Besides this, a wider choice of cations and anions for use as dopant ions is available in the electrochemical polymerization process. Free-standing as well as self-supporting conductive polymer films of desired thickness or geometry can be obtained. Using this novel technique, a variety of conductive polymers like polypyrrole, polythiophene, polyaniline, polyphenylene oxide pyrrole and polyaniline/polymeric acid composite have been generated. Pyrrole in aqueous acetonitrile solvent containing tetraethyl ammonium tetra-fluoroborate was electropolymerized in a two-electrode electrochemical cell. Polypyrrole containing the BF_4^- ion (dopant) was obtained as a film deposited on the platinum electrode surface [59, 60].

The polymers were thought of as electrical insulators until the discovery that iodine-doped polyacetylene (which was already described on previous pages of thesis)

exhibited electrical conductivity many orders of magnitude higher than neutral polyacetylene. This discovery was published [61], and as a result of this pioneering work, the researchers received the 2000 Nobel Prize in Chemistry. The development of this new class of polymeric materials continues to offer the promise of a wide range of novel applications including molecular electronics [62], actuators [63], electrochromic windows/displays [64], supercapacitors [65], transistors [66], photovoltaics [67] and corrosion protection [68]. This discovery opened up new areas of research with many commercial products now incorporating polymers as electrical conductors [69]. CPs consist of conjugated chains containing p-electrons delocalized along the polymer backbone. In their neutral form, CPs are semiconductive materials that can be doped and converted into electrically conductive forms. The doping can be either oxidative or reductive, though oxidative doping is more common. There are three states of CPs: non-conducting (uncharged), oxidized (p-doped) where electrons are removed from the backbone, and the reduced (n-doped) (least common), where electrons are added to the backbone. The doping processes are usually reversible, and typical conductivities can be switched between those of insulators ($0 - 10^{-10}$ S/cm) and those of metals (10^5 S/cm) [70].

Until about 30 years ago all carbon based polymers were rigidly regarded as insulators. The notion that plastics could be made to conduct electricity would have been considered to be absurd. Indeed, plastics have been extensively utilized by the electronics industry for their insulating property. They were all used as inactive packaging and insulating materials. This very narrow perspective is rapidly changing as a new class of polymers known as intrinsically conductive polymers or electroactive polymers are being discovered. Although this class of polymer is in its infancy, much like the plastic industry was between the 1930's and 50's, the potential uses of these polymers are quite significant [71, 72]. The first conducting plastics were discovered by accident at the Plastics Research Laboratory of BASF in Germany. When they made polyphenylene and polythiophene while they were attempting the oxidative coupling of aromatic compounds, they noticed that these polymers showed electrical conductivities, up to 0.1 S/cm [215].

The applications of conductive polymers can be classified mainly under two groups, as it is shown in Table 2.9. While the first group of applications use their

conductivity as main property, the second group utilizes their electroactivity. π -conjugated polymers are quite sensitive to electrochemical oxidation and reduction effects, and these processes drastically change the optical and electrical properties of the polymer. As a result, it is possible to precisely control these properties of a π -conjugated polymer, even between a conducting state and an insulating state, by controlling oxidation and reduction, since these are often reversible reactions [62,76,143,159,186,276,282,284].

Table 2.11 : The applications of conductive polymers.

Conductive Polymers	Electroactive Polymers
Electrostatic materials	Molecular electronics
Conducting adhesives	Electrical displays
Electromagnetic shielding	Chemical, biochemical and thermal sensors
Printed circuit boards	Rechargeable batteries
Artificial nerves	Drug release systems
Antistatic clothing	Optical computers
Piezoceramics	Ion exchange membranes
Active electronics (diodes, transistors)	Electromechanical actuators
Aircraft structures	"Smart" structures
	Actuators-Switches

Uses of conductive polymers

This applicational group uses the basic property of conductivity of polymeric materials, such as coating an insulator with a very thin layer of conducting polymer, therefore having ability to prevent the build-up of static electricity. Such an end-use is especially important where such an electrical-discharge is hazardous, for instance, in an environment with flammable gasses and liquids, or in the explosives industry. In the electronics industry, a sudden discharge of static electricity can damage microcircuits. This problem gained high importance in recent years with the development of modern integrated circuits, i.e. decreasing sizes of components and the production technique which already minimized to nanometric scale. Also, in such microcircuits, to increase processing-speed and to reduce power consumption of the system, junctions and connecting lines are getting much finer and closer to each other. Thus, modern circuits are more sensitive, and can be easily damaged by static discharge even at a very low voltage. As a solution to this problem, modifying the thermoplastic material used for casing by adding a suitable amount of conducting

polymer into the resin results in a composite plastic material that can be used for the protection against electrostatic discharge [73].

Conductive adhesives are used to join two or more pieces of electrically conductive objects together by sticking and also allowing electric current passing through them. Such a system requires applying monomer between the conducting surfaces which were desired to be stucked and allowing it to polymerize between them.

Most of the electrical devices, especially computers, tablet-PCs and cellular phones, they all generate electromagnetic radiation, often at a range of radio and microwave frequencies. This can cause interference, therefore malfunctions in nearby electrical devices. Here the electromagnetic-shielding materials are subject to solve such a problem. The plastic cases used in many of these electrical devices are transparent to electromagnetic radiation. This radiation can be adsorbed by an electrically conductive surface coated the inside of casing. Conductive polymers are the best alternatives for such an application, as they can be easily and cost-effectively applied, and be well working even if it is applied as a very thin layer of a wide range of resin-types. Such a coating has good adhesion, gives a good coverage, thermally expands approximately the same as the polymer it is coating, needs just one-step and gives a good thickness [74].

The printed circuit boards are used in manufacture of almost all electrical devices. These are made of copper-coated epoxy-resins. To connect the multiple components to each other in order to produce a working system, on such a board the copper is selectively etched to produce conducting lines. All the components on a board are placed in holes specially cut into the resin material. To get a good electrically-connection between the hole surface and the placed component, these holes need to be lined with a conductive material. In conventional method, surface of these holes were lined by electroless copper plating, which has several problems such as its expense of a multistage production and poor-adhesion onto resin material of the board. Today, this process is already replaced by appliance of a conductive polymer as interfacial material. For instance, if the board is etched with potassium permanganate solution a thin layer of manganese dioxide is produced only on the surface of the resin. This will then initiate polymerization of a suitable monomer to

produce a layer of conductive polymer. This new method is much cheaper, easy and quick to apply, is very selective and has very good adhesion [75].

Some biocompatible conductive polymers can act as artificial nerves, i.e. they may be used to transport small electrical signals through the body. It can be even considered to achieve modifications to the human-brain by such biological applications of conductive polymers, as a vision for future [76].

For spaceships and airplanes, weight is extremely important. It is much more attractive to use polymers with a density of about 1 g/cm^3 rather than 10 g/cm^3 for metals. Moreover, the power ratio of the internal combustion engine is about 676.6 watts per kilogramme. This compares to 33.8 watts per kilogramme for a battery-electric motor combination. A drop in weight could give similar ratios to the internal combustion engine [77]. Modern airplanes are already made of light-weight composites, which makes them much lighter, but also vulnerable to damage from lightning bolts. Coating exterior surface of an airplane with a conductive polymer, the vulnerable internals can be protected by directing the electrical charge away.

Uses of electroactive polymers

Conducting polymers can be used to produce a molecular electronic system which is an electronic structure assembled atom by atom. For this application, a modified polyacetylene with an electron accepting group (acceptor) at one end and a withdrawing group (donor) at the other, can be used. A short section which is known as a “spacer” or “modulable barrier” of the chain should be saturated in order to separate the functional groups from each other (Figure 2.44). Such a structure can be used to create a logic device. There would be two inputs, one light pulse which excites one end and another which excites the modulable barrier. There is one output, a light pulse to see if the other end has become excited. [78].



Figure 2.44 : Insertion of a “spacer” to separate the donor and acceptor (functionalized chain ends).

Today's electrical displays require materials with faster response and higher contrast. Conductive polymers are really very good materials to produce display panels. Depending on the chosen conductive polymer, the doped and undoped states can be either colourless or intensely coloured. However, the colour of the doped state is greatly red-shifted from that of the undoped state. The colour of doped state can be varied by using dopant ions that absorb in visible light. Because conductive polymers are intensely coloured, even a very thin layer is enough for display panels with a high contrast and large viewing angle. Unlike liquid crystal displays (LCD), the image formed by redox of a conductive polymer can have a high stability even in the absence of an applied field. The switching time (refresh rate) achieved with such systems has been as low as about 2 ms. The cycle lifetime is generally about 10^6 cycles. Experiments are already being done to try to increase cycle lifetime to above 10^7 cycles [79].

Conductive polymers are very useful to produce sensors, because of their chemical properties. Due to the drastically change in their electrical properties during reaction with various redox agents (dopants), or via their instability to moisture and heat; they give chance to use this change as an indicator and to form it into an electronic signal. The gas sensors are good examples of such an application, using this principle. It has been shown that, PPy behaves as a quasi 'p' type material. The electrical resistance of PPy increases when a reducing gas such as ammonia interacts its surface, and decreases in the presence of an oxidizing gas such as nitrogen dioxide. The gases cause a change in the near surface charge carrier (here electron holes) density by reacting with surface adsorbed oxygen ions. Another type of sensor developed is a biosensor that utilizes the ability of triiodide to oxidize polyacetylene as a means to measure glucose concentration. Glucose is oxidized with oxygen with the help of glucose oxidase. This produces hydrogen peroxide which oxidizes iodide ions to form triiodide ions. Therefore, conductivity is proportional to the peroxide concentration which is proportional to the glucose concentration [80].

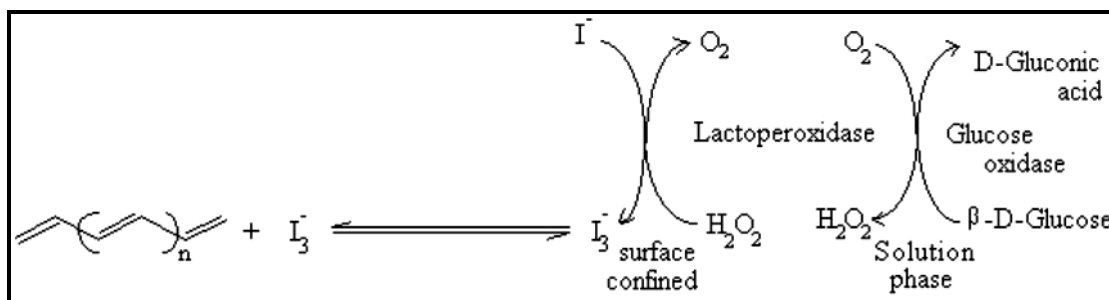


Figure 2.45 : Application of Polyacetylene to a glucose sensor.

Because of modern life-style and mobile electronic devices, maybe the most effective and highly anticipated application is producing the rechargeable batteries with lighter in weight. Lithium-ion and some lithium-polymer cells are comparable to, or better than nickel-cadmium cells now already on the market.

The polymer battery, such as a polypyrrole-lithium cell operates by the oxidation and reduction of the polymer backbone. During charging process, the polymer oxidizes, and anions in the electrolyte enter the porous polymer to balance the charge created; and the lithium ions in electrolyte are electrodeposited at the lithium surface. During discharging (while usage) of the battery, the electrons are removed from the lithium, causing lithium ions to reenter the electrolyte and to pass through the load and into the oxidized polymer. The positive sites on the polymer are reduced, releasing the charge-balancing anions back to the electrolyte. This process can be repeated about as often as a typical secondary battery cell [81].

In Figure 2.46, a recently developed ultracapacitor design is shown. These electrodes are helpful in designing electrochemical capacitors that combines the battery's high energy density and the capacitor's power performance, paving the way to advance energy storage technology. The research team showed the high-performance electrochemical capacitors made of graphene. These electrochemical capacitors, also called as ultracapacitors or supercapacitors, retain superior electrochemical qualities even under high mechanical stress, making them suitable for high-power flexible electronics [323].

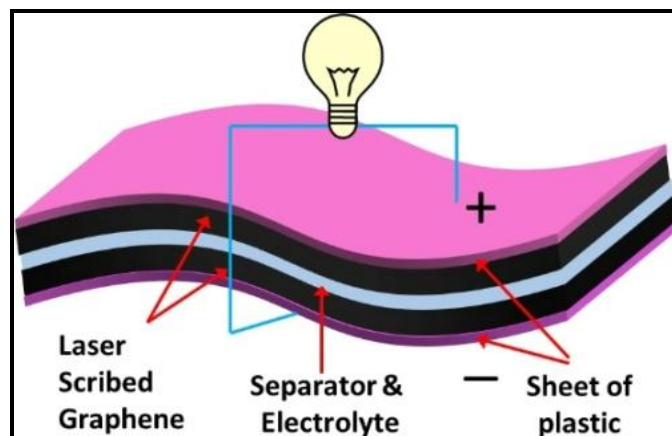


Figure 2.46 : An application of laser scribed graphene ultracapacitor.

Conducting polymers are able to do mimics when they vary their states as doped and undoped, thus, they can be used to directly convert the electrical energy into the mechanical energy. Such a system utilizes large changes that can be as large as 10% in size undergone during the doping and dedoping of many conducting polymers. Electrochemical actuators can function by using changes in a dimension of a conducting polymer, changes in the relative dimensions of a conducting polymer and a counter electrode and changes in total volume of a conducting polymer electrode, electrolyte and counter electrode. The method of doping and dedoping is very similar to that used in rechargeable batteries, and requires the anodic strip and the cathodic strip changing size at different rates during charging and discharging. The applications of this include microtweezers, microvalves, micropositioners for microscopic optical elements, and actuators for micromechanical sorting (such as the sorting of biological cells) [82].

In Fig 2.47, electrochemical transfer of dopant from the outer layer to the inner layer of each bimorph causes opening the tweezers. A bimorph is a cantilever that consists of two active layers: piezoelectric and metal.

These layers produce a displacement via thermal activation (a temperature change causes one layer to expand more than the other), or electrical activation as in a piezoelectric bimorph (electric field causes one layer to extend and the other layer to contract). A piezoelectric unimorph has one active (i.e. piezoelectric) layer and one inactive (i.e. non-piezoelectric) layer [1-10, 16, 18, 20, 63].

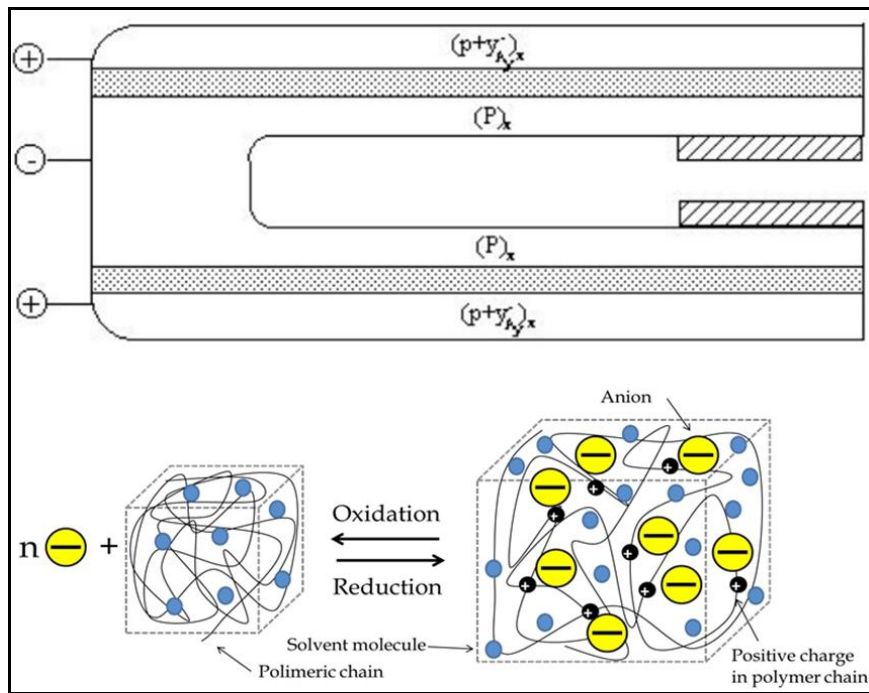


Figure 2.47 : Proposed use of paired bimorph actuators as micro-electrochemical tweezers.

Smart structures are items which change themselves to be better and more suitable. An example of such a futuristic application is a golf club which adapt in real time to a person's tendency to slice or undercut their shots. A more realizable application is vibration control [83]. Smart skins have been developed which do not vibrate during skiing. Vibration control is achieved by using the force of the vibration to apply a force opposite to the vibration [84]. Other applications of such smart structures include active suspension systems on cars, trucks and train; traffic control in tunnels and on roads and bridges; damage assessment on boats; automatic damping of buildings and programmable floors for robotics and AGV's [83]. An AGV is an "automated guided vehicle" or "automatic guided vehicle", a mobile robot that follows markers or wires in the floor, or uses vision, magnets, or lasers for navigation.

Much research is necessary to see some of the above applications will become a reality [84]. The stability and processibility both need to be substantially improved if they are to be used in the market place. The cost of such polymers must also be substantially lowered. However, it must be considered that, although conventional polymers were synthesized and studied in laboratories around the world, they did not become widespread until years of research and development had been done. In a

way, conducting polymers are at the same stage of development as their insulating ones were some 50-60 years ago. Regardless of the practical applications which are eventually developed for them, they will certainly challenge researchers in the years to come with new and unexpected phenomena.

2.6 Pyrrole and Polypyrrole

Pyrrole is a heterocyclic aromatic organic compound, a five-membered ring with the formula C_4H_4NH [218]. It is a colourless volatile liquid that darkens readily upon exposure to air. Pyrrole has very low basicity compared to conventional amines and some other aromatic compounds like pyridine. This decreased basicity is attributed to the delocalization of the lone pair of electrons of the nitrogen atom in the aromatic ring. Like many amines, pyrrole slowly decomposes on exposure to air and light [219]. Over time, it turns brown over time due to accumulation of impurities such as polypyrrole and various amine. The simplest member of the pyrrole family is pyrrole itself, a basic heterocyclic compound; colorless to pale yellow, toxic oil with pungent taste and similar to chloroform odor; insoluble in water; soluble in alcohol, ether, and dilute acids; boils at 129–131°C; polymerizes in light. It is usually purified by distillation immediately before use. Pyrrole oligomers are easier to oxidize than the corresponding pyrrole monomers. The formula of pyrrole is shown in the Fig 2.48.

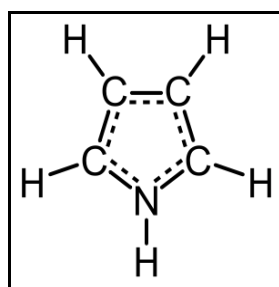


Figure 2.48 : Pyrrole.

Pyrrole ring system is involved in coloured products in nature. Pyrrole was first detected by F. F. Runge in 1834, as a constituent of coal tar. In 1857, it was isolated from the pyrolysate of bone. Its name comes from the Greek “pyrros” (fiery), from the reaction used to detect it; the red color that it imparts to wood when moistened with hydrochloric acid [220]. Pyrrole and its derivatives are widely used as an intermediate in synthesis of pharmaceuticals, medicines, agrochemicals, dyes, photographic chemicals, perfumes and other organic compounds. They are used in

metallurgical processes. They are useful in the intensive study of transition-metal complex catalyst chemistry for uniform polymerization, luminescence chemistry and spectrophotometric analysis.

Polypyrrole (PPy) is a chemical compound formed from a number of connected pyrrole ring structures. The formula of PPy is shown in the Figure 2.49. Polypyrroles are conducting polymers of the rigid-rod polymer host family, all basically derivatives of polyacetylene. PPy films thinner than 1 mm have different spectral properties depending on the conditions of synthesis and degree of PPy oxidation; with the increasing degree, the colour of the films changes from yellow to the blue and, ultimately, black. The stability in air of the doped PPy films is relatively high; their degradation occurs only above 150 - 300 °C. Thermal degradation of PPy starts with the loss or decomposition of dopant.

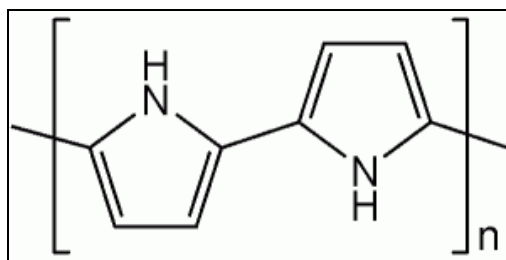


Figure 2.49 : Formula of Polypyrrole.

Polypyrrole is a conducting polymer that has attractive characteristics for the use as a radar absorbing material [85]. The polymer's conductivity can be varied over several orders of magnitude, covering a range that is suitable for microwave absorption.

Polypyrrole (PPy) can be formed chemically or electrochemically through oxidative polymerization of pyrrole monomer,

The oxidation process mentioned above proceeds via a one electron oxidation of pyrrole to a radical cation, which subsequently couples with another radical cation to form the 2,2'-bipyrrole. This process is then repeated to form longer chains.

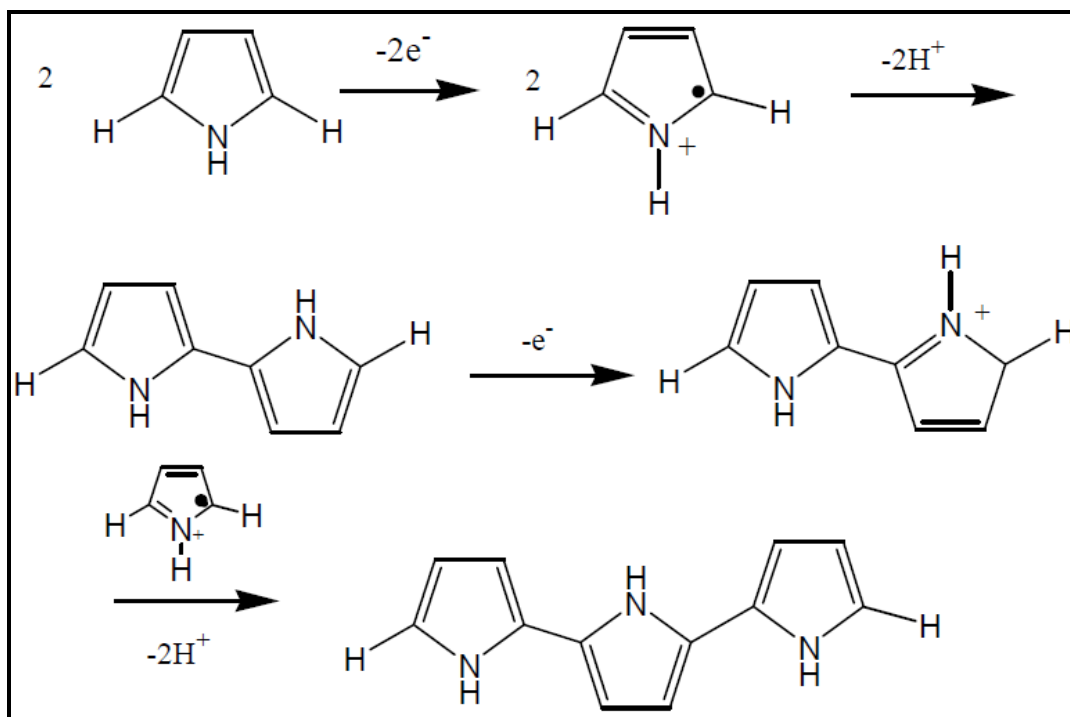


Figure 2.50 : Oxidative polymerization of Pyrrole to Polypyrrole.

The final form of polypyrrole is that of a long conjugated backbone as seen in Figure 2.50. The polymer has resonance structures that resemble the aromatic or quinoid forms. In this neutral state the polymer is not conducting and only becomes conducting when it is oxidized. The charge associated with the oxidized state is typically delocalised over several pyrrole units and can form a radical cation (polaron) or a dication (bipolaron) (Figure 2.51). The physical form of polypyrrole is usually an intractable powder resulting from chemical polymerization and an insoluble film resulting from electropolymerization.

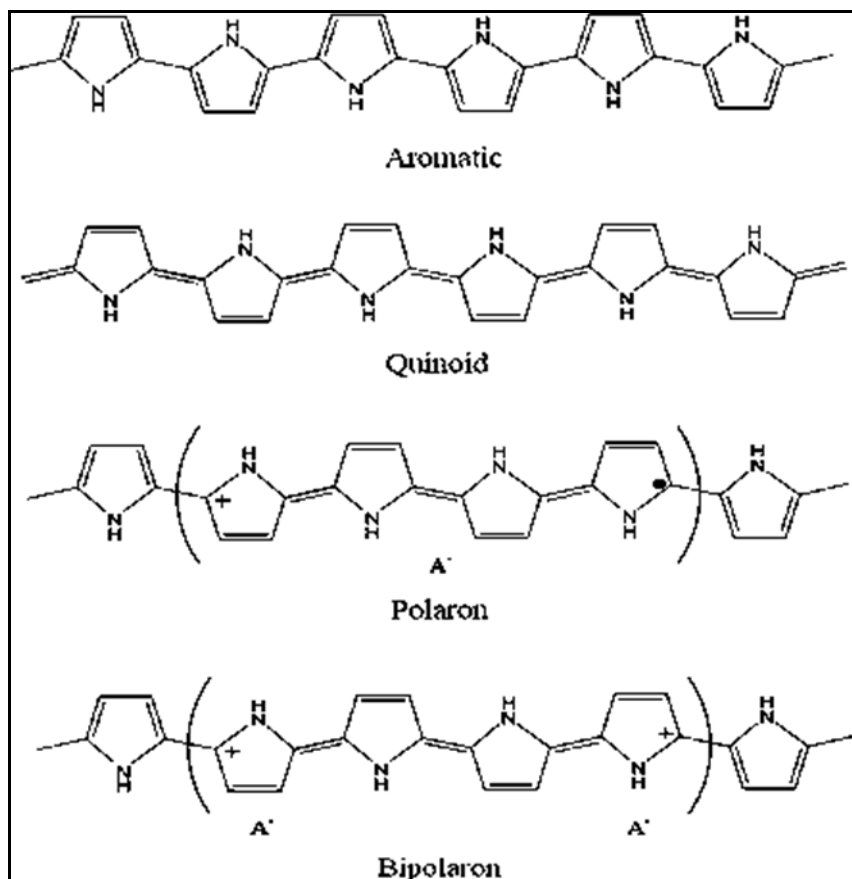


Figure 2.51 : Chemical structures of PPy in neutral aromatic and quinoid forms and in oxidized polaron and bipolaron forms.

2.6.1 Polymerization of Pyrrole

2.6.1.1 Electropolymerization of Pyrrole

Electrochemical oxidation of pyrrole forms a film of conducting polymer at the electrode surface. The electropolymerization of pyrrole to polypyrrole follows as in Figure 2.52.

Initiation. Formation of monomer radical cation by electrochemical oxidation, +0.8 V vs SCE.

Propagation. Combination of two radical cation monomers (or oligomers) followed by loss of two hydrogen ions. The linkage formed is at the 2 position of the pyrrole ring, forming 2,2'-bipyrrole. 2,5-disubstituted pyrroles do not polymerize and 2-monomers only form dimers. Propagation continues by re-oxidation of the bipyrrole and further combination of radicals.

Termination. Occurs when no further monomer is present for oxidative polymerization or side reactions terminate the PPy chain. An example of a termination reaction is the reaction with water to form the amide group.

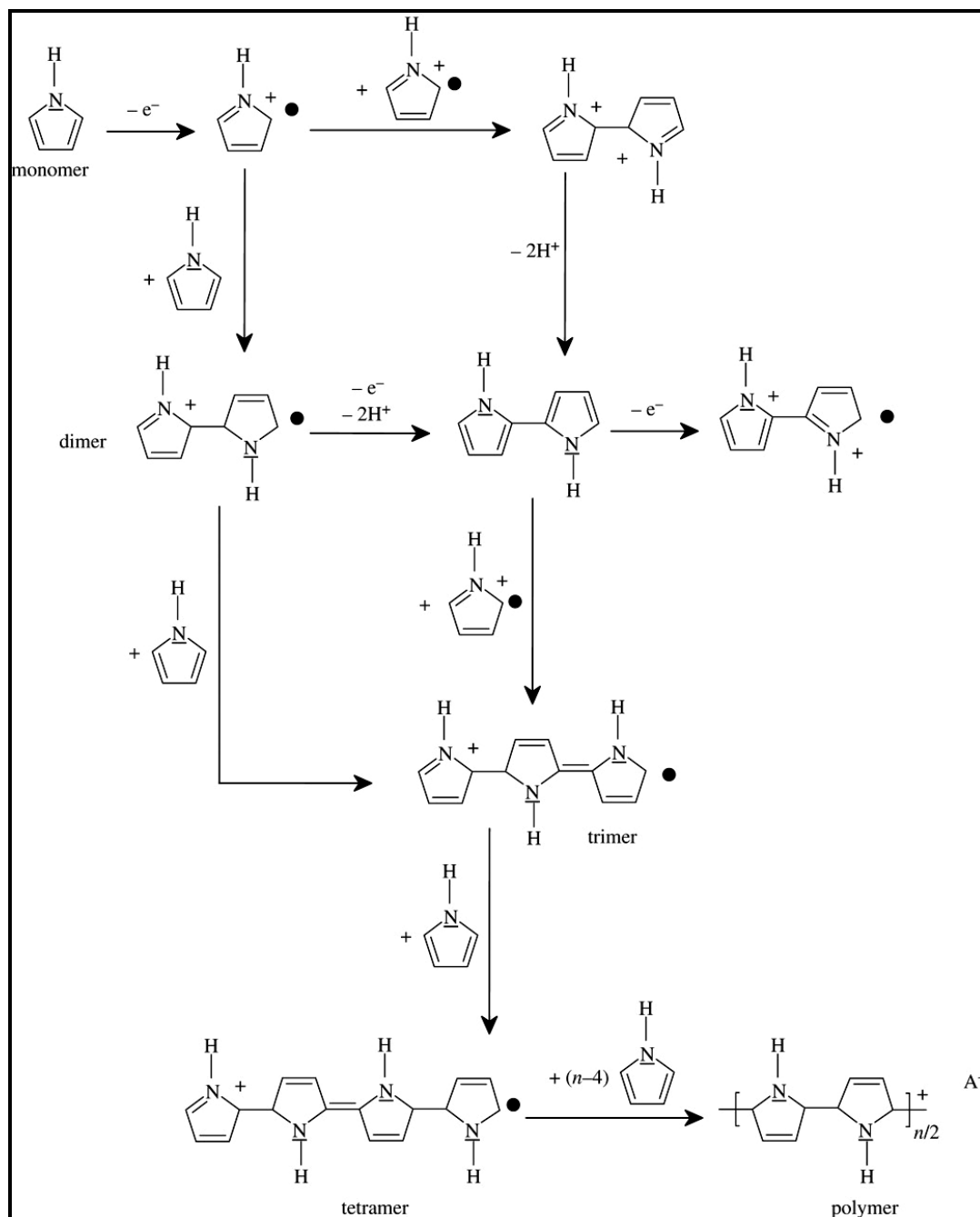


Figure 2.52 : Electropolymerization mechanism of Pyrrole.

Monomer units are adsorbed onto the surface of the working electrode resulting in one-electron oxidation to form a pyrrole cation radical. These cations then couple with themselves, with other cations or with neutral monomers from solution. In each

case, this leads to the formation of a dimer dication, which undergoes a double deprotonation to give a neutral molecule. These more stable dimer radicals have a lower oxidation potential compared with the monomer units and chain growth then occurs by preferential coupling between the dimers and monomers. Anion (A^-) is required to maintain electroneutrality.

The success of electropolymerization of pyrrole is due to the stability of the radical through charge delocalization, and the ease of electro-oxidation. The loss of the hydrogen ions makes the dimer (oligomer) formation irreversible so proton acceptors, such as water, pyridine and bases, enhance electropolymerization. Good solvents for electropolymerization [86] include water, acetonitrile, butanone, propylene carbonate, dimethylformamide (DMF) and ethanol though the presence of a bit of water (1 v/v%) enhances the polymer formation. Water can also result in chain termination. Potentiostatic, potential cycling, and galvanostatic methods can be used to electropolymerize pyrrole. Potentiostatic methods (constant potential) and cycling the potential yield the most consistent films of about the same quality. Galvanostatic deposition (constant current), does not produce as good a quality film as the other methods, but is useful for controlling film thickness.

Electrochemical oxidation of a 5-member pyrrole oligomer [87] shows two reversible one-electron oxidation processes at $E_o = -0.28$ and -0.08 V vs Ag/Ag⁺. These correspond to the formation of the radical cation and dication, respectively, which are stable and do not polymerize. Another oxidation peak at $E_p=0.75$ V marks the start of polymerization. Extrapolation of the E_o value to infinite chain length for the first one electron oxidation gives a value of -0.59 V, compared to the measured value of -0.57 V for polypyrrole from the pentamer [88].

AFM studies of polypyrrole production indicate that time and substrate influence the final film morphology [88, 89]. Supporting electrolyte was found to affect deposition kinetics [89]. Cyclic voltametry and NIR-Vis spectroscopy have also been used to show the affect of pH and counter ion [90]. Neutral polypyrrole is noted to be very unstable in water or air. In basic solutions the polymer was doped with hydroxide ions and other anions in acidic solutions. Incorporation of polymeric counter ions has been investigated for imbuing other properties such as thermoresponsiveness [91].

2.6.1.2 Chemical polymerization of Pyrrole

Polypyrrole can also be synthesized via chemical polymerization, using a chemical oxidant such as ferric chloride (FeCl_3) [221, 222]. During chemical polymerization, pyrrole and a water soluble counter-ion salt are added to an aqueous FeCl_3 solution. The FeCl_3 initiates pyrrole polymerization, and the black polymer falls out of solution. This method can be used to coat fabrics or other non-conducting surfaces with polypyrrole, as the polypyrrole will deposit on any surface exposed to the reaction solution. Alternatively, anhydrous FeCl_3 can be dissolved in an organic solvent. When pyrrole is mixed into this solvent, it will be oxidized, and the resulting polypyrrole will precipitate out of solution. Both methods of chemical polymerization produce powdery products that are not free-standing, and are generally used when one wants to coat, a non-conductive surface [221-223], or to make polypyrrole with a very large surface area for capacitor applications [224, 225]. The mechanism of chemical polymerization of Py is similar to that for electropolymerization of pyrrole and conductivities are comparable. The resulting polymer in its oxidized form is conducting with charge compensation afforded by FeCl_4^- . The conductivity of polypyrroles formed from different ferric salts (effect of dopant ion) has been related to the $\text{Fe}^{2+}/\text{Fe}^{3+}$ redox potential with strong acid anions providing the most oxidizing ferric species. Weaker acid anions typically coordinate Fe^{3+} ions more strongly, reducing its oxidizing potential [86]. An investigation into the ferric ion equilibria in aqueous solutions showed that above a concentration of 0.5 M HClO_4 there was no change in the amount of available $\text{Fe}(\text{H}_2\text{O})_6^{3+}$ [92].

The solvent the reaction occurs in also changes the redox potential. For example the $\text{Fe}^{2+}/\text{Fe}^{3+}$ redox potential is lower in water than acetonitrile. If the redox potential is too high, an irreversible dissolution of polypyrrole can occur, as for ferric perchlorate in acetonitrile [93]. Methanol has been found to produce the best conducting polymer based on conductivity and morphology [94, 95]. The conductivity was related to the redox potential of the $\text{Fe}^{2+}/\text{Fe}^{3+}$ system and could be varied by adding FeCl_2 . The optimum redox potential in methanol was +0.5 V vs SCE. The solvent also has an influence on the dopant ion that remains in the PPy film. In ether using FeCl_3 as oxidant leaves FeCl_4^- as the dopant ion, while in methanol, the dopant is mainly Cl^- with some FeCl_4^- [86]. Water was found to be trapped in the PPy with formation of

pyrrolidinone rings at chain terminations similar to electrochemically produced films [86].

Other counter ions to the ferric ion will also be incorporated into the PPy film [86] as will ions present in solution. Dopants whose bonds are variable / unstable such as Cl-O, B-F, P-F, should be avoided for sake of polymer stability [96]. Polymerization of pyrrole in the presence of surfactants such as dodecylbenzyl sulphonic acid or a salt like sodium dodecyl sulphate, leads to an increase in mass yield due to incorporation of the salt/surfactant into the polymer [97]. Cationic surfactants were found to inhibit the polymerization of pyrrole. Polymerization of pyrrole in the presence of polystyrene sulphonate (PSS) produced particles (non-colloidal) with the size being inversely proportional to the concentration of ferric chloride oxidant [98]. The size effect is due to the affinity of pyrrole and the ferric ion to PSS. The acid concentration affects the polymerization process.

The conductivity of polypyrrole increases as the synthesis temperature is reduced. This is thought to be due to a reduction in the number of side reactions. Polypyrrole's conductivity as a function of temperature is studied as well as reflectivity, and classified into metallic, critical and insulating regions [99]. Polypyrrole's conductivity is strongly dependent on temperature. but the type of dependence (metallic vs. insulating) depends on the conditions under which the sample was made. In general. polypyrrole's conductivity decreases with decreasing temperature until a minimum of $T = 10$ to 20 K. Below this point, the conductivity increases with decreasing temperature for highly doped (metallic) samples. and continues to decrease for less highly doped (insulating) samples [318,320,321]. Whether a particular sample is metallic or insulating is determined by whether the Fermi energy is above or below the mobility edge (the critical energy that differentiates localized and non-localized states) [319].

The density of polypyrrole has been determined to be 1.48 g/cm^3 and $1.44 \pm 0.05 \text{ g/cm}^3$ [98,100]. Polypyrrole derivatives have been prepared and their properties studied. By blocking the 3-, 4- positions on the pyrrole ring, unwanted side reactions at these sites are eliminated. This has been noted to yield higher conductivity in the case of poly 3,4- dimethoxypyrrole [101,102]. Various alkylendoxypyrroles have been synthesised and studied including a series of soluble species [101,103,104]. N-

substituted pyrroles tend to induce twisting relative to adjacent pyrrole rings, thus limiting the conjugation length and conductivity. Solid state NMR has been used to elucidate some of the conducting mechanisms and structures [105]. Bipolarons appear to be the charge carriers and conductivity is linked to the loss or decomposition of the dopant ions. Elevated temperatures in air reduce the quinoid content and oxidise the 3,4-positions. Dodecyl sulphate is less stable than *p*-toluene sulphonate at elevated temperatures. Under argon the dodecyl sulphate doped film become brittle indicating cross linking at elevated temperatures [105].

The polymer produced by electrochemical or chemical synthesis is generally an intractable solid or powder. In following section 2.6.2, there are some of the strategies that have been investigated for the purpose of producing useable material.

2.6.2 Processability of Polypyrrole

Researchers have been looking at a number of methods for making conducting polymers practical [106]. The trade off is often lower conductivities, though sometimes there is the serendipitous gain of stability. Some of these methods include direct polymerization onto polymers sheets, glass, polymer and inorganic particles, clays, zeolites, porous membranes, fibres and textiles and soluble matrices. The methods used to coat these materials are reviewed below to highlight potential avenues for the development of radar absorbing materials.

2.6.2.1 Solutions of Polypyrrole

The solubility of polypyrrole is limited due to its rigid structure and cross-linking. Attempts at increasing the solubility have been made by derivatizing the pyrrole ring at the 3- and 4- positions with alkyl groups, or substituents on the pyrrole's nitrogen. Another techniques that has been proven successful for some conducting polymers is to use long chain surfactant dopants like sodium dodecyl benzene sulfonate [104-106], di(2-ethylhexyl) sulfosuccinate sodium salt [107], or polystyrene sulfonate [95]. These polymers are then soluble in *m*-cresol, NMP, DMSO, DMF and THF.

2.6.2.2 Chemical preparation of Polypyrrole composites

Since polypyrrole is generally intractable, attempts have been made to polymerize pyrrole onto or into the material where it is desired. In one strategy, the oxidant is

mixed with the substrate and then exposed to pyrrole [108]. For instance, ferric chloride has been mixed with polyvinyl alcohol [109], polyvinyl acetate [110], polyethylene oxide [111], poly(styrene-butyl acrylate-hydroxethyl acrylate) [31], poly(methyl acrylate-co-acrylic acid) [112], or rubber [113], and exposed to pyrrole vapours. The variation of this method is to soak the substrate with the pyrrole monomer and then immerse it in an oxidant solution [108, 114].

Polypyrrole can be deposited directly onto a substrate surface, by placing the object in a solution containing pyrrole and oxidant. This coating strategy has been applied to fabrics [115] and is discussed in greater detail in section 2.6.5.

Surfaces have been modified with dopant groups to facilitate polypyrrole-substrate adhesion and deposition. Low density polyethylene has been sulphonated and used as a template for the polymerization of pyrrole yielding PPy layers up to 80 nm thick and conductivity up to 150 S/cm [116,117]. A similar system was investigated using a sulphonic acid derivative of polystyrene grafted polyethylene [118], and compression molded sulphonated polystyrene objects [119]. Other researchers have attempted to improve deposition and adhesion of the polypyrrole by graft polymerization of other polymers to the polyethylene [140]. Polypyrrole has been deposited onto acrylic, polystyrene, polyimide and polyurethane foam [123]. Composites have been made by dispersing polypyrrole powder in melted LDPE, HDPE and PS [141], or by dispersing polypyrrole powder or flakes in silicone rubber or vinyl ester and curing the material [142]. Colloidal PPy has been made by stabilisation with methylcellulose [143].

2.6.3 Copolymers and graft copolymers of Polypyrrole

Processable or soluble polypyrrole has been formed by graft copolymerization of pyrrole. This has been accomplished by coupling pyrrole to a reactive monomer, polymerizing the monomer and then polymerizing the pyrrole as was done for methylmethacrylate [144-146]; or by modification of a preformed polymer with pyrrole and then polymerizing the pyrrole as has been done for polystyrene-co-poly(chlorostyrene) [147]. These materials were initially soluble with a tendency to become insoluble at high pyrrole content.

Direct copolymerization of pyrrole with other monomers has produced soluble conducting product. Examples include the polymerization of pyrrole with various aniline derivatives [148-150], and methyl ethyl ketone formaldehyde resin [151]. The conductivity and solubility depends on the feed ratio of pyrrole.

2.6.4 Electrochemically synthesis of Polypyrrole

Pyrrole has been electrochemically copolymerized with a liquid crystal derivatised thiophene forming an insoluble film [152].

2.6.5 Polypyrrole studies on textiles

Conductive textiles [153] can be produced by weaving thin metallic or carbon wires, impregnating fibre materials with conducting powders, metallizing material, or by blending filament-sized fibres of stainless steel or carbon fibre. Conducting fibres have also been made from conducting polymers by solution spinning, however, they are typically brittle, expensive to produce and hard to manufacture on a large scale [154]. Conducting powder (carbon) incorporation is most cost effective, though the high content required to yield percolation reduces the mechanical properties of the fibres. Core/shell strategies, where normal textile fibres are coated with a conducting material, maintain the original mechanical strength. Conducting polymers have been used for this application, and yield conductivities that fall between metallized fabrics and carbon-based blends.

One of the earliest reports of the deposition of polypyrrole onto fibres involved a two-step process, whereby paper was soaked in a ferric chloride solution before immersion in a pyrrole solution [134]. Variations on this method include exposing the ferric chloride to pyrrole monomer in the vapour phase [155,156] and soaking the substrate in monomer before polymerization in an oxidizing solution [157]. The process is also applicable to the use of various solvents [158].

The easiest method of applying conductive polymer to a textile is from a solution of the conducting polymer. The solubility of highly conducting polymers (PPy, PANI and Polythiophene) is limited to solvents that are not generally compatible with the textiles [126]. Water-based systems have been used for coating textiles such as the PANIPSS system and emulsion polymerized monomers to form latex [159,160].

In-situ polymerization is another method for producing conductive coatings on textile substrates [161-163]. The mechanism for conducting polymer deposition proceeds through the adsorption of oligomeric species onto the textile surface, nucleation, from which subsequent polymerization occurs, growth, forming a smooth continuous film. Neither the monomer nor the oxidant is adsorbed to produce nucleation sites. In the presence of a fibrous surface, little or no polymer is found in solution. The coatings made by this method do not form significant fibre-to-fibre bonds, unlike solution and emulsion methods.

Polymer deposition is independent of surface material yielding films less than 1 μm thick and very uniform for coverages of 1-5%. Substrate material does not have a significant effect on the polymerization of pyrrole, yielding essentially the same conductivity for the same mass of textile. Clean glass fabric is reported to not coat well with PPy [153], though its adhesion can be improved by the use of aminosilane or pyrrole-silane molecules that chemically bond to the glass surface [164-166]. Factors important to determining the conductivity include surface area, hydrophobicity, surface polarity and porosity. Porous fibres (nylon and polyacrylonitrile) and materials with polar groups tend to increase adhesion and polymer deposition while non-polar fibres such as polyethylene and polytetrafluoroethylene and dense crystalline fibres such as polyester yield poorer adhesion. The conductivity is not a linear function of the mass of polypyrrole deposited [52]. Fabrics prepared from continuous filament yarns produce better conducting films than those prepared from spun fiber yarns [167]. The conductivity of PPy-Textiles does not vary greatly as a function of humidity.

Kinetics of the polypyrrole deposition on textiles has been studied.[168] The rate of polymerization is dependent on the concentration of monomer and type of oxidizing agent. Ammonium persulfate, APS, is much faster than FeCl_3 . Acidic FeCl_3 is much faster than more basic FeCl_3 as the acid drives the equilibrium $\text{Fe}(\text{H}_2\text{O})_6^{+3} \rightarrow \text{Fe}(\text{H}_2\text{O})_5(\text{OH})^{+2} + \text{H}^+$ to the left. The hydrated species is smaller and not as tightly coordinated, so the reaction is more facile. Highly coordinating ligands or high pH slows the reaction rate. Comparing reactions with and without the presence of fibres in the reaction vessel, the reaction rate is faster with fibres present and second order, though first order reaction rates can be achieved if the Fe^{3+} concentration is

significantly increased. Without fabric, the reaction rate is second order and slower. Pure solvents such as methanol, methylene chloride or acetonitrile permit polymerization to occur in the solution phase, so no PPy is deposited on the fabric.

Pure solvents have already been noted to inhibit the deposition of PPy on the textile, whereas mixed solvents give mixed results. For instance, 20 g/L acetone in water inhibits PPy deposition, whereas the same concentration of methanol does not interfere. Textiles may be scoured with surfactants before sale and these may have an effect on PPy formation. Surfactants that are cationic or nonionic do not promote adsorption while dodecylbenzene sulfonic acid, DBSA, marginally decreases adsorption. Hydrophobic surfactants such as alkyl naphthylsulfonate promote film formation.

Other additives, such as 1,4-dihydroxybenzene, reduce adsorption while p-nitrophenol does not interfere. PPy – Fabric (Polyethyleneterephthalate and Polyethylene) samples have been chemically polymerized, using Poly (vinyl alcohol) as a surfactant to improve PPy coating on non-woven materials and NSA as a dopant with APS as oxidant [116]. The DC conductivity (T) indicates 3-D variable range hopping.

Conducting fibres have been fabricated by electropolymerizing pyrrole with a cotton, silk or wool fibre wrapped around the electrode [168]. A considerable body of work exists for polyaniline, PANI, coated textiles [169]. Polyaniline on glass fibres has been studied [170]. The glass was cleaned in sulphuric acid to remove impurities before polymerization in HCl, aniline and PTSA. Conductivities up to 1.79 S/cm were realized based on the thickness of the film rather than the thickness of the fabric. It is pointed out here that in the rinsing stages of the PANI/HCl or PANI/PTSA fabrics, a solution containing the counterion must be used as rinsing with pure water leaches out the dopant [170].

2.7 Electrospinning

As the diameters of polymer fiber materials are reduced from micrometers (e.g. 10–100 nm) to nanometers, several amazing characteristics appear such as high surface area to volume ratio (this ratio for a nanofiber can be as large as 10³ times of that microfiber), flexibility in surface functionalities, and high-qualified mechanical

performance (e.g. stiffness and tensile strength) compared with any other known form of the material. These properties make the polymer nanofibers to be optimal precursors for many significant applications. In recent years, series of processing techniques such as drawing [171], template synthesis [172,173], phase separation [174], self-assembly [175, 176], electrospinning [177, 178], etc. have been used to obtain polymer nanofibers. Even though the term “electrospinning”, derived from “electrostatic spinning”, was used relatively recently (in around 1994), its fundamental idea dates more than 60 years earlier. A series of patents [179–183] were published from 1934 to 1944, which describe an experimental setup for the production of polymer filaments using an electrostatic force. A polymer solution was entered into the electric field, then the polymer filaments were formed from the solution; between two electrodes bearing electrical charges of opposite polarity. One of the electrodes was placed into the solution and the other onto a metal collector. Once ejected out of a metal spinnerette with a small hole, the charged solution jets evaporated to become fibers which were collected on the collector. The potential difference depended on the properties of the spinning solution, such as polymer molecular weight and viscosity. If the distance between the spinnerette and the collector was short, spun fibers tended to stick to the collecting device as well as to each other, due to incomplete solvent evaporation. The schematic draft of electrospinning is shown in the Figure 2.54.

In recent years since 1980s the electrospinning process essentially similar to that described by [184] has attracted more probably due in part to a surging interest in nanotechnology, as ultrafine fibers or fibrous structures of various polymers with diameters down to submicrons or nanometers can be easily fabricated with this process.

There are mainly three components to complete the process: a high voltage supplier, a capillary tube with a pipette or needle of small diameter, and a metal collecting screen. In the electrospinning process a high voltage is used to create an electrically charged jet of polymer solution or melt out of the pipette (Figure 2.53). Before reaching the collecting screen, the solution jet evaporates or solidifies, and is collected as an interconnected web of small fibers [177, 178].

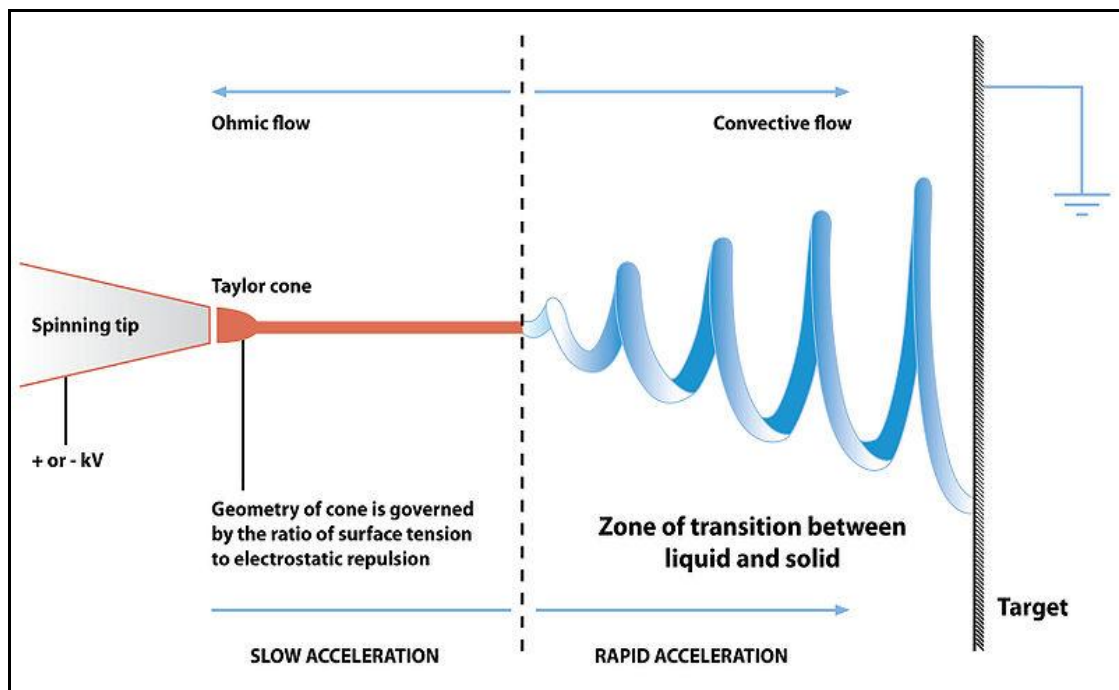


Figure 2.53 : Schematic of electrospinning setup and process.

One electrode is placed into the spinning solution/melt and the other attached to the collector. In most cases, the collector is simply grounded, the electric field is subjected to the end of the capillary tube that contains the solution fluid held by its surface tension. This induces a charge on the surface of the liquid. Mutual charge repulsion and the contraction of the surface charges to the counter electrode cause a force directly opposite to the surface tension. When the intensity of the electric field is increased, the hemispherical surface of the fluid at the tip of the capillary tube elongates to form a conical shape known as the Taylor cone [185]. Further increasing the electric field, a critical value is attained with which the repulsive electrostatic force overcomes the surface tension and the charged jet of the fluid is ejected from the tip of the Taylor cone. The discharged polymer solution jet undergoes an instability and elongation process, which allows the jet to become very long and thin. Meanwhile, the solvent evaporates, leaving behind a charged polymer fiber. In the case of the melt the discharged jet solidifies when it travels in the air.

Both the dissolution and the electrospinning are conducted at room temperature with atmosphere condition. However, some polymers may cause unpleasant or even harmful smells, therefore the processes should be conducted within chambers having a ventilation system. Furthermore, a DC voltage in the range of several to several

tens of kVs is necessary to generate the electrospinning. One must be careful to avoid touching any of the charged jet while manipulation. It is noted that the same polymer dissolved in different solvents may all be electrospun into nanofibers.

There are many parameters that affects the transformation of polymer solutions into nanofibers through electrospinning. These parameters include (a) the solution properties such as viscosity, elasticity, conductivity, and surface tension, (b) governing variables such as hydrostatic pressure in the capillary tube, electric potential at the capillary tip, and the gap (distance between the tip and the collecting screen), and (c) ambient parameters such as solution temperature, humidity, and air velocity in the electrospinning chamber [186].

Consequently these fibers have a large surface area per unit mass so that nanowoven fabrics of these nanofibers collected on a screen can be used for example, for filtration of submicron particles in separation industries and biomedical applications, such as wound dressing in medical industry, tissue engineering scaffolds and artificial blood vessels. The use of electrospun fibers at critical places in advanced composites to improve crack resistance is also promising [187, 188].

2.8 Emulsion Polymerization

Emulsion polymerization is a largely used process that helps to obtain waterborne resins that contains several colloidal and physicochemical properties. A hydrophobic monomer is added into the water with emulsifier and the reaction is continued with the initiation reaction by the water-soluble initiator (such as NaPS) in this free-radical non-homogenous polymerization type [189-195]. This polymerization mainly involves the reaction of free radicals with relatively hydrophobic monomer molecules within submicron polymer particles dispersed in a continuous aqueous phase (Figure 2.54). This unique polymerization process that is heterogeneous in nature exhibits very different reaction mechanisms and kinetics compared to bulk or solution free radical polymerization. Surfactant is generally required to stabilize the colloidal system; otherwise, latex particles nucleated during the early stage of polymerization may experience significant coagulation in order to reduce the interfacial free energy. This feature may also come into play in determining the

number of reaction loci (i.e., polymer particles) available for the consumption of monomer therein.

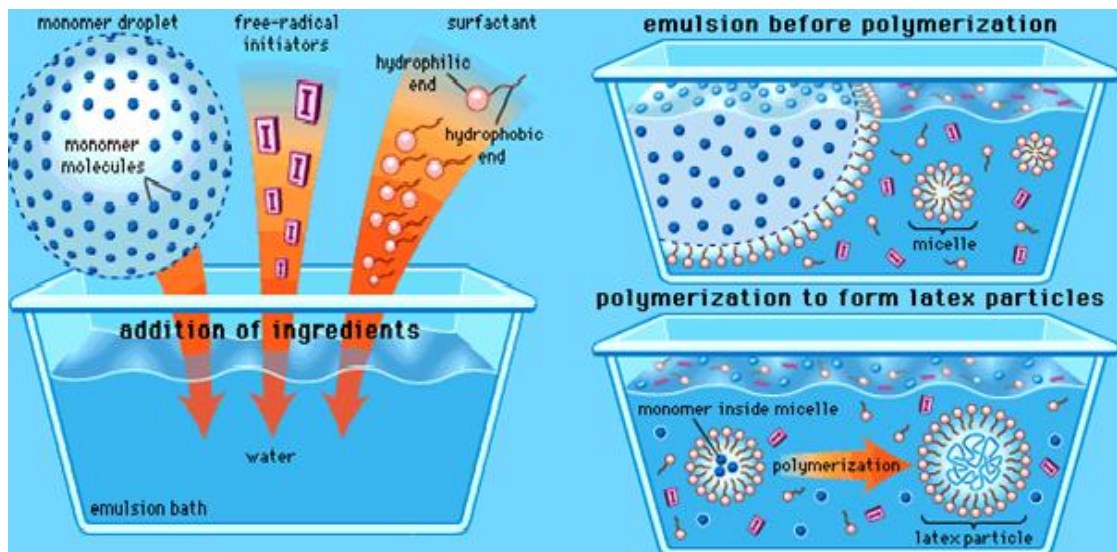


Figure 2.54 : Schematic view of emulsion polymerization.

The spontaneous latex form of particles are obtained from polymerization at the very beginning of the reaction process. These latex particles are normally 100 nm in size, and are made of many individual polymer chains. The particles do not coagulate with each other due to the surrounding of the surfactant on the particles. also the electrostatic force coming from the surfactant makes the particles repel each other.

A large oil–water interfacial area is created as the particle nuclei form and particle size increases with the continuing of the polymerization. Therefore an effective stabilizer that contains ionic and non-ionic surfactants, also protective colloid (e.g. hydroxyethyl cellulose and polyvinyl alcohol), is needed to prevent the latex particles from coagulation thanks to the physically or chemically integrated on the particle surface [196]

Since growth and stabilization, nucleation of polymer particles are controlled by the free radical polymerization mechanisms in combination with several colloidal occurrences, emulsion polymerization is considered as a relatively complex process.

3. EXPERIMENTAL PART

3.1 Materials

All the studies included in this thesis were performed using the following materials: Butyl Acrylate (BuA) ($\text{CH}_2\text{CHCOOC}_4\text{H}_9$), Acrylonitrile (AN) ($\text{C}_3\text{H}_3\text{N}$), Pyrrole (Py) ($\text{C}_4\text{H}_5\text{N}$), Dimethylformamide (DMF) ($\text{C}_3\text{H}_7\text{NO}$), Dimethylsulphoxide (DMSO) ($\text{C}_2\text{H}_6\text{OS}$), Sodium Dodecyl Benzene Sulfonate (SDBS) ($\text{C}_{18}\text{H}_{29}\text{NaO}_3\text{S}$), Cerium (IV) Ammonium Nitrate (CAN) ($\text{H}_8\text{N}_8\text{CeO}_{18}$), Potassium Peroxydisulphate (KPS) ($\text{K}_2\text{S}_2\text{O}_8$), and Ammonium Persulphate (APS) ($(\text{NH}_4)_2\text{S}_2\text{O}_8$) were all reagent degree and were purchased from Sigma Aldrich. Sodium Chloride (NaCl), Ethanol ($\text{C}_2\text{H}_5\text{OH}$) and Methanol (CH_3OH) were obtained from Merck. Distilled water was obtained from our laboratory. All the reagents were used as taken without further purification.

3.2 Analyses and Instruments

3.2.1 Spectroscopic analyses

3.2.1.1 ATR-FTIR analysis

Analyses were carried out on an ATR-FTIR reflectance spectrophotometer (Perkin Elmer, Spectrum One, with a Universal ATR attachment with a diamond and ZnSe crystal). The advantage of using this instrument with such an ATR attachment is, having chance to perform analyses by simply taking a sample in its solid form and to put it onto the crystal eye of the instrument to begin an analyzing process of just a few seconds.

All the spectra obtained from the analyses performed on this ATR-FTIR instrument were taken as absorbance / wavelength graphs in a $4000 - 650 \text{ cm}^{-1}$ band.

3.2.1.2 UV-Vis analysis

Ultraviolet–visible spectroscopy or ultraviolet-visible spectrophotometry (UV-Vis or UV/Vis) refers to absorption spectroscopy or reflectance spectroscopy in the ultraviolet-visible spectral region. The absorption or reflectance in the visible range directly affects the perceived color of the chemicals involved. In this region of the electromagnetic spectrum, molecules undergo electronic transitions. Molecules containing π -electrons or non-bonding electrons (n-electrons) can absorb the energy in the form of ultraviolet or visible light to excite these electrons to higher anti-bonding molecular orbitals. The more easily excited the electrons (i.e. lower energy gap between the HOMO and the LUMO), the longer the wavelength of light it can absorb.

All the UV-Visible Spectroscopy analyses were performed by using the Perkin Elmer Lambda 45 UV-Visible Spectrometer. The spectra were obtained between 0-5 absorbance and 190 – 1100 nm wavelength bands, with a 1 nm of sensitivity.

3.2.1.3 EIS analysis

A dielectric material (dielectric for short) is an electrical insulator that can be polarized by an applied electric field. When a dielectric is placed in an electric field, electric charges do not flow through the material as they do in a conductor, but only slightly shift from their average equilibrium positions causing dielectric polarization. Because of dielectric polarization, positive charges are displaced toward the field and negative charges shift in the opposite direction. This creates an internal electric field that reduces the overall field within the dielectric itself. If a dielectric is composed of weakly bonded molecules, those molecules not only become polarized, but also reorient so that their symmetry axis aligns to the field. The study of dielectric properties concerns storage and dissipation of electric and magnetic energy in materials. Dielectrics are important for explaining various phenomena in electronics, optics, and solid-state physics.

Dielectric spectroscopy (sometimes called impedance spectroscopy), and also known as electrochemical impedance spectroscopy (EIS), measures the dielectric properties of a medium as a function of frequency. It is based on the interaction of an external field with the electric dipole moment of the sample, often expressed by permittivity.

It is also an experimental method of characterizing electrochemical systems. This technique measures the impedance of a system over a range of frequencies, and therefore the frequency response of the system, including the energy storage and dissipation properties, is revealed. Often, data obtained by EIS is expressed graphically in a Bode plot or a Nyquist plot.

Impedance is the opposition to the flow of alternating current (AC) in a complex system. A passive complex electrical system comprises both energy dissipater (resistor) and energy storage (capacitor) elements. If the system is purely resistive, then the opposition to AC or direct current (DC) is simply resistance.

For the EIS analyses performed, it was used the Parstat 2263 Electrochemical Analyzer instrument, as shown in Figure 3.1.



Figure 3.1 : Parstat 2263 Electrochemical Analyser.

3.2.1.4 Broad-band dielectric spectrometry

The interaction of electromagnetic waves with matter in the frequency range between 10^{-6} and 10^{12} Hz is the domain of broadband dielectric spectroscopy. In this extraordinarily extended dynamic range molecular and collective dipolar fluctuations, charge transport and polarisation effects at inner and outer boundaries take place and determine the dielectric properties of the material being studied. Hence, broadband dielectric spectroscopy enables one to gain a wealth of information on the dynamics of bound (dipoles) and mobile charge carriers depending on the details of a molecular system.



Figure 3.2 : Novocontrol BDS-40 Broadband Dielectric/Impedance Spectrometer.

The film and thin films samples which are subjected to this thesis study were analyzed in the instrument shown in Fig 3.2, to make a conclusion about the electromagnetic shielding performances and conductivity levels of the sampled materials.

3.2.2 Morphological analyses

The morphology of the samples were diverting from eachother in various ways because of their raw materials, production methods and production and preparing conditions such as humidity, temperature, residual solvent, etc. The Scanning Electron Microscope (SEM) and Atomic Force Microscope (AFM) analyses were performed to enlighten the morphological properties of various samples studied in this thesis.

3.2.2.1 SEM analysis

Some of SEM analyses were performed on a desktop model of SEC SEN-3000M Mini-SEM instrument in Electropol-Nanotech Res. Grp. Laboratories of ITU (Figure 3.3), which can perform taking SEM pictures in a range of 50x – 30,000x magnification, according to the sample type. And the detailed SEM analyses in a larger scale (50,000 – 400,000) were performed by FEI - Quanta FEG 250 instrument (Figure 3.4) of MEMTEK laboratories in Istanbul Technical University.



Figure 3.3 : SEC SEN-3000M Mini-SEM instrument.



Figure 3.4 : FEI - Quanta FEG 250 instrument.

3.2.2.2 AFM analysis

Atomic force microscopy (AFM) or scanning force microscopy (SFM) is a very high-resolution type of scanning probe microscopy, with demonstrated resolution on the order of fractions of a nanometer, more than 1000 times better than the optical diffraction limit. The precursor to the AFM, the scanning tunneling microscope, was developed by Gerd Binnig and Heinrich Rohrer in the early 1980s at IBM Research - Zurich, a development that earned them the Nobel Prize for Physics in 1986. Binnig, Quate and Gerber invented the first atomic force microscope (also abbreviated as AFM) in 1986. The first commercially available atomic force microscope was introduced in 1989. The AFM is one of the foremost tools for imaging, measuring, and manipulating matter at the nanoscale. The information is gathered by "feeling" the surface with a mechanical probe. Piezoelectric elements that facilitate tiny but

accurate and precise movements on (electronic) command enable the very precise scanning. In some variations, electric potentials can also be scanned using conducting cantilevers. The AFM instrument used in this thesis study is shown in Figure 3.5.



Figure 3.5 : Nanosurf Easy Scan 2 AFM-STM instrument.

3.2.3 Dynamic Mechanical Analysis

Dynamic mechanical analysis (termed shortly as DMA, also known as dynamic mechanical spectroscopy) is a technique used to study and characterize materials. It is most useful for studying the viscoelastic behavior of polymers. A sinusoidal stress is applied and the strain in the material is measured, allowing one to determine the complex modulus. Depending on the desired measurement method, the temperature of the sample or the frequency of the stress can be varied while performing test, leading to variations in the complex modulus; this approach can be used to locate the glass transition temperature of the material, as well as to identify transitions corresponding to other molecular motions. DMA instrument used while this thesis study is shown in Figure 3.6.

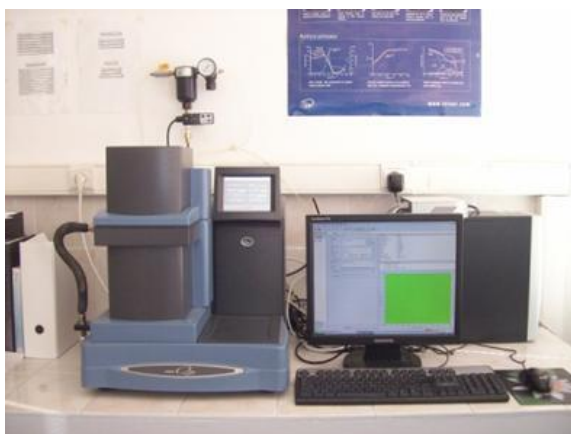


Figure 3.6 : TA Instruments DMA Q800 Dinamic Mechanical Analyzer.

3.3 Synthesis of Polyacrylonitrile (PAN)

In this study, it was used first, bulk polymerization; and then emulsion polymerization for synthesis of PAN.

3.3.1 Bulk polymerization of Acrylonitrile (AN)

3.3.1.1 Materials

Cerium ammonium (IV) nitrate $(\text{NH}_4)_2[\text{Ce}(\text{NO}_3)_6]$ (CAN), nitric acid (HNO_3), and oxalic acid were all Merck reagents. Acrylonitrile was supplied from Aksa, Turkey. All these chemicals and monomers were used as received. Distilled water was used for preparing solutions and stock solutions.

3.3.1.2 Polymerization procedure of Acrylonitrile

Polymerization was carried out in a flat-bottomed flask equipped with a stirrer and a condenser by the addition of Ce(IV) (CAN) dissolved in HNO_3 -water to an aqueous solution of monomer and oxalic acid. All operations were conducted in water at 25 °C. Polymerization started with addition of Ce(IV) solution at 25 °C water bath temperature and reaction concentrations of oxidant, monomer, and acid as following: $[\text{Ce}(\text{IV})] = 2 \times 10^{-2} \text{M}$, $[\text{HNO}_3] = 0.1 \text{M}$, $[\text{OA}] = 2 \times 10^{-2} \text{M}$, $[\text{AN}] = 2.4 \text{M}$. After 1 hour, the temperature was increased up to 60°C and was kept at this temperature for 1 hour. After 2 hours of polymerization, the resulting polymer was precipitated, filtered and washed with distilled water. The filtered polymer was dried at room temperature. Polymerization mechanism is given below:

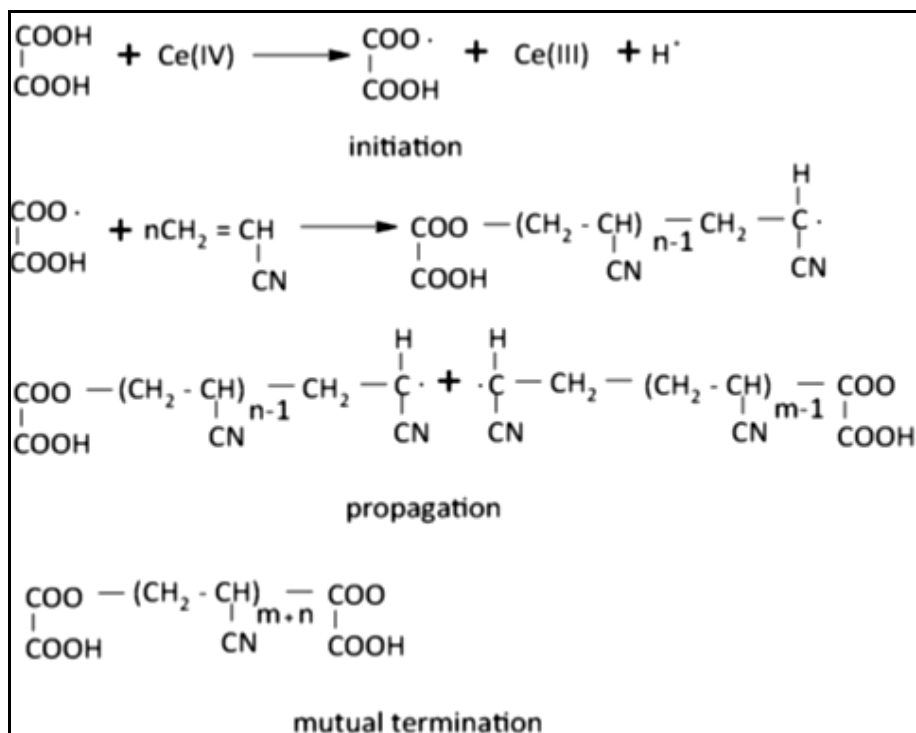


Figure 3.7 : Polymerization scheme of AN with Oxalic Acid-CAN couple.

3.3.2 Emulsion polymerization of AN

3.3.2.1 Materials

Ammonium persulphate (APS) $[(\text{NH}_4)_2\text{S}_2\text{O}_8]$, Sodium dodecylbenzenesulphonate (SDBS) $[\text{CH}_3(\text{CH}_2)_{11}\text{C}_6\text{H}_4\text{SO}_3\text{Na}]$, Methanol (CH_3OH), were all Aldrich reagents. Acrylonitrile was supplied from Aksa, Turkey. Distilled water was used as polymerization medium and to prepare solutions. All the materials were used as taken, without further purification.

Table 3.1 : Ingredients and their amounts in reaction medium.

Ingredients	Molar Mass (g/mol)	Mole	Molarity	Weight (g)
AN	53.06	0.10000	1.00000	5.30600
SDBS	348.48	0.00152	0.01523	0.53060
APS	228.18	0.00150	0.01500	0.34227

3.3.2.2 Polymerization procedure

Polymerization was carried out in a round-bottomed reaction-bulb equipped with a magnetic-stirrer and a condenser by the addition of APS-dissolved-in-water to the aqueous emulsion of AN monomer. The emulsion medium was carefully prepared before the polymerization process by addition of SDBS into the required amount of distilled water, and after SDBS was completely solved, the AN monomer was added into the medium while vigorous stirring. When the milky-emulsion was observed, the medium was heated up, and the polymerization started with addition of APS solution at 70°C. After 5 hours of polymerization, the resulting polymer was precipitated, filtered and washed 5 times respectively with excess amount of distilled water and methanol. The filtered and washed polymer was dried first in laboratory-oven under 1 atm of vacuum pressure at 60°C for 1 day, and then left to the atmospheric conditions of laboratory at room temperature.

3.4 Synthesis of Polybutyl acrylate (PBuA)

3.4.1 Materials

Butyl acrylate, Cerium (IV) ammonium nitrate (CAN), methanol and distilled water were used to synthesize PBuA. The reagents were all purchased from Aldrich, and were used as they are taken, i.e. without further purification.

3.4.2 Polymerization process of BuA

CAN was dissolved in HCl/water medium to obtain initiator solution, Butyl acrylate was solved in required amount of water, and polymerization took place at 40 °C. The yield was more than 70%.

3.5 Synthesis of P(AN-co-BuA) Copolymer

The different molar compositions of P(AN-co-BuA) copolymers were synthesized from its comonomers, AN and BuA, with these AN/BuA% molar ratios, 95/5, 90/10, 85/15, 80/20, 75/25, 67/33, 50/50 and 25/75. The receipt to synthesize the P(AN-co-BuA) was taken directly from the receipt previously already used to successfully polymerize AN monomer. While the AN monomer ratio is excessively more than BuA monomer as feeding rate, the copolymer was able to be synthesized without

problem and the yield was not that bad. But, when the BuA monomer is more than AN monomer as weight while feeding to the polymerization medium, the polymerization was usually failed or resulted with a very low yield. The optimization of the reaction time, the temperature of the reaction medium, the monomer feeding composition of the copolymer to clearly see the differences in resultant polymer, and the washing/filtering/drying conditions, were all done after multiple of polymerization attempts.

P(AN-co-BuA) copolymer was synthesized firstly via bulk polymerization by using Ce(IV) as a free-radical initiator and oxalic acid as redox-agent, in HNO₃ acid medium. The yield was higher than 90%, but the resultant polymer was almost impossible to solve in any organic solvent, because of the strong crosslinks between molecular chains caused by high-reactant CAN initiator.

Because of the faced problems while processing the polymer, the polymerization method was changed to the emulsion polymerization that includes the use of a surfactant to disperse monomer drops in water medium at micro/nano dimensions, and the initiator as KPS (Potassium persulphate)/APS (Ammonium persulphate). Ammonium persulphate is a salt that works as a free radical initiator in water medium, and it results high yields and high molecular weight of synthesized polymer. The related literature claims the interaction between the surfactant molecules and the resultant polymer, thus easier the solubility and so the processability. Most of the copolymers synthesized by emulsion polymerization were able to be fully dissolved in any organic solvent at room temperatures in less than half hour.

The visual, morphological and spectroscopic analyses were done to characterize the synthesized copolymer products.

3.6 Thin Film Production

Most of laboratory analyzing techniques and devices are suitable to analyze materials in film form, which polymeric materials are easier to handle and to observe, especially while mechanical analyzes such as stress/strain test on a dynamic mechanic analyzer. Thus, in this study, the thin films were prepared from synthesized (AN-co-BuA) copolymer within a range of 20-100 microns thickness.

3.6.1 Materials

Synthesized copolymers of various monomer ratios (5/95, 10/90, 15/85, 20/80, and 33/67 %BuA/AN) were used to produce polymeric film samples. To produce each film sample, 0.25 g of taken polymer was dissolved via stirring in Dimethylformamide (DMF) on magnetic stirrer system for 1-2 hours to obtain a 10 ml total volume of polymer solution.

3.6.2 Procedure

Polymer solutions were casted onto smooth surfaces of specially prepared glass-cells, and left to the vacuum atmosphere which was already set to -1 bar pressure and +60 °C temperature for 72 hours. After this solution-casting and drying stage, the prepared films were carefully removed from glass-cells and left into the standard atmospheric conditions (25 C, 1 atm, 65% RH) of laboratory for 24 hours and then packed to keep in safety for further analyses.

3.7 Electrospun-Nanofiber Production

3.7.1 Materials

Synthesized polymer/copolymer, Dimetyl formamide (DMF), Dimetyl sulphoxide (DMSO). DMF and DMSO were purchased from Sigma-Aldrich, at analytical grade. Polymers were previously synthesized in the laboratory.

3.7.2 Procedure

Electrospinning method was used to produce nanofibers of synthesized polymers. In this process a high potential (1 – 50 kV) electrical field is applied between polymer extruder/syringe system and metal collector surface. In this method, with suitable amount of polymer feeding rate, average value of fiber diameter can be easily arranged. While many other parameters such as atmospheric pressure, temperature, relative humidity, temperature of polymer solution are all effecting parameters in electrospinning process, the most important and determining parameters are syringe-tip diameter and shape, concentration of polymer solution, electrical potential applied and distance between tip and collector.

Nanofibers were obtained by electrospinning method from two different solutions including 300 μ l polymerized Py in copolymer matrix, and the copolymer itself; which were previously described and prepared. 90/10 mol% AN/BuA copolymer was used at a 5wt% concentration rate in DMF for both of the solutions.

In this study, all polymer solutions were prepared with 5-10% concentration at standard room conditions (25°C, 1 atm), and electrospinning process was run under about 1-3 kV/cm electrical potential/distance ratio (Table 3.2). From literature it was already known that the fiber diameter increases with increase in concentration of polymer solution, and polymer feeding rate; and decreases with increase in syringe-collector distance, and applied electrical potential. Thus, nanofibers were produced with desired properties, and samples were taken for analyses.

Table 3.2 : Electrospinning parameters used to produce nanofibers.

	Feeding Rate (ml/h)	Applied Voltage (kV)	Distance (cm)
co-1	0.3	10	10
co-2	0.15	10	10
co-3	0.15	15	10
co-4	0.15	20	10
coPy-1	0.15	20	5
coPy-2	0.15	15	5
coPy-3	0.15	10	5
coPy-4	0.15	20	7.5
coPy-5	0.15	25	7.5
coPy-6	0.15	30	7.5
coPy-7	0.15	20	10
coPy-8	0.15	25	10
coPy-9	0.15	30	10

3.8 Matrix polymerization of Pyrrole

3.8.1 Composite-thin-film production

Different amounts of Pyrrole (Py) added composite thin films were produced by casting from Dimethylformamide (DMF) solutions of synthesized -via oxidative polymerization with Ceric ammonium nitrate as initiator- Poly(Acrylonitrile-co-Butyl Acrylate) [P(AN-co-BuA)] onto smooth glass-surfaces. SEM, ATR-FTIR, and Dynamic Mechanical Analyses of products revealed a change in morphological view

and mechanical behavior correlated with Polypyrrole (PPy) content. And electrical impedance measurements were conducted to reveal electrical conductivity change with increasing PPy content.

In some previous studies of literature, PAN and its various related copolymers/terpolymers were used as polymer electrolytes, or to produce conductive thin films, and/or fibers by its own, with/without adding salts or electronic active self-dopant polymers to improve electronic interaction of structure in order to have improved electrical conductivity and impedance properties, and they were characterized by spectroscopic, mechanical, visual, and/or electrical impedance techniques.

In this study, Cerium ammonium nitrate (CAN) was used as initiator for Poly(Acrylonitrile-co-Butyl acrylate) [P(AN-co-BuA)] synthesis by free radical polymerization. Pyrrole (Py) was polymerized on the synthesized copolymer matrix by using the same oxidant (CAN) as initiator. CAN was chosen as an initiator because of well distribution in reaction medium, its strong oxidation ability, and homogeneity in various solutions' media, thus it is our difference from previous studies, to achieve polymerization process in an easier and faster way, and to reach good results in all visual, mechanical, and electrical properties. Because CAN is a well oxidant as initiator metal salt, our synthesizing conditions do not require high temperatures and/or nitrogen usage in vacuum atmosphere while process.

3.8.1.1 Synthesis of the polymeric matrix

Poly(AN-co-BuA) (both monomers, AN and BuA, from Aldrich, commercial grade; and used in 95% / 5% molar ratios) was obtained by free-radical polymerization in the presence of cerium ammonium nitrate (CAN) as initiator.

The reaction was carried out in distilled water media at 70°C for 3 hours. The polymer was washed several times first with nitric acid solution to remove salts and with distilled water and ethanol to purify it free from monomers, and dried under dynamic vacuum for 24 hours. The reaction yield was over 95%. The T_g value of the copolymer determined on the basis of DSC analysis from the second heating cycle was equal to 93°C. A tentative structure can be seen in Fig. 3.8 with interactions between DMF and PPy molecules as resultant product.

3.8.1.2 Preparation of composite thin films

The composite thin films were obtained by the casting technique on smooth glass-surfaces from synthesized copolymer with/without adding Pyrrole (Py) monomer to solution in dimethylformamide (DMF). In Py added solutions, in order to polymerize Py in polymer matrix, CAN was added as free-radical polymerization initiator at a 30% mass ratio of added Py amount. The solvent was removed under dynamic vacuum under a 600 mm Hg vacuum pressure for 24 hours, and then composite thin films were left to laboratory atmospheric conditions. The solvent was used readily as taken.

3.8.2 Composite-electrospun-nanofiber production

To obtain electrospun-nanofibers, the same polymer/DMF and also PPy/polymer ratios were used with the solutions which were previously prepared for film casting. After various trials for optimizing the solution concentration, applied voltage, distance from syringe-needle-tip to the collector plate, temperature; consequently the electrospinning solutions were prepared at a 5% concentration, and applied voltage between the needle and the collector was approximately 1 kilovolt per centimeter (1 kV/cm). The concentration parameter was held stable, and the other parameters such as distance (5 cm, 10 cm, 15 cm) and the applied potential (5 kV, 10 kV, 15 kV) were changed and applied.

Table 3.3 : Compositions of electrospinning solutions.

	Polymer Type	Concentration(wt%)	Monomer	Amount	Initiator (CAN)	Solvent (DMF)
1st Solution	90A/10B	5%	0	0	0	10 ml
2nd Solution	90A/10B	5%	Py	600 μ l	0.174 g	10 ml

Before electrospinning process, a 4 hours of stirring was applied to obtain homogenous solutions. Various parameters such as distance, applied voltage, and/or feeding ratios were tried and then the visual characterizations were performed on SEM analyses.

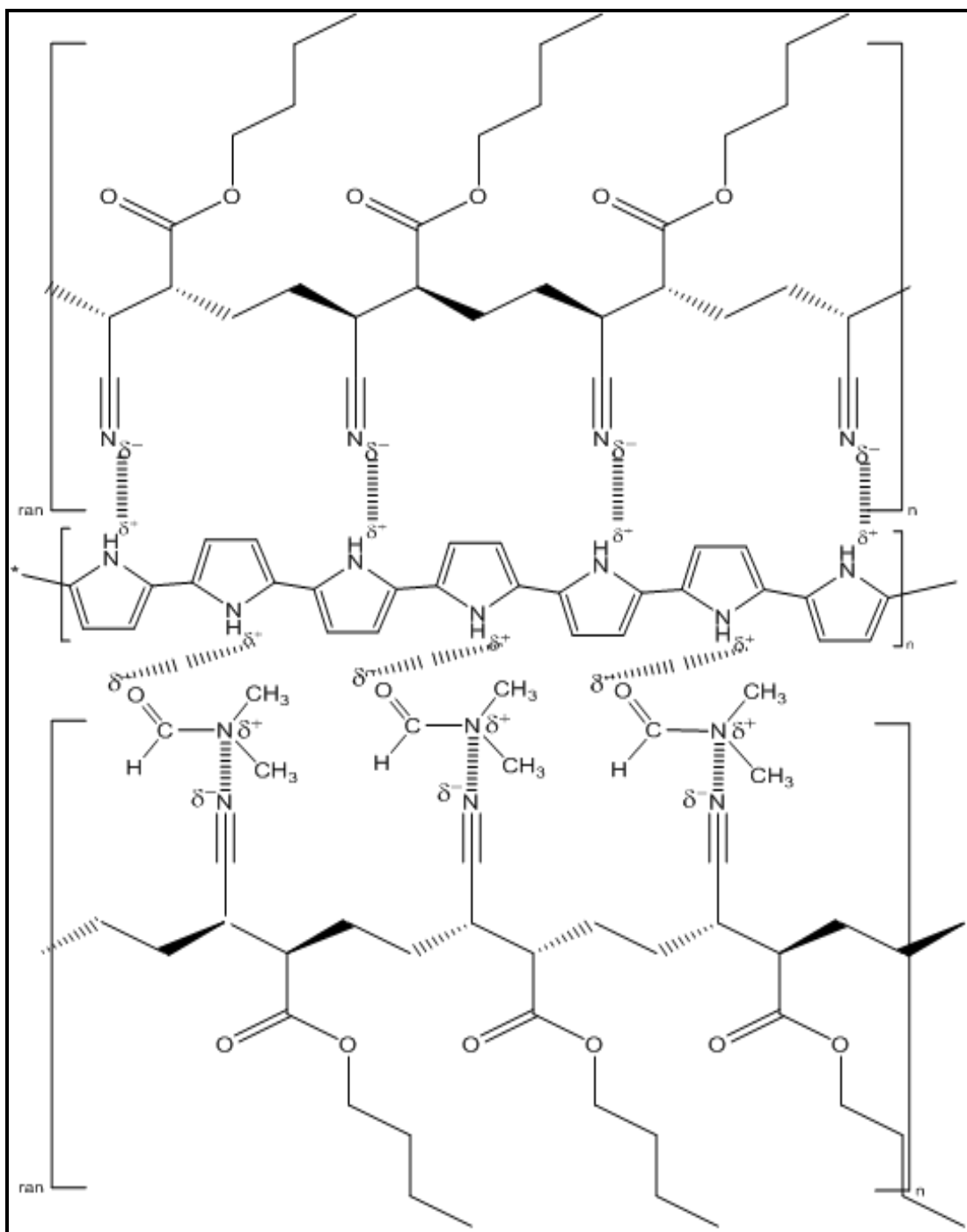


Figure 3.8 : Synthesized P(AN-co-BuA) random copolymer structure and interactions between molecules of copolymer matrix, PPy and DMF.

3.9 Production of Composite Core-Shell Nanoparticles

The Polypyrrole/(Acrylonitrile-co-Butyl acrylate) core-shell nanoparticles were obtained by a simple and cost-effective single-batch micro-emulsion polymerization. Polymerization of Acrylonitrile (AN) and Butyl acrylate (BuA) was performed in an aqueous medium with the presence of Sodium Dodecyl Benzene Sulphonate (SDBS)

as anionic surfactant and Potassium/Ammonium Persulfate (KPS/APS) as initiator. Unlike the conventional emulsion polymerization process, the micro-emulsion polymerization process includes not only vigorously-stirring the monomers in water-surfactant medium, but also a sonification process which held carefully on an Ultrasonic Cleaner. Because of the ultrasonic vibrations applied to the monomer droplets in water-surfactant medium, the droplets become much smaller, and the surfactant molecules keep those new micro/nano droplets stable in reaction medium. After such a copolymerization process which was performed for 5 hours at 70°C temperature in water-bath, the resultant polymer emulsion was milky-yellowish-white, and it was cooled down to the room temperature and the total reaction volume was divided into small-glass-containers-with-stainless-steel-caps to keep the samples safe for further analyses/experiments. Into each container, only different amounts of Pyrrole (Py) droplets (without use of any extra initiator) were added at room temperature, and the polymerization of Py occurred inside each container, so their milky-yellowish-white color turned to bluish-gray till black, and at extreme amounts of Py it was observed brownish-black. At the end of Py polymerization in AN-co-BuA emulsion medium, nanoparticles of PPy/(AN-co-BuA) were sampled by help of a micropipette, and the morphology was characterized by Scanning Electron Microscopy (SEM) on nanoparticle samples which were prepared by dispersing and diluting in ethanol and then dropping on a glass-substrate. Other than SEM analysis to have an idea about the particles' average sizes; the average nanoparticle size was also determined by a Particle Size Analyzer (via light-scattering method). Nanoparticles were successfully obtained as approximately 170-250 nm diameter changing by the different Polypyrrole (PPy) amounts. Then, the emulsions with/without PPy were all precipitated with a 5000 RPM centrifuge machine, washed 5 times with distilled-water, and then left to drying in vacuum-oven under -1 atm pressure and 60°C temperature for 3 days. Powder-like nanoparticle samples were obtained at the end of drying process. These samples were used for further analyses and/or experiments. Nanoparticle powders were characterized by both Fourier Transform Infrared-Attenuated Total Reflectance (ATR-FTIR), UV-Visible Spectroscopy to reveal their polymeric contents, and also by DMF-Gas Permeation Chromatography (DMF-GPC) to have an idea about their approximate molecular-weights. UV-Visible Spectroscopy results are examined with particle sizes and it was

observed that the UV-Visible absorption is directly proportional with the particle size of nanoparticles.

Conductive polymers and their composites are being interested frequently in recent years due to their usability for sensors, batteries, smart windows, electronic devices, bio-applications, smart-textile applications etc. Polypyrrole is one of the most commonly used types of conjugated conductive polymers. However it has not only advantages such as easy polymerization, high conductivity, and good thermal stability; but also some disadvantages such as brittleness and hard-processibility. The researchers are trying to minimize this problem by interacting the Polypyrrole with other polymers using various methods such as matrix-polymerization (includes polymerization of Pyrrole in polymer matrix in organic solvent medium), template-shell (or core-shell) particle production (produces shorter molecular chains of PPy, as result increases the solubility of Pyrrole, so its processability), or directly copolymerizing it with some chemical compounds which are already with high solubility.

In this study, Acrylonitrile is chosen, since it is one of the most popular monomers of textile industry due to its common usage as a precursor of carbon fibers by copolymerizing with some other monomers. Butyl acrylate monomer is chosen for its hydrophobicity and suitability for being copolymer with acrylonitrile. Hydrophobicity is a critical factor to have core-shell nanostructures in emulsion media with existence of a suitable surfactant.

3.9.1 Synthesis of P(AN-co-BuA) nanoparticles

0.1 mol monomer that consists of AN-BuA was emulsified in aqueous media with the presence of 10wt% SDBS (percentage by weight of monomer amount). 90%AN-10%BuA composition by moles was used. The reaction volume is completed to 100 ml with distilled water. All the ingredients and their amounts are demonstrated at Table 3.4. The monomers are shown in the Figure 3.9.

Table 3.4 : The total monomer, AN, BuA, SDBS and APS composition in feed.

Total Monomer (moles)	AN (%)	BuA (%)	SDBS (wt%monomers)	APS (mol%monomers)
0.1	90	10	10	1.5
	4.775 g	1.282 g	0.606 g	0.342 g

The three necked reaction flask is covered with aluminum folio in order to avoid sunlight that may start polymerization. The condenser is tied to one neck of the flask so that the evaporating monomer could be gained back. While 30 minutes stirring with magnetic stirrer in the hot water bath, the temperature was kept at 70°C. Then required amount of APS is added as solved in distilled water to the emulsion and the polymerization had started. After 3 hours (normally, the emulsion polymerizations take 5-6 hours; here it was stopped after 3 hours to keep polymer particles as small as possible), the polymer emulsion was cooled down till room temperatures, and the milky-yellowish-white liquid samples were taken from the emulsion to characterize the synthesized copolymer particles by SEM and Particle Size Analyzer in further steps. Total volume of resultant emulsion was then poured into the desired number of small glass-containers in equal volumes. In one of these containers, the precipitation by NaCl/distilled-water solution was performed to stop in the medium the possible reactions which could go on increasing particle-size. The other containers were kept for further stages of this study. Precipitated polymer particles were characterized by ATR-FTIR, UV-Visible Spectrometer and SEM.

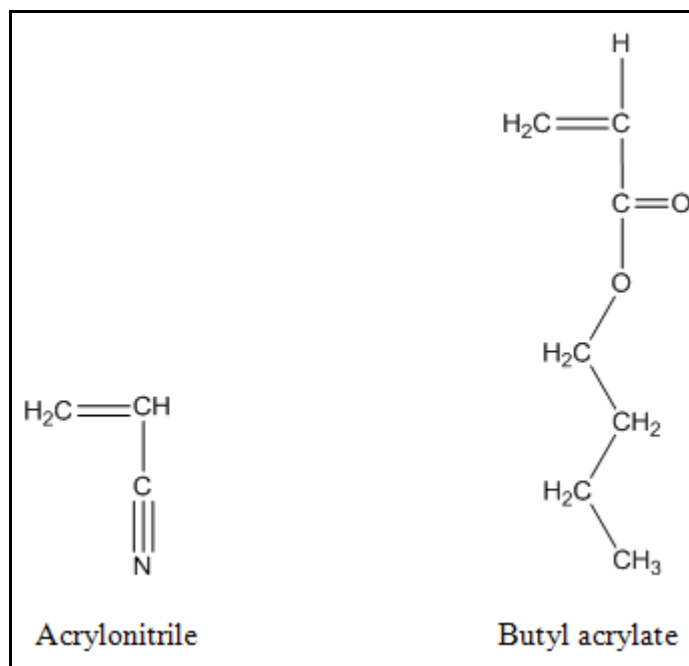


Figure 3.9 : Monomers used in synthesis of Poly(AN-co-BuA) template nanoparticles.

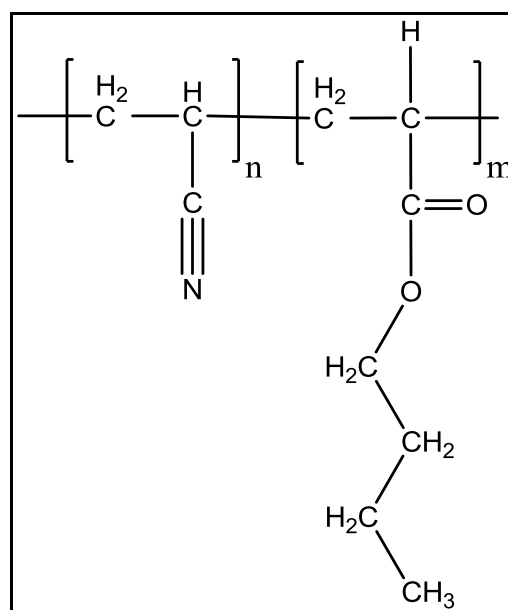


Figure 3.10 : P(AN-co-BuA) structure.

3.9.2 Synthesis of P(AN-co-BuA)/PPy core/shell nanoparticles

AN-BuA copolymers were prepared as given above. At the end of 3 hours polymerization, after waiting for equalizing the reaction with room temperature, without any initiator addition, pyrrole droplets were added into the emulsion medium

with the help of sonication process, and reaction continued 24 hours. Figure 3.11. shows the tentative mechanism of composite formation. Increasing amounts of pyrrole droplets are added as 10, 15, 20, 25, 30, 35, 40, 80, 120, 240, and 360 microliters. Samples were taken from this latex to characterize by SEM and Particle Size Analyzer. And then nanoparticles were precipitated and 5 times washed with distilled water and by the help of a 5000rpm centrifuge. The resulting nanomaterials were characterized by ATR-FTIR, UV-Visible Spectrometer and DMF-GPC.

3.10 Production of Electrospun Nanomats

Nanomats were produced from in-which 40, 80, 120, 160, and 200 μl Py in-situ-polymerized Acetonitrile+DMF (50/50 vol%) solutions onto the glass cover-slides via electrospinning/electrospraying method. The resultant samples were characterized by light-microscopy, SEM, and ATR-FTIR analyses.

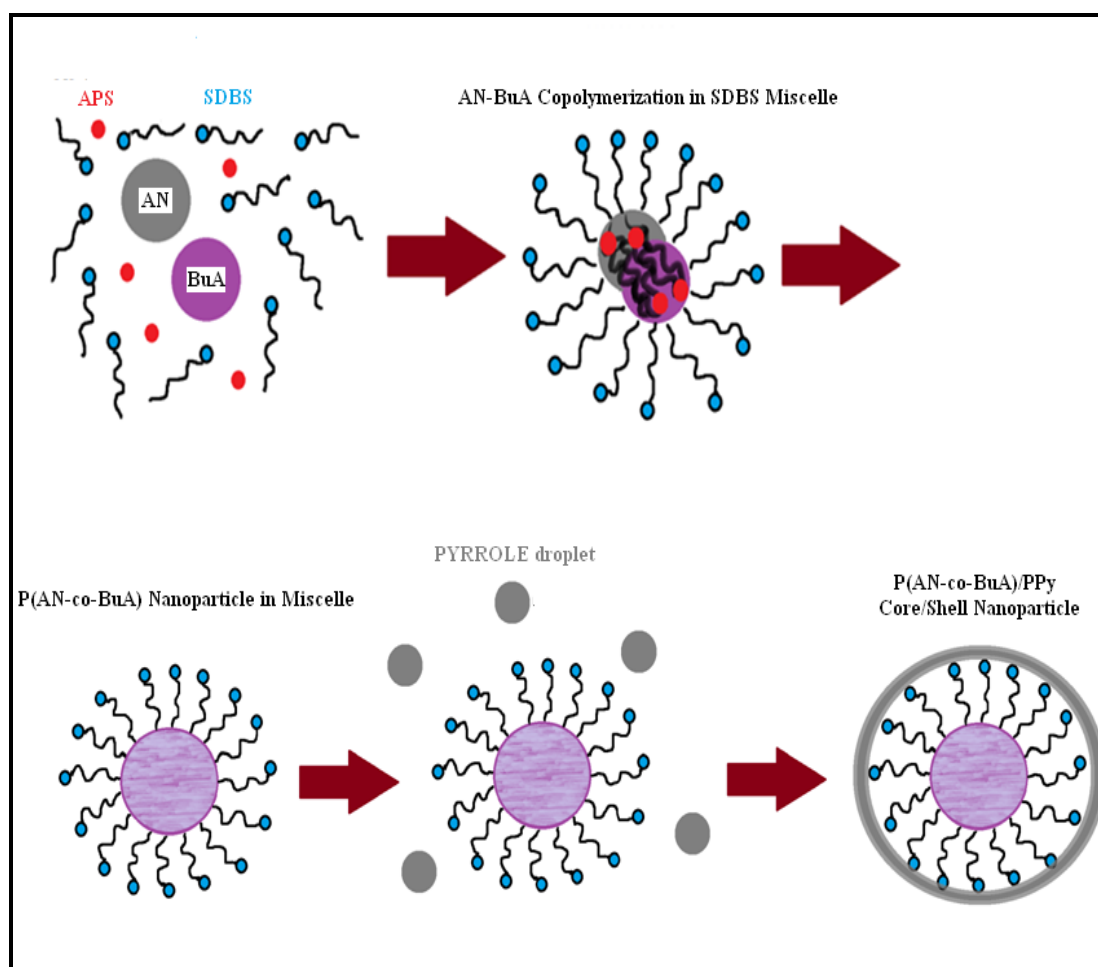


Figure 3.11 : Tentative mechanism of studied core-shell formation.

3.11 Solvent Effect on Electrical Conductivity of Composites

It is well known from the literature that, doping the polymers with ferroelectrical metal atoms and/or strong-ionic functional groups increases the electrical conductivity. For instance, FeCl_3 is not only as an initiator, but is widely used also to achieve this aim while polymerization of electroactive monomers.

In this study, a special doping process was not used on PPy including composite products, but dielectrical properties of different solvents were taken into account, and from the related literature it was seen that, Dimethylformamide (DMF) is superior to many of other solvents as its dielectric constant is much higher, so, for example, while electrospinning it has a superiority to the others, and also because of its higher polarity, it dissolves most of the polymeric compounds without problem even at room temperatures; but, DMF has a disorder effect on conjugated polymeric chains, and even if it leaves the film/thin-film/nanoweb structure after a well designed evaporating process, permanent is the damage to the interaction between intramolecular chains of conjugated polymer. On the other hand, Dimethylsulphoxide (DMSO) has a lower polarity degree compared to DMF, and its higher melting point (18.6°C) is creating problems while trying to process some polymers, but; because of its $-\text{Sulfo}$ group, it is showing a doping effect, and keeping/increasing the conductivity of conjugated polymers.

Here in this part of the study, the thin-films were prepared onto ITO-PET surfaces using DMSO as solvent, and the electrical impedance spectroscopy results showed high admittance values for those samples.

4. RESULTS AND DISCUSSION

4.1 Characterization of Synthesized Polymers

After the synthesis of PAN polymer, the spectroscopic characterization was done by ATR-FTIR spectroscopy. When the comparison was done with the related literature, it was clearly understood that PAN polymer was successfully synthesized at a high yield such as 70-80%.

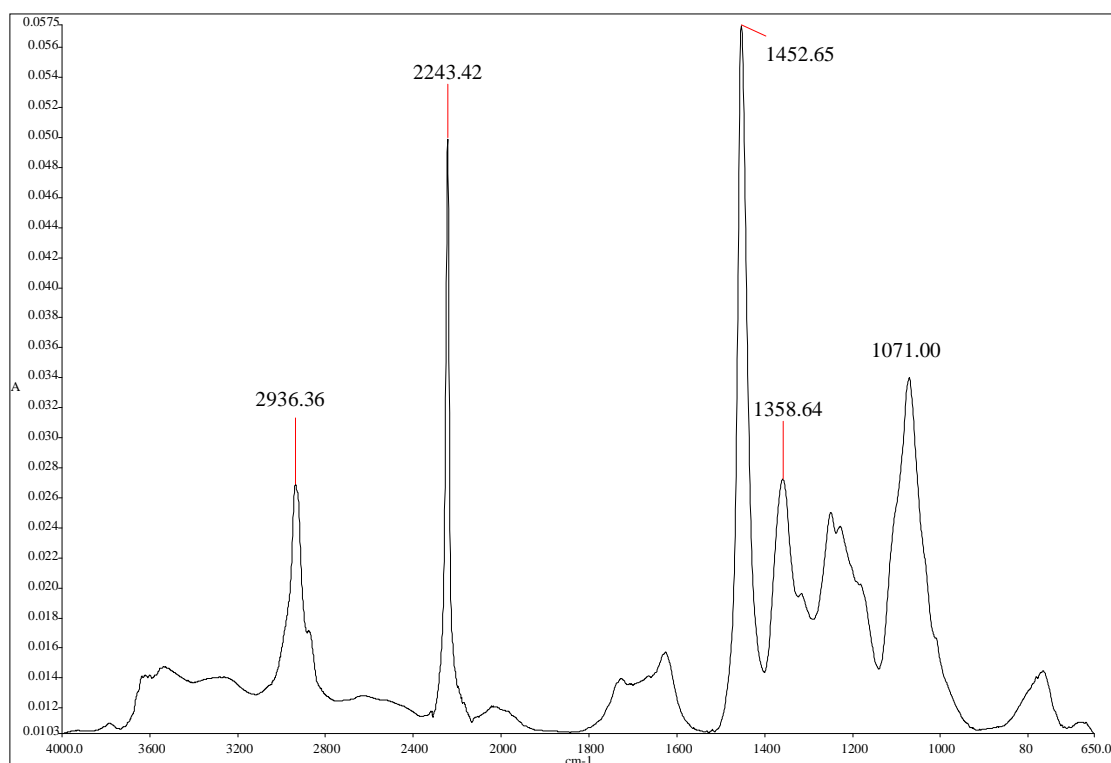


Figure 4.1 : ATR-FTIR spectra of synthesized PAN polymer.

The vibrations characteristics of the PAN structure are those of C=N nitrile group at ca. 2244 cm⁻¹ and the bands in the regions 2944–2870, 1460–1450, 1380–1350, and 1270–1220 cm⁻¹ are assigned to the aliphatic CH group vibrations of different modes in CH, CH₂, and CH₃, respectively. ATR-FTIR characterization was applied on all synthesized polymers and copolymers, which were with 100/0, 95/5, 90/10, 85/15,

80/20, 75/25, 67/33, 50/50, 25/75 molar ratios as AN/BuA% monomer initial feeds while the polymerization process.

After the taken photos of the synthesized polymers of different monomer ratios, it was seen that the more BuA monomer in polymer structure results the larger polymer particles and the yellowish color; while the more AN monomer in polymer structure results the smaller polymer particles and a smoother-powder form, and whiter the color. The light microscope views reveal the change in the morphology of synthesized polymers in a bigger scale. The SEM pictures show the differences between the shapes and the average sizes of the synthesized copolymer particles, by changing the fed monomer ratios. The more the fed BuA monomer, the larger the particles and assymetrical as shape; the more the fed AN monomer, the smaller the particles and more spherical particles were obtained.

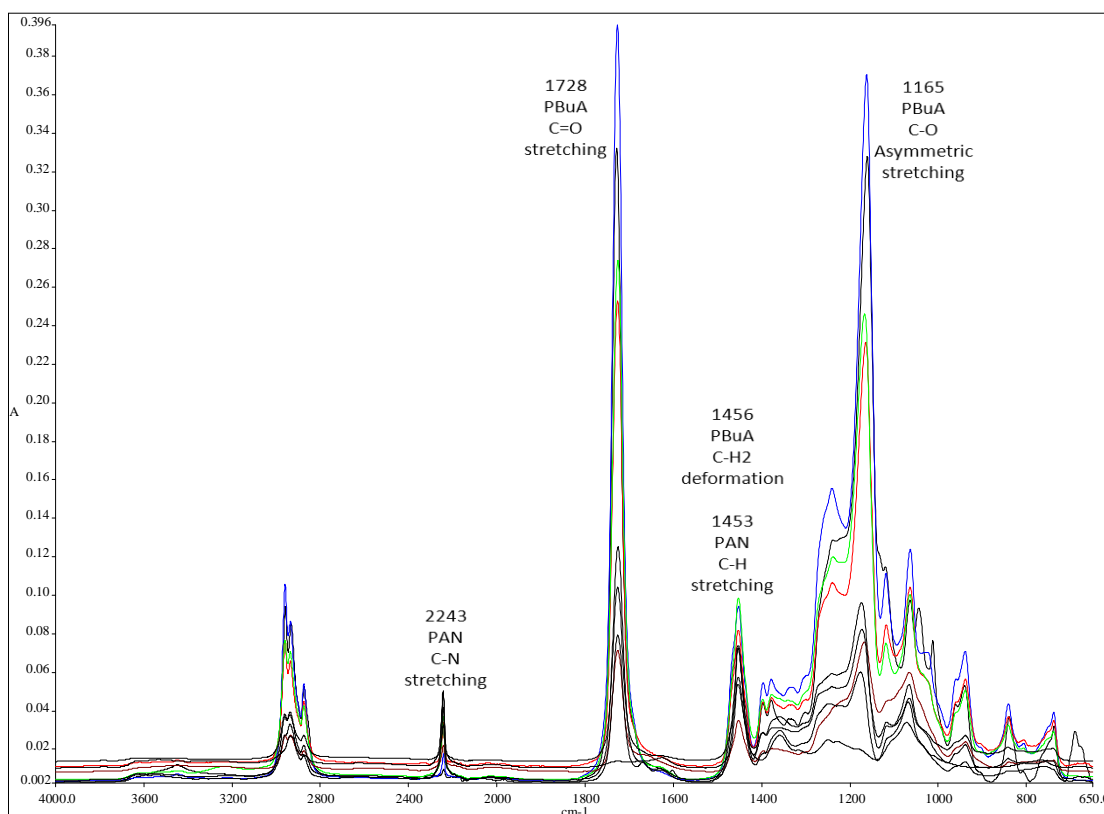


Figure 4.2 : ATR-FTIR spectra of synthesized AN-BuA copolymers.

In ATR-FTIR spectral graph above (Figure 4.2), it is possible to see all the characteristic peaks of synthesized polymers related to PAN and PBuA. Here we understand that the polymers contain not the exact monomer feed ratios but there exists a linear correlation between monomer feeds and resultant polymer. Mass

(bulk) polymerization and emulsion polymerization methods are well known with their hard-to-control molecular weight distribution in resultant polymer and their different initial/resultant monomer ratios, thus, this is not a surprising result. On the other hand, from the analyses it is obvious that the synthesized copolymers contain different molar ratios of monomers. In Figure 4.3, the correlation between AN monomer feed rates and ATR-FTIR absorbance ratios of synthesized polymers' related characteristic peaks is shown, which reveals as result the increase of AN existence in resultant polymers.

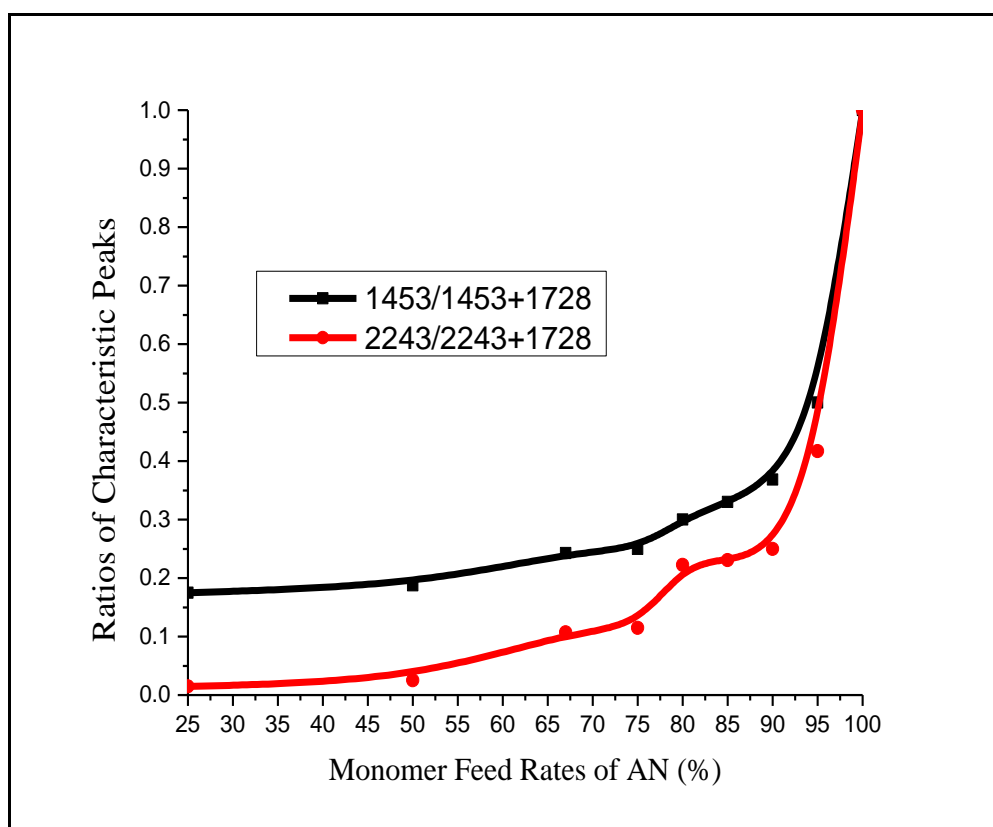


Figure 4.3 : Absorbance ratios of characteristic peaks in copolymer (related to AN feed rates)

4.2 Characterization of Copolymeric Films

Films made by solution casting from 95/5, 90/10, 80/20 and 67/33 AN/BuA mol% copolymers were characterized by ATR- FTIR spectra and Dynamic Mechanical analyses to reveal how they differ from each other as composition and mechanical behavior.

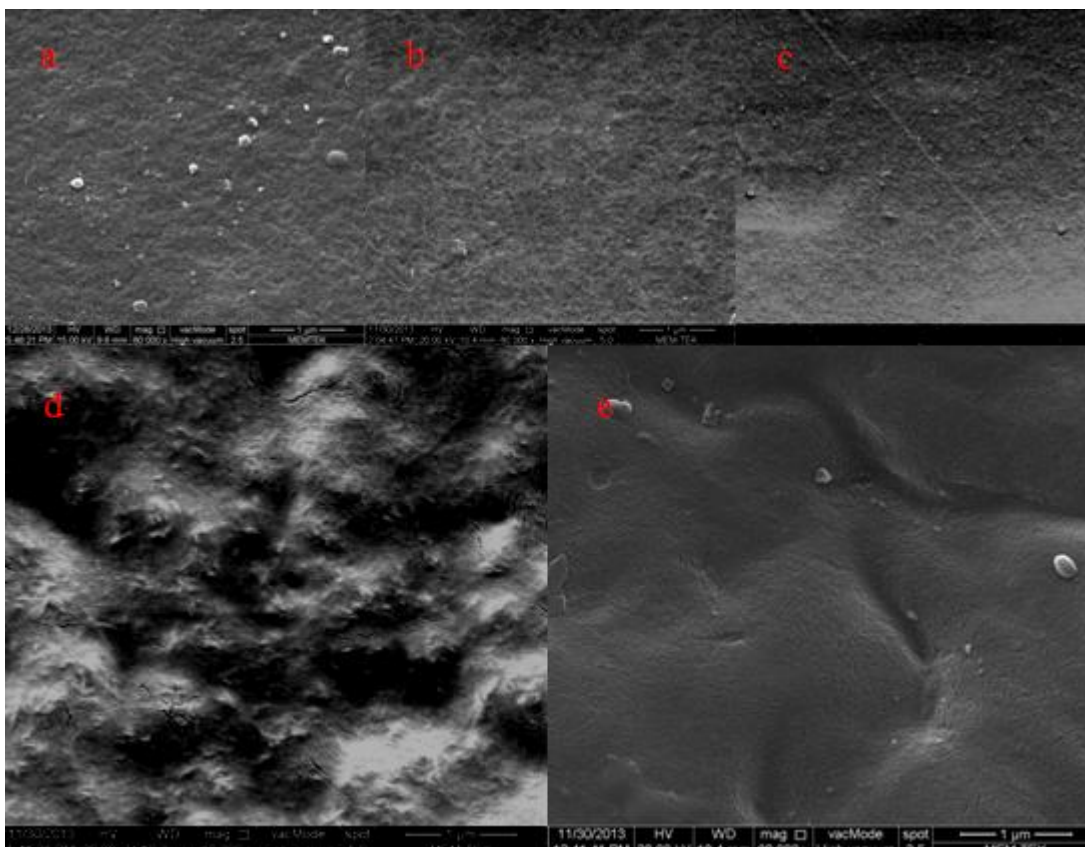


Figure 4.4 : The morphological change of polymeric film surfaces with increasing BuA mol% amount in copolymer structure (a: 100% PAN film, b: 95/5 AN/BuA, c: 90/10 AN/BuA, d: 80/20 AN/BuA, e: 67/33 AN/BuA).

As it is seen in Figure 4.4, the film samples show a change to smoother surface morphology from granular structure, by decreasing AN/BuA ratio. A similar tendency was observed in case of synthesized copolymer particles. It was mentioned before that, the polymer particles change their morphology from white powder-like particles to pale-yellowish latex granules which are larger as particle diameter and which tend to stick to each other, with increasing amount of BuA in resultant copolymer. Long side groups of BuA are responsible creating inter-molecular interactions between molecular chains of the copolymer, and the molecular chains slide and fit onto each other in a better packed form of polymer, and this is resulting the elasticity of polymer with better mechanical characteristics , also the smoother morphology on film surfaces. Furthermore, when a conjugative polymer will be included into the copolymer matrix to create a electrical conductive composite, the negative impact of conjugative polymer on mechanical and morphological properties of resultant product can be compensated with required amount of BuA co-monomer.

4.2.1 FTIR spectroscopy

Films show the expected variation from each other in FTIR spectra (Figure 4.5), because of their different monomer compositions. The characteristic absorbance peaks of related compounds are also clearly seen. Thus, the spectra shows good correlation between absorbance values and monomer contents, as a proof of copolymer structure and composition.

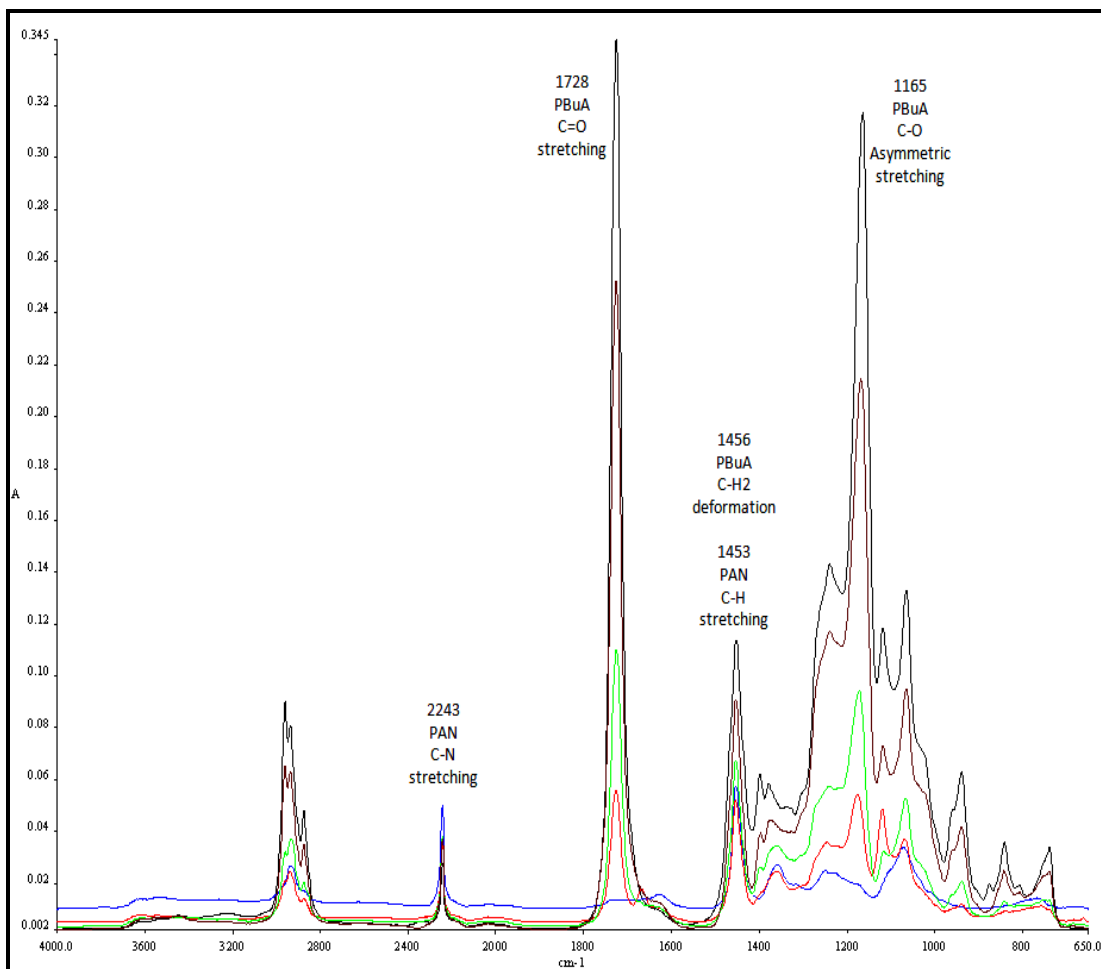


Figure 4.5 : ATR-FTIR spectra of the films made by solution casting from AN-BuA copolymers.

4.2.2 DMA analysis

Stress-Strain tests and Multifrequency-Strain tests were performed on Dynamic Mechanical Analyzer, to reveal the effect of monomer composition on mechanical behavior and Glass-transition temperature (T_g) values of film products.

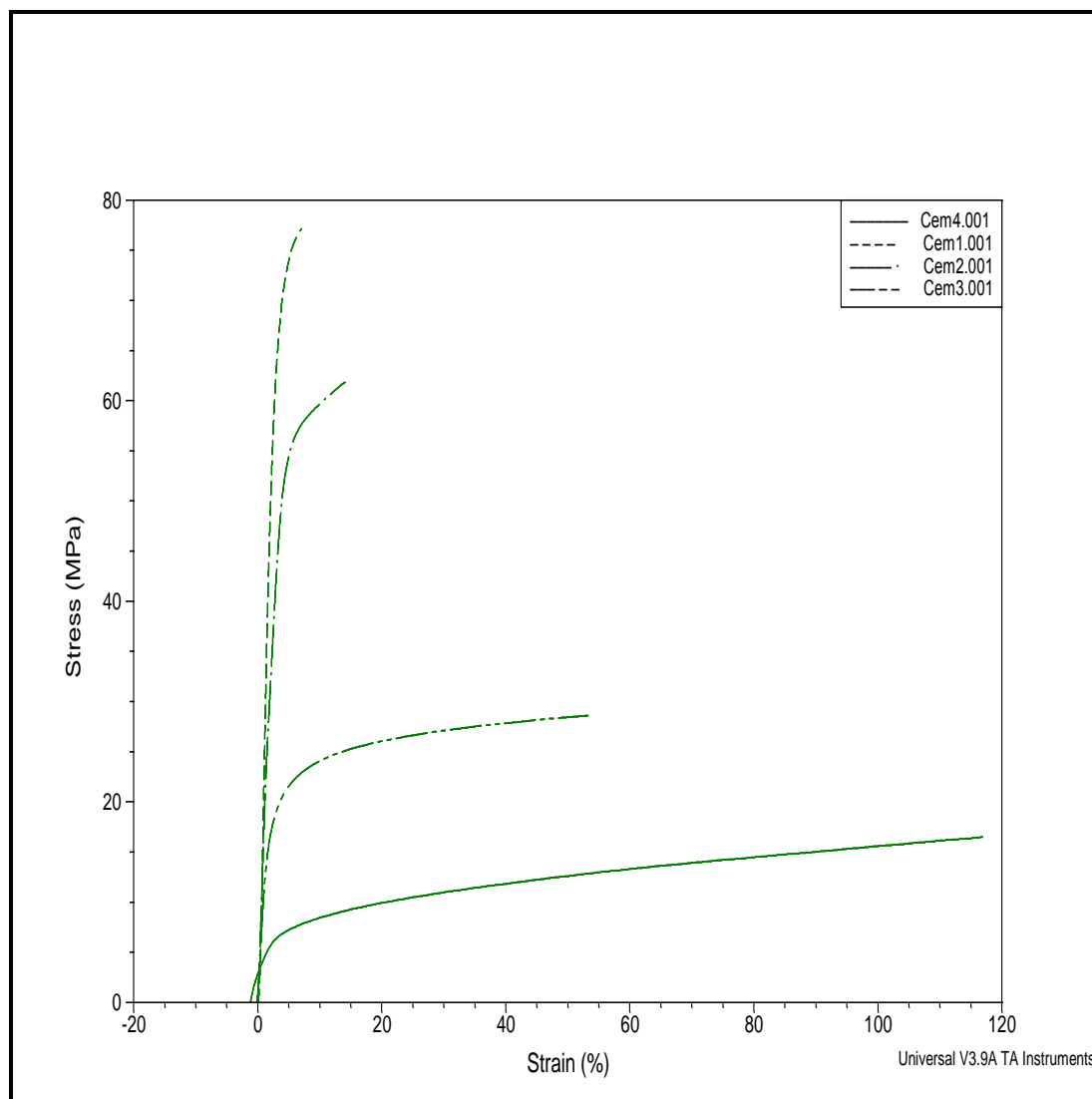


Figure 4.6 : Stress-strain curves of 95/5, 90/10, 80/20 and 67/33 AN/BuA mol% fed copolymeric films (C1 : 95/5, C2 : 90/10, C3 : 80/20, C4 : 67/33).

The stress-strain curves in Fig 4.6 shows how the mechanical behavior drastically changes with increasing BuA monomer content in copolymer structure. Here between DMA film samples the maximum BuA content exists in 67/33, and it shows elastomeric behavior; i.e. it has very high level of strain (120% elongation) when even a very low level of stress (12-13 MPa) was applied.

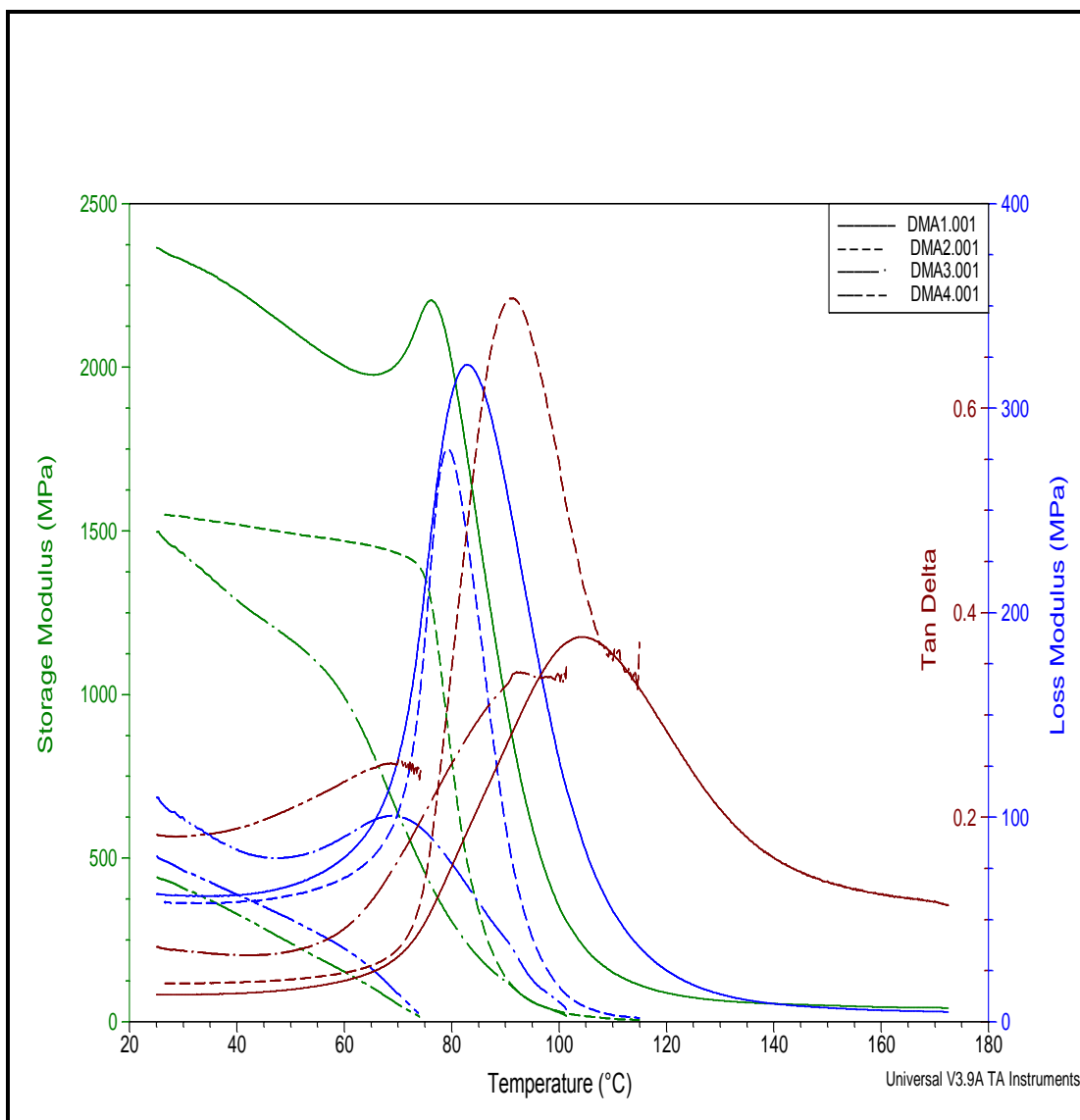


Figure 4.7 : Storage Modulus, Loss Modulus and Tan Delta Curves of Copolymeric Films according to Multifrequency-strain Test Results (DMA1 : 95/5, DMA2 : 90/10, DMA3 : 80/20, DMA4 : 67/33 AN/BuA).

Figure 4.7, both curves show the logical order according to the BuA monomer content of copolymeric films. The BuA content increases, the T_g value decreases. According to Tan Delta peak, the T_g values are approximately 105, 95, 90, 72°C for DMA1, DMA2, DMA3, DMA4 film samples; and according to Storage Modulus peak, the T_g values are about 80, 75, 60, 40-45°C for same order of samples.

4.2.3 Thermal gravimetric analysis (TGA)

Thermal analyses were performed on prepared polymeric samples to understand the change in their decomposition behavior by applied heat. The decomposition behavior

is a critical point especially for end-uses which include high temperatures as ambient conditions, such as filtering-systems, protective coatings, protective clothings, etc.

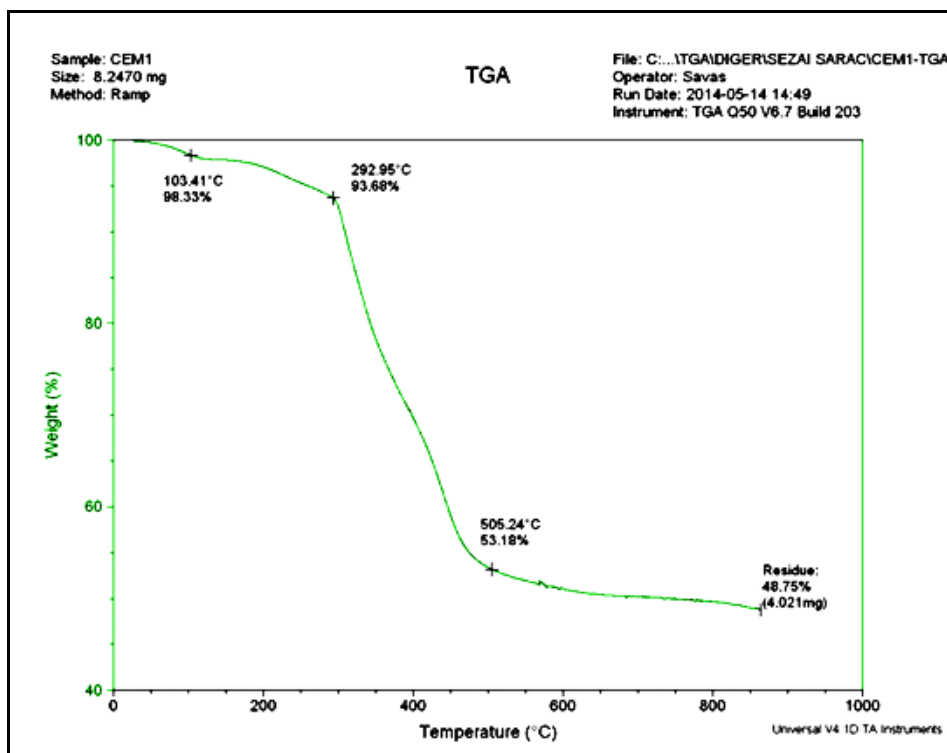


Figure 4.8 : Decomposition analysis of 100% PAN film.

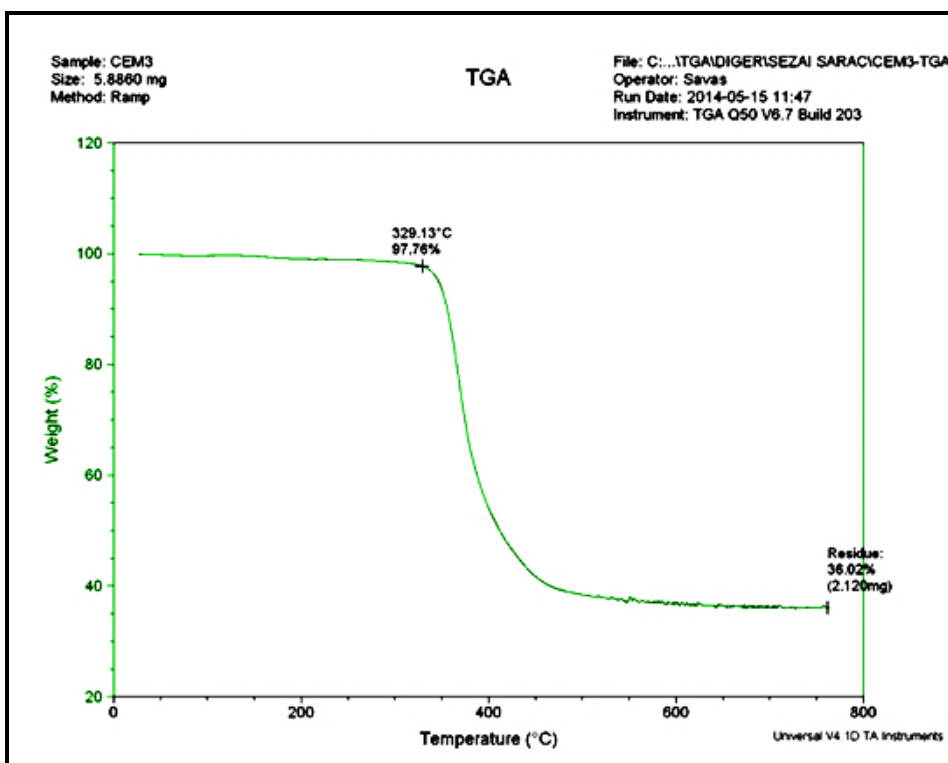


Figure 4.9 : Decomposition analysis of 95/5 mol% AN/BuA copolymeric film.

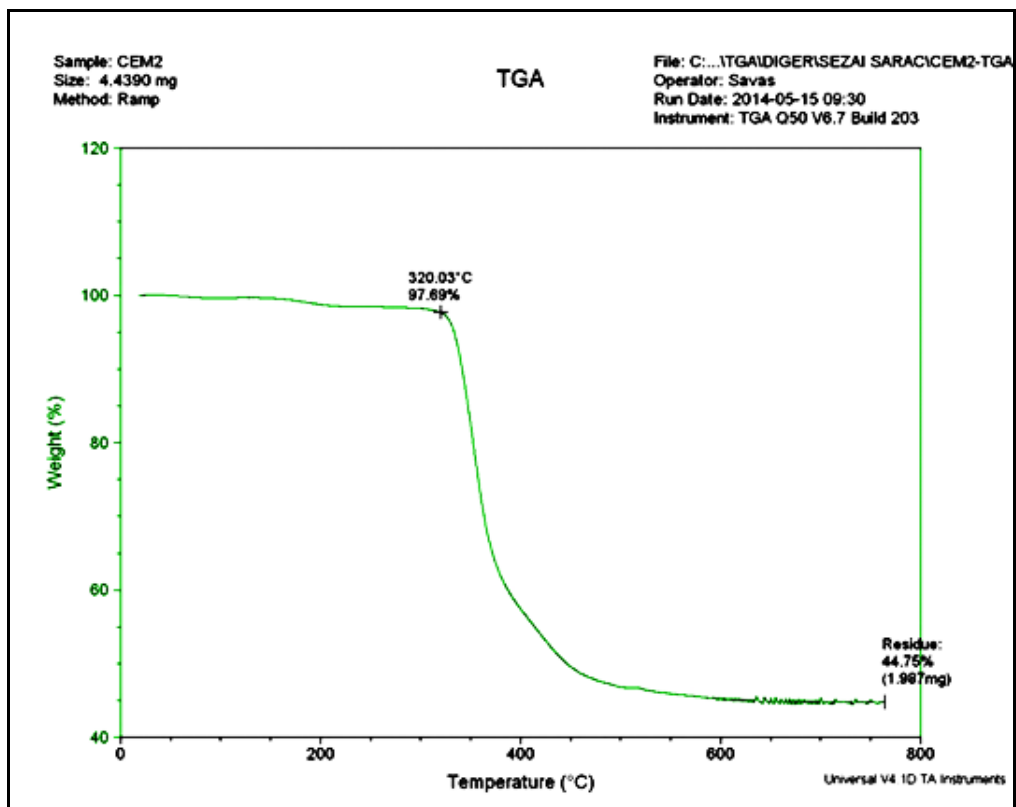


Figure 4.10 : Decomposition analysis of 90/10 mol% AN/BuA copolymeric film.

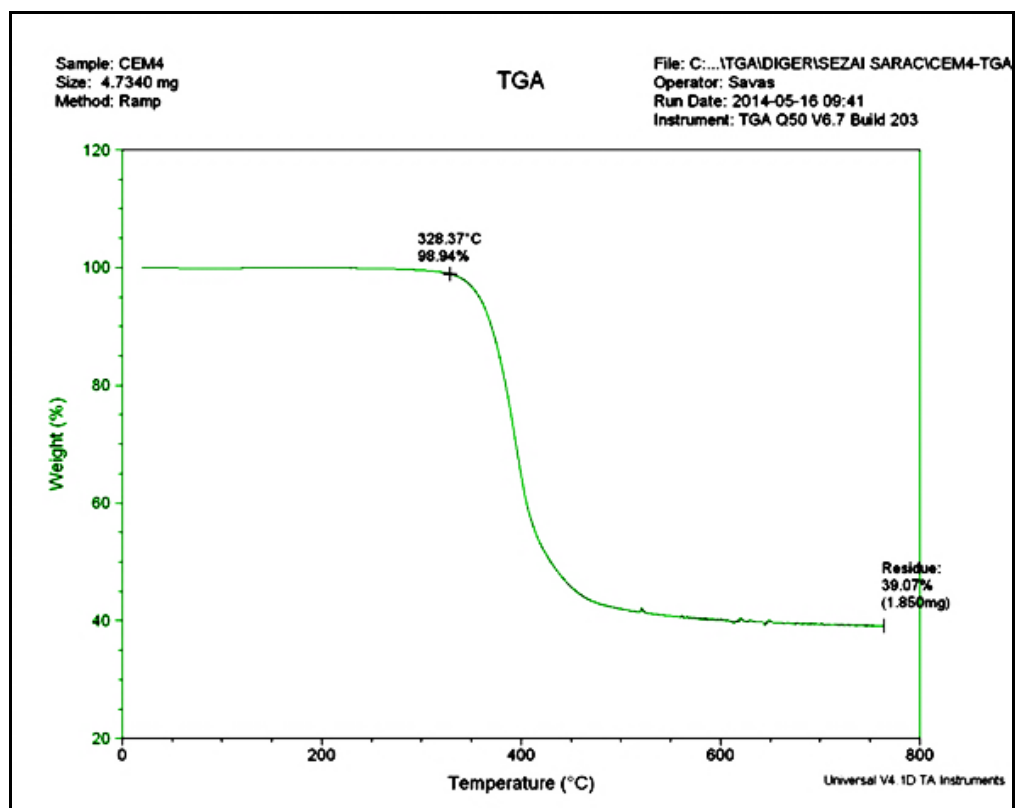


Figure 4.11 : Decomposition analysis of 85/15 mol% AN/BuA copolymeric film.

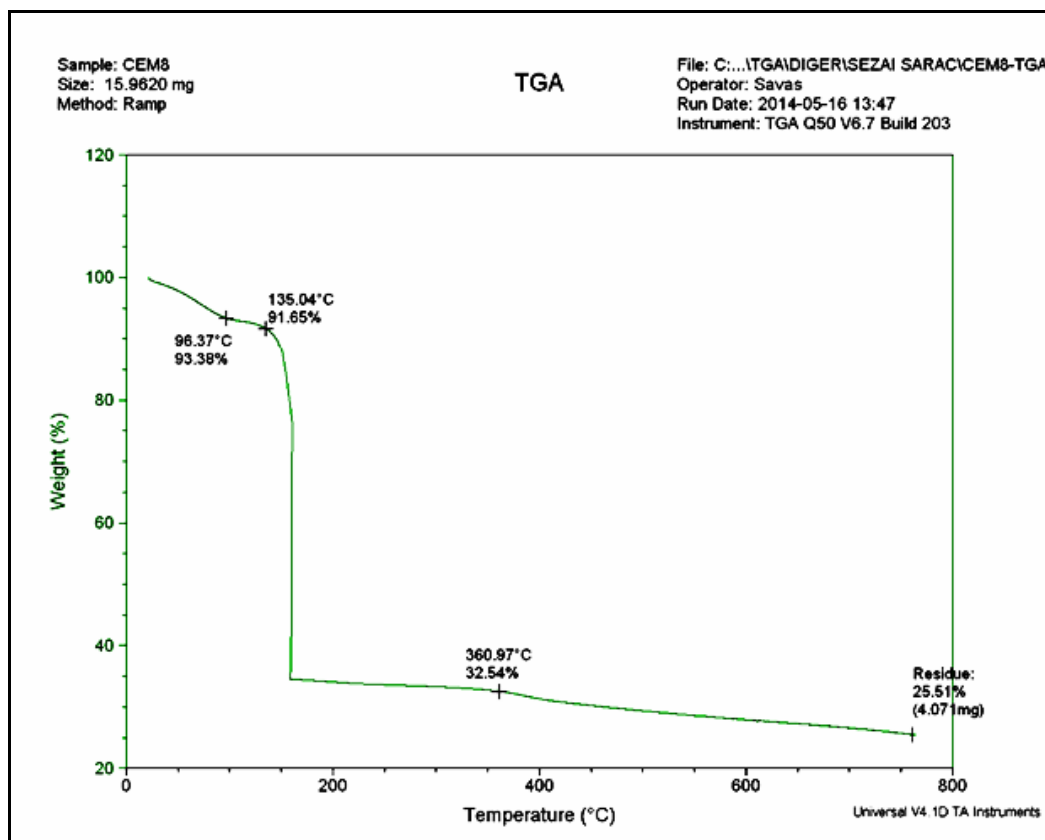


Figure 4.12 : Decomposition analysis of 90/10 mol% AN/BuA + 200Py copolymeric film by TGA.

As it can be seen in the TGA graphs in Figure 4.8 to 4.12, 100% PAN polymeric film showed a decomposition between 280-290°C; while the samples with BuA in polymer structure showed around 325-330°C. This increase indicates that BuA comonomer improved thermal stability. On the other hand, the residue material left after completely burning was decreased from approximately 50% to 30-40% of initial mass at the end of process. Also, PPy inclusion in copolymer matrix drastically affected the thermal resistance, which it was already expected as electroactive polymers show low thermal resistances.

4.3 Characterization of Composite Films

4.3.1 FTIR spectroscopy

ATR-FTIR spectroscopic analysis revealed all the characteristic absorbance peaks of DMF, PAN, PBuA, and PPy in P(AN-co-BuA) and P(AN-co-BuA)/PPy composite films (Fig. 4.14). It was already expected to see some shifts of the absorbance bands because of inter-molecular and inter-planary interactions. The peak observed at 1315

cm^{-1} can be assigned to C-H in plane vibration [208-210], as well as inclusion of Cerium into structure by doping of conductive polymer due to further oxidation (see in Fig. 4.13). Linear and significant dependency of absorbance of C-N stretching (at 1454 cm^{-1}) versus increase in initial Py amount indicates the increase in PPy content [211] in composite while absorbance changes in characteristic peaks of DMF and P(AN-co-BuA) matrix in composite stay constant (Fig. 4.13, Fig. 4.14).

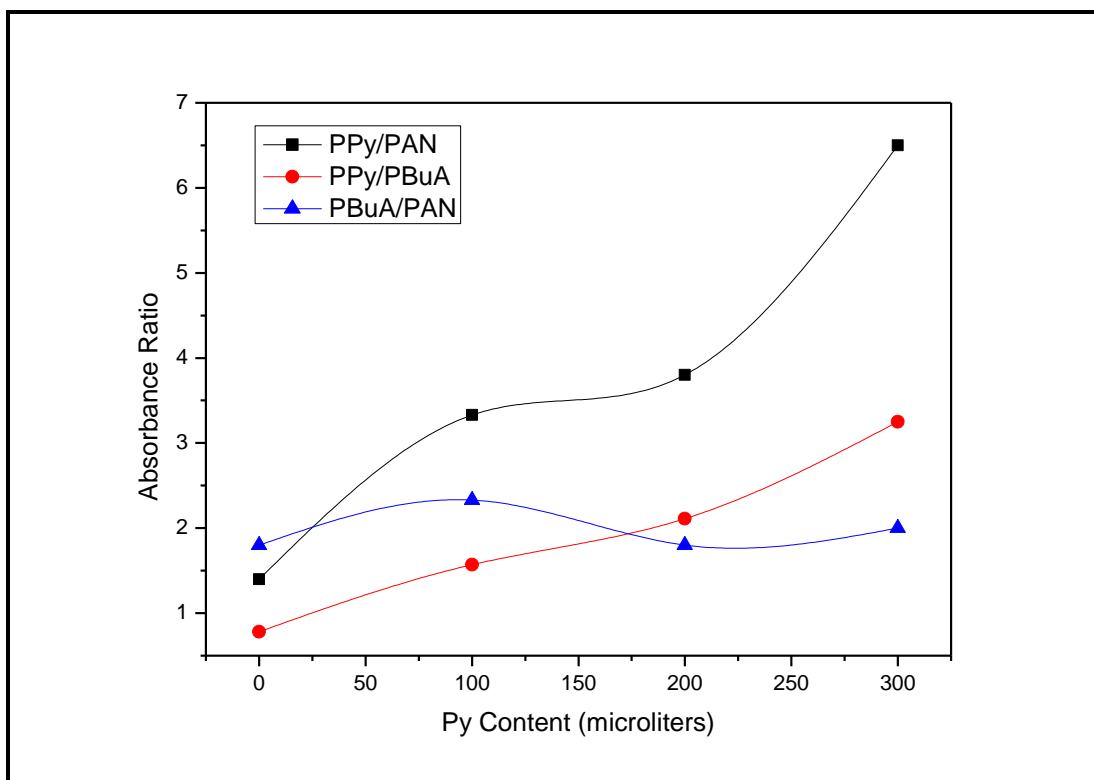


Figure 4.13 : The changes of characteristic peaks' ratios of copolymer matrix and PPy related to Py contents.

Fig. 4.13 shows how the characteristic absorbance peak of PPy increases while others almost do not show any change. To reveal this relation, only three absorbance peaks were taken to account. Because as be seen in Fig. 4.14, other absorbance peaks are in the shared absorbance bands of more than one components. For instance, characteristic absorbance peak of DMF (1666 cm^{-1} C=O stretching) and C-C stretching absorbance peak (1644 cm^{-1}) make some shift and meet in the same band, and occurs as one absorbance peak in ATR-FTIR spectra.

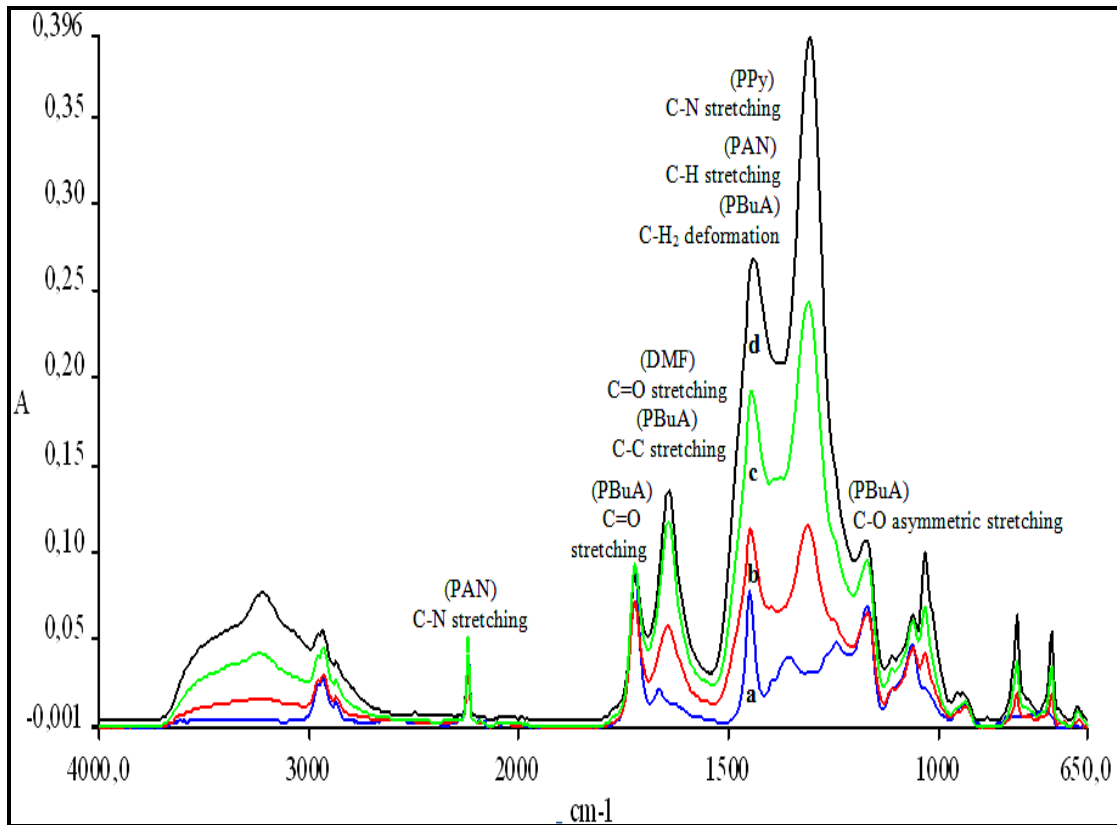


Figure 4.14 : ATR-FTIR spectra comparison graph of composite thin films with various Py contents (a: 0µl, b: 100µl, c: 200µl, d: 300µl).

4.3.2 DMA characterization

Homopolymer form of PPy is well known with its fragile structure and bad mechanical behaviour. Thus, it is expected to see worse mechanical behaviour with increasing initially Py content of composite thin films.

Homopolymer of BuA (PBuA) is a resin-like material, and when it is in copolymer structure with another monomer like Acrylonitrile (AN), it improves the mechanical properties of that copolymer. So, it is possible to say that, existence of BuA in copolymer matrix has a contrary effect with Py content. Thus, in order to avoid the fragile structure of composite thin films with increasing Py content, the molar ratio of BuA monomer within copolymer can be increased.

Stress/strain curves were obtained on DMA instrument, and in Fig. 4.15, curves show all the expected results [314,315]. In figure it is also important to see the enhancement in mechanical behavior with BuA inclusion. 95/5 mol% AN/BuA film shows a better characteristic than the film produced using commercial PAN-Aldrich.

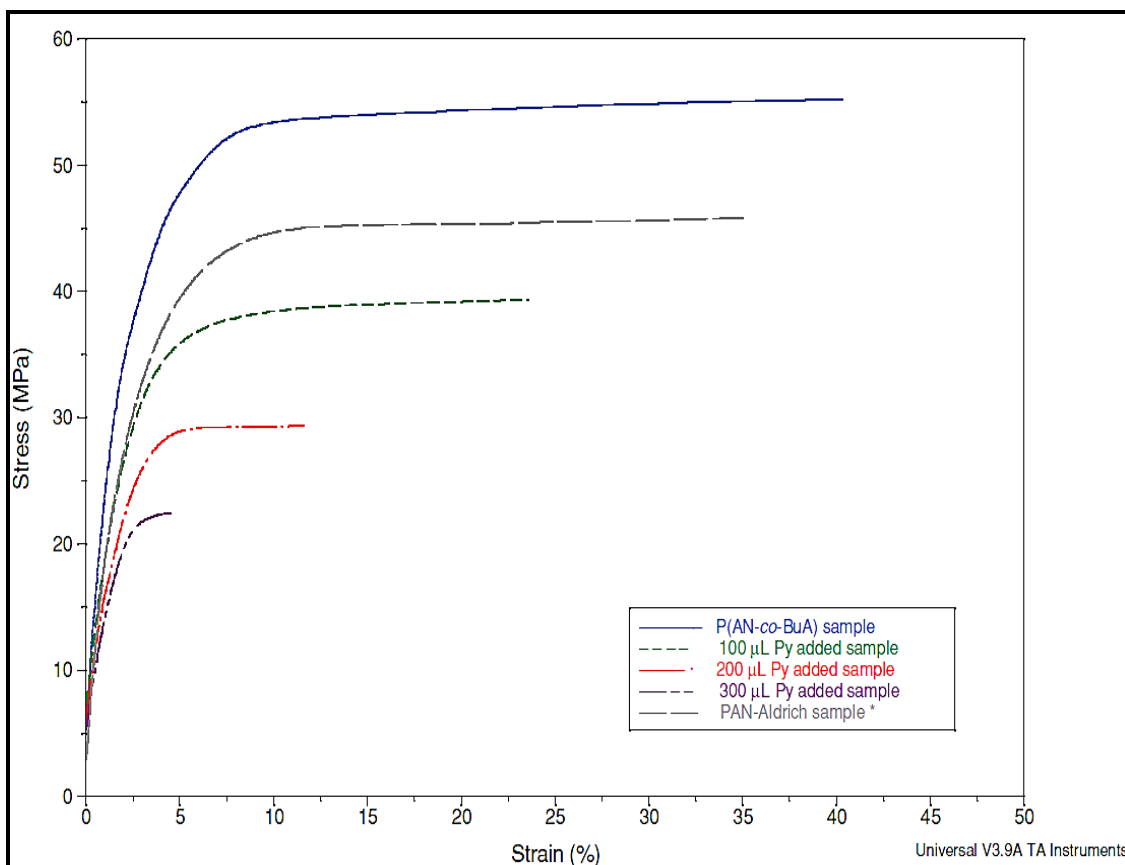


Figure 4.15 : Stress / Strain curves of composite thin films with various Py contents.

4.3.3 Morphological characterization

Two extreme composite thin films (thin film with no Py added, and thin film with 300 μl Py added) were chosen to see more clearly the difference between the surface visual appearance. Scanning Electron Microscope (SEM) images revealed the visual change more with increasing magnification as can be seen in Fig. 4.16 and Fig. 4.17.

In SEM images, it is possible to see that the composite thin film with no Py added has a much more smooth surface view, and the 300 μl Py added composite thin film has many pore-like (or Polypyrrole core-shell) structures and segmental surface, can be measured as having an approximately 800-900 nm width in Fig. 4.17. For deep understanding, it is needed to make further visual analyses on composite thin film surfaces. As a result, it can be simply said that, film surface characteristic is changing to a rougher morphology with increasing PPy content (Fig. 4.16 and Fig. 4.17).

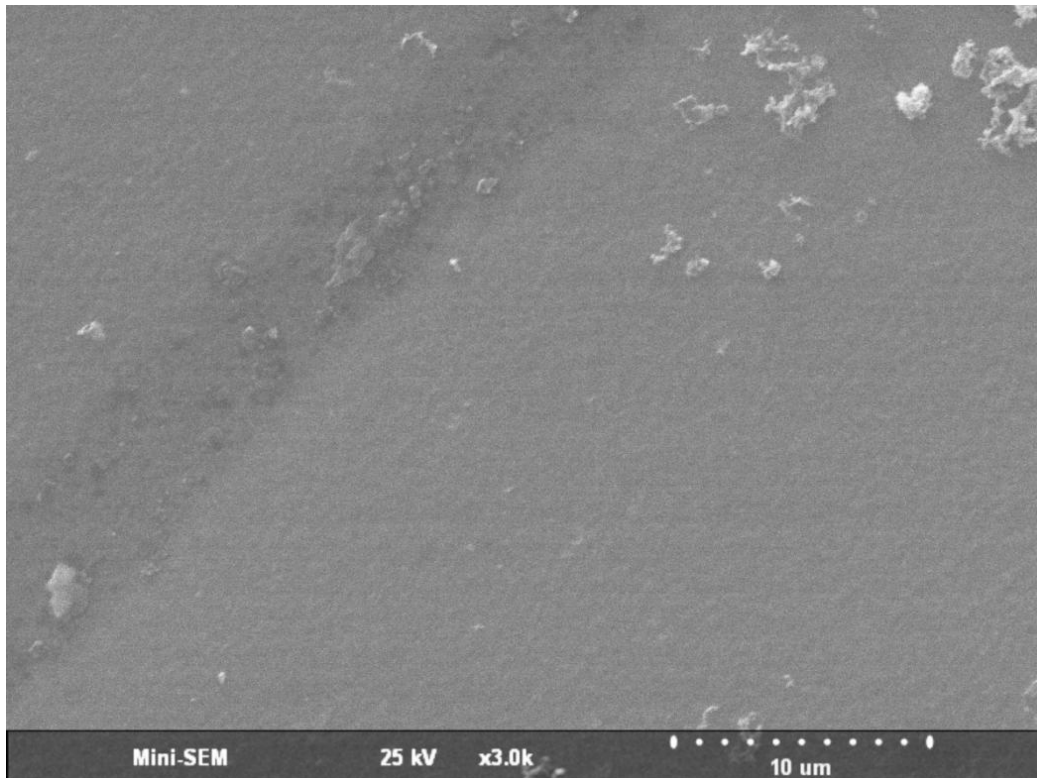


Figure 4.16 : SEM image of composite thin film with no Py added (X3000 magnification).

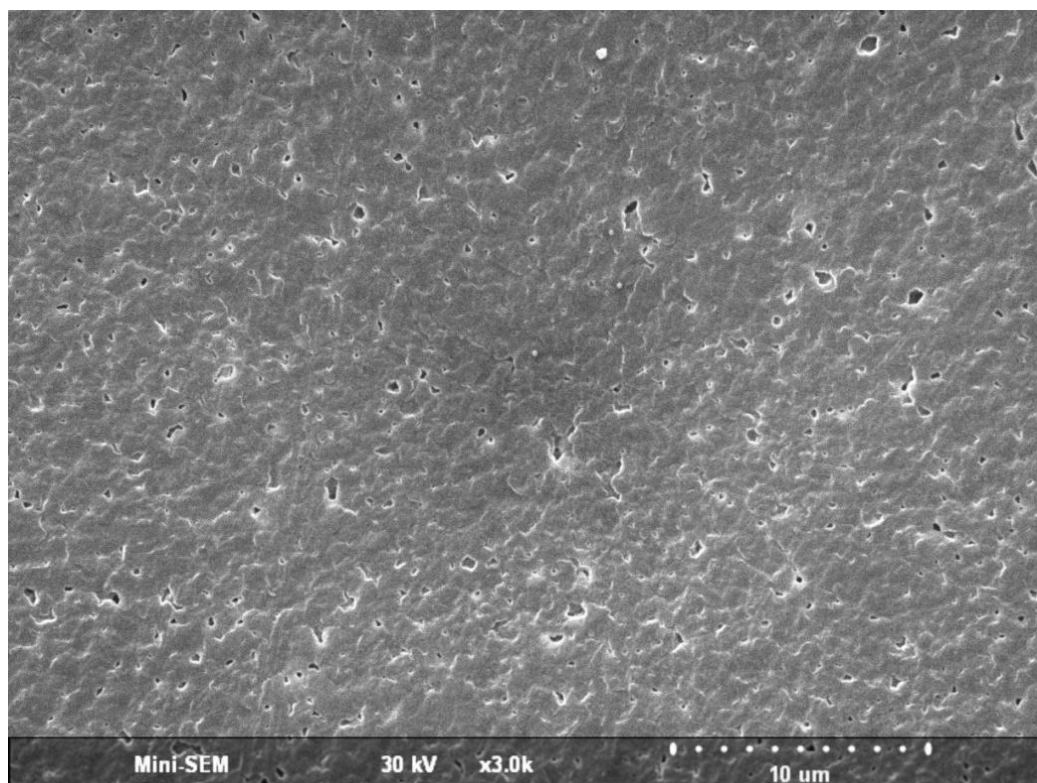


Figure 4.17 : SEM image of composite thin film with 300 μ l Py added (X3000 magnification).

4.3.4 Impedance spectroscopy

Electrical impedance analyses were performed on composite thin films to see their dielectric constants, electrical conductivity, and impedance values [315].

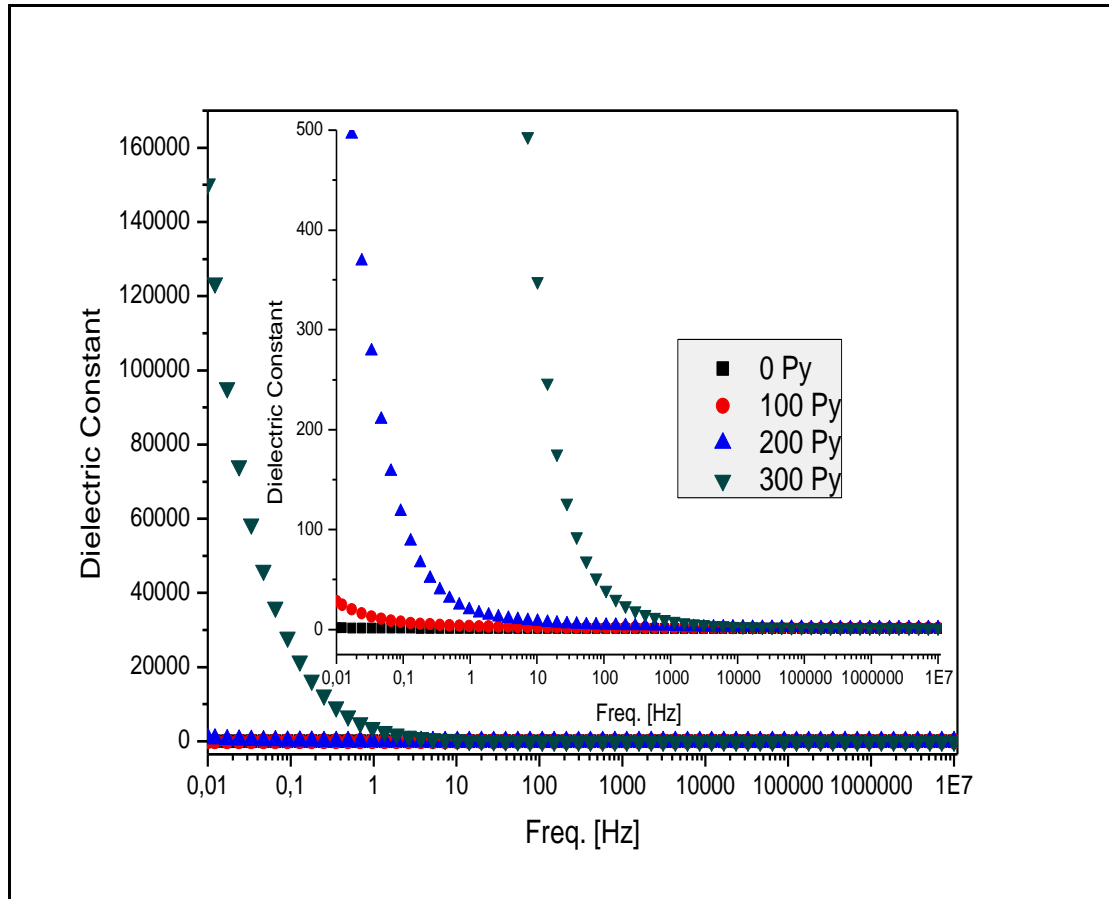


Figure 4.18 : Variation of dielectric constants of the composite thin films with 0, 100, 200, and 300 μl Py (INSET: Extended view of the curves).

Within 0.01–10 Hz frequency band, dielectric constant values show positive correlation with PPy contents of composite thin films. This tendency can be seen better in inset of Fig 4.18. Because 300 μl Py added composite film has a very high dielectric constant at 0.01 Hz as seen in Fig. 4.18, an extended view is shown on the same figure to reveal diversity in a larger detail.

Dielectric constants are differing in lower frequency values, but they approach to zero value at the ranges higher than 1 - 10 Hz band (Fig. 4.18).

Conductivity values (calculated via both Real and Imaginary Conductivity values) are not showing a direct correlation since a frequency band of 46 kHz - 64kHz ; but

at lower frequencies there is a positive correlation between conductivity and Py content values (Fig. 4.19).

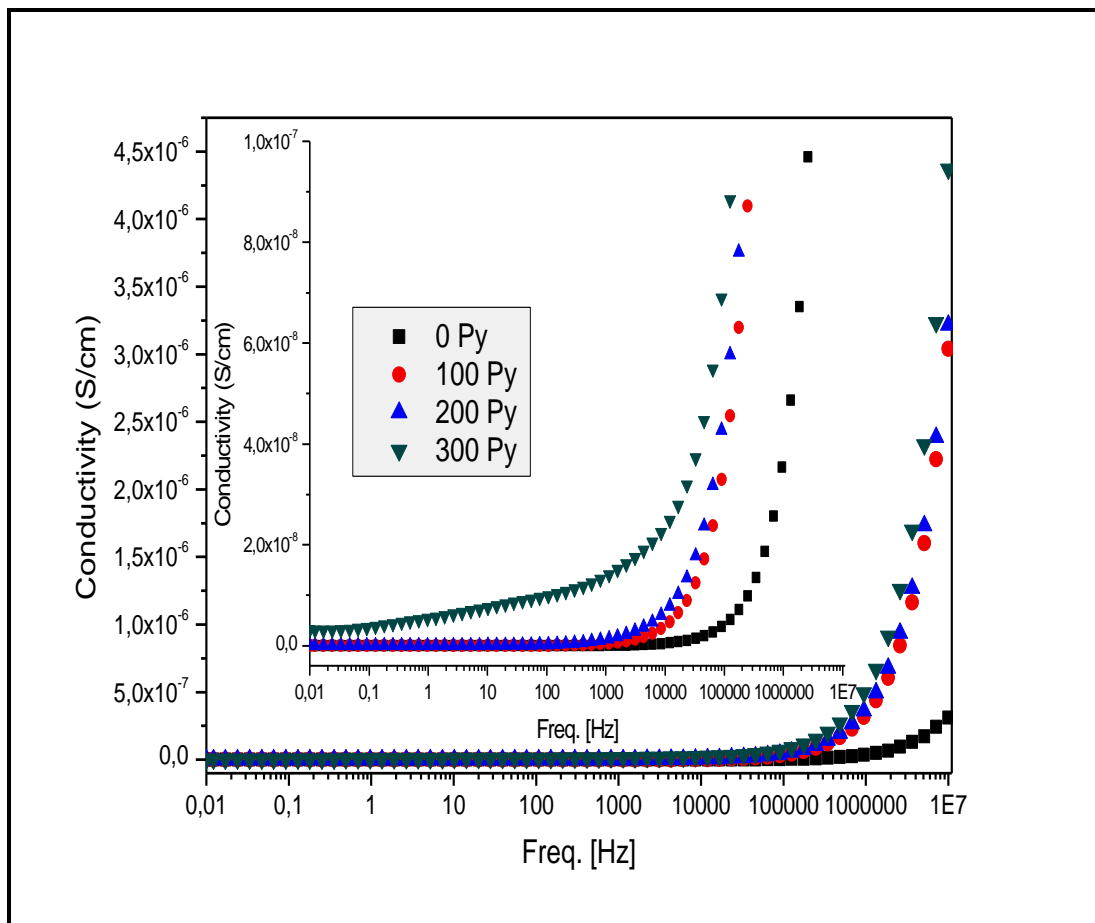


Figure 4.19 : Conductivity curves of composite thin films (INSET: Extended view of the curves).

As can be seen in Fig. 4.20, impedance curves of composite films are ordered in an inverse correlation with Py contents, and the curves start to differ more from each other starting from the 10 Hz – 100 Hz frequency band to the lower frequencies.

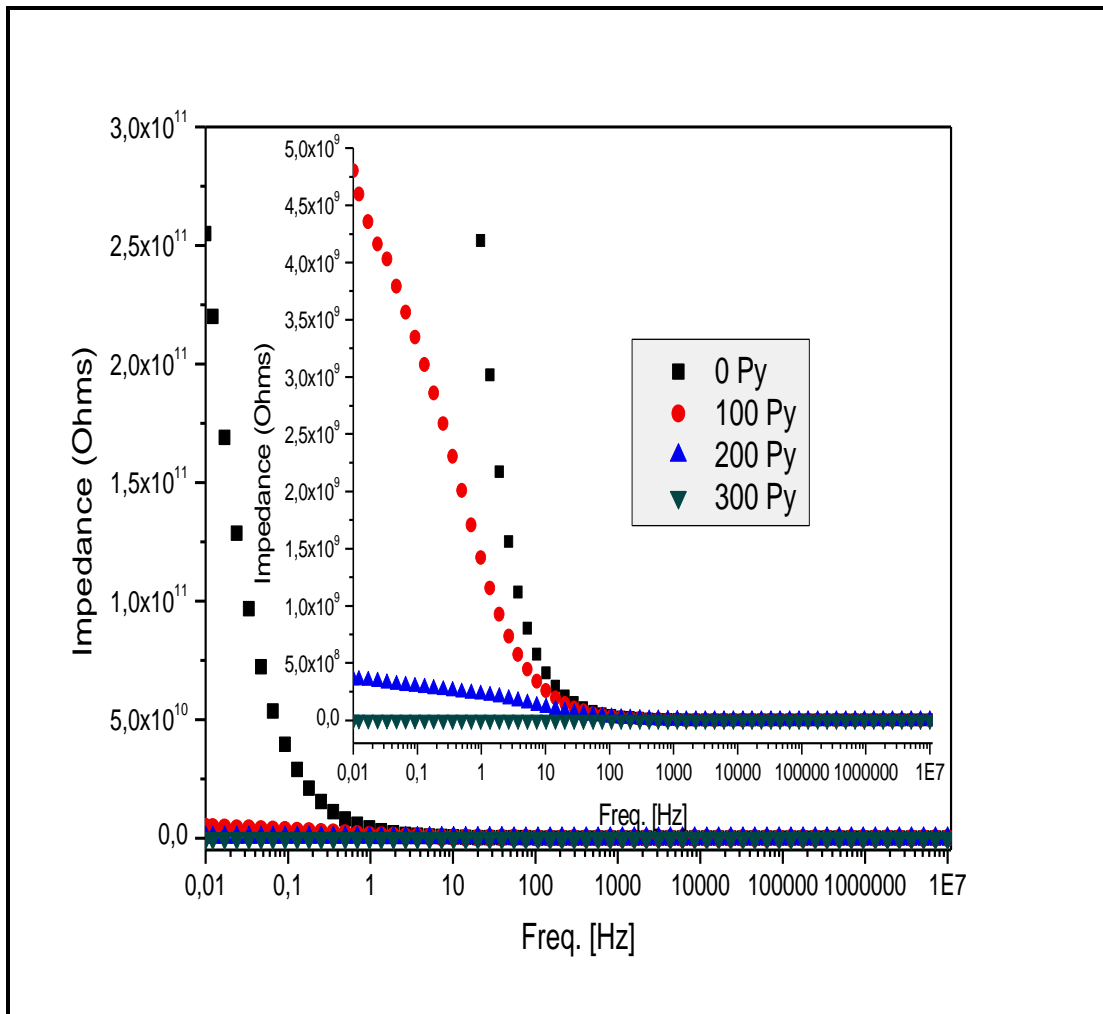


Figure 4.20 : Impedance curves of composite thin films (INSET: Extended view of the curves).

The relation between impedance curves of composite thin films can be seen more clearly in zoomed part of the same figure which shows the impedance curves comparison graph in a larger view. Figure 4.21 shows the relation between initial Py contents, mechanical breakdown stress, and conductivity values of composite thin film samples.

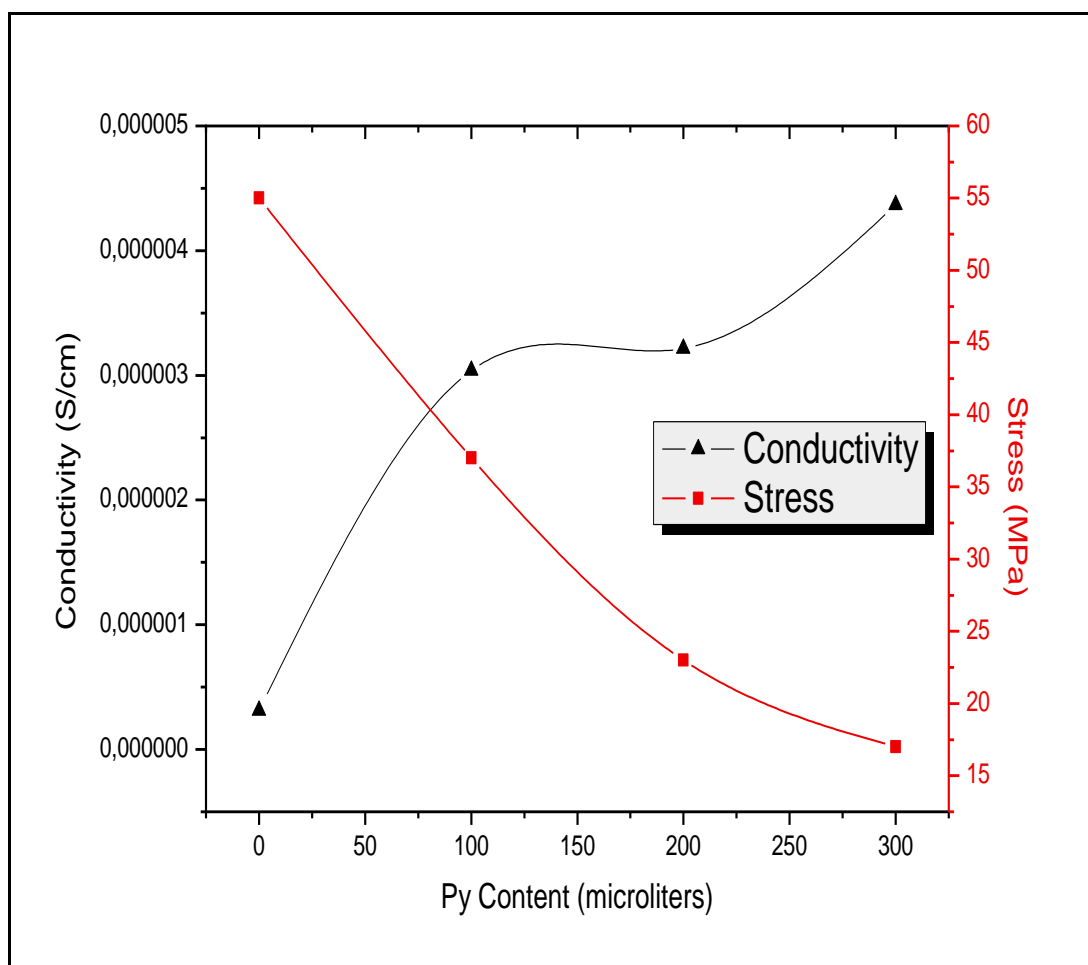


Figure 4.21 : 2-Y graphical view of relation between Py contents, breakdown stresses, and conductivity values (at 10^7 Hz) of composite thin films.

The results of this study on produced composite thin films reveal that, with increasing amount of added Py to polymerize in P(AN-co-BuA) matrix, the absorbance peaks of PPy polymer also increase. This was clearly observed by ATR-FTIR spectrophotometric results. The increased PPy content in copolymer matrix results worse mechanical properties, causing both lower breakdown force and shorter elongation under applied tensile stress while dynamic mechanical analyzes. PPy content also results in different and rougher visual apperance on composite thin film surface. Electrical properties of composites showed interestingly different tendencies with various subjects of analysis, including dielectric constants, conductivities, and impedances. While dielectric constants and impedance values of composites were showing positive correlation with PPy content, the conductivity values were not in a similar order within whole applied frequency range, but under all frequencies lower than 46 kHz. This situation can be explained by the different

surface characteristics of each composite thin film, and/or different PPy distribution ratio in copolymer matrix. But also it gives future hopes to create new ideas of various application areas which need different mechanical properties while suitable electrical conductivities.

4.4 Nanofiber Characterization

Because nanofibers are difficult to handle in their stand-alone form, mechanical analyses were not made, but were only optical and statistical analyses.

In addition to optical microscopic measurements, for further details Scanning Electron Microscope (SEM) images were taken. The samples' surfaces were coated with Gold-Palladium (Au-Pd) particles prior to SEM analyses.

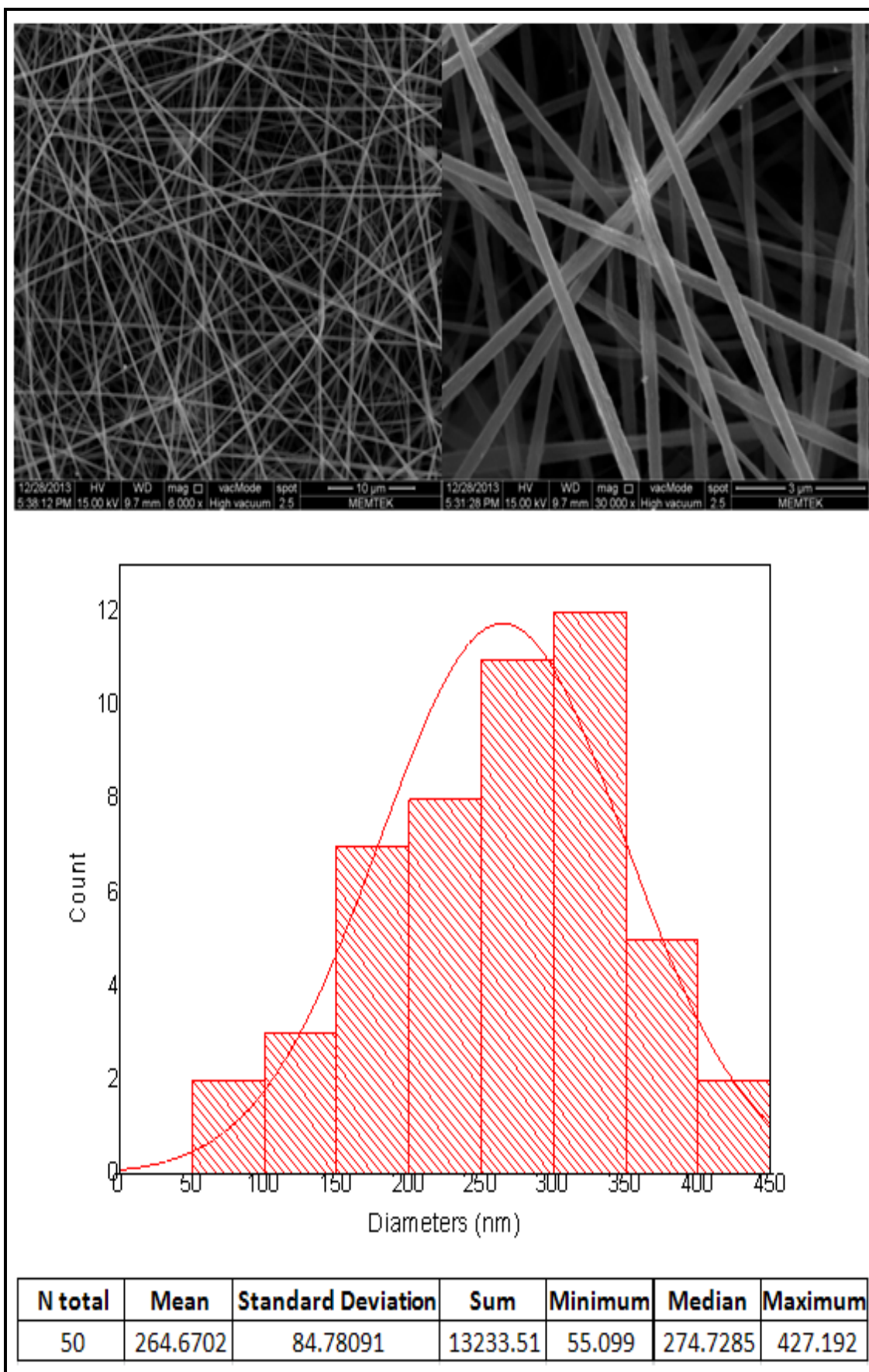


Figure 4.22 : SEM pictures and average diameter analyses of co-1 nanofibers.

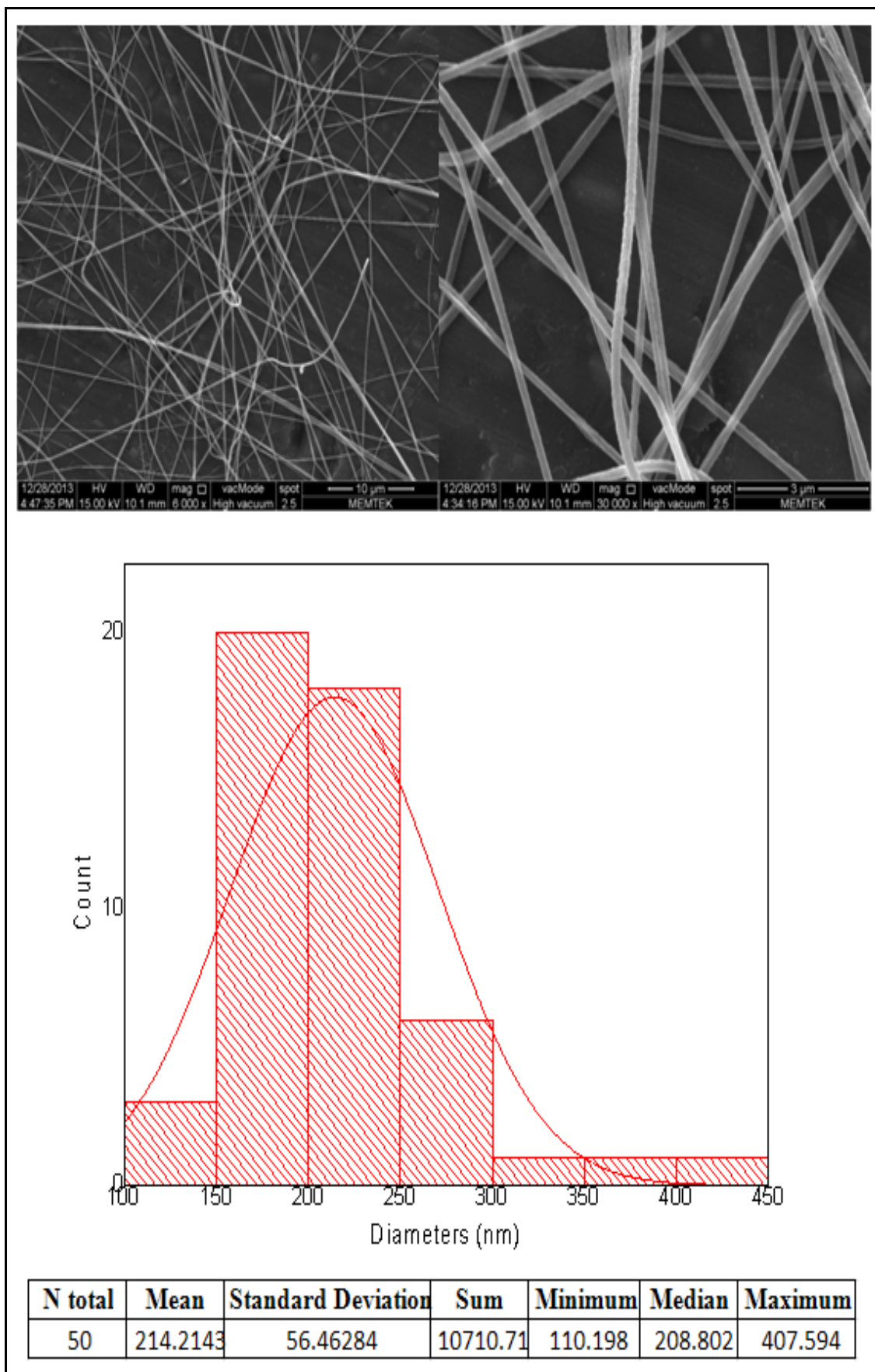
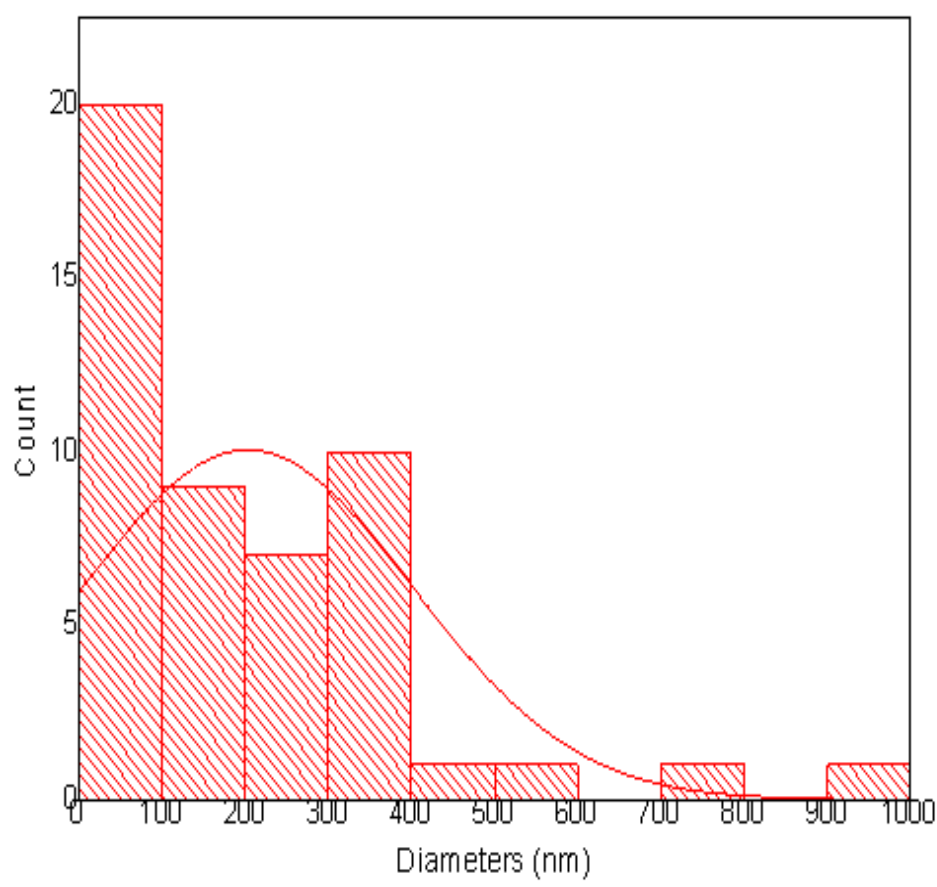
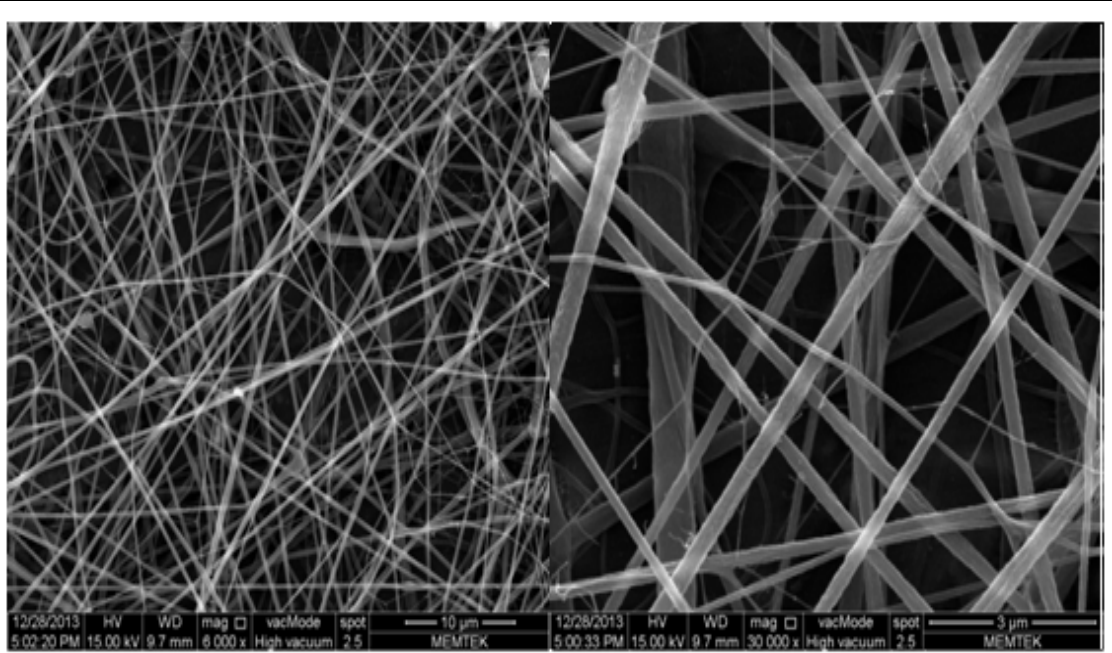


Figure 4.23 : SEM pictures and average diameter analyses of co-2 nanofibers.



N total	Mean	Standard Deviation	Sum	Minimum	Median	Maximum
50	203.1654	198.39475	10158.27	12.987	131.7885	966.63

Figure 4.24 : SEM pictures and average diameter analyses of co-3 nanofibers.

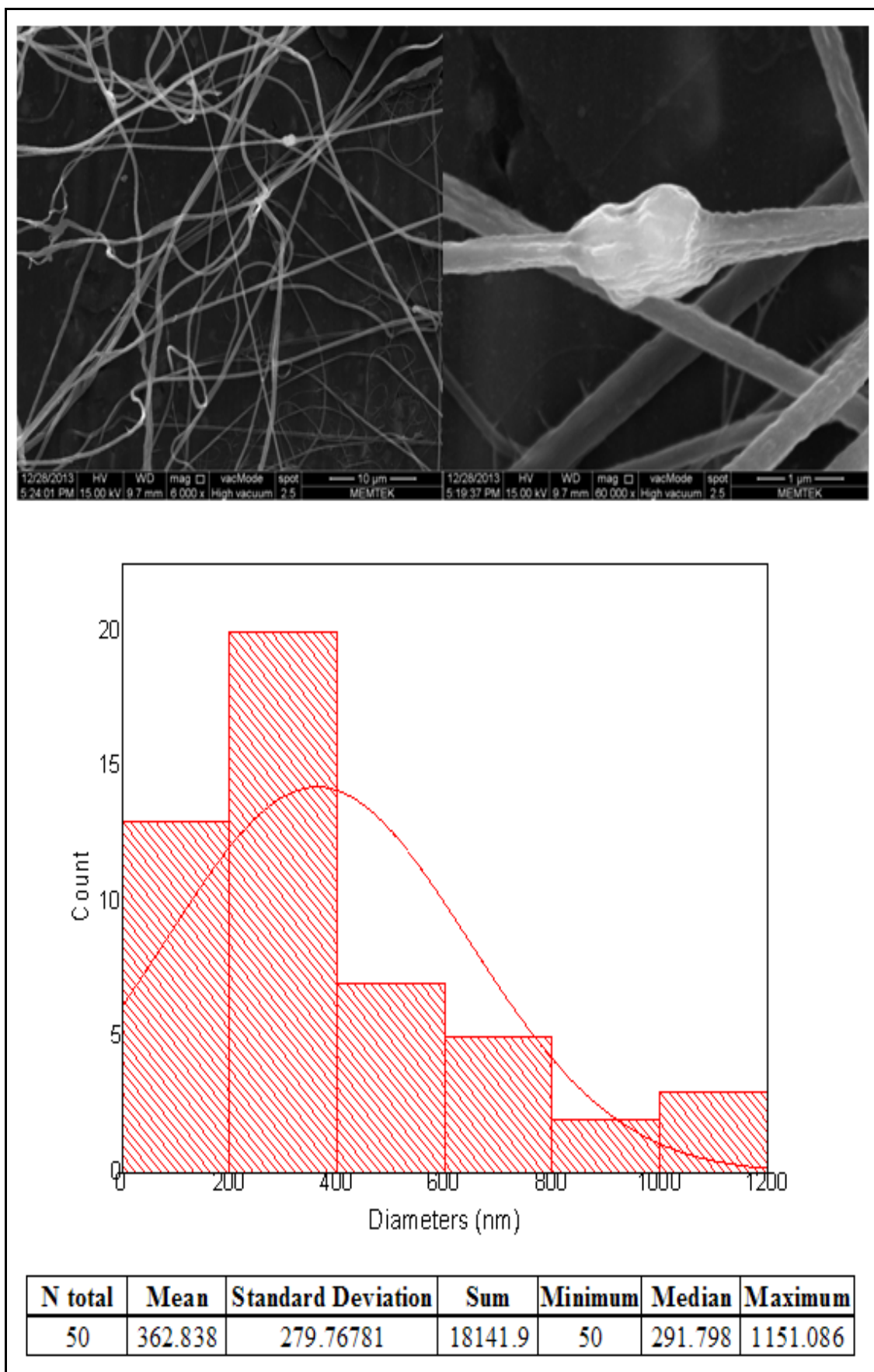


Figure 4.25 : SEM pictures and average diameter analyses of co-4 nanofibers.

First four nanofiber samples (from Figure 4.22 to 4.25) were electrospun from DMF solutions of AN-BuA copolymer. The samples co-1 and co-2 have same applied voltage (10 kV) and tip-collector distance (10 cm), but different feeding rates (0.3 ml/h and 0.15 ml/h). And, the samples co-2, co-3, and co-4 have constant feeding rate and tip-collector distance as 0.15 ml/h and 10 cm; but the only variable parameter they have is the applied voltage, as 10, 15, and 20 kV.

Co-1 and Co-2 samples give smooth fiber surfaces, with a low-deviated fiber diameter distribution. Furthermore, decreasing the feed-rate (Co-1: 0.3 ml/h, Co-2: 0.15 ml/h) resulted in thinner nanofibers (mean value of fiber diameters decreased from 265 nm to 214 nm).

A great deviation from mean fiber diameter is observable with increasing applied voltage, for Co-2, Co-3, and Co-4 samples. Especially in SEM pictures of Co-3 and Co-4, ultra-thin fiber formation can be seen. Such a formation was thought to be happened because of higher voltages per cm. All the four nanofiber samples were prepared from the same solution, thus, it is not possible to say that such a non-uniform diameter distribution can happen due to non-homogeneous electrospinning solution; because the first two samples (Co-1 and Co-2) give quite uniform and smooth fibers from the same solution, with different electrospinning parameters.

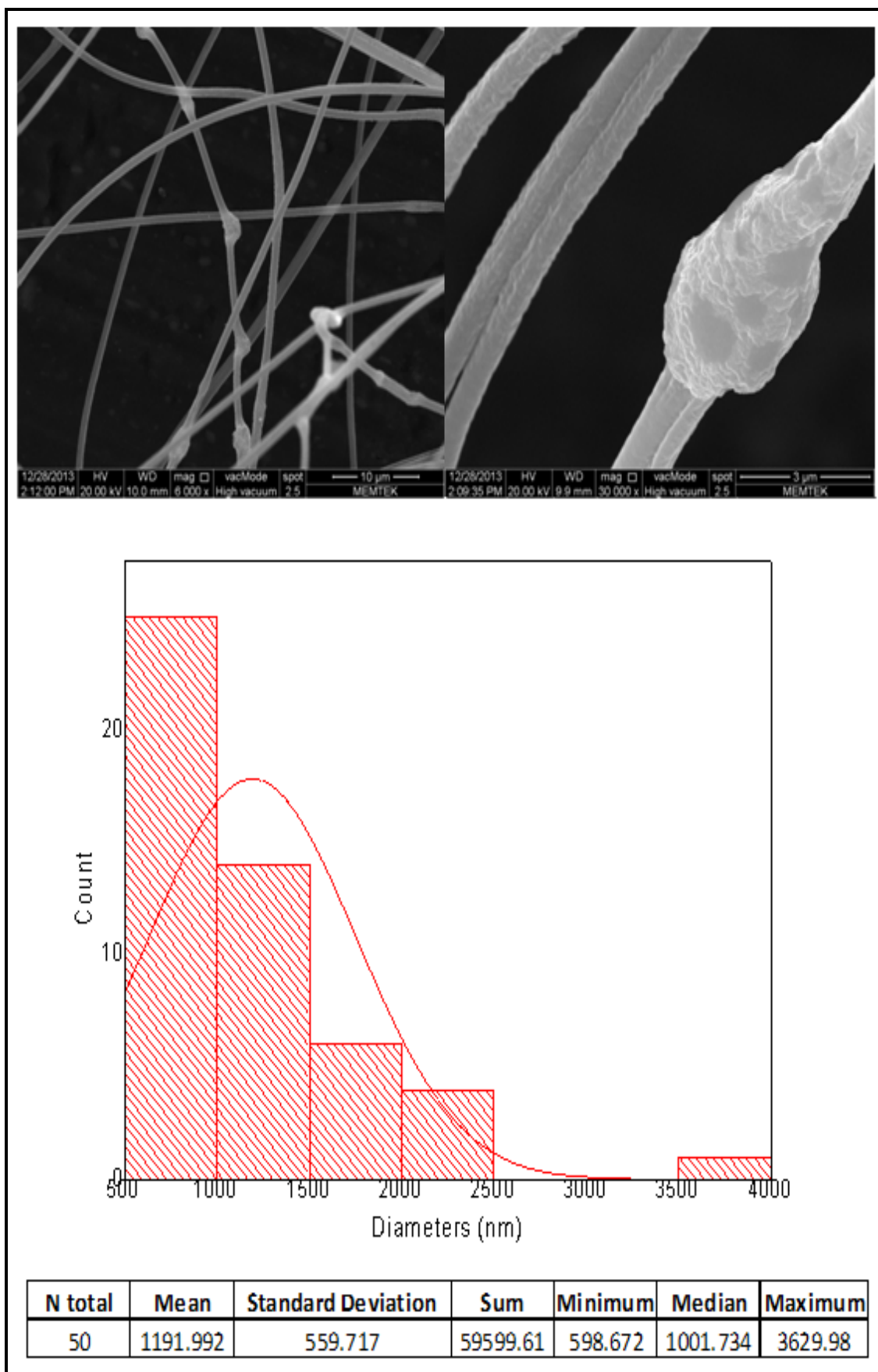
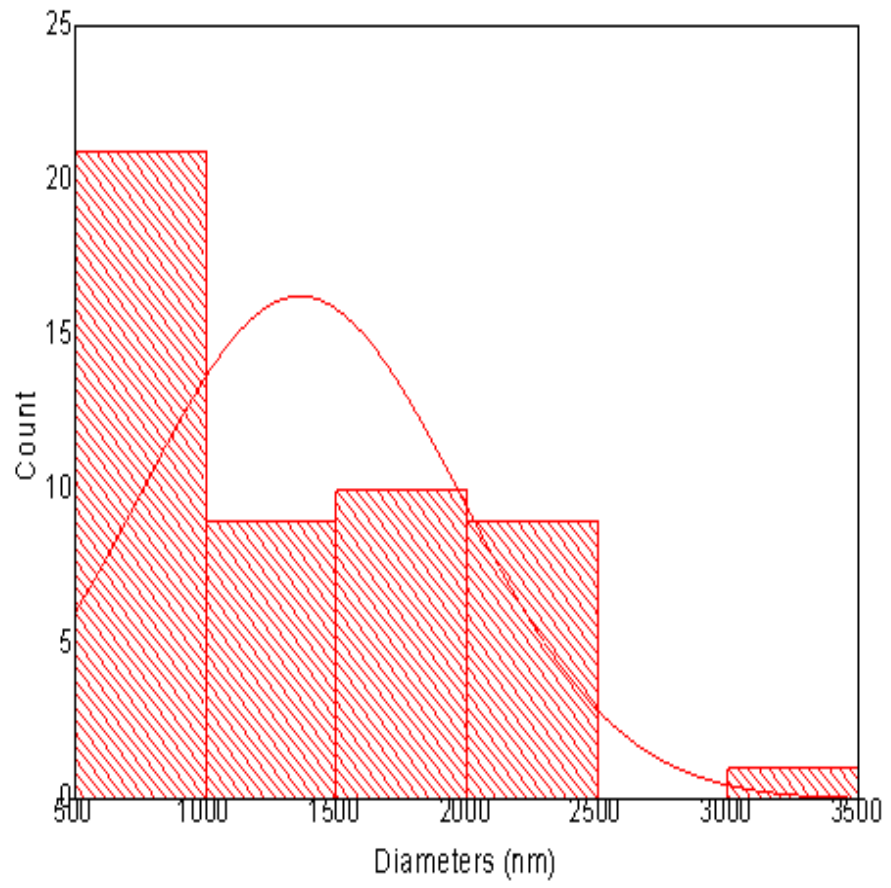
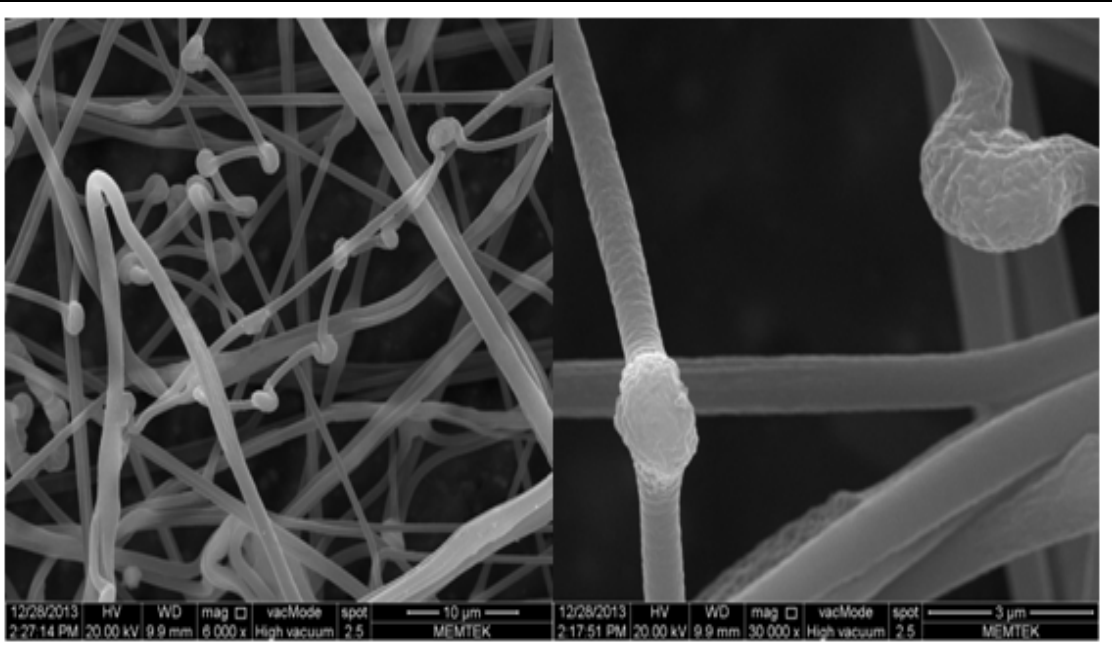


Figure 4.26 : SEM pictures and average diameter analyses of coPy-1 nanofibers.



N total	Mean	Standard Deviation	Sum	Minimum	Median	Maximum
50	1362.333	612.49798	68116.64	589.063	1148.458	3117.198

Figure 4.27 : SEM pictures and average diameter analyses of coPy-2 nanofibers.

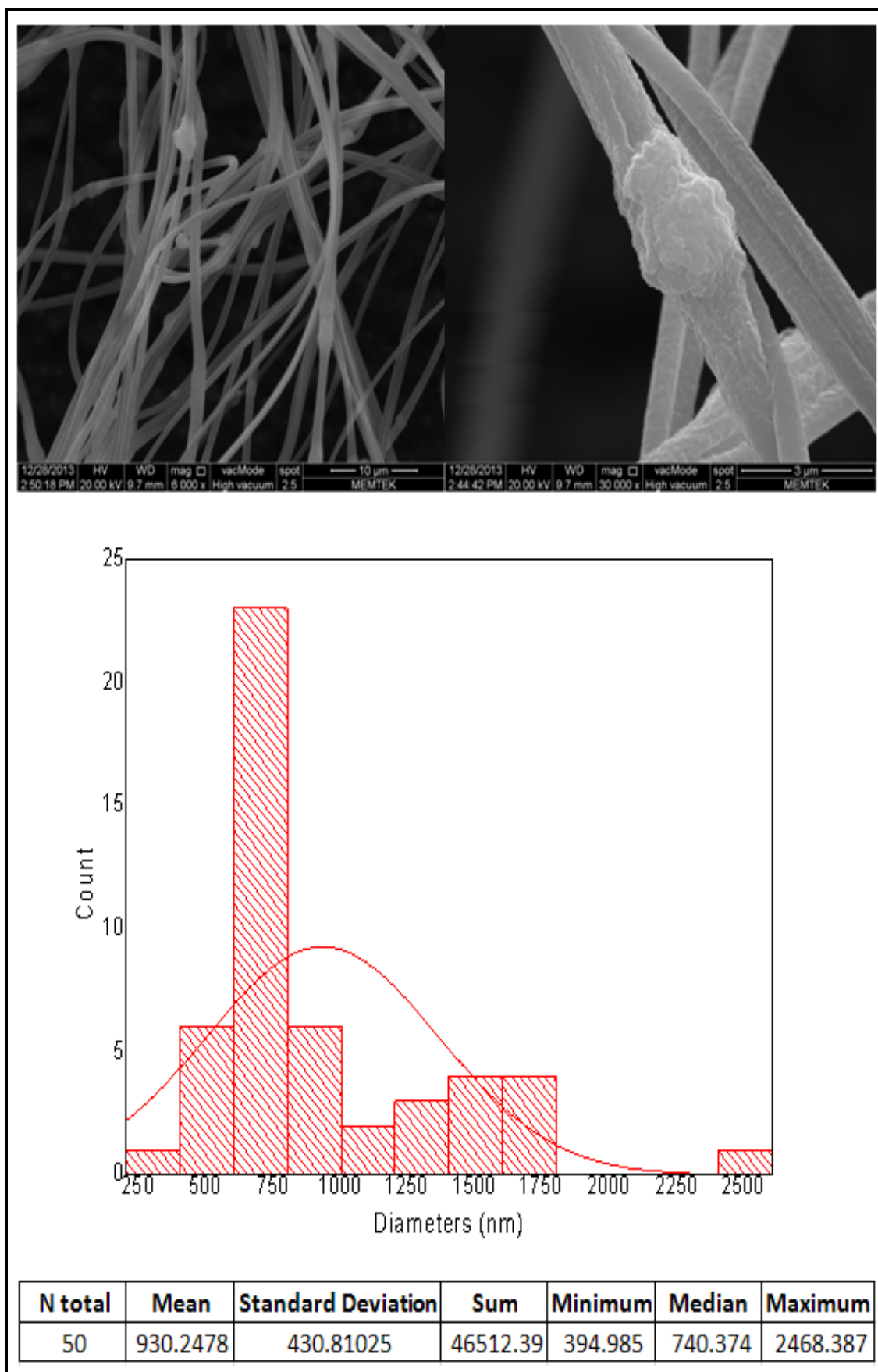


Figure 4.28 : SEM pictures and average diameter analyses of coPy-3 nanofibers.

The nanofiber samples coPy-1, coPy-2, and coPy-3 are shown in Figure 4.26, 4.27 and 4.28. They are produced with constant parameters of feeding rate (0.15 ml/h) and tip-collector distance (5 cm), but with variable applied-voltage as 20 kV, 15 kV, and 10 kV. There is not an obvious correlation between values of mean fiber diameter. Such a non-uniformity and high thickness of nanofibers can be explained with very small tip-collector distance (5 cm), thus, lack of space and lack of time to form nanofibers after Taylor-cone.

Another interesting point is the neck-formation which is much larger than fiber diameter. The rough surface of nanofibers are expected to be resulted due to PPy inclusion into the copolymer matrix, and neck-formation is, too. Such necks could be formed because of low-solubility of PPy which is embedded into the copolymer matrix, and/or due to the difference in dielectricities of PPy and copolymer matrix, thus, the charge carriers are not distributed uniformly in composite electrospinning solution, therefore, resulted a deviance in interaction of solution with electrical field that shapes the fiber body.

AN-BuA/PPy composite nanofibers (named as coPy) are thicker compared to the nanofibers which were produced only from AN-BuA the copolymer. This indicates the PPy formation in copolymer matrix and possible porous structure in fiber body which inflates it to result larger diameters.

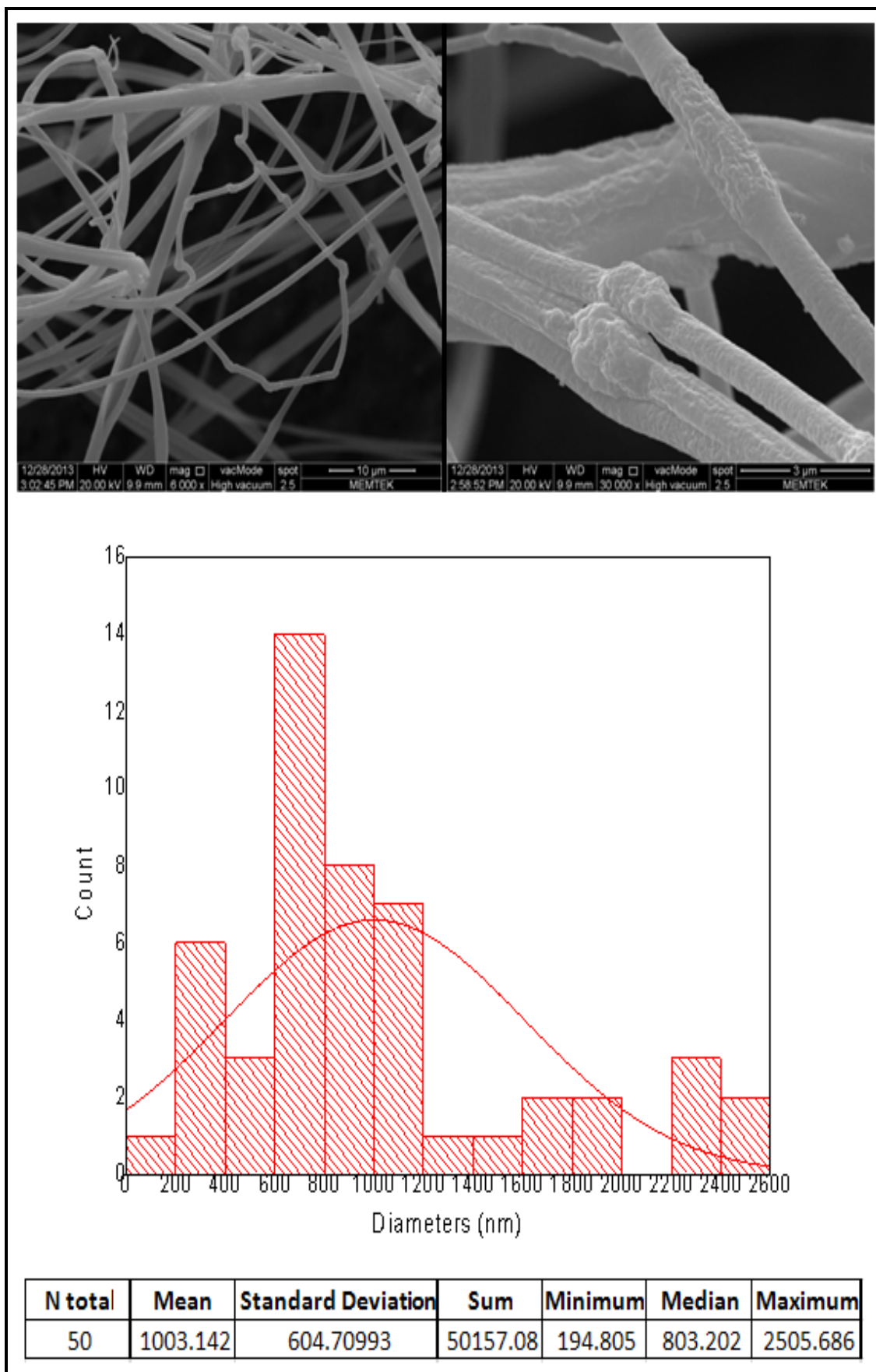


Figure 4.29 : SEM pictures and average diameter analyses of coPy-4 nanofibers.

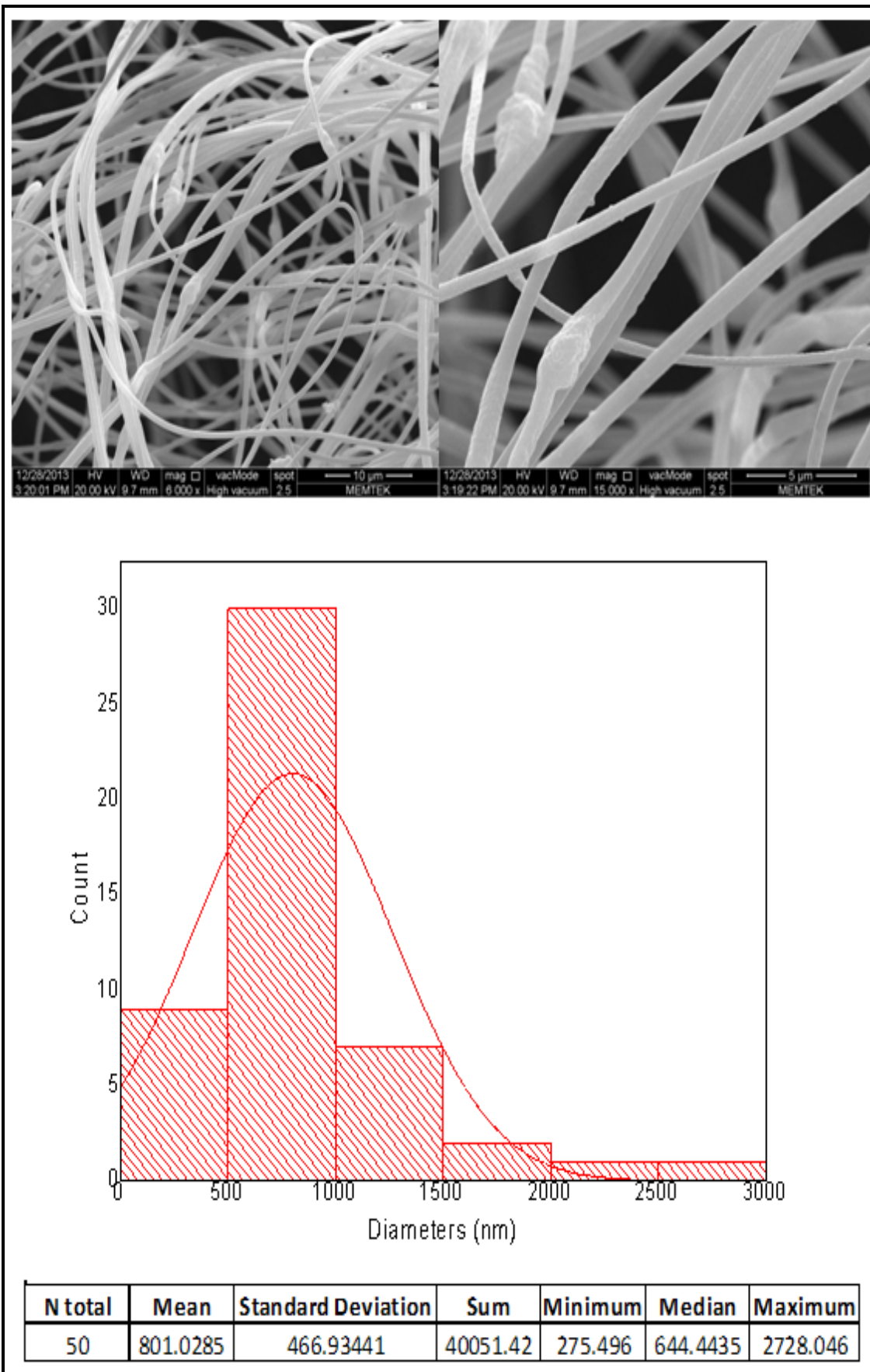


Figure 4.30 : SEM pictures and average diameter analyses of coPy-5 nanofibers.

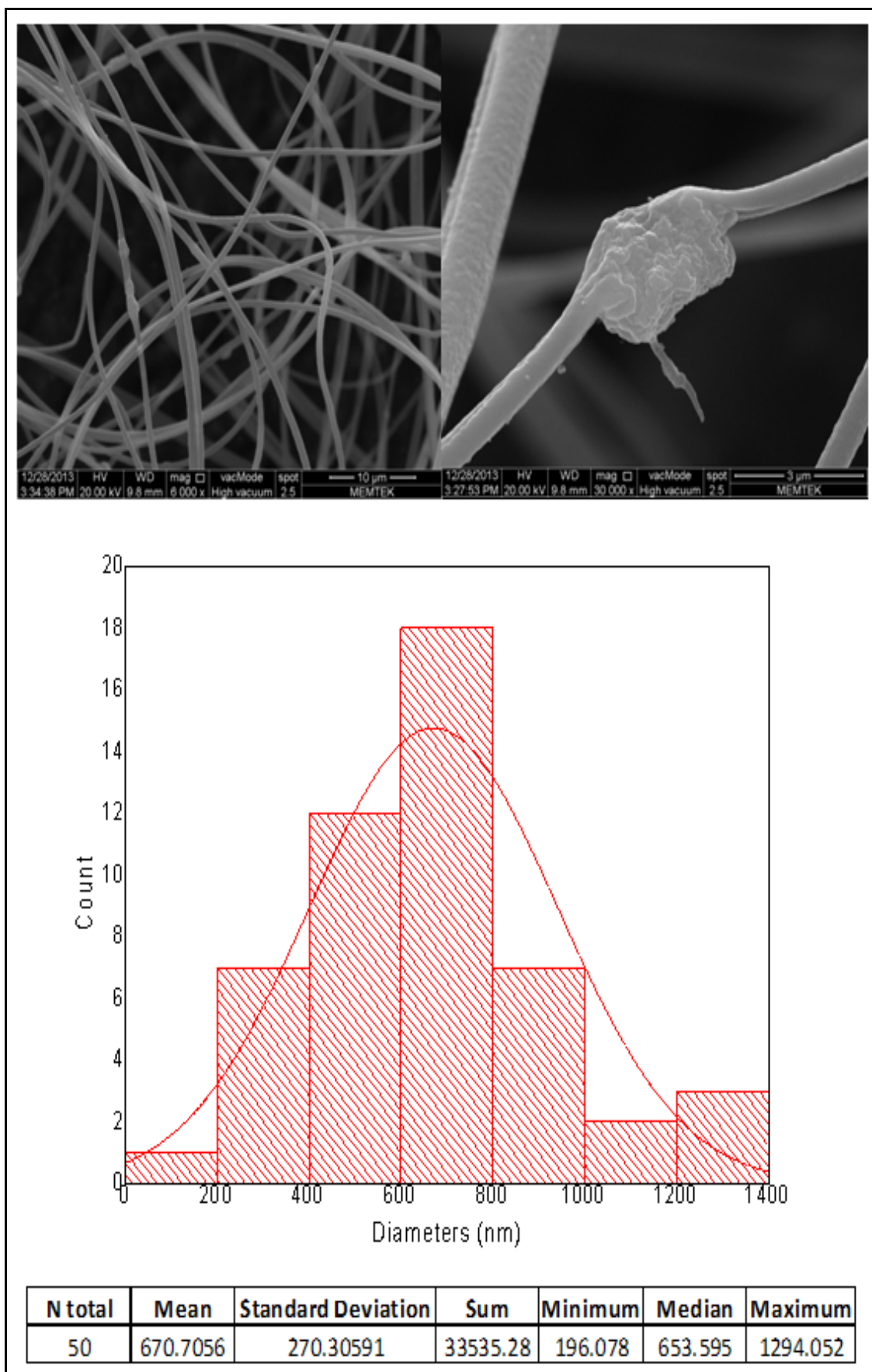


Figure 4.31 : SEM pictures and average diameter analyses of coPy-6 nanofibers.

The samples coPy-4, coPy-5, and coPy6 can be seen in Figure 4.29, 4.30, and 4.31. They were produced with a constant feeding rate (0.15 ml/h) and constant tip-collector distance (7.5 cm), but with variable applied voltages as 20 kV, 25 kV, and 30 kV. The mean values of fiber diameters and also standard deviations show an important decrease with increasing applied voltage.

While fibers are with a rough surface due PPy inclusion, they also lose uniformity of diameter distribution, i.e., very thick micron-level fibers are forming, but ultra-thin fibers accompany those thick fibers. Neck-formations are again noticeable, since it is already thought to be a result of PPy formation in copolymer matrix.

In Figure 4.32, 4.33, and 4.34, it is shown the samples coPy-7, coPy-8, and coPy-9 produced with constant feeding rate of 0.15 ml/h and constant tip-collector distance of 10 cm, but with variable applied voltages as 20 kV, 25 kV, and 30 kV. The decrease in fiber diameters and standard deviations again show a decrease due to increasing applied voltages. But, the overall fiber diameter is showing an important decrease compared to the previous “coPy” samples which were produced with shorter tip-collector distances. The applied voltage increases the amount and intensity of electrical field, thus, it increases the force that protrudes fiber from polymer solution and flies it through the space between the needle-tip and the collector. At this point, the tip-collector distance is very critical for fiber formation as it describes the time, rate and distance for evaporation of the solvent that has to leave the polymer solution to form also to strain the fiber body. While very small tip-collector distance does not give enough time and space to the solvent to leave the polymer solution, it also lacks the possibility to strain and elongate the fiber body to decrease its thickness. Therefore, it is possible to tell that a critical balance exists between the applied voltage and the tip-collector distance, as well as between other parameters such as feeding rate, temperature, viscosity, humidity, solvent type, etc, to produce the nanofibers with desired characteristics.

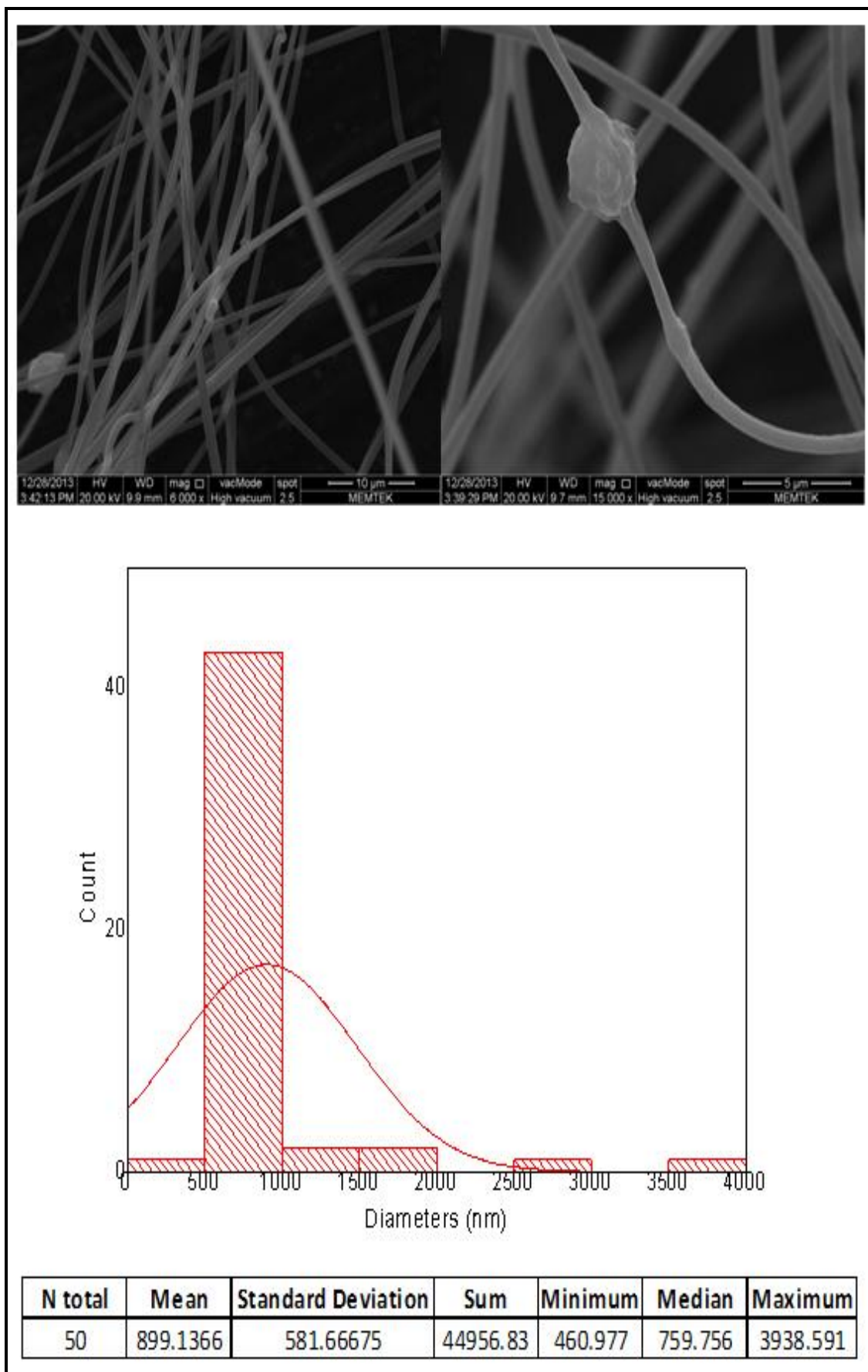
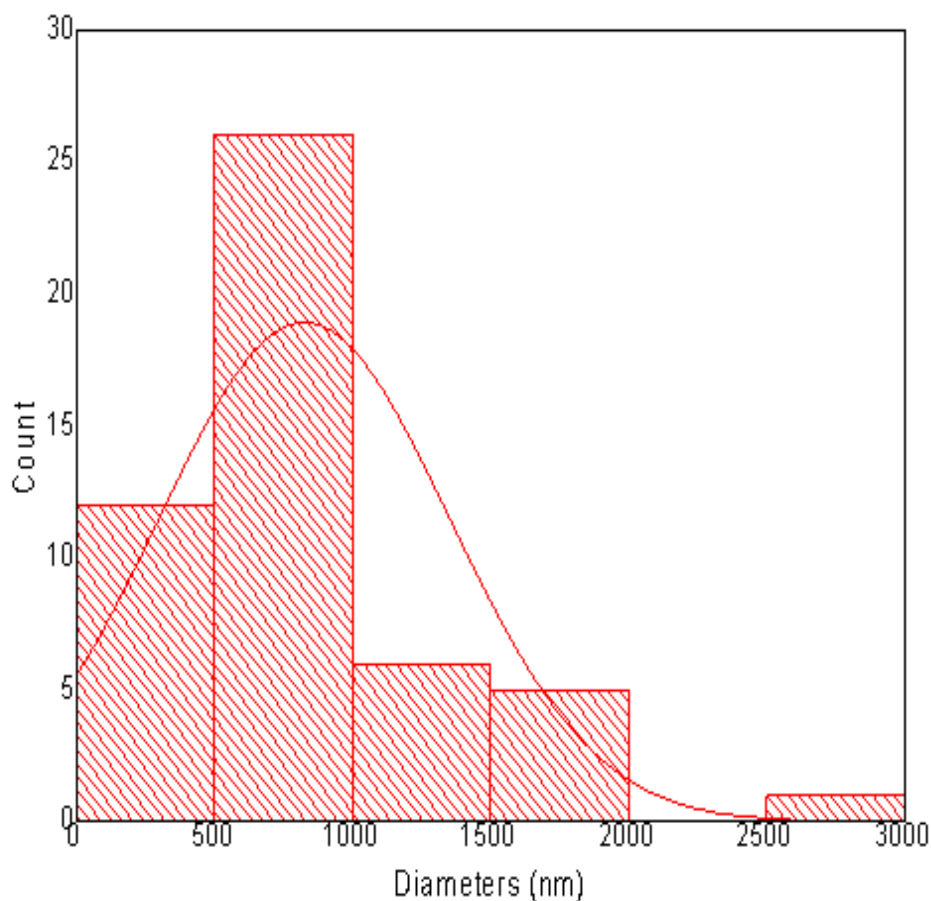
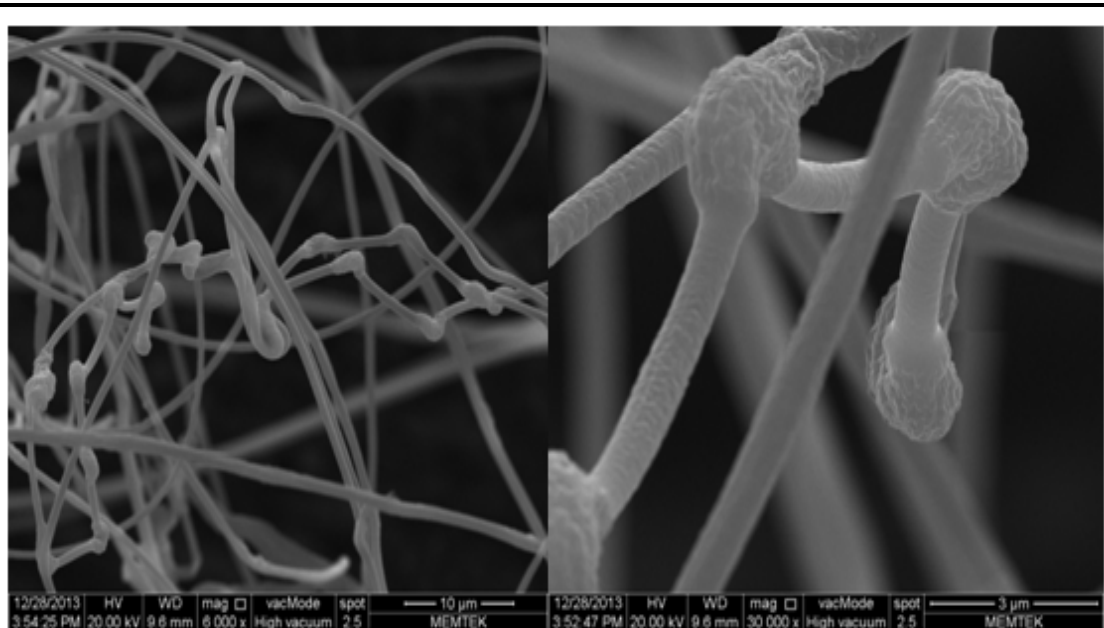


Figure 4.32 : SEM pictures and average diameter analyses of coPy-7 nanofibers.



N total	Mean	Standard Deviation	Sum	Minimum	Median	Maximum
50	825.6907	527.49402	41284.54	112.365	704.414	2715.428

Figure 4.33 : SEM pictures and average diameter analyses of coPy-8 nanofibers.

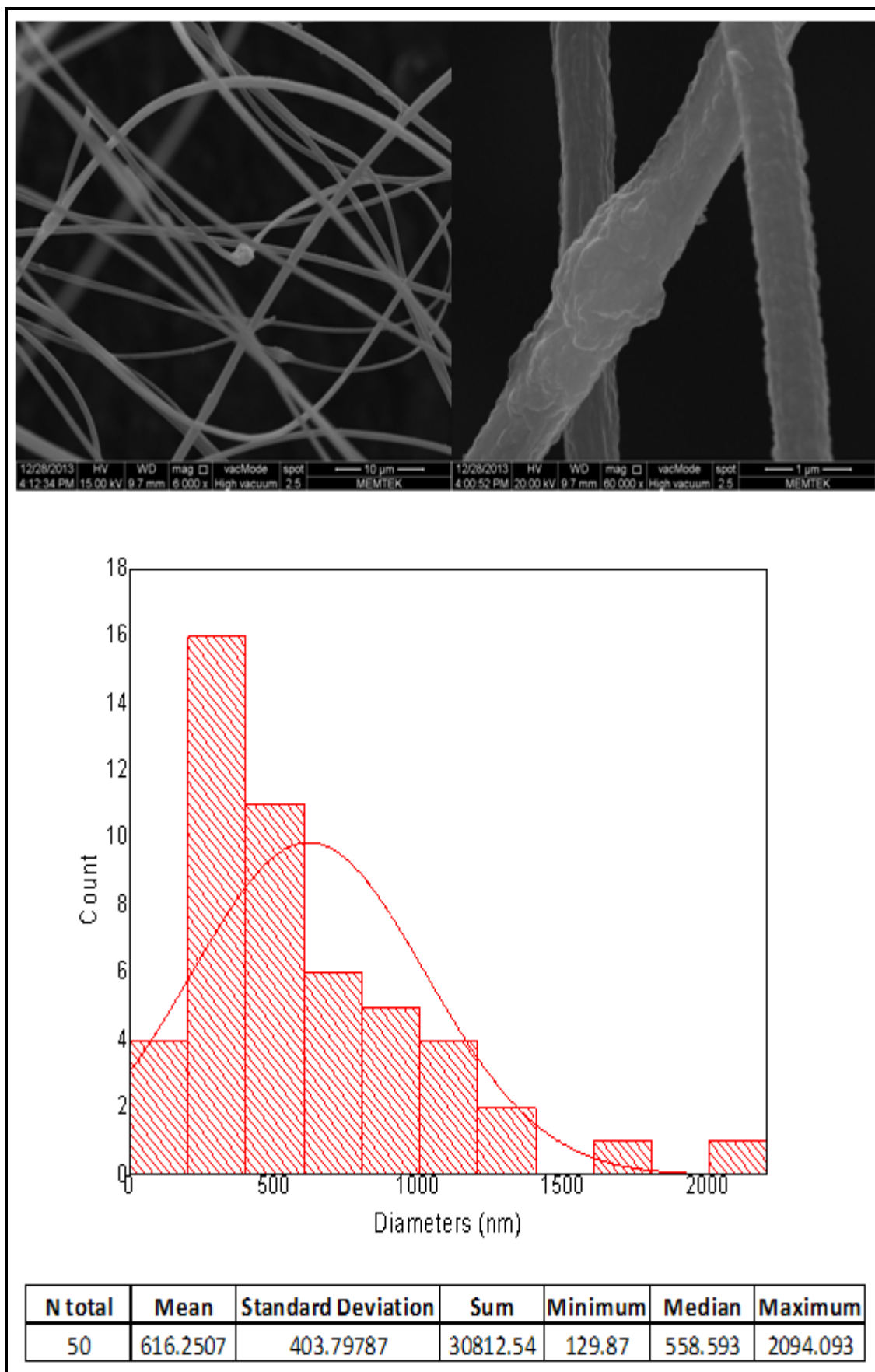


Figure 4.34 : SEM pictures and average diameter analyses of coPy-9 nanofibers.

Table 4.1 : Electrospinning parameters and resultant average fiber diameters.

	Feeding Rate (ml/h)	Applied Voltage (kV)	Distance (cm)	Fiber Diameter (nm)
co-1	0.3	10	10	265 ± 85
co-2	0.15	10	10	214 ± 57
co-3	0.15	15	10	203 ± 198
co-4	0.15	20	10	363 ± 290
coPy-1	0.15	20	5	1192 ± 560
coPy-2	0.15	15	5	1362 ± 613
coPy-3	0.15	10	5	930 ± 431
coPy-4	0.15	20	7.5	1003 ± 605
coPy-5	0.15	25	7.5	801 ± 467
coPy-6	0.15	30	7.5	671 ± 270
coPy-7	0.15	20	10	899 ± 582
coPy-8	0.15	25	10	826 ± 528
coPy-9	0.15	30	10	616 ± 404

After all these statistical diameter analyses, it is generally seen that increasing applied potential and decreasing feeding rate results thinner fibers; and the decreasing syringe tip – collector distance results in thicker structure. Polypyrrole content in “coPy” termed samples is affecting the surface morphology of nanofibers, which form cauli-flower morphology due to PPy’s characteristic. Furthermore, the nanofibers with PPy show a tendency to have lower standard deviation from the mean diameter values by increasing applied voltage, while the nanofibers without PPy vice versa. Generally, it is possible to say that, the higher mean diameters have also higher deviations; a reflection of this result can be seen also in related SEM images (Figure 4.22 to 4.34). For instance, in some samples, thick fibers are formed (1-3 micron), while ultra-thin fibers (20-50 nm) accompanying these thick ones.

4.5 Characterization of Composite Nanomats

The optical characterizations of composite nanomat samples are shown below, in Figure 4.35. The color change from blackish-gray to light gray can be seen by decreasing PPy content in the polymer matrix of composite nanomats.

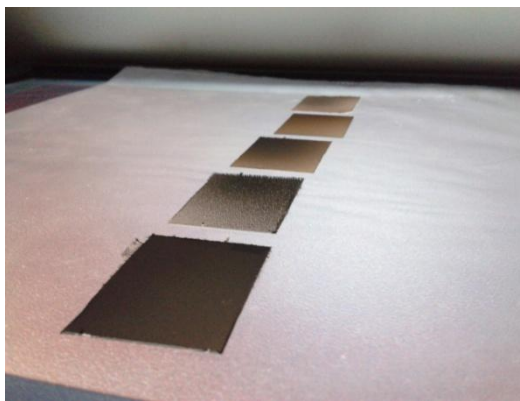


Figure 4.35a : Color change of nanomats due to changing Polypyrrole content.

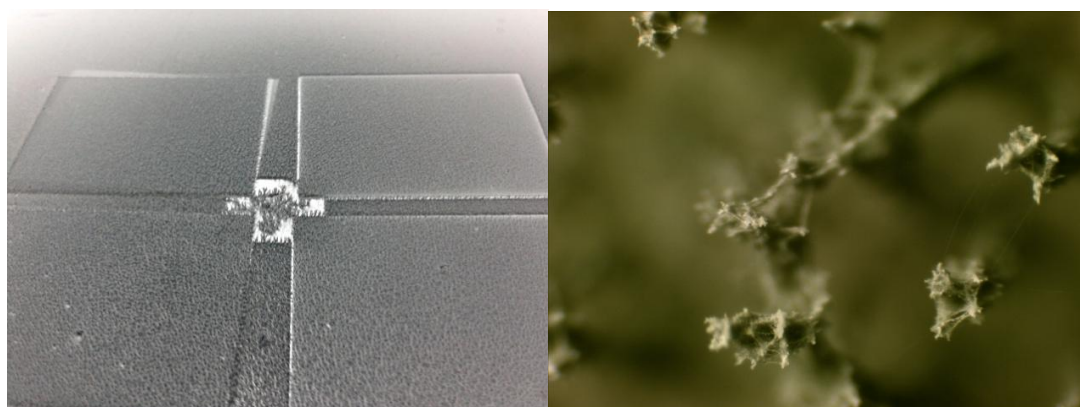


Figure 4.35b : Optical characterizations of nanomats (picture on the left is the photo view, and the picture on the right is the light-microscope view of 150x magnification).

As seen in Figure 4.35b, tree-like structures are clearly observed on nanomat sample surfaces. The reason of such interesting morphology is thought to be high-electroactivity of PPy in composite nanofibers. Because of the high electrical-potential applied between syringe-tip and collector while electrospinning-process, the nanofibers are forming a thin layer of electroactive composite nano-web, and then the consecutive nanofibers are collecting onto it which it can form a latter-surface to reach to the syringe-tip in extremely-strong electrical field of electrospinning setup (in Figure 4.36 it is clearly seen the double-layer morphology of nanomat surface in SEM shot of 1000x magnification).

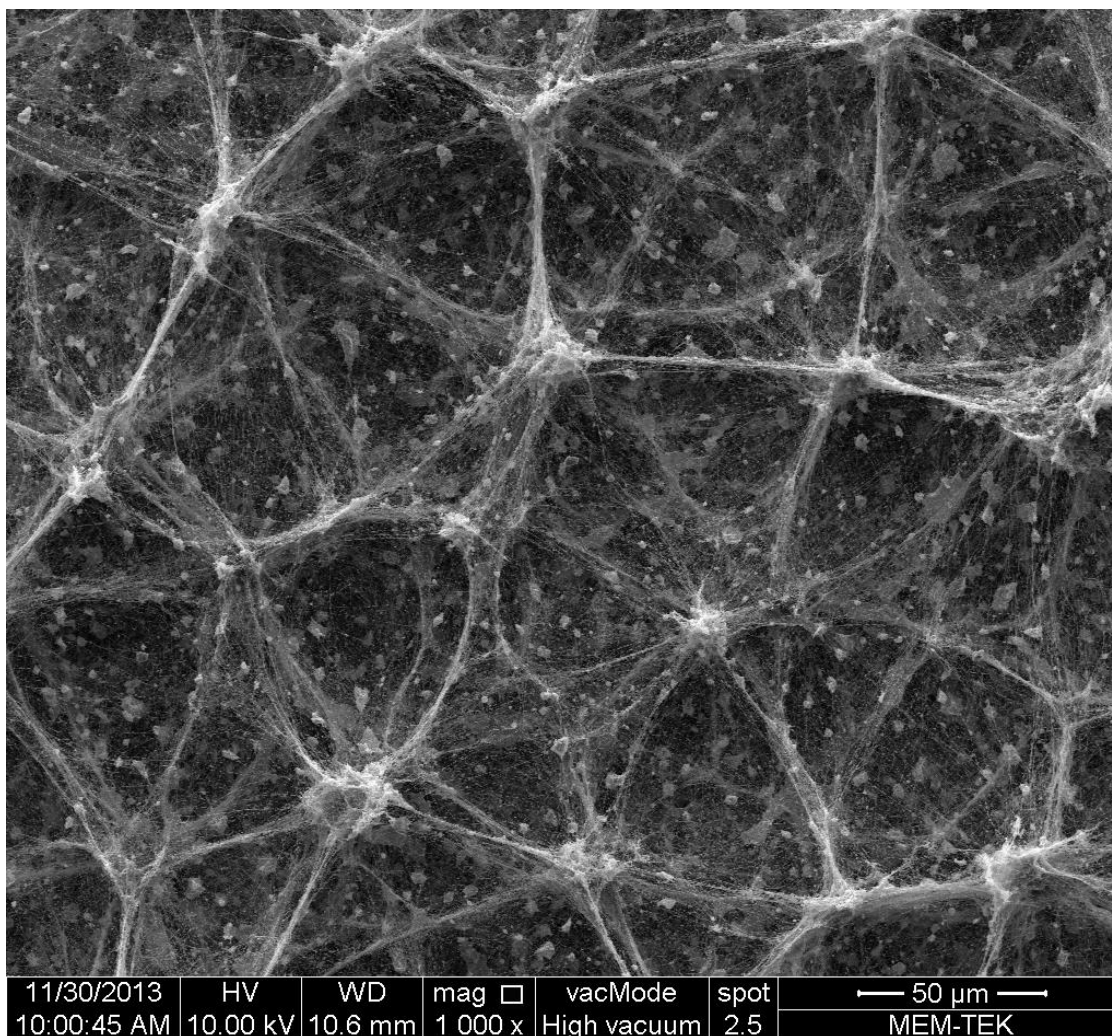


Figure 4.36 : SEM view of a produced nanomat sample.

The correlation exists between the three parameters, which follows as; initial Py contents added into the polymer solutions to form PPy in polymer matrix, PPy's FTIR absorbance peaks and the tree-like morphology of nanomat surfaces. The increasing amount of PPy and also the higher conductivity levels of PPy due to its doping by initiator-solvent system in composite structure, the surface morphology of nanomat sample (Figure 4.36) showed a change to this interesting form.

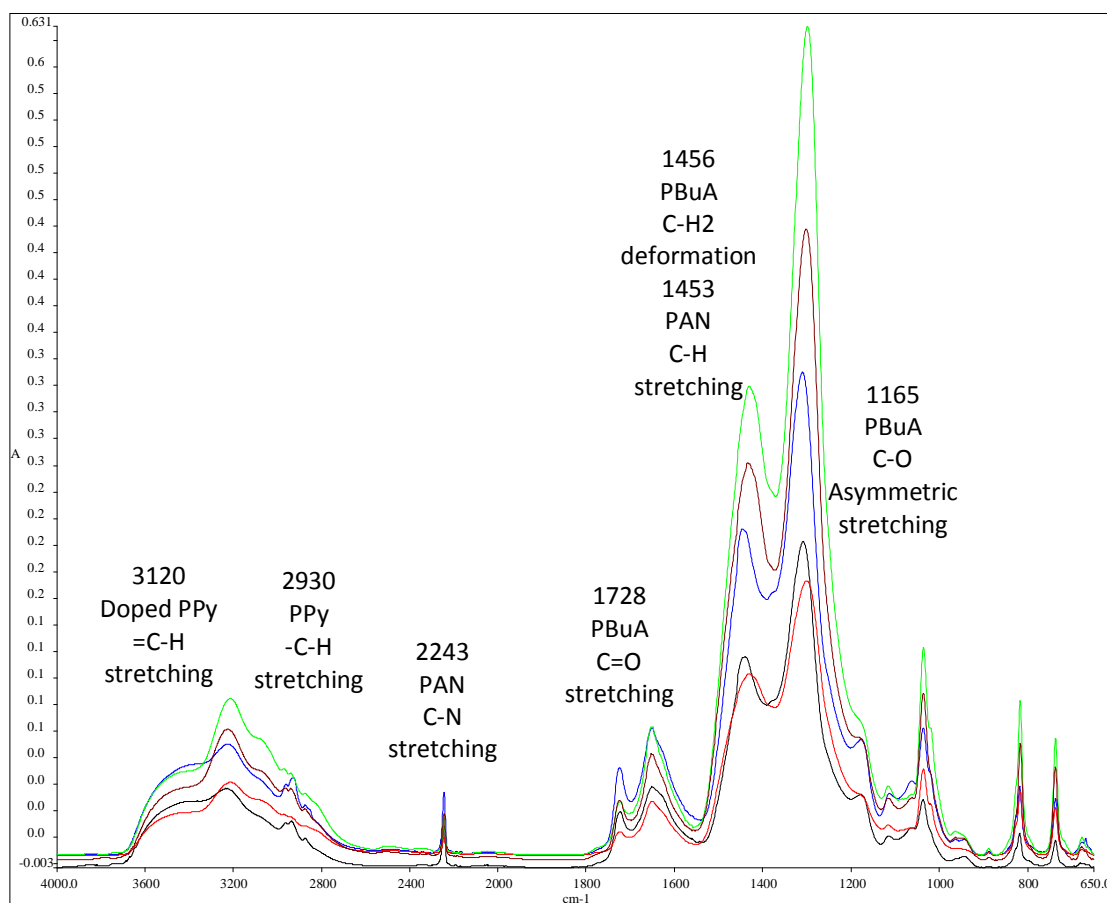


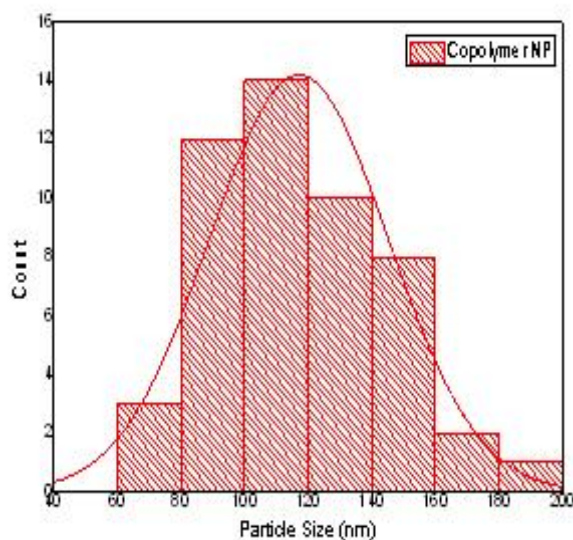
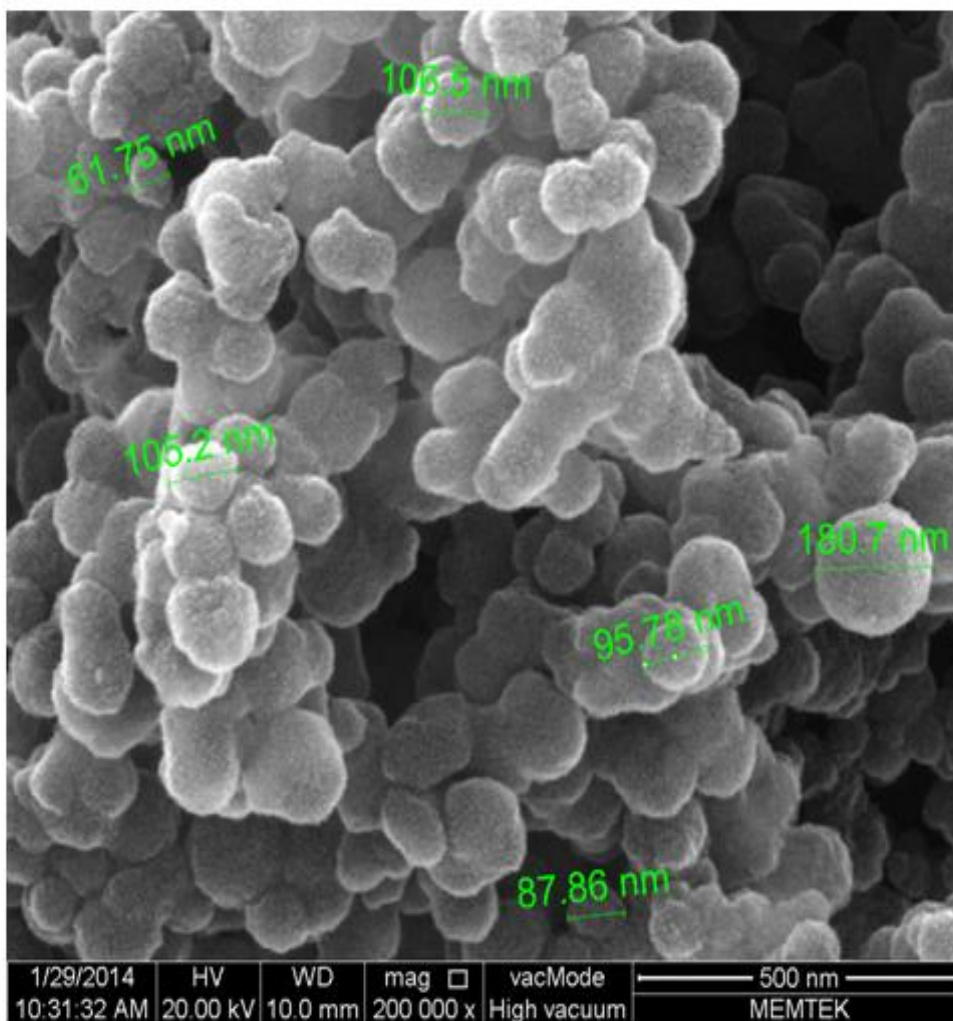
Figure 4.37 : ATR-FTIR spectra of 40, 80, 120, 160, and 200 µl Py polymerized nanomats.

In Figure 4.37, the spectra shows the change in characteristic peaks regarding to PPy formation in polymer matrix used to produce nanomats. Especially the absorbance peaks seen in 2800-3600 cm^{-1} band are thought to be related to the doped form of PPy, indicating also its high electrical conductivity.

4.6 Characterization of Core-Shell Nanoparticles

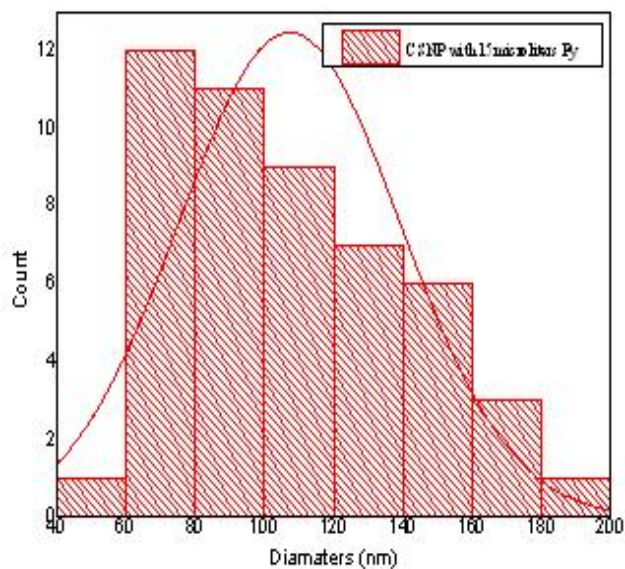
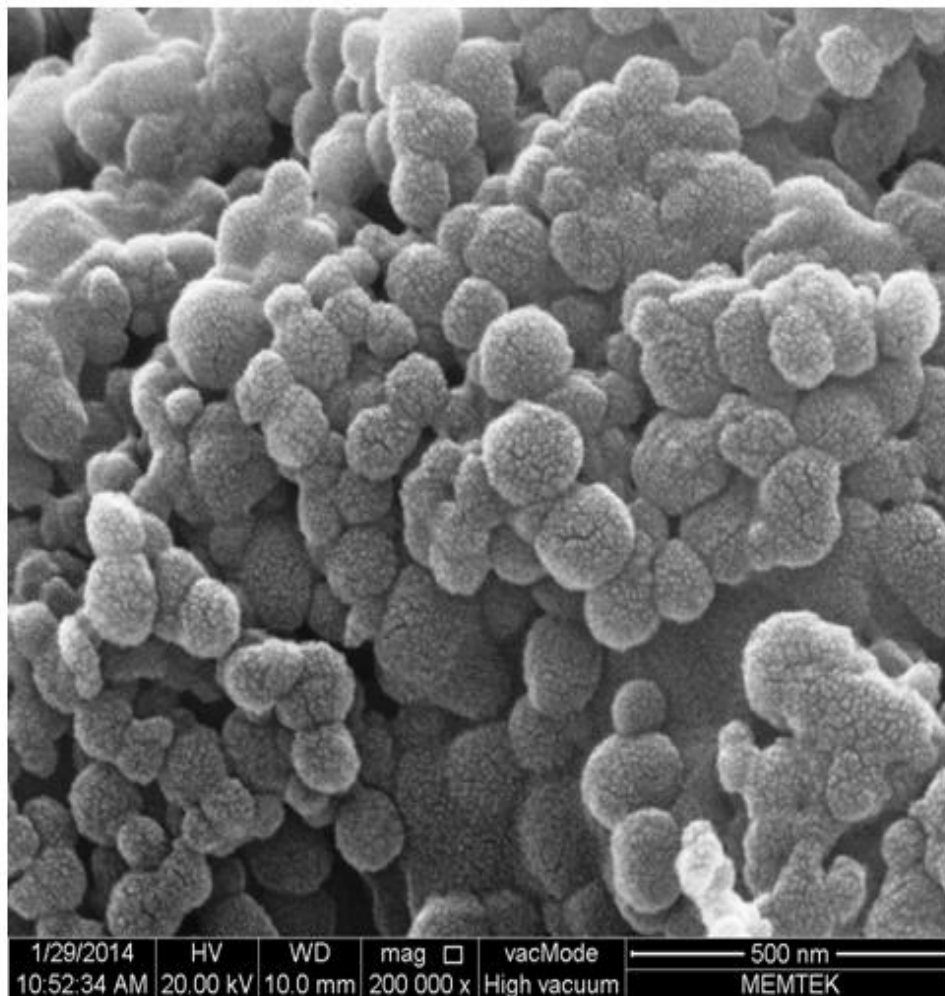
4.6.1 SEM analysis of P(AN-co-BuA) and PPy/P(AN-co-BuA) nanoparticles

Nanoparticles were sampled from emulsions by diluting in ethanol, then dripping the diluted dispersion onto glass substrates and then drying at room temperature. The samples were characterized morphologically by Scanning Electron Microscope and they were coated with gold-palladium prior to analyses.



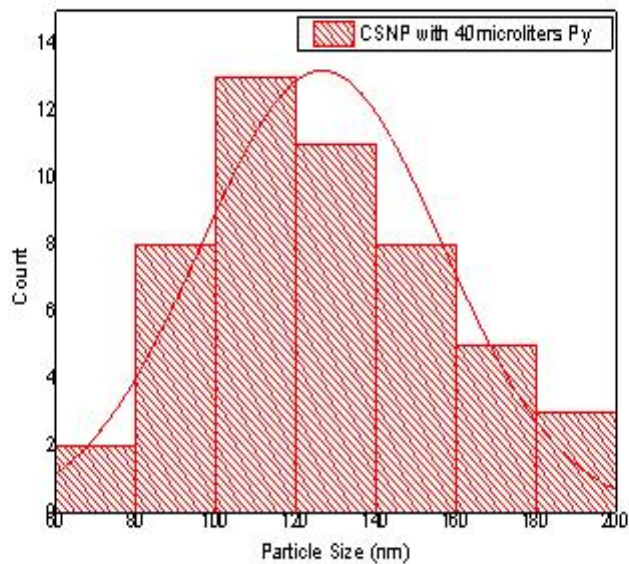
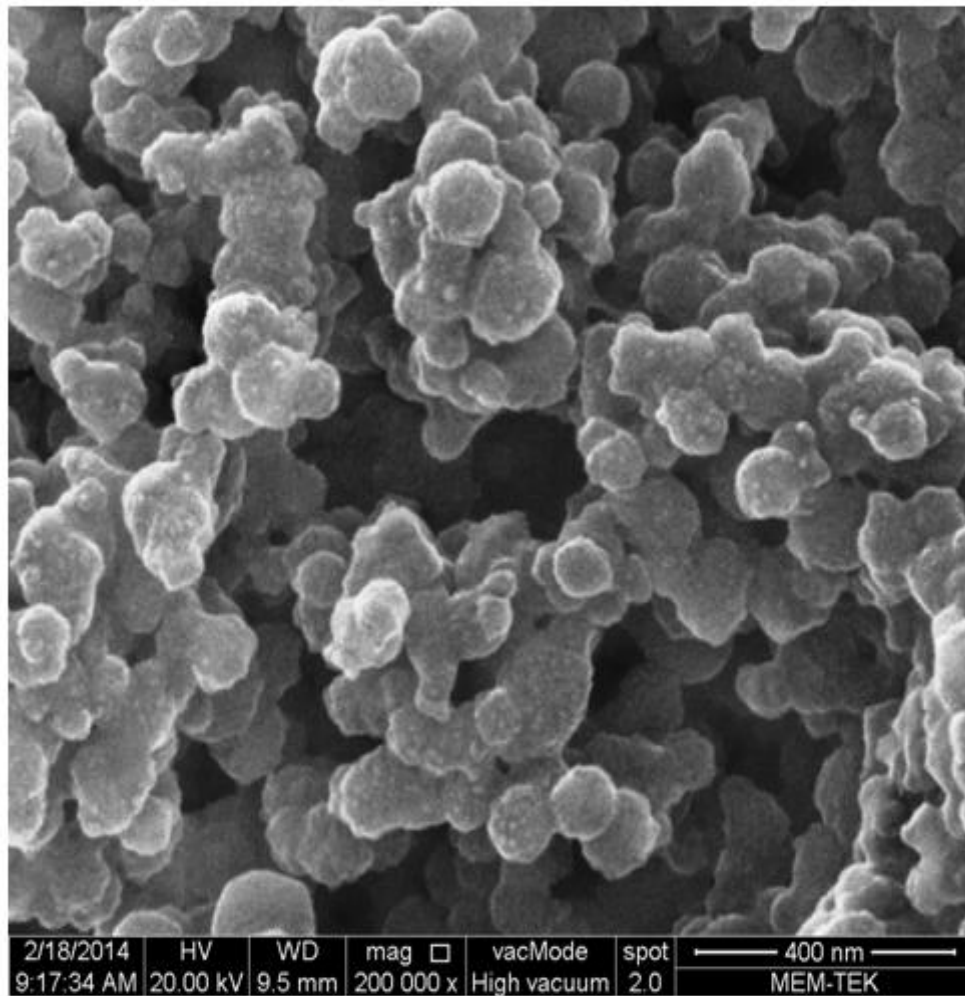
OPy	N total	Mean	Standard Deviation	Sum	Minimum	Median	Maximum
nm	50	117.1316	28.12596	5856.581	60.979	109.246	183.206

Figure 4.38 : P(AN-co-BuA) nanoparticles.



15Py	N total	Mean	Standard Deviation	Sum	Minimum	Median	Maximum
nm	50	107.18	32.00457	5359	57.615	100.651	182.61

Figure 4.39 : P(AN-co-BuA)/PPy core/shell nanoparticles (15 microliters Py).



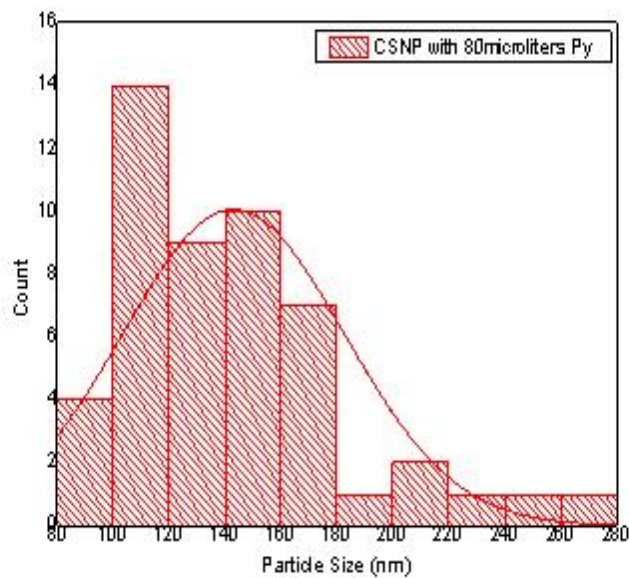
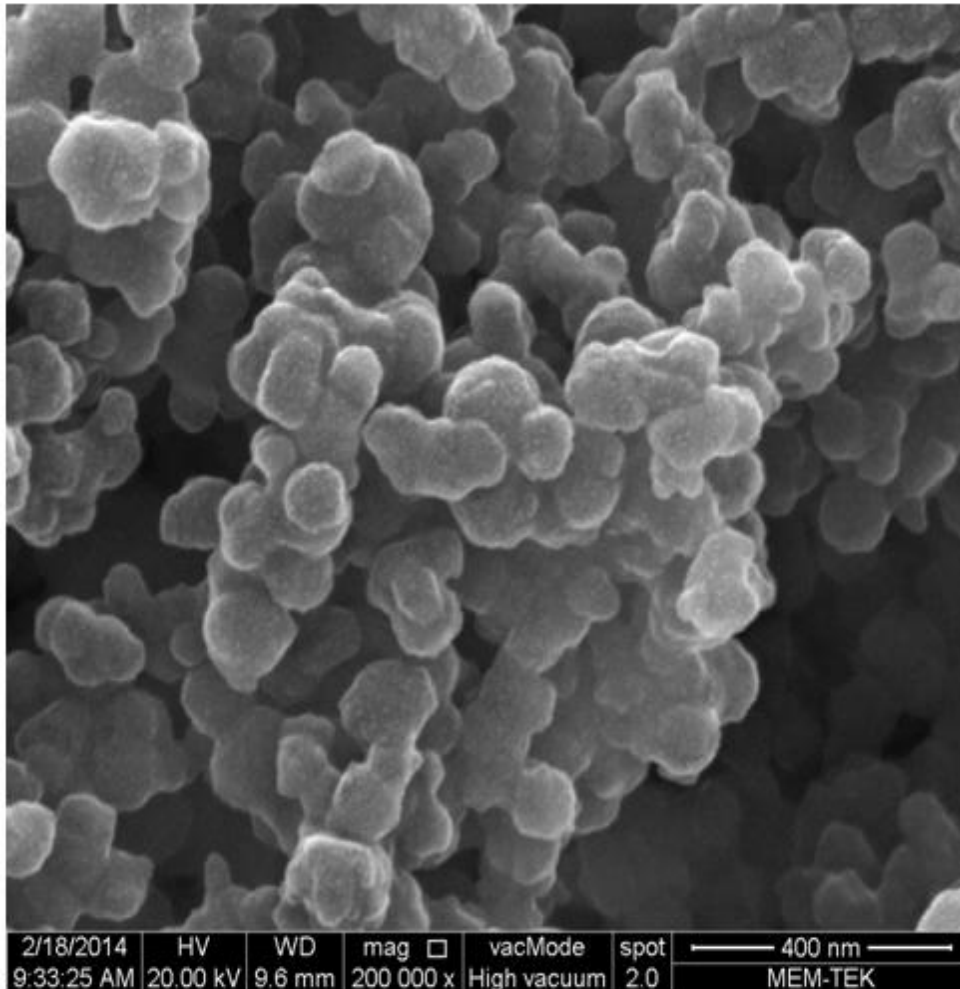
40Py	N total	Mean	Standard Deviation	Sum	Minimum	Median	Maximum
nm	50	126.5101	30.16607	6325.503	70.27	122.164	187.336

Figure 4.40 : P(AN-co-BuA)/PPy core/shell nanoparticles (40 microliters Py).

Figure 4.38, 4.39, 4.40, 4.41. and 4.42 show the SEM images of P(AN-co-BuA) and PPy/P(AN-co-BuA) nanoparticles obtained from emulsions. Spherical structures occurred by the emulsion polymerization method, by the stirring in high rpm of magnetic stirrer. Adding Pyrrole into the emulsion medium while continuing reaction, provides a core-shell structure since the surfactant SDBS create a nano/micro-reactor vessel by providing micelle formation where the monomers are encapsulated in. Hydrophobic part of the surfactant molecules adsorb on the produced conducting polymer, a surfactant thus becoming a part of the resulting material. And this is also increasing the solubility so the processability of PPy. Therefore, P(AN-co-BuA) are encapsulated in SDBS miscelle by the hydrophobic tail, since the BuA monomer is hydrophobic, too. Then, Pyrrole polymerized by the adsorption on the surface of the miscelle. As seen in the Table 4.2, nanoparticle sizes are decreased by the addition of pyrrole first; but then increased by the increasing amounts of Py added.

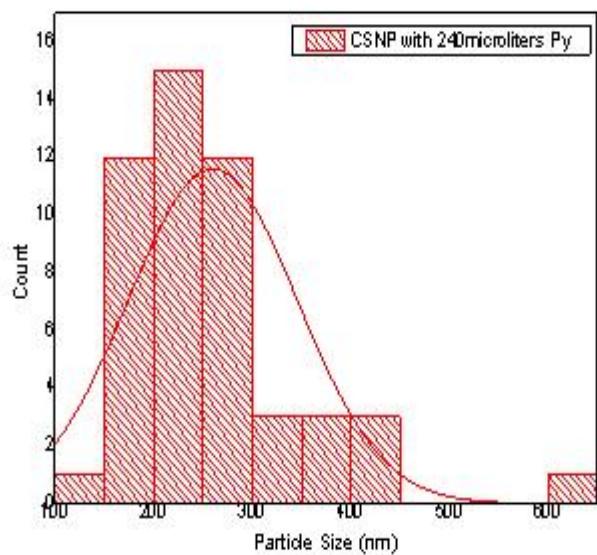
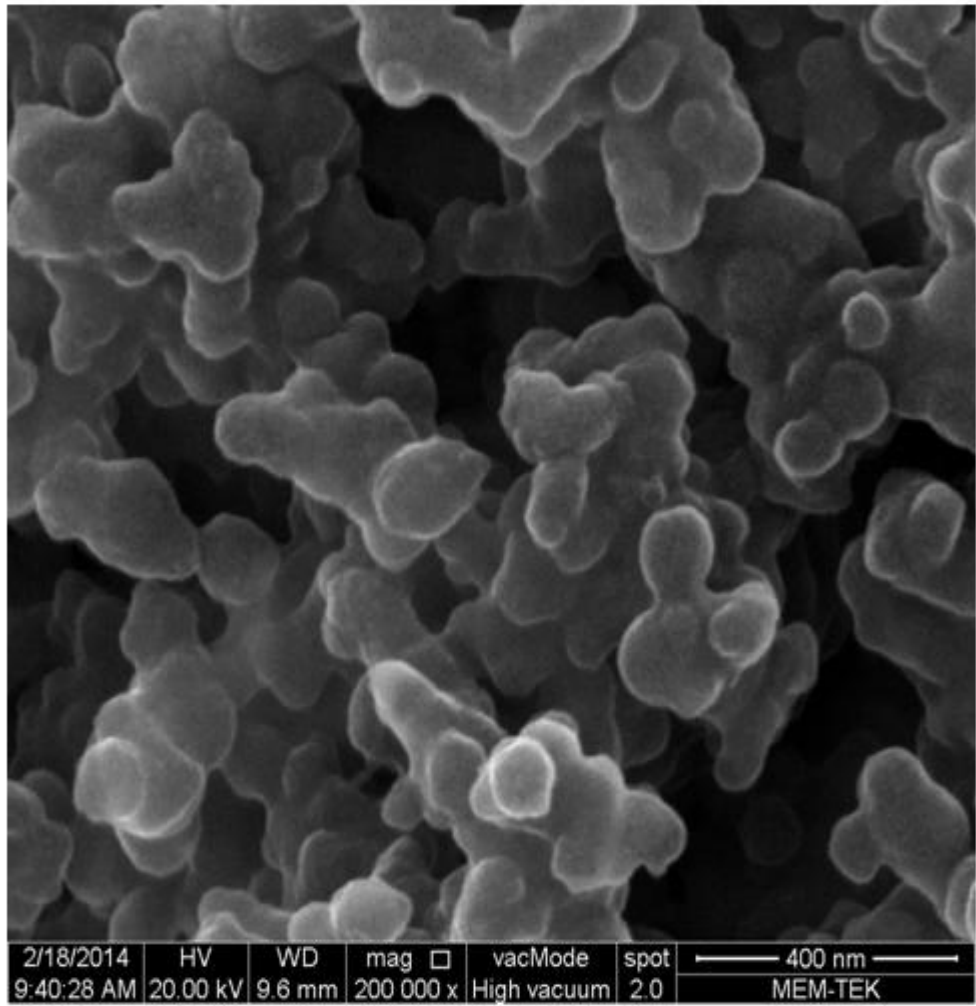
Table 4.2 : P(AN-co-BuA) and PPy/P(AN-co-BuA) nanoparticle sizes estimated from SEM images.

Nanoparticles	Fed Pyrrole (μl)	Average Particle Size (nm)
P(AN-co-BuA)	0	117 \pm 28
PPy/(AN-co-BuA)	15	107 \pm 32
PPy/(AN-co-BuA)	40	127 \pm 30
PPy/(AN-co-BuA)	120	143 \pm 40
PPy/(AN-co-BuA)	240	260 \pm 86



120Py	N total	Mean	Standard Deviation	Sum	Minimum	Median	Maximum
nm	50	142.9892	39.6767	7149.46	91.803	136.246	268.849

Figure 4.41 : P(AN-co-BuA)/PPy core/shell nanoparticles (120 microliters Py).



240Py	N total	Mean	Standard Deviation	Sum	Minimum	Median	Maximum
nm	50	260.0374	85.98062	13001.87	130.439	242.1925	619.034

Figure 4.42 : P(AN-co-BuA)/PPy core/shell nanoparticles (240 microliters Py).

4.6.2 Particle size analysis of P(AN-co-BuA) and PPy/P(AN-co-BuA) NP

The particle size analyses of synthesized nanoparticles were performed also with another method, i.e. Light Scattering method, on Particle Size Analyzer - Malvern Mastersizer Microplus Ver.2.19 device. Samples that containing different amount of pyrrole addition were taken from emulsion latexes and sent to the Organik Kimya A.Ş. in order to analyze particle size. As seen in the Figure 4.43, the colour of each emulsion sample changes from gray to darker gray-bluish-black by increasing pyrrole content. The colour change indicates the polymerization of Pyrrole, the change in color-tones indicates different amounts of PPy formation.

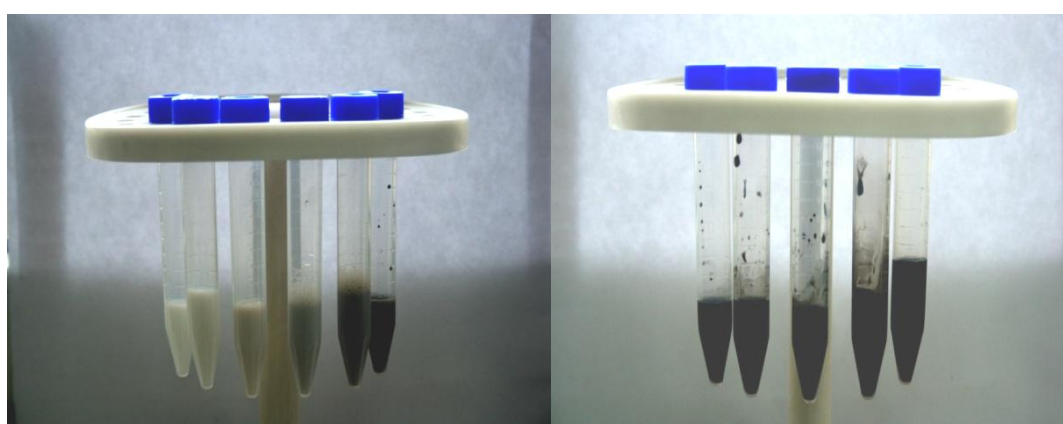


Figure 4.43 : The colour change of CSNP emulsions by increasing PPy content.

By increasing amounts of polypyrrole in the structure, particles get larger as shown in the Table 4.4. These diameters were measured by Particle Size Analyzer and the results differ from the results obtained by SEM image analyzing, this is thought to be caused from the aggregation due to electrostatic interactions and structure of polypyrrole.

4.6.3 Atomic Force Microscope (AFM) analysis of nanoparticles

Polymer template nanoparticles and 35microliters Py polymerized core-shell composite nanoparticles were sampled via dispersing in ethanol and then dripping onto glass substrates; and the morphological change was observed between these two samples, as an indication of PPy formation on polymer template NPs. As it can be seen below in Figure 4.44, the sample morphologies show a change from smooth to rough.

Table 4.3 : P(AN-co-BuA) and PPy/P(AN-co-BuA) CSNP sizes measured by particle size analyzer via light-scattering.

Nanoparticles	Fed Pyrrole Content (μl)	Particle Size (nm)
PPy/(AN-co-BuA)	0	362
PPy/(AN-co-BuA)	15	435
PPy/(AN-co-BuA)	20	477
PPy/(AN-co-BuA)	25	486
PPy/(AN-co-BuA)	30	630
PPy/(AN-co-BuA)	40	666
PPy/(AN-co-BuA)	80	1337
PPy/(AN-co-BuA)	120	1360
PPy/(AN-co-BuA)	240	1816
PPy/(AN-co-BuA)	360	2158

In Figure 4.44, the surface morphologies of the nanoparticle samples prepared by dripping their diluted ethanol dispersion onto glass substrates. The roughness seem to be decreased in latter, it is not because the sample with PPy give smaller particles and so less roughness; but it is because the analysis area is smaller, the AFM tip works on a smaller area, so the roughness is less affected by sample slope. Slope of the sample surface, so the scanning area is a critical factor while AFM analyses. Thus, it has to be taken into account also the morphological view, which is indeed changing to a rougher topography with PPy formation.

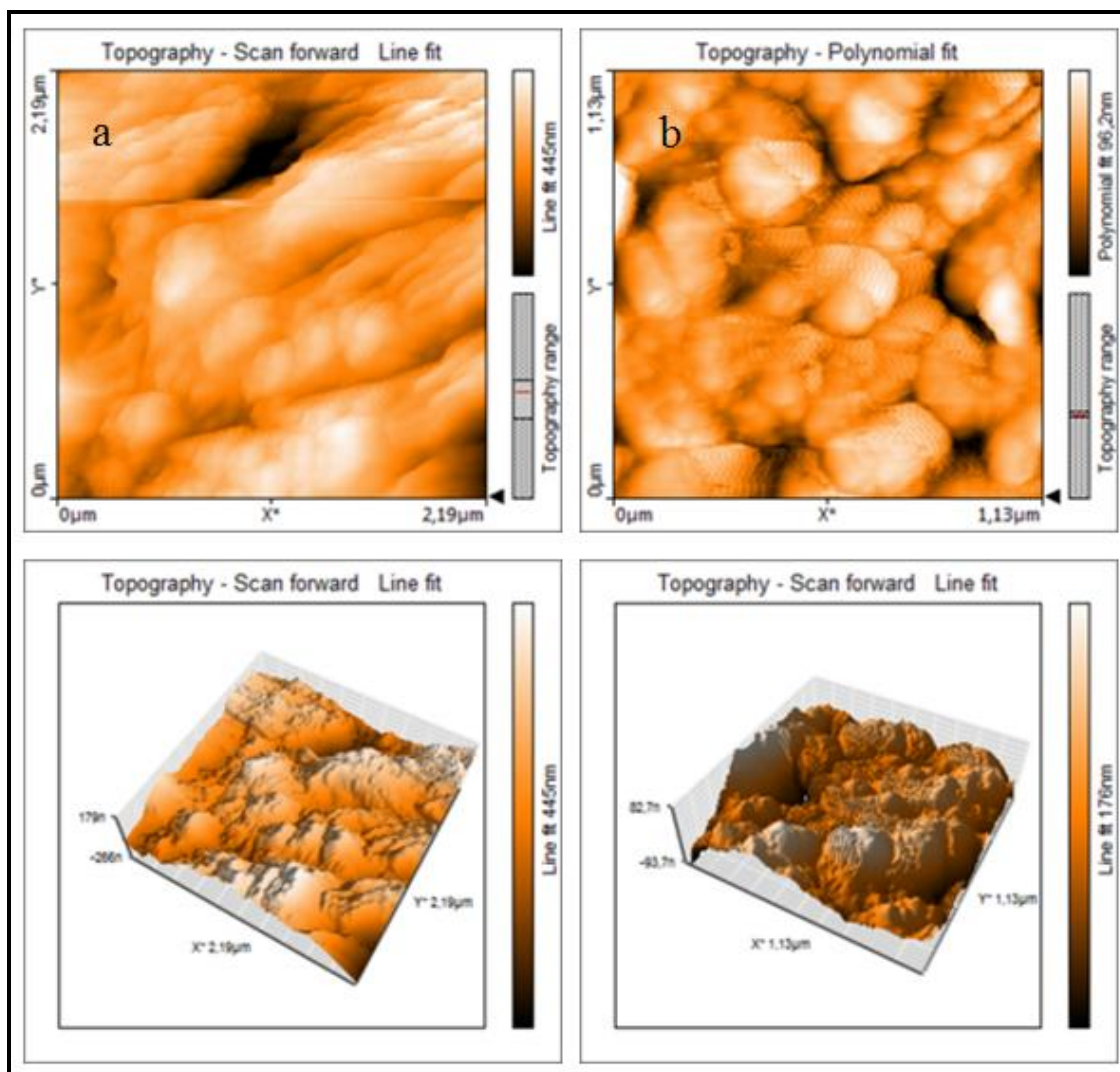


Figure 4.44 : The surface topographies of (a) polymer template and (b) CSNPs.

4.6.4 ATR-FTIR characterization of nanoparticles

After washing five times with distilled water by centrifuge process at 5000 rpm revolution speed, all the particle samples were dried, and taken in powder form to the further analyses. The ATR-FTIR spectra of P(AN-co-BuA) and PPy/P(AN-co-BuA) nanoparticles are shown in Figure 4.45 and it was recorded in the absorbance mode. Peak at 3430 cm^{-1} shows the N-H stretching from P(AN-co-BuA), peak at 1449 cm^{-1} refers to N-C ring vibration from P(AN-co-BuA), peaks at 2954 and 1055 cm^{-1} are assigned to C-H stretching from P(AN-co-BuA). The peak at 2242 cm^{-1} is the characteristic peak of $\text{C}\equiv\text{N}$ nitrile group from AN. C=O stretching from BuA can be seen at 1726 cm^{-1} as a characteristic. The peak at 1634 cm^{-1} may be coming from O-H bending.

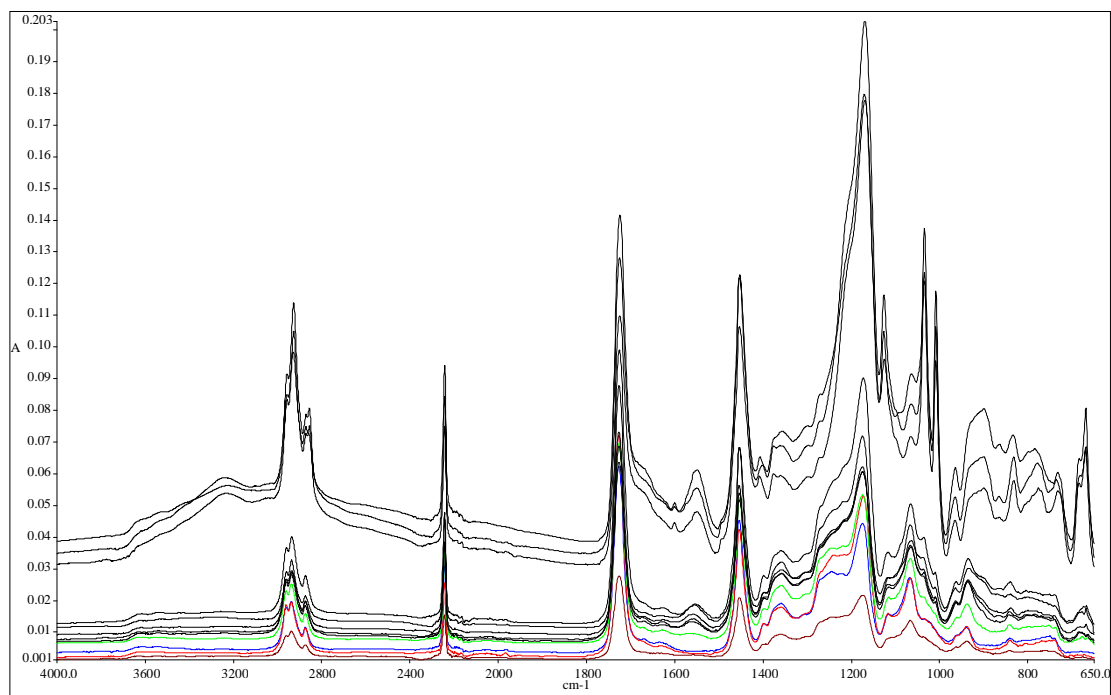


Figure 4.45 : ATR-FTIR spectra of nanoparticles and core-shell nanoparticles.

The characteristic peaks can be easily seen by the ATR-FTIR graphs of PPy / p(AN-co-BuA) nanoparticles in Figure 4.45 above. The peak at 1554 cm^{-1} shows the PPy ring vibration and also peak at 1449 cm^{-1} shows the PPy ring vibration (C=C stretching) too. At the 1166 cm^{-1} C-H in-plane deformation of PPy is observed. 1045 cm^{-1} peak refers to N-H in-plane deformation. Peaks at 967 and 911 cm^{-1} are the =C-H out of plane vibration of PPy. The appearance of the peak at 1554 cm^{-1} above a certain Py addition concentration is due to PPy formation in the structure strongly. Figure 4.40 indicates that the 1554 cm^{-1} peak is appearing and increasing sample by sample as the added pyrrole amount is increased up to $360\text{ }\mu\text{l}$. Also, the samples with more PPy content (120 , 240 and 360 microliters of initial Py), show a floating-high absorbance curves between $4000 - 1800\text{ cm}^{-1}$ interval, some of the literature informs such a behavior as an indicator of high-electroactivity.

Furthermore, the absorbance peaks around 720 cm^{-1} wavenumber band is known as indicating the conjugation length of PPy polymer chains. Longer the conjugation results higher the conductivity.

The FTIR spectrum obtained for nanoparticles shows the presence of PPy's characteristic absorption bands at 1543 , 1458 cm^{-1} (C=C stretching of pyrrole ring), 1311 cm^{-1} (C-N stretching vibration in the ring), 1166 cm^{-1} (C-H in-plane

deformation), 1041 cm^{-1} (N-H in-plane deformation), 908 cm^{-1} (C-H out-of-plane deformation), 783 cm^{-1} (C-H out-of-plane ring deformation) and 673 cm^{-1} (C-C out-of-plane ring deformation or C-H rocking).

In Figure 4.46, PPy's characteristic peak at 1554 cm^{-1} (the PPy ring vibration peak, which does not occur on FTIR of copolymer nanoparticles) is taken into account to show the increase in PPy content of nanoparticles.

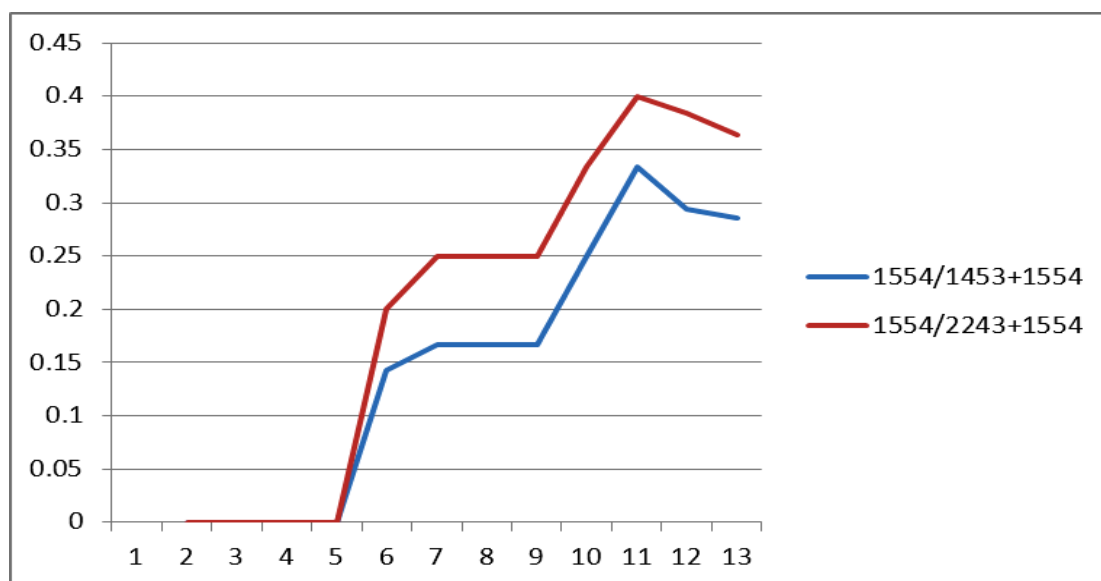


Figure 4.46 : The change in ratio of PPy/PAN characteristic peaks by initial Py amount.

As seen in Figure 4.46, first four samples (copolymer np, and core-shell np with 10, 15, 20 μl initial Py feed) do not show a clear characteristic peak of PPy, then the peak absorbance shows an increase with Py amount, but last two samples (core-shell np with 240 and 360 μl Py) show a decrease. The maximum absorbance ratio is clearly seen at core-shell np sample with 120 μl initial amount of Py. It indicates also the evidence of the highest amount of PPy formation on this sample.

4.6.5 UV-Visible spectroscopic characterization of nanoparticles

While UV-Visible Spectroscopy characterization, two types of sampling were performed prior to the analyses. First, 10 microliters of emulsion from each sample were taken into and dispersed in 10 ml of distilled water, and UV-Vis spectroscopy analysis was achieved (Fig 4.47). The second type of sampling technique includes precipitation and isolating the nanoparticles from their own emulsions, and washing and drying them, and then dissolving 0.001 g nanoparticle powder was in 10 ml

DMF and after calibration of the spectrometer with pure DMF, taking the measurements (Figure 4.48).

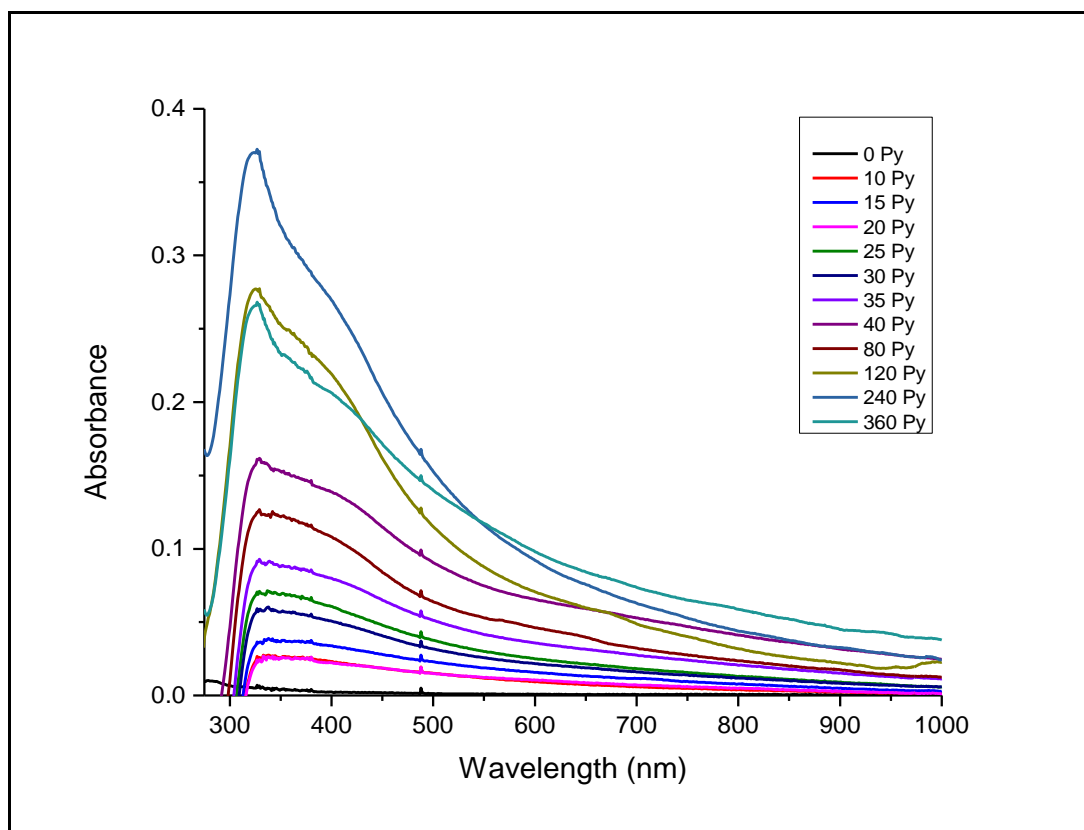


Figure 4.47 : UV-Visible spectrum of P(AN-co-BuA) and PPy/P(AN-co-BuA) nanoparticles in distilled water medium (emulsion/water 1/1000 dilution).

The UV-Visible spectroscopy results show the absorbance increase by the increasing pyrrole addition into the reaction media. 0, 10, 15, 20, 25, 35, 40, 80, 120, 240, and 360 microliters of Py added nanoparticles were analyzed and after 40 microliter PPy added, the characteristic peak at 460 nm appears and shows the $\pi-\pi^*$ transition band of PPy [316]. This peak appears at 80, 120, 240, and 360 μl pyrrole added samples as seen in the Figure 4.48.

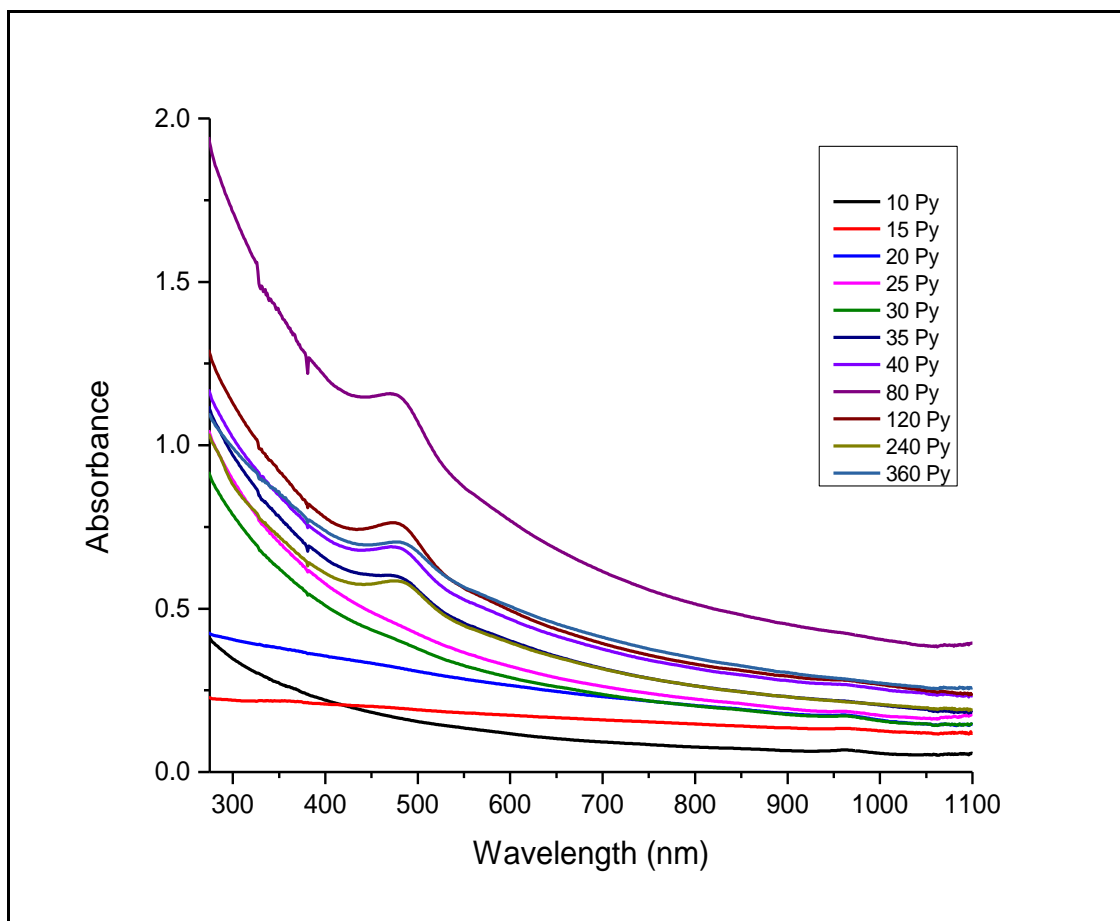


Figure 4.48 : UV-Visible spectrum of PPy/P(AN-co-BuA) nanoparticles in DMF solvent (0.001 g of particles / 10 ml DMF).

4.6.6 Thin-films of CSNP and their EIS characterization

Thin-films (with about 2-3 microns of thickness) of previously synthesized core-shell nanoparticles were produced by dripping their 20 μ l of 2,5wt% DMSO solution onto 1cm x 2cm Indium tinoxide-Polyethyleneterephthalate (ITO-PET) surfaces arranging to cover about half of the surface (to leave an open surface to attach the resultant samples to the analyzer in order to conduct Electrochemical Impedance Spectroscopy analyzes), and then drying them for a few hours in vacuum-oven under -1 atm pressure and 60°C temperature to evaporate and remove excess of DMSO, so to obtain thin-film surface.



Figure 4.49 : Preparation stages of thin-films and the resultant samples.

After obtaining the thin films of PPy/AN-co-BuA composite CSNPs on ITOPET substrates, they were taken into 10 ml of 0.1 M $\text{NaClO}_4/\text{H}_2\text{O}$ solution to perform Electrochemical Impedance Spectroscopy (EIS) analyses. The Nyquist, Bode Phase, Bode Magnitude and Admittance results were obtained and their graphs were plotted as comparison to each other as can be seen in Figures 4.51 to 4.54.

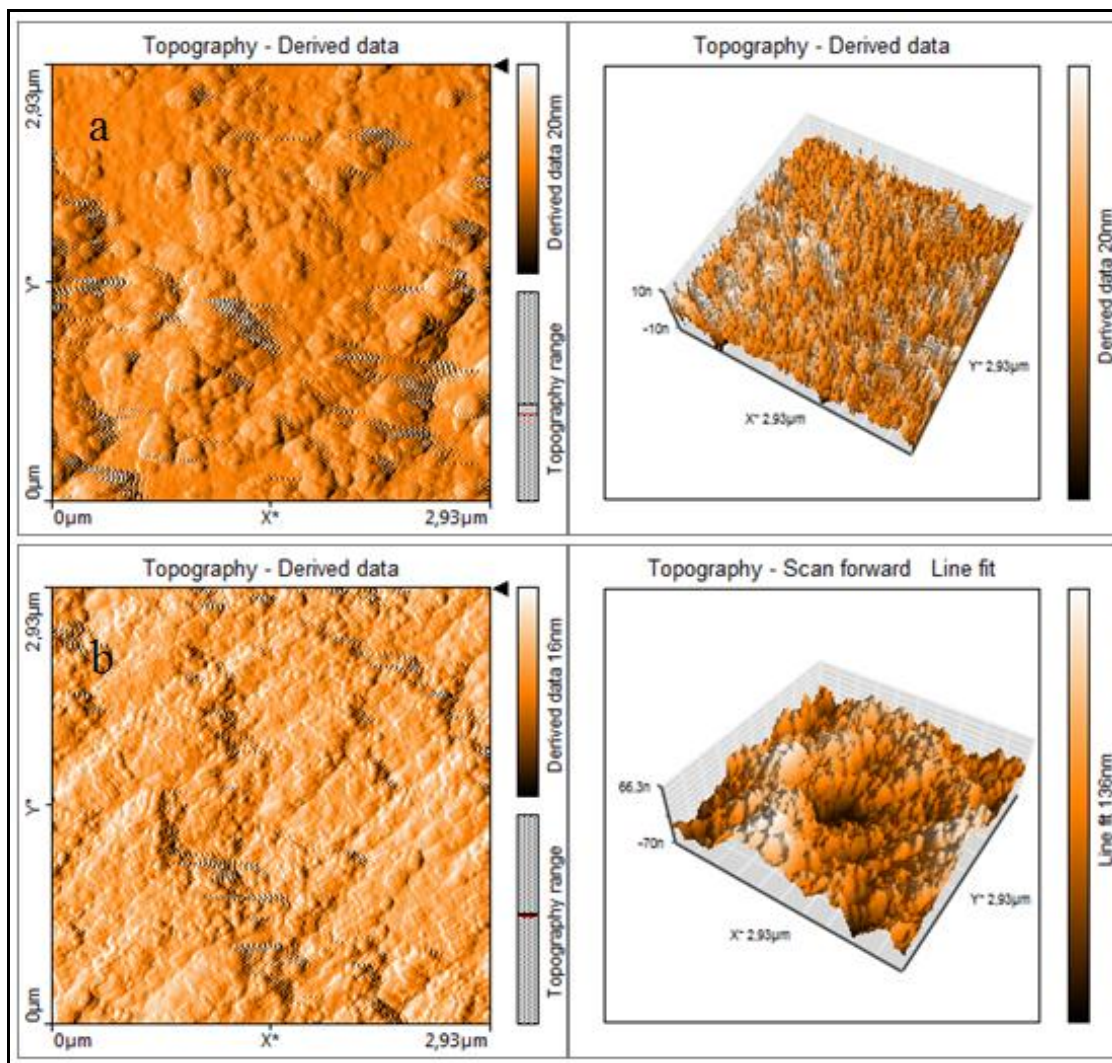


Figure 4.50 : The morphology change on surfaces of CSNPs' thin-films (a: thin-film obtained from 20µl Py polymerized CSNPs, b: thin-film obtained from 40µl Py polymerized CSNPs).

Above in resultant views of AFM analyses (Figure 4.50), it is shown the topographical views of two thin-film samples which were produced by using CSNPs with different PPy contents. As it can be easily noticed, the increasing amount of PPy formation shows itself either as changes in topography of film surfaces, whereas granular surface is more obvious on latter because of larger particles sizes; and as an obvious difference also in roughness values. Here it would be wise to take into account that the analyzed surface areas are identical for both samples, so it is possible to evaluate the roughness value as an indication to compare morphological changes caused by different amounts of PPy formation on surfaces of copolymeric nanoparticles which were used as templates.

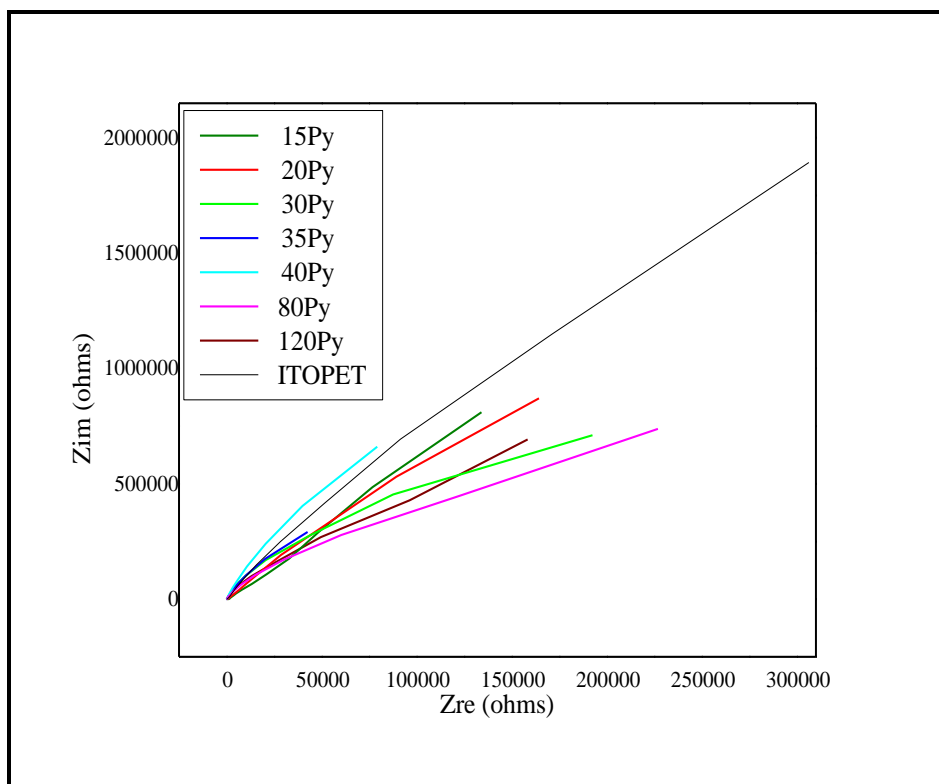


Figure 4.51 : Nyquist plots' comparison on EIS (analyses were performed in 10 ml 0,1 M NaClO₄/H₂O).

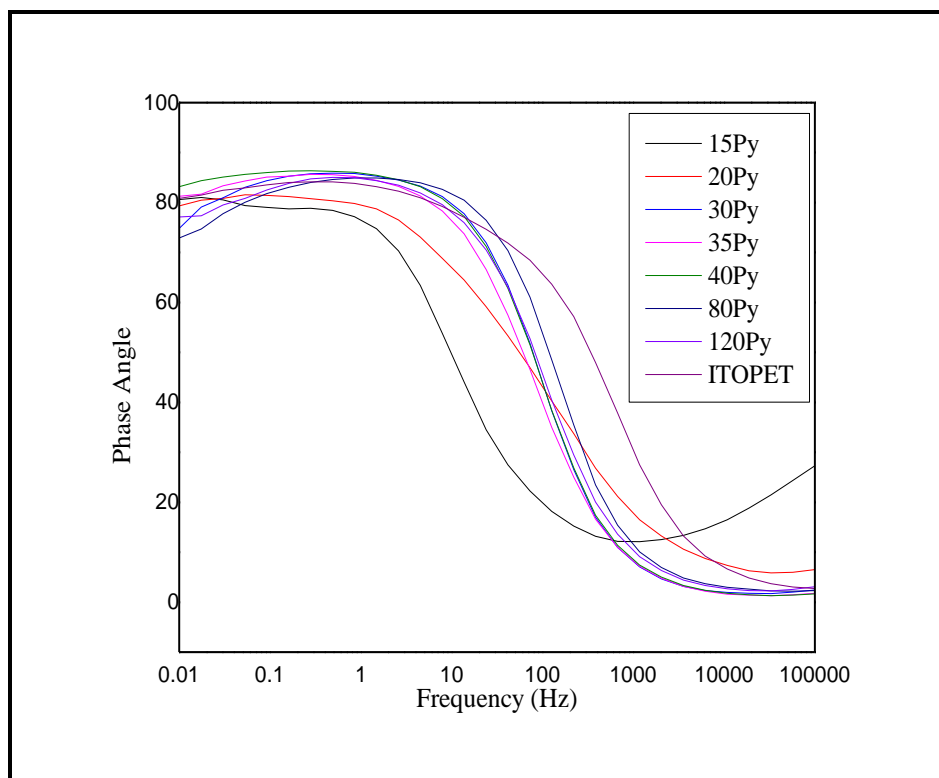


Figure 4.52 : Bode Phase plots' comparison on EIS (analyses were performed in 10 ml 0,1 M NaClO₄/H₂O).

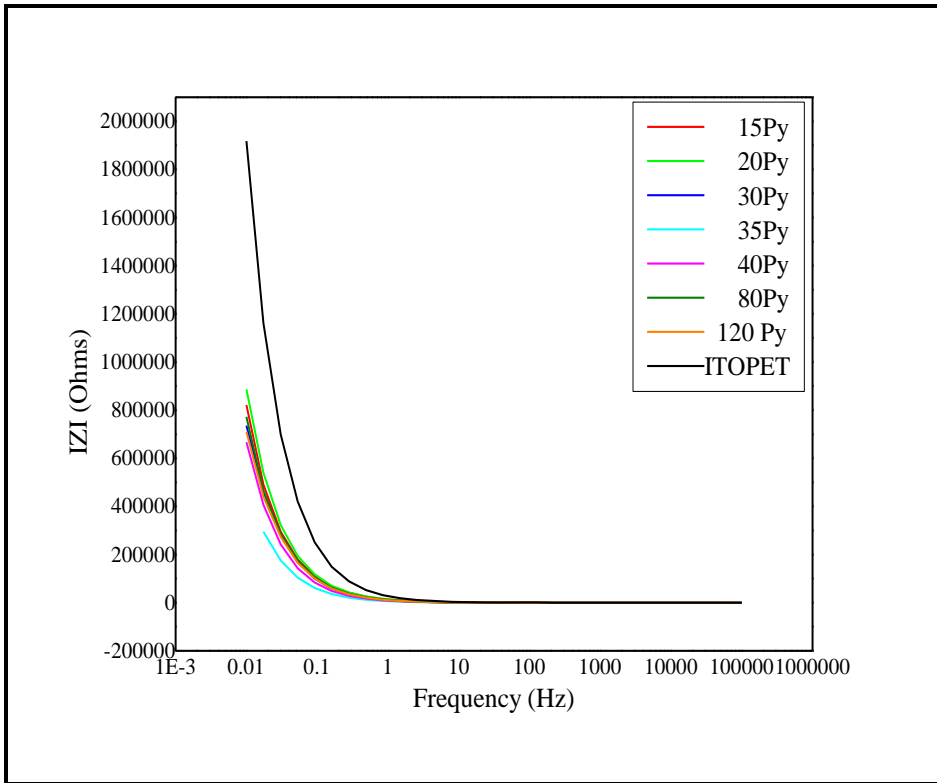


Figure 4.53 : Bode Magnitude plots' comparison on EIS (analyses were performed in 10 ml 0,1 M NaClO₄/H₂O).

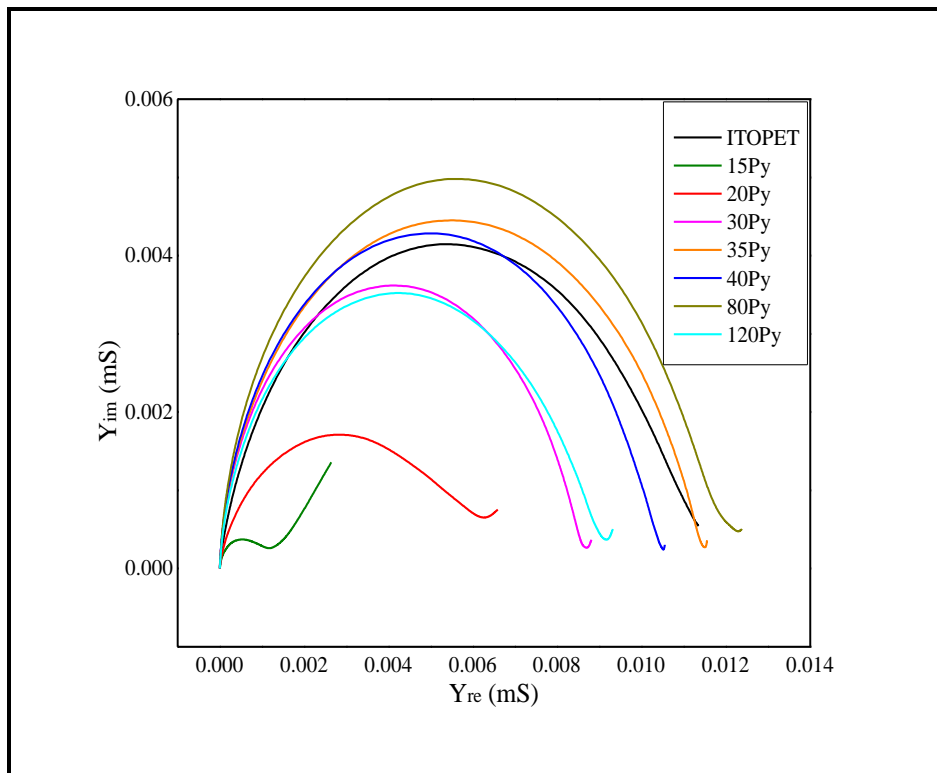


Figure 4.54 : Admittance curves' comparison on EIS (analyses were performed in 10 ml 0,1 M NaClO₄/H₂O).

From the related literature it is well known that usually the maximum peak of semi-circle curves are evaluated as “conductivity” of the sample-system which is subjected to EIS analysis. Thus, it can be seen above in Figure 4.54, the sample labeled as “40 Py” is showing a conductivity even higher than ITO/PET surface itself. And this result can be related to the polymerization method for Py here in this study was used, and the doping effect of DMSO in the temperature of vacuum-oven which was used to obtain thin-films. Some of the literature already reports doping effect of annealing the film samples were casted on substrates with DMSO as solvent.

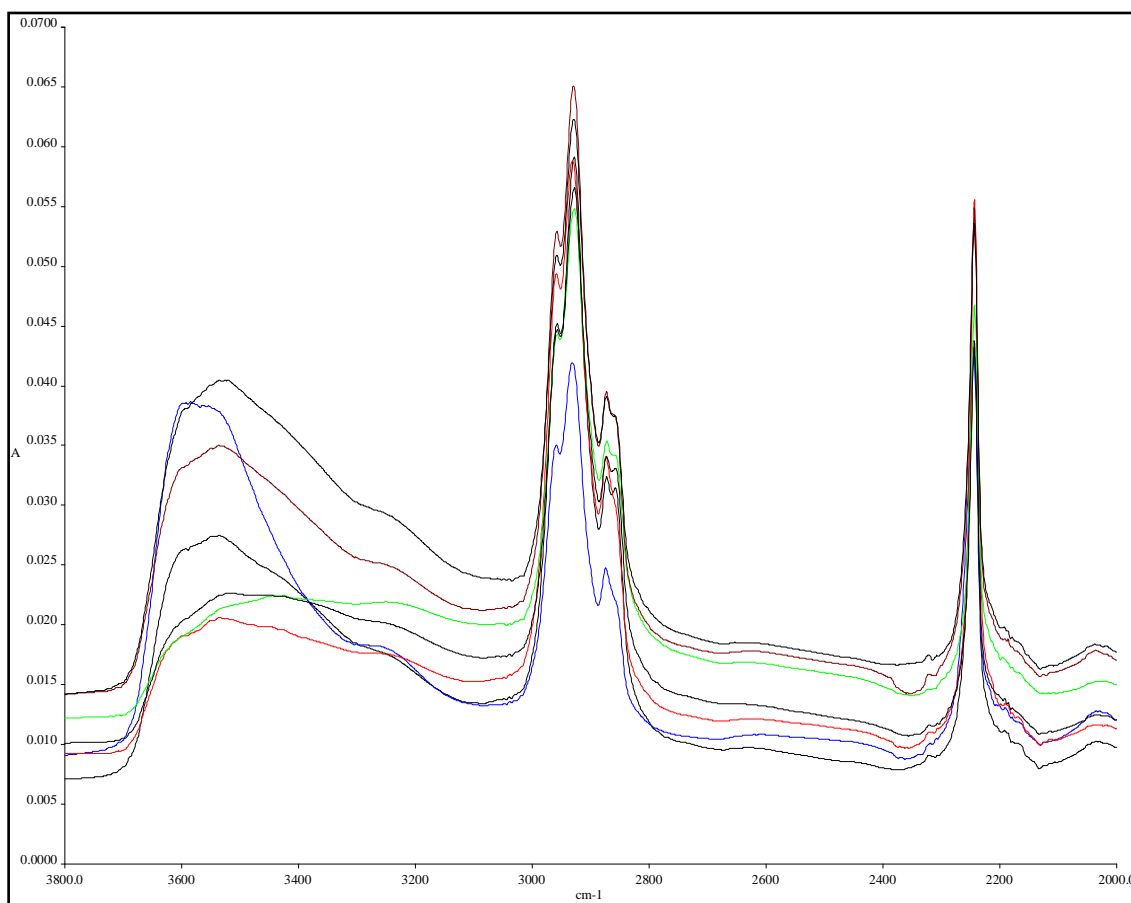


Figure 4.55 : FTIR spectra of CSNP thin-films between 3800-2000 cm^{-1} band.

In extended view of spectra above it is shown (Figure 4.55), FTIR absorbance curves of 15, 20, 30, 35, 40 (top black curve), 80 (lowest black curve) and 120 μl Py polymerized CSNP-thin film samples. Here it is focused on the characteristic peaks of PPy. (3558 cm^{-1} : O-H stretching covalently bound due to lack of O-H bending at 1620 cm^{-1} in undoped PPy; 3400 cm^{-1} N-H stretching; 3110 cm^{-1} : Aromatic C-H stretching) [212]. 35 and 40 microliters Py polymerized CSNP thin films have the maximum absorbance, as they showed also better performance than other samples in

EIS analyses. For instance, FTIR absorbance peaks show a good correlation with Admittance peaks of EIS.

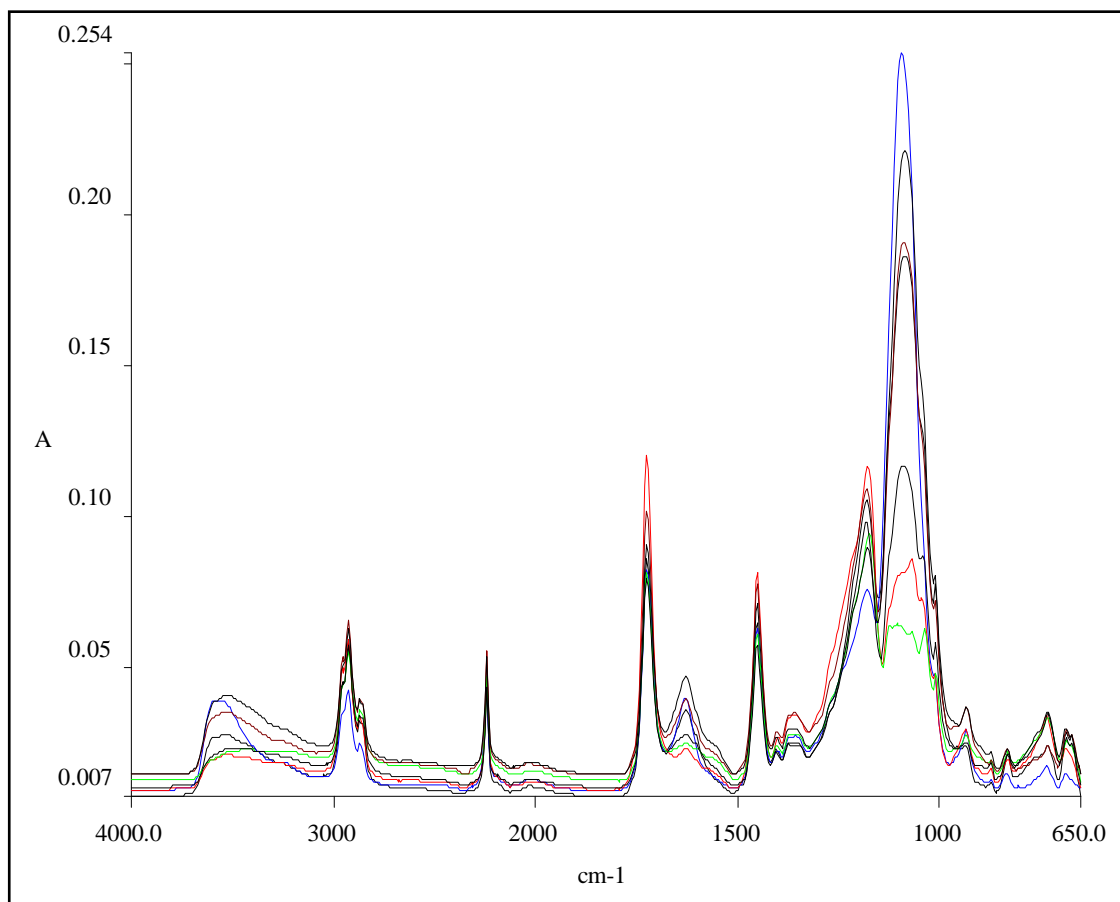


Figure 4.56 : FTIR spectra of CSNP thin-films between 4000-650 cm^{-1} band.

In Table 4.4, the characteristic absorbance peaks related to PAN, PBuA, and PPy are listed. Here it is seen and also from the literature it is known that 2959 cm^{-1} absorbance peak is related to PPy formation, and it is -C-H deformation stretching of PPy.

Figure 4.57 shows the correlation between the related PPy absorbance peaks from FTIR and the Admittance curves' maximums from EIS which are regarded to the electrical conductivity performance to the sample subjected to EIS analysis.

Table 4.4 : Absorbance peaks regarding to PPy, PAN and PBuA of CSNP thin films.

		15 Py	20 Py	30 Py	35 Py	40 Py	80 Py	120 Py
	cm-1							
	736	0.01	0.03	0.03	0.02	0.03	0.03	0.02
PPy	1403	0.02	0.02	0.02	0.02	0.02	0.02	0.02
	1453	0.06	0.08	0.06	0.07	0.07	0.05	0.06
	2190	0.01	0.01	0.01	0.01	0.01	0.01	0.01
	2959	0.03	0.04	0.04	0.05	0.05	0.04	0.04
	3564	0.03	0.02	0.02	0.03	0.04	0.02	0.02
PAN	1453	0.06	0.08	0.06	0.07	0.07	0.05	0.06
	2243	0.04	0.05	0.04	0.05	0.05	0.04	0.04
PBuA	1728	0.08	0.12	0.08	0.1	0.09	0.07	0.08

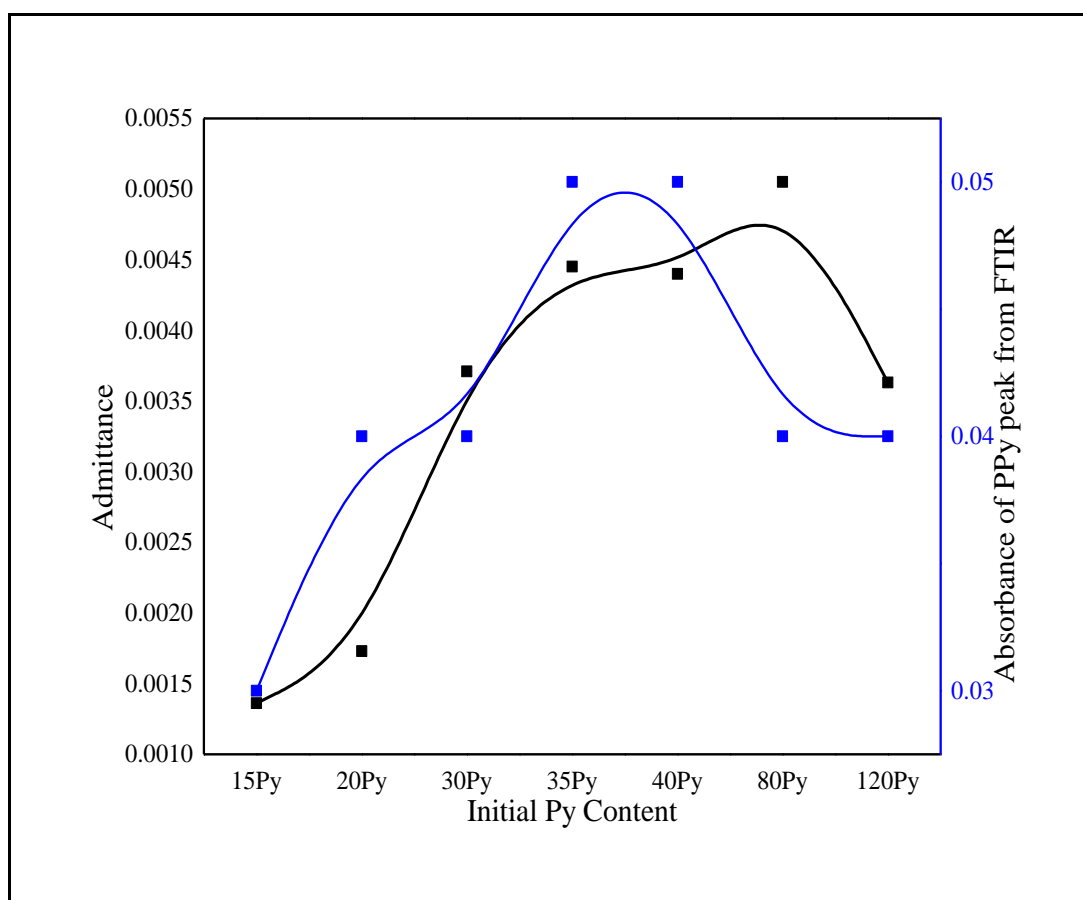


Figure 4.57 : PPy FTIR absorbance peaks – admittance maximums correlation.

Except some points, almost all the points regarding to absorbance maximums of chosen characteristic FTIR peak of PPy (here it is at 2959 cm^{-1}) and admittance values of thin-film samples, are showing a good correlation with each other. Some samples are showing a bias from the expected tendency, due to side-chains formation on molecular chains of PPy because of either excessive Py amount, and the decreasing initiator/Py ratio with increasing Py monomer, while the initiator amount is stable for all samples. To obtain higher conductivity, it is of course important to polymerize more Py so to result more PPy formation, but also to keep the initiator/Py ratio as high as possible, and also to use a suitable solvent system while either producing CSNPs and preparing the composite samples, to keep the PPy chains in oriented and regular form, also to obtain them with higher doping levels.

5. CONCLUSIONS

In this study, first it was investigated the bulk and emulsion polymerizations of Acrylonitrile (AN) and Butyl acrylate (BuA), and then, their homopolymers and copolymers with different mol% monomer ratios were synthesized. Each copolymeric product differs in morphological, mechanical, electrical and chemical character by change in monomer fractions of its' raw materials, first due to its polymer, and then the solvent type which has to be used to solve and than also to shape it into composite products such as film, thin-film, coating, nanofibers via casting/spin-coating/dripping/electrospraying/electrospinning methods. Pyrrole (Py) and its derivatives were also used to enhance the electrical behavior of polymeric products, and all the performed analyses proved the existence of electroactive polymer in composites, while changing drastically their morphological, mechanical and spectroscopic characteristics. For the better mechanical properties, BuA amount plays a critical role. Electroactive composites could be produced in various forms according to the end-use, thus, while the composite films/thin-films are suitable for anti-corrosive coatings for metal surfaces or electromagnetic shielding material for walls, ship/aircraft bodies, or as electrochromic film coating on automobile, seacraft, and airplane glasses; on the other hand, nanofiber forms of electroactive composites are more suitable for a wide range of applications such as gas-sensors, bioactive-synthetic-tissues, antibacterial and/or antiviral air-conditioner filters, etc., because of their porous structure at nano scale, so their large total surface area. In this thesis study, as last stage, P(AN-co-BuA) copolymer was synthesized via micro-emulsion polymerization method. Py monomer at different Py/Polymer wt% ratios in this emulsion medium was polymerized, and this process was carried out without using any extra initiator nor surfactant. Polymerization of Py in emulsion medium, so its deposition onto each polymer particle as "shell" was performed at room temperature, and thus to produce polymer-composite core-shell nanoparticles (CSNP) was obtained by using such an easy and cost-effective single-batch method. Then, these core-shell nanoparticles (CSNP) were used also to produce thin-films by dripping onto electrically-conductive Indiumtin oxide Polyethyleneterephthalate (ITO-PET)

substrates from their DMSO-solutions. The increasing BuA amount in copolymer structure results better mechanical characteristics which can be compared even to elastomers; lower Glass-transition temperatures (T_g), but better thermal resistance, which also means higher curing temperatures; on the other hand, increasing PPy formation results cauliflower surface structure, so an increasing surface roughness, brittleness as mechanically, but higher electrical conductivity. It is possible to enhance electrical behavior while keeping mechanical properties at an acceptable level, with increasing PPy amount, but also BuA comonomer in composites. Already some samples showed a good potential for the future applications, as their electrical and mechanical behaviors are much better than their homopolymeric precursors.

REFERENCES

- [1] **Bar-Cohen, Y.** (2004). *Electroactive Polymer (EAP) Actuators as Artificial Muscles Reality, Potential and Challenges* (2nd ed., Vol. 136, pp.1-765). SPIE Press.
- [2] **Bar-Cohen, Y. & Breazeal, C.** (2003). *Biologically-Inspired Intelligent Robots*, (Vol. 122, pp.1-393). SPIE Press.
- [3] **Roentgen, W. C.** (1880). About the changes in shape and volume of dielectrics caused by electricity, Section III. In G. Wiedemann (Ed.), *Annual Physics and Chemistry Series* (Vol. 11, pp.771-786). Leipzig : John Ambrosius Barth Publisher.
- [4] **Bar-Cohen, Y., Xue, T., & Lih S. S.** (1996). Polymer Piezoelectric Transducers For Ultrasonic NDE, *1st International Internet Workshop on Ultrasonic NDE, Subject: Transducers, organized by R. Diederichs*, UOnline Journal, Germany.
- [5] **Bar-Cohen, Y.** (Ed.). (1999). Proceedings of the first SPIE's Electroactive Polymer Actuators and Devices (EAPAD) Conf. *Smart Structures and Materials Symposium*, 3669, pp.1-414.
- [6] **Zhang, Q. M., Huang, C., Xia, F., & Su, J.** (2004). Electric EAP, Chapter 4. In Y. Bar-Cohen, (Ed.), *Electroactive Polymer (EAP) Actuators as Artificial Muscles* (2nd ed., Vol. 136, pp.95-148). SPIE Press.
- [7] **Sherrit, S., Bao, X., & Bar-Cohen, Y.** (2004). Methods of Testing and Characterization, Chapter 15. In Y. Bar-Cohen, (Ed.), *Electroactive Polymer (EAP) Actuators as Artificial Muscles* (2nd ed., Vol. 136, pp.467-526). SPIE Press.
- [8] **Mussa-Ivaldi, S.** (2000). Real brains for real robots. *Nature*, 408, 305-306.
- [9] **Wessberg, J., Stambaugh, C. R., Kralik, J. D., Beck, P. D., Lauback, M., Chapin, J. C., Nicolelis, M.A.** (2000). Real-time prediction of hard trajectory by ensembles of cortical neurons in primates. *Nature*, 408, 361-365.
- [10] **Bar-Cohen, Y., Olazábal, V., Sansiñena, J., & Hinkley, J.** (2004). Processing and Support Techniques, Chapter 14. In Y. Bar-Cohen (Ed.), *Electroactive Polymer (EAP) Actuators as Artificial Muscles - Reality, Potential and Challenges* (2nd ed., Vol. 136, pp.431-463). SPIE Press.
- [11] **Fisch, A., Mavroidis, C., Bar-Cohen, Y., & Melli-Huber, J.** (2003). Haptic and Telepresence Robotics, Chapter 4. In Y. Bar-Cohen and C. Breazeal (Eds.), *Biologically-Inspired Intelligent Robots* (Vol. 122, pp.73-101). SPIE Press.

- [12] **de Rossi, D., Della Santa, A., & Mazzoldi, A.** (1997). Dressware: wearable piezo- and thermo-resistive fabrics for ergonomics and rehabilitation, *Proceedings of the 19th Annual International Conference of the IEEE Engineering in Medicine and Biology Society*, Chicago, IL, USA.
- [13] **Schreyer, H. B., Gebhart, N., Kim, K. J., & Shahinpoor, M.** (2000). Electric activation of artificial muscles containing polyacrylonitrile gel fibers. *Biomacromolecules J., ACS Publications, 1*, 642-647.
- [14] **Della Santa, A., Mazzoldi, A., & De Rossi, D.** (1996). Steerable microcatheters actuated by embedded conducting polymer structures. *Journal of Intelligent Material Systems and Structures, 7* (3), 292-301.
- [15] **Bar-Cohen, Y.** (Ed/Co-author). (2005). *Biologically Inspired Technologies*, CRC Press.
- [16] **Kornbluh, K., Pelrine, R., Pie, Q., Rosenthal, M., Standford, S., Bowit, N., Sharstri, S. V.** (2004). Application of Dielectric Elastomer EAP Actuators, Chapter 16. (pp.529-581).
- [17] **Jager, E. W. H., Inganäs, O., & Lundström, I.** (2000). Microrobots for Micrometer-Size Objects in Aqueous Media: Potential Tools for Single Cell Manipulation. *Science, 288*, 2335-2338.
- [18] **Herr, H.M. & Kornbluh, R. D.** (2004). New horizons for orthotic and prosthetic technology: artificial muscle for ambulation. In Y. Bar-Cohen (Ed.), *Proceedings of SPIE's Smart Structures and Materials: Electroactive Polymer Actuators and Devices (EAPAD)*, (Vol. 5385, pp.1-9).
- [19] **Heydt, R. & Chhokar, S.** (2003). Refreshable Braille display based on electroactive polymers. In records of *23rd Intl. Display Research Conference, sponsored by the Society for Information Display*, Phoenix, Arizona, USA : September 16–18, 2003, (pp.111-114).
- [20] **Jung, K., Nam, J., & Choi, S. H.** (2004). Micro-inch worm robot actuated by artificial muscle actuator based on dielectric elastomer, *Proceedings of the 2004 SPIE's EAP Actuators and Devices (EAPAD)*, San Diego, CA, USA : 14-18 March, 2004, (Vol. 5385, pp.47).
- [21] **Allcock, H. R., Lampe, F. W., & Mark, J. E.** (2003). *Contemporary Polymer Chemistry*. 3rd ed., Pearson Education.
- [22] **Cowie, J. M. G.** (1991). *Polymers: Chemistry and Physics of Modern Materials* (2nd ed.). Blackie (in USA : Chapman and Hall).
- [23] **Ezrin, M.** (1996). *Plastics Failure Guide: Cause and Prevention*. Hanser-SPE.
- [24] **Lewis, P. R., Reynolds, K., & Gagg, C.** (2004). *Forensic Materials Engineering: Case studies*. CRC Press.
- [25] **Wright, D. C.** (2001). *Environmental Stress Cracking of Plastics*. RAPRA.
- [26] **Nuyken, O. & Lattermann, G.** (1991). *Handbook of Polymer Synthesis Part A* (1st ed., pp.223). (H. R. Kricheldorf, ed.), New York, USA : Marcel Dekker.

- [27] **Warson, H. & Finch, C. A.** (2001). *Applications of Synthetic Resin Latices: Fundamental chemistry of latices and applications of adhesives*. John Wiley & Sons Inc.
- [28] **Fittig, R. & Paul, L.** (1887). *Justus Liebigs Ann. Chem.*, 188, 55.
- [29] **Fittig, R. & Engelhorn, F. R.** (1880). *Justus Liebigs Ann. Chem.*, 200, 70.
- [30] **Kahlbaum, G. W. A.** (1880). *Über polymere Acrylsäuremethylester*, *Ber. Dtsch. Chem. Ges.*, 13, 2348.
- [31] **Röhm, O.** (1901). *On the Polymerization Products of Acrylic Acid* (Doctoral dissertation).
- [32] **Röhm, O.** (1914). *U.S. Patent No. 1,121,134*; CA : USA, vol:09, 395 A.
- [33] **Barker, A. L. & Skinner, G. S.** (1924). *J. Am. Chem. Soc.*, 46, 403.
- [34] **Riddle, E. H.** (1954). *Monomeric Acrylic Esters*. Reinhold, New York, USA.
- [35] **Kautter, C. T.** (1975). *Plastics Handbook, Polymethacrylate (Polymethacrylates) Kunststoff Handbuch*, (Vol. 9, p.1). Edited by R. Vieweg and F. Esser. Carl Hanser Verlag, München, Germany.
- [36] **Kine, B. B. & Novak, R. W.** (1985). In H. F. Mark, N. M. Bikales, C. G. Overberger, and G. Menges, eds., *Encyclopedia of Polymer Science and Engineering* (2nd ed., pp.234). New York, USA : Wiley.
- [37] **Charles, E. C., Jr.** (2003). *Giant molecules; Essential Materials for everyday living and problem solving* (2nd ed., pp.45). John Wiley & Sons Inc.
- [38] **Thompson, L. F., Willson, C. G., & Frechet, J. M. J.** (1984). Materials for Microlithography: Radiation-Sensitive Polymers. *American Chemical Society*, 266, 5020–5026.
- [39] **Htoo, M. S.** (1989). *Microelectronic Polymers*. New York, USA : Marcel Dekker.
- [40] **Gonzalez, I., Asua, J. M., & Leiza J. R.** (2007). The role of methyl methacrylate on branching and gel formation in the emulsion copolymerization of BA/MMA. *Polymer*, 48, 2542-2547.
- [41] **Clements, A., Dunn, M., Firth, V., Hubbard, L., Lazonby, J., & Waddington, D.** (2010). *The essential chemical industry*. 5th ed. CIEC Promoting Science, University of York.
- [42] **Semegen, S. T.** *Encyclopedia of Physical Science and Technology, Polymers* (3rd ed., pp.395-405). Academic Press.
- [43] **Liang, Y., Ji L., Guo, B., Lin, Z., Yao, Y. F., Li, Y., Zhang, X.** (2011). Preparation and electrochemical characterization of ionic-conducting lithium anthranum titanate oxide/polyacrylonitrile submicron composite fiber-based lithium-ion battery separators. *J Pow. Sour.*, 196, 436–441.
- [44] **Schildknecht, C. E.** (1952). *Vinyl and related polymers; their preparations, properties and applications in rubbers, plastics and in medical and industrial arts* (pp. 3878). New York: Wiley-Interscience.

- [45] **Perepelkin, K. E., Klyuchnikova, N. V., & Kulikova N. A.** (1989). Experimental evaluation of man-made fibre brittleness. *Fibre Chem.*, *21*, 145–148.
- [46] **Rahaman, M. S. A., Ismail A. F., & Mustafa A.** (2007). A review of heat treatment on polyacrylonitrile fiber. *Polym. Degrad. Stab.*, *92*, 1421–1432.
- [47] **Litmanovich, A. D. & Plate N. A.** (2000). Alkaline hydrolysis of polyacrylonitrile on the reaction mechanism. *Macromol. Chem. Phys.*, *201*, 2176–2180.
- [48] **Khajuria, A. & Balaguru, P. N.** (1992). *Plastic shrinkage characteristics of fiber reinforced cement composites* (pp.82–90). London, Routledge, UK : Taylor & Francis.
- [49] **Bai, Y. J., Wang C. G., Lun, N., Wang, Y. X., Yu, M. J., & Zhu, B.** HRTEM microstructures of PAN precursor fibers. *Carbon*, *44* (9), 1773-1778.
- [50] **Bredas, J. I. & Street, G. B.** (1985). Polarons, Bipolarons, And Solitons In Conducting Polymers. *Accounts of Chemical Research*, *18* (10), 309-315.
- [51] **Scherf, U. & Mullen, K.** (1992). *Design And Synthesis Of Extended Pi-Systems - Monomers, Oligomers, Polymers, Synthesis* (Vol. 1-2, pp.23-38). Stuttgart, Germany.
- [52] **Roncali, J.** (1992). Conjugated Poly(thiophenes) - Synthesis, Functionalization, and Applications. *Chemical Reviews*, *92* (4), 711-738.
- [53] **Tolbert L. M.** (1992). Solitons In A Box - The Organic Chemistry of Electrically Conducting Polyenes. *Accounts of Chemical Research*, *25* (12), 561-568.
- [54] **Toshima, N. & Hara, S.** (1995). Direct Synthesis Of Conducting Polymers From Simple Monomers. *Progress In Polymer Science*, *20* (1), 155-183.
- [54] **Feast, W. J., Tsibouklis, J., Pouwer, K. L., Groenendaal, L., & Meijer, E. W.** (1996). Synthesis, Processing and Material Properties of Conjugated Polymers. *Polymer*, *37* (22), 5017-5047.
- [55] **Novak, P., Muller, K., Santhanam, K., & Haas, O.** (1997). Electrochemically Active Polymers For Rechargeable Batteries. *Chemical Reviews*, *97* (1), 207-281.
- [56] **Roncali, J.** (1997). Synthetic Principles for Bandgap Control in Linear Pi-Conjugated Systems. *Chemical Reviews*, *97* (1), 173-205.
- [57] **Hide, F., Diazgarcia, M. A., Schwartz, B. J., & Heeger, A. J.** (1997). New Developments In The Photonic Applications of Conjugated Polymers. *Accounts Of Chemical Research*, *30* (10), 430-436.
- [58] **Leclerc, M. & Faid, K.** (1997). Electrical and Optical Properties of Processable Polythiophene Derivatives: Structure-Property Relationships. *Advanced Materials*, *9* (14), 1087-1094.
- [59] **Nataraj, S. K.** (2012). Polyacrylonitrile-based nanofibers - A state-of-the-art review, *Progress in Polymer Science*, *37*, 487– 513.

- [60] **Curran, D., Grimshaw, J., & Perera, S. D.** (1991). Polypyrrole as a support for electrocatalytic materials. *Chem. Soc. Rev.*, 20, 391.
- [61] **Shirakawa, H., Louis, E., MacDiarmid, A., & Heeger, A.** (1977). Synthesis of electrically conducting organic polymers: halogen derivatives of polyacetylene, (CH)_x. *Chem. Commun.*, 578–580.
- [62] **Tour, J. M.** (2000). Molecular wires for electronic applications. *Polym. News*, 25, 329–336.
- [63] **Maw, S., Smela, E., Yoshida, K., Sommer-Larsen, P., & Stein, R. B.** (2001). The effects of varying deposition current density on bending behaviour in PPy(DBS)- actuated bending beams. *Sensors Actuators A*, 89, 175–184.
- [64] **Sonmez, G., Scotland, P., Zong, K., & Reynolds, J. R.** (2001). Highly transmissive and conductive poly[(3,4-alkylenedioxy)pyrrole-2,5-diyl] (PXDOP) films prepared by air or transition metal catalyzed chemical oxidation. *J. Mater. Chem.*, 11, 289–294.
- [65] **Ferraris, J. P., Brotherston, I. D., Loveday, D. C., Mudigonda, D. S. K., & Li, L.** (1999). Type III electrochemical capacitors based on poly(3-phenylthiophene) derivatives. *Proc. Electrochem. Soc.*, 98, 671–682.
- [66] **Lovinger, A. J., Bao, Z., Katz, H. E., and Dodabalapur, A.** (1999). Structural, morphological and orientational requirements for high-performance polymeric and organic thin-film transistors. *Polym. Mater. Sci. Eng.*, 81, 234–235.
- [67] **Gratzel, M.** (2001). Molecular photovoltaics that mimic photosynthesis. *Pure Appl. Chem.*, 73, 459–467.
- [68] **MacDiarmid, A. G.** (1985). *Short Course on Conductive Polymers*. SUNY, New Platz, NY, USA.
- [69] **Zarras, P. & Irvin, J. A.** (2003). Electrically active polymers. In: *Encyclopedia of Polymer Science and Technology* (3rd Edition). New York, USA : John Wiley & Sons.
- [70] **Epstein, A. J.** (1997). Electrically conducting polymers: science and technology. *MRS Bull.*, 22 (6), 16–23.
- [71] **Kaner, R. B. & MacDiarmid, A. G.** (1988). *Scientific America*, 60–65.
- [72] **Naarmann, H.** (1993). *Polymers to the Year 2000 and Beyond* (Chapter 4), John Wiley & Sons.
- [73] **Margolis, J.** (1989). *Conductive Polymers and Plastics* (pp.121). Chapman and Hall.
- [74] **Margolis, J.** (1989). *Conductive Polymers and Plastics* (pp.120). Chapman and Hall.
- [75] **Barlow, A.** (1997). Entone-OMI representative.
- [76] **Alcacer, L.** (1987). *Conducting Polymers Special Applications* (pp.5). D. Reidel Publishing Company.
- [77] **Salaneck, W. R., Clark, D. T., & Samuelsen, E. J.** (1991). *Science and Application of Conducting Polymers* (pp.135). IOP Publishing.

- [78] **Salaneck, W. R., Clark, D. T., & Samuelsen, E. J.** (1991). *Science and Application of Conducting Polymers* (pp.55). IOP Publishing.
- [79] **Alcacer, L.** (1987). *Conducting Polymers Special Applications* (pp.192). D. Reidel Publishing Company.
- [80] **Margolis, J.** (1989). *Conductive Polymers and Plastics* (pp.121). Chapman and Hall.
- [81] **Margolis, J.** (1989). *Conductive Polymers and Plastics* (pp.33). Chapman and Hall.
- [82] **Salaneck, W. R., Clark, D. T., & Samuelsen, E. J.** (1991). *Science and Application of Conducting Polymers* (pp.52). IOP Publishing.
- [83] **Salaneck, W. R., Clark, D. T., & Samuelsen, E. J.** (1991). *Science and Application of Conducting Polymers* (pp.168). IOP Publishing.
- [84] *Tomorrow World.* (1997). BBC TV.
- [85] **Olmedo, L., Hourquebie, P., and Buvat, P.** (1997). *Antec*, 952, 1320.
- [86] **Walker, J. A., Warren, L. F., & Witucki, E. F.** (1988). New chemically prepared conducting "pyrrole blacks". *J. Polym. Sci.: Part A: Polym. Chem.*, 26 (5), 1285.
- [87] **Martina, S., Enklemann, V., Schluter, A. D., Wegner, G., Zotti, G., & Zerbi, G.** (1993). Synthesis and electrochemical and spectroscopical studies of 2.5-pyrrole oligomers and well-defined short-chain poly(2.5-pyrrole). *Synthetic Metals*, 55-57, 1096.
- [88] **Miles, M. J., Smith, W. T., & Shapiro, J. S.** (2000). Morphological investigation by atomic force microscopy and light microscopy of electropolymerised polypyrrole films. *Polymer*, 41, 3349.
- [89] **Suarez, M. F. & Compton, R. G.** (1999). In situ atomic force microscopy study of polypyrrole synthesis and the volume changes induced by oxidation and reduction of the polymer. *Journal of Electroanalytical Chemistry*, 462, 211.
- [90] **Li, Y. & Qian, R.** (1989). Effect of anion and solution pH on the electrochemical behavior of polypyrrole in aqueous solution. *Synth. Met.*, 28, 127.
- [91] **Kim, B. C., Spinks, G. M., Too, C. O., Wallace, G. G., Bae, Y. H., & Ogata, N.** (2000). Incorporation of novel polyelectrolyte dopants into conducting polymers. *Reactive & Functional Polymers*, 44, 245.
- [92] **van den Schoor, R. C. G. M., van de Leur, R. H. M., & de Wit, J. H. W.** (1999). Synthesis of a polypyrrole film on a non-conducting substrate: the influence of the acid concentration on the Fe^{3+} equilibria. *Synthetic Metals*, 102, 1404.
- [93] **Audebert, P. & Bidan, G.** (1986). Comparison of carbon paste electrochemistry of polypyrroles prepared by chemical and electrochemical oxidation paths. Some characteristics of the chemically prepared polyhalopyrroles. *Synthetic Metals*, 14, 71.

- [94] **Machida, S., Miyata, S., & Techagumpuch, A.** (1989). Chemical synthesis of highly electrically conductive polypyrrole. *Synthetic Metals*, 31, 311.
- [95] **Whang, Y. E., Han, J. H., Nalwa, H. S., Watanabe, T., & Miyata, S.** (1991). Chemical synthesis of highly electrically conductive polymers by control of oxidation potential. *Synthetic Metals*, 41-43, 3043.
- [96] **Druy, M. A.** (1986). The role of the counterion in the reactivity of conducting polymers. *Synth. Met.*, 15, 243.
- [97] **Stejskal, J., Omastova, M., Fedorova, S., Prokes, J., & Trchova, M.** (2003). Polyaniline and polypyrrole prepared in the presence of surfactants: a comparative conductivity study. *Polymer*, 44, 1353.
- [98] **Qi, Z. & Pickup, P.G.** (1997). Size Control of Polypyrrole Particles. *Chem. Mater.*, 9, 2934.
- [99] **Mithra, L. M. M., Cao, Y., Cho, S., Sutar, D., Lee, K., Subramanyam, S. V.** (2001). Electrical transport and reflectance studies on polypyrrole-CF₃SO₃⁻ in the vicinity of metal-insulator transition. *Synthetic Metals*, 119, 437.
- [100] **Lei, J., Cai, Z., & Martin, C. R.** (1992). Effect of reagent concentrations used to synthesize polypyrrole on the chemical characteristics and optical and electronic properties of the resulting polymer. *Synthetic Metals*, 46, 53.
- [101] **Zotti, G., Zecchin, S., Schiavon, G., & Groenendaal, L. B.** (2000). Conductive and magnetic properties of 3,4-dimethoxy- and 3,4-ethylenedioxy-capped polypyrrole and polythiophene. *Chem. Mater.*, 12, 2996.
- [102] **Gassner, F., Graf, S., & Merz, A.** (1997). On the physical properties of conducting poly(3,4-dimethoxypyrrole) films. *Synth. Met.*, 87, 75.
- [103] **Zong, K. & Reynolds, J. R.** (2001). 3,4-Alkylenedioxyppyroles: Functionalized Derivatives as Monomers for New Electron-Rich Conducting and Electroactive Polymers. *J. Org. Chem.*, 66, 6873.
- [104] **Sonmez, G., Schottland, P., Zong, K., & Reynolds, J. R.** (2001). Highly Transmissive and Conductive Poly[(3,4-alkylenedioxy)pyrrole-2,5-diyl] (PXDOP) Films Prepared by Air or Transition Metal Catalyzed Chemical Oxidation. *J. Mater. Chem.*, 11, 289.
- [105] **Forsyth, M. & Smith, M. E.** (1993). Solid state NMR characterization of polypyrrole: The nature of the dopant in PF₆⁻ doped films. *Synth. Met.*, 55-57, 714.
- [106] **Malinauskas, A.** (2001). Chemical deposition of conducting polymers. *Polymer*, 42, 3957.
- [107] **Kim, C. Y., Lee, J. Y., & Kim, D. Y.** (1998). *Patent No.* 5,795,953.
- [108] **Kim, I. W., Lee, J. Y., & Lee, H.** (1996). Solution-cast polypyrrole film: the electrical and thermal properties. *Synthetic Metals*, 78, 117.
- [109] **Lee, G. J., Lee, S. H., Ahn, K. S., & Kim, K. H.** (2002). Synthesis and characterization of soluble polypyrrole with improved electrical conductivity. *J. Appl. Poly. Sci.*, 84, 2583.

- [110] **Oh, E. J. & Jang, K. S.** (2001). Synthesis and characterization of high molecular weight, highly soluble polypyrrole in organic solvents. *Synth. Met.*, *119*, 109.
- [111] **Nicolau, Y. F., Davied, S., Genoud, F., Nechtschein, M., & Travers, J. P.**, (1991). Polyaniline, polypyrrole, poly(3-methylthiophene) and polybithiophene layer-by-layer deposited thin films. *Synth. Met.*, *42* (1-2), 1491.
- [112] **Jousse, F. & Olmedo, L.** (1991). Parametric study of vapor-phase polymerization of pyrrole: An improvement in reproducibility. *Synth. Met.*, *41*, 385.
- [113] **Chakraborty, M., Mukherjee, D. C., & Mandal, B. M.** (1999). Interpenetrating polymer network composites of polypyrrole and poly(vinyl acetate). *Synthetic Metals*, *98*, 193.
- [114] **Khedkar, S. P. & Radhakrishnan, S.** (1997). Application of dip-coating process for depositing conducting polypyrrole films. *Thin Solid Films*, *303*, 167.
- [115] **Yin, W., Liu, H., Li, J., Li, Y., & Gu, T.** (1997). Conducting composite films based on polypyrrole and crosslinked poly(styrene-butyl acrylate-hydroxyethyl acrylate). *J. App. Poly. Sci.*, *64*, 2293.
- [116] **Zoppi, R. A. & De Paoli, M. A.** (1996). Chemical preparation of conductive elastomeric blends: polypyrrole/EPDM—II. Utilization of matrices containing crosslinking agents, reinforcement fillers and stabilizers. *Polymer*, *37*, 1999.
- [117] **Bjorklund, R. B. & Lundstroem, I.** (1984). Some properties of polypyrrole-paper composites. *J. Electron. Mat.*, *13*, 211.
- [118] **Kuhn, H. H.** (1997). Adsorption at the liquid/solid inter-face: conductive textiles based on polypyrrole. *Textile Chemist and Colorist*, *29*, 17.
- [119] **Onoda, M., Fujita, D., Isaki, K., & Nakayama, H.** (1999). Preparation and functions of conductive polymer/insulating polymer composite films using molecular self-assembly. *Electrical Engineering in Japan*, *128*, 1.
- [120] **Onoda, M. & Tada, K.** (1999). *Proceedings of the 6th International Conference on Properties and Applications of Dielectric Materials*. Xi'an, China : Xi'an Jiaotong University, June 21-26, 2000.
- [121] **Zinger, B. & Kijel, D.**, (1991). Electrically conducting polyethylene/polypyrrole films. *Synthetic Metals*, *41* (3), 1013.
- [122] **De Jesus, M. C., Weiss, R. A., & Chen, Y.** (1997). The development of conductive composite surfaces by a diffusion-limited in situ polymerization of pyrrole in sulfonated polystyrene ionomers. *Journal of Polymer Science: Part B: Polymer Physics*, *35*, 347.
- [123] **Neoh, K. G., Teo, H. W., Kang, E. T., & Tan, K. L.** (1998). Enhancement of Growth and Adhesion of Electroactive Polymer Coatings on Polyolefin Substrates. *Langmuir*, *14*, 2820.

- [124] **Chen, X. B., Issi, J. P., Devaux, J., & Billaud, D.** (1997). The Stability of Polypyrrole and Its Composites. *Journal of Materials Science*, 32, 1515.
- [125] **Truong, V. T., Codd, A. R., & Forsyth, M.** (1995). Dielectric properties of conducting polymer composites at microwave frequencies, *Journal of Materials Science*, 29 (16), 4331.
- [126] **Bjorklund, R. B. & Liedberg, B.** (1986). Electrically conducting composites of colloidal polypyrrole and methylcellulose. *J. Chem. Soc. Chem. Commun.*, 16, 1293.
- [127] **Stanke, D., Hallensleben, M. L., & Toppare, L.** (1995). Graft copolymers and composites of poly(methyl methacrylate) and polypyrrole. *Synthetic Metals*, 72, 89.
- [128] **Stanke, D., Hallensleben, M. L., & Toppare, L.** (1995). Graft copolymers and composites of poly(methyl methacrylate) and polypyrrole. *Synthetic Metals*, 72, 95.
- [129] **Ng, S. C., Chan, H. S. O., Xia, J. F., & Yu, W.** (1998). Electrically conductive graft copolymers of poly(methyl methacrylate) with varying polypyrrole and poly(3-alkylpyrroles) contents, *J. Mater. Chem.*, 8 (11), 2347.
- [130] **Nazzal, A. I. & Street, G. B.** (1985). Pyrrole–styrene graft copolymers. *J. Chem. Soc., Chem. Commun.*, 375.
- [131] **Li, X. G., Huang, M. R., Wang, L. X., Zhu, M. F., & Menner, A.** (2001). Synthesis and characterization of pyrrole and *m*-toluidine copolymers. *Synthetic Metals*, 123, 435.
- [132] **Li, X. G., Wang, L. X., Jin, Y., Zhu, Z. L., & Yang, Y. L.** (2001). Preparation and identification of a soluble copolymer from pyrrole and *o*-toluidine. *J. Appl. Poly. Sci.*, 82, 510.
- [133] **Li, X. G., Wang, L. X., Huang, M. R., Lu, Y. Q., Zhu, M. F., & Menner, A.** (2001). Synthesis and characterization of pyrrole and anisidine copolymers. *Polymer*, 42 (14), 6095.
- [134] **Ustamehmetoglu, B., Kizilcan, N., Sarac, A. S., & Akar, A.** (2001). Soluble polypyrrole copolymers. *J. Appl. Poly. Sci.*, 82, 1098.
- [135] **Cirpan, A., Alkan, S., Toppare, L., Cianga, I., & Yagci, Y.** (2002). Synthesis and characterization of conducting copolymers of thiophene-3-yl acetic acid cholesteryl ester with pyrrole. *Journal of Materials Science*, 37, 1767.
- [136] **Kuhn, H. H. & Child, A. D.** (1998). Electrically Conducting Textiles. In Skotheim, T. A., Elsenbaumer, R.L., Reynolds, J.R., (Eds.), *Handbook of Conducting Polymers* (pp. 993). New York, USA : Marcel Dekker.
- [137] **Gregory, R. V.** (1998). Solution Processing of Conductive Polymers: Fibres and Gels from Emeraldine Base Polyaniline. In Skotheim, T. A., Elsenbaumer, R. L., Reynolds, J. R., (Eds). *Handbook of Conducting Polymers* (pp.437). New York, USA : Marcel Dekker.

- [138] **Miyata, S. & Ozio, T.** (1997). *US Patent No.* 4699804.
- [139] **Maus, L., Witucki, E. F., & W., L.F.** (1987). *US Patent No.* 4696835.
- [140] **Newman, P., Warren, L., & Witucki, E.** (1986). *US Patent No.* 4617228.
- [141] **Mizuki, T. & Watanabe, K.** (1989). *Japan Patent No.* 01,266,280.
- [142] **Wiersma, A. E.** (1994). *European Patent App Patent No.* 0 589 529 A1.
- [143] **Wiersma, A. E., vd Steeg, L. M. A., & Jongeling, T. J. M.** (1995). Waterborne core-shell dispersions based on intrinsically conducting polymers for coating applications. *Synthetic Metals*, 77, 2269.
- [144] **Genies, E. M., Petrescu, C., & Olmedo, L.** (1991). Conducting materials from polyaniline on glass textile. *Synthetic Metals*, 41 (1-2), 665.
- [145] **Gregory, R. V., Kimbrell, W. C., & Kuhn, H. H.** (1989). Conductive textiles. *Synthetic Metals*, 28 (1-2), 823.
- [146] **Bartholomew, G. W., Jongchul, K., Volpe, R. A., & Wenzel, D. J.** (1993). *US Patent No.* 5211810.
- [147] **Faverolle, F., Attias, A. J., Bloch, B., Audebert, P., & Andrieux, C. P.** (1998). Highly Conducting and Strongly Adhering Polypyrrole Coating Layers Deposited on Glass Substrates by a Chemical Process. *Chemistry of Materials*, 10 (3), 740.
- [148] **Nagasubramanian, G.** (1991). *US Patent No.* 5066748.
- [149] **Cho, G., Jang, J., Moon, I., Leeb, J. S., & Glatzhofer, D. T.** (1999). Enhanced adhesion of polypyrrole film through a novel grafting method. *Journal of Materials Chemistry*, 9 (2), 345.
- [150] **Kuhn, H. H.** (1992). *US Patent No.* 5,108,829.
- [151] **Bhadani, S. N., Kumari, M., Gupta, S. K. S., & Sahu, G. C.** (1997). Preparation of conducting fibers via the electrochemical polymerization of pyrrole. *Journal of Applied Polymer Science*, 64, 1073.
- [152] **Barry Jr., C. N.** (1993). *U.S. Patent No.* 5,176,851.
- [153] **MacDiarmid, A. G., Chiang, J. C., Richter, A. F., & Somasiri, N. L. D.** (1987). Synthesis and Characterization of Emeraldine Oxidation State by Elemental Analysis. In Alcacer, L., (Ed.). *Conducting Polymers* (pp.105). Reidel: Dordrecht.
- [154] **Jousse, F., Delnaud, L., & Olmedo, L.** (1995). *40th Int. SAMPE Symp. Exhib.* (pp.360).
- [155] **Sengupta, L. C. & Spurgeon, W. A.** (1992). *6th Int. SAMPE Electronics Conference.*
- [156] **Wong, T. C. P., Chambers, B., Anderson, A. P., & Wright, P. V.** (1992). Large area conducting polymer composites and their utilisation in microwave absorbing material. *Electronics Letters*, 28 (17), 1651.

- [157] **Wong, T. C. P., Chambers, B., Anderson, A. P., & Wright, P. V.** (1993). *Proc. 8th International Conference on Antennas and Propagation*. Edinburgh, UK.
- [158] **Wong, T. C. P., Chambers, B., Anderson, A. P., & Wright, P. V.** (1995). *9th International Conference on Antennas and Propagation*.
- [159] **Wong, T. C. P., Chambers, B., Anderson, A. P., & Wright, P. V.** (1993). *Proc. 3rd Int Conference on Electromagnetics in Aerospace Applications*. Turin, Italy. September 14-17, 1993.
- [160] **Gangopadhyay, R. & De, A.** (2000). Conducting Polymer Nanocomposites: A Brief Overview, *Chemistry of Materials*, 12 (3), 608.
- [161] **Armes, S. P. & Vincent, B.** (1987). Dispersions of electrically conducting polypyrrole particles in aqueous media. *J.Chem.Soc.,Chem.Commun.*, (4), 288.
- [162] **Armes, S. P., Miller, J. F., & Vincent, B.** (1987). Aqueous dispersions of electrically conducting monodisperse polypyrrole particles. *J. Colloid and Interface Sci.*, 118 (2), 410.
- [163] **Armes, S. P. & Aldissi, M.** (1990). Preparation and characterization of colloidal dispersions of polypyrrole using poly(2-vinyl pyridine)-based steric stabilizers. *Polymer*, 31, 569.
- [164] **Simmons, M. R., Chaloner, P. A., Armes, S. P., Greaves, S. J., & Watts, J. F.** (1998). Synthesis and Characterization of Colloidal Polypyrrole Particles Using Reactive Polymeric Stabilizers. *Langmuir*, 14 (3), 611.
- [165] **Armes, S. P. & Aldissi, M.** (1989). Novel colloidal dispersions of polyaniline. *J. Chem. Soc., Chem. Commun.*, (2), 88.
- [166] **Cooper, E. C. & Vincent, B.** (1989). Electrically conducting organic films and beads based on conducting latex particles. *J. Phys. D.: Appl. Phys.*, 22, 1580.
- [167] **Chehimi, M. M., Abel, M. L., Sahraoui, Z., Fraoua, K., Lascelles, S. F., & Armes, S. P.** (1997). Time-dependent variation of the surface energy of conducting polypyrrole. *Int. J. Adhesion and Adhesives*, 17 (1), 1.
- [168] **Khan, M. A. & Armes, S. P.** (2000). Conducting Polymer-Coated Latex Particles. *Adv. Mater.*, 12 (9), 671.
- [169] **Lascelles, S. F. & Armes, S. P.** (1995). Synthesis and characterization of micrometersized polypyrrole-coated polystyrene latexes. *Adv. Mater.*, 7 (10), 864.
- [170] **Barthet, C., Armes, S. P., Lascelles, S. F., Luk, S. Y., & Stanley, H. M. E.** (1998). Synthesis and Characterization of Micrometer-Sized, Polyaniline-Coated Polystyrene Latexes. *Langmuir*, 14 (8), 2032.
- [171] **Ondarcuhu T. & Joachim C.** (1998). Drawing a single nanofibre over hundreds of microns. *Europhys Lett.*, vol. 42 (2), 215–220.
- [172] **Feng, L., Shuhong, L., Zhai, J., Song, Y., Jiang, L., & Zhu, D.** (2002). Super-Hydrophobic Surface of Aligned Polyacrylonitrile Nanofibers. *Angewandte Chemie Int. Ed.*, 41 (7), 1221–1223.

- [173] **Martin, C. R.** (1996). Membrane-based synthesis of nanomaterials. *Chemistry of Materials*, 8 (8), 1739-1746.
- [174] **Ma, P. X. & Zhang, R.** (1999). Synthetic nano-scale fibrous extracellular matrix. *J Biomed Mat Res.*, 46, 60–72.
- [175] **Liu, G., Ding, J., Qiaol, L., Guol, A., Dymov, B. P., Saijo, K.** (1999). Polystyrene-block poly (2-cinnamoyl ethyl methacrylate) nanofibers-Preparation, characterization, and liquid crystalline properties. *Chem-A European J.*, 5 (9), 2740-2749.
- [176] **Whitesides G. M. & Grzybowski B.** (2002). Self-assembly at all scales. *Science*, 295, 2418–2421.
- [177] **Deitzel J. M., Kleinmeyer J., Hirvonen J. K., & Beck T. N. C.** (2001). Controlled deposition of electrospun poly(ethylene oxide) fibers. *Polymer*, 42 (19), 8163-8170.
- [178] **Fong, H. & Reneker, D. H.** (2001). Electrospinning and formation of nanofibers. In: Salem, D. R. (Ed.), *Structure formation in polymeric fibers* (pp.225-246). Munich, Germany: Hanser.
- [179] **Formhals, A.** (1934). *US Patent No.* 1,975,504.
- [180] **Formhals, A.** (1939). *US Patent No.* 2,160,962.
- [181] **Formhals, A.** (1940). *US Patent No.* 2,187,306.
- [182] **Formhals, A.** (1943). *US Patent No.* 2,323,025.
- [183] **Formhals, A.** (1944). *US Patent No.* 2,349,950.
- [184] **Baumgarten, P. K.** (1971). Electrostatic spinning of acrylic microfibers. *Journal of Colloid and Interface Science*, 36 (1), 71-79.
- [185] **Taylor G. I.** (1969). Electrically driven jets. *Proc R Soc London, Ser A.*, 313, 453-475.
- [186] **Doshi J. & Reneker D. H.** (1995). Electrospinning process and applications of electrospun fibers. *J. Electrostatics*, 35 (2-3), 51-60.
- [187] **Kenawy, E. R., Layman, J. M., Watkins, J. R., Bowlin, G. L., Matthews, J. A., Wnek, G. E.** (2003). Electrospinning of Poly(Ethylene-co-Vinyl Alcohol) Fibers. *Biomaterials*, 24 (6), 907-913.
- [188] **Stankus J. J., Guan J., & Wagner W. R.** (2004). Fabrication of biodegradable elastomeric scaffolds with sub-micron morphologies. *J. Biomed Mater Res Part A*, 70A (4), 603-614.
- [189] **Bovey, F. A., Kolthoff, I. M., Medalia, A. I., & Meehan, E. J.** (1965). *Emulsion polymerization*. New York, USA : Interscience Publishers.
- [190] **Blakely, D. C.** (1975). *Emulsion polymerization: Theory and practice*. London, UK : Applied Science.
- [191] **Eliseeva, V. I., Ivanchev, S. S., Kuchanov, S. I., & Lebedev, A. V.** (1981). *Emulsion polymerization and its applications in industry*. New York, USA : Consultants Bureau.
- [192] **Barton, J. & Capek, I.** (1994). *Radical polymerization in disperse systems* (pp.48). New York, USA : Ellis Horwood.

- [193] **Gilbert, R. G.** (1995). *Emulsion polymerization: a mechanistic approach*. London, UK : Academic Press.
- [194] **Fitch, R. M.** (1997). *Polymer colloids: a comprehensive introduction*. London, UK : Academic Press.
- [195] **Verwey, E. J. W. & Overbeek, J. Th. G.** (1943). *Theory of the stability of lyophobic colloids*. New York, USA : Elsevier.
- [196] **Gupta, A. K., Paliwal, D. K., & Bajaj, P.** (1998). *Journal of Applied Polymer Science*, 70, 2703-2709.
- [197] **Bajaj, P., Sreekumar, T. V., & Sen, K.** (2001). Effect of Reaction medium on Radical Polymerization of Acrylonitrile with Vinyl acids. *J. Appl. Polym. Sci*, 79, 1640.
- [198] **Serkov, A. & Radishevskii, M.** (2008). Status and Prospects for Production Of Carbon Fibres Based on Polyacrylonitrile. *Fibre Chemistry*, 40 (1), 24–31.
- [199] **Delong, Liu** (2011). Synthesis of Polyacrylonitrile by Single-electron Transfer-living Radical Polymerization Using Fe(0) as Catalyst and Its Absorption Properties After Modification. *Journal of Polymer Science Part A: Polymer Chemistry*, 2916–2923.
- [200] **Polyacrylonitrile (PAN) Carbon Fibers Industrial Capability Assessment**. United States of America Department of Defense. Retrieved December 4, 2013, from http://www.acq.osd.mil/mibp/docs/pan_carbon_fiber_report_to_congress_10-2005.pdf
- [201] **Top 9 Things You Didn't Know about Carbon Fiber**. Department of Energy. Retrieved March 29, 2013, from <http://energy.gov/articles/top-9-things-you-didn-t-know-about-carbon-fiber>
- [202] **Manufacturing advances bring carbon fiber closer to mass production**. By John McElroy RSS feed. Autoblog. Retrieved December 8, 2013, from <http://www.autoblog.com/2012/11/27/manufacturing-advances-bring-carbon-fiber-closer-to-mass-product/>
- [203] **Papkov, D., Zou, Y., Andalib, M. N., Goponenko, A., Cheng, S. Z. D., & Dzenis, Y. A.** (2013). Simultaneously Strong and Tough Ultrafine Continuous Nanofibers. *ACS Nano*, 7 (4), 3324–3331.
- [204] **Discovery yields supertough, strong nanofibers**. Retrieved April 26, 2013, from <http://www.kurzweilai.net/discovery-yields-supertough-strong-nanofibers>.
- [205] **Aykut, Y., Pourdeyhimi, B., & Khan, S. A.** (2013). Effects of Surfactants on the Microstructures of Electrospun Polyacrylonitrile Nanofibers and Their Carbonized Analogs. *Journal of Applied Polymer Science*, 3726–3735.
- [206] **Hou, C.** (2013). Synthesis of High Performance Polyacrylonitrile by RASA SET–LRP in the Presence of Mg Powder. *Journal of Polymer Science Part A: Polymer Chemistry*, 3328–3332.

- [207] **Polyacrylonitrile.** Retrieved April 25, 2014, from <http://www.pslc.ws/macrog/pan.htm>
- [208] **Bhat, N. V., Gadre, A. P., & Bambole, V. A.** (2003). Investigation of Electropolymerized Polypyrrole Composite Film: Characterization and Application to Gas Sensors. *J. Appl. Polym. Sci.*, 88, 22–29.
- [209] **Cheng, Q., Pavlinek, V., Li, C., Lengalova, A., He, Y., & Saha, P.** (2006). Synthesis and Structural Properties of Polypyrrole/Nano-Y₂O₃ Conducting Composite. *Appl. Surf. Sci.*, 253, 1736–1740.
- [210] **Sahoo, N. G., Jung, Y. C., So, H. H., & Cho, J. W.** (2007). Polypyrrole Coated Carbon Nanotubes: Synthesis, Characterization and Enhanced Electrical Properties, *Synth. Met.*, 157, 374–379.
- [211] **Al-Mashat, L., Tran, H.D., Wlodarski, W., Kaner, R.B., & Kalantar-Zadeh, K.** (2008). Conductometric Hydrogen Gas Sensor Based on Polypyrrole Nanofibers. *IEEE Sensor.J.*, 8 (4), 365–370.
- [212] **Lei, J. & Martin, C. R.** (1992). *Synthetic Metals*, 48, 331.
- [213] **Dams, R., Vangeneugden, D., & Vanderzande, D.** (2013). Atmospheric Pressure Plasma Polymerization of *In Situ* Doped Polypyrrole. *The Open Plasma Physics Journal*, 6 (1), 10.
- [214] **Acrylonitrile (ACN): 2014 World Market Outlook and Forecast up to 2018.** Retrieved May 20, 2014, from <http://mcgroup.co.uk/researches/acrylonitrile-acn>
- [215] **Pratt, C.** (2003). *Conjugated Polymers: Electronic Conductors*. London: Kingston Univ.
- [216] **Ebewele, R. O.** (2000). *Polymer Science and Technology* (chapter 15). New York, USA : CRC Press LLC.
- [217] **Rasmussen, S. C.** (2011). Electrically Conducting Plastics: Revising the History of Conjugated Organic Polymers, *ACS Symposium Series*, 1080 (10), 147–163.
- [218] **Loudon, M. G.** (2002). Chemistry of Naphthalene and the Aromatic Heterocycles. *Organic Chemistry* (4th ed., pp.1135-1136). New York, USA : Oxford University Press.
- [219] **Armarego, W. L. F. & Chai, C. L. L.** (2003). *Purification of Laboratory Chemicals* (5th ed., pp.346). Elsevier.
- [220] **Harreus, A. L.** (2002). *Ullmann's Encyclopedia of Industrial Chemistry*. Weinheim : Wiley-VCH.
- [221] **Malinauskas, A.** (2001). Chemical deposition of conducting polymers, *Polymer*, 42, 3955-3972.
- [222] **Spinks, G., Wallace, G., Ding, J., Zhou, D., Xi, B., & Gillespie, J.** (2003). Ionic liquids and polypyrrole helix tubes: Bringing the electronic braille screen closer to reality. In *SPIE Smart Structures and Materials 2003 : Electroactive Polymer Actuators and Devices* (Vol. 5051, pp.372). San Diego, CA, USA.

- [223] **Collins, G. E. & Buckley, L.** (1996). Conductive polymer-coated fabrics for chemical sensing. *Synthetic Metals*, 78, 93-101.
- [224] **Ishizu, K., Tsubaki, K., & Uchida, S.** (2002). Encapsulation of polypyrrole by internal domain modification of double-cylinder-type copolymer brushes. *Macromolecules*, 35, 10193-10197.
- [225] **He, B. L., Zhou, Y. K., Zhou, W. J., Dong, B., & Li, H. L.** (2004). Preparation and characterization of ruthenium-doped polypyrrole composites for supercapacitor, *Materials Science and Engineering, A*, 374, 322-326.
- [226] **Karim, M. R., Lim, K. T., Lee, C. J., & Lee, M. S.** (2007). A facile synthesis of polythiophene nanowires. *Synthetic Metals*, 157, 1008-1012.
- [227] **Silva, A. J. C., Ferreira, S. M. F., Santos, D. P., Navarro, M., Tonholo, J., & Ribeiro, A. S.** (2012). A multielectrochromic copolymer based on pyrrole and thiophene derivatives, *Solar Energy Materials & Solar Cells*, 103, 108-113.
- [228] **Qiao, Y., Shen, L., Wu, M., Guo, Y., & Meng, S.** (2014). A novel chemical synthesis of bowl-shaped polypyrrole particles, *Materials Letters*, 126, 185-188.
- [229] **Waghuley, S. A., Yenorkar, S. M., Yawale, S. S., & Yawale, S. P.** (2008). Application of chemically synthesized conducting polymer-polypyrrole as a carbon dioxide gas sensor. *Sensors and Actuators B*, 128, 366-373.
- [230] **Chen, S. & Zhitomirsky, I.** (2014). Capacitive behaviour of polypyrrole, prepared by electrochemical and chemical methods. *Materials Letters*, 125, 92-95.
- [231] **Sezer, E., Ustamehmetoğlu, B., & Saraç, A. S.** (1999). Chemical and electrochemical polymerization of pyrrole in the presence of N-substituted carbazoles. *Synthetic Metals*, 107, 7-17.
- [232] **Champagne, S. D., Duchet, J., & Legras, R.** (1999). Chemical and electrochemical synthesis of polypyrrole nanotubules. *Synthetic Metals*, 101, 20-21.
- [233] **Tan, Y. & Ghandi, K.** (2013). Kinetics and mechanism of pyrrole chemical polymerization. *Synthetic Metals*, 175, 183-191.
- [234] **Lee, H. S. & Hong, J.** (2000). Chemical synthesis and characterization of polypyrrole coated on porous membranes and its electrochemical stability. *Synthetic Metals*, 113, 115-119.
- [235] **He, C., Yang, C., & Li, Y.** (2003). Chemical synthesis of coral-like nanowires and nanowire networks of conducting polypyrrole. *Synthetic Metals*, 139, 539-545.
- [236] **Benhaddad, L., Bernard, M. C., Deslouis, C., Makhloufi, L., Messaoudi, B., Takenouti, H.** (2013). Chemical synthesis of hollow sea urchin like nanostructured polypyrrole particles through a core-shell redox mechanism using a MnO₂ powder as oxidizing agent and sacrificial nanostructured template. *Synthetic Metals*, 175, 192-199.

- [240] **Duchet, J., Legras, R., & Champagne, S. D.** (1998). Chemical synthesis of polypyrrole: structure-properties relationship. *Synthetic Metals*, 98, 113-122.
- [241] **Guimard, N. K., Gomez, N., & Schmidt, C. E.** (2007). Conducting polymers in biomedical engineering. *Progress in Polymer Science*, 32, 876-921.
- [242] **Lange, U., Roznyatovskaya, N. V., & Mirsky, V. M.** (2008). Conducting polymers in chemical sensors and arrays. *Analytica Chimica Acta*, 614, 1-26.
- [243] **Bator, B. P., Blaz, T, Migdalski, J., & Lewenstam, A.** (2007). Conducting polymers in modeling transient potential of biological membranes. *Bioelectrochemistry*, 71, 66-74.
- [244] **Bator, B. P., Migdalski, J., & Lewenstam, A.** (2006). Conducting polymer films as model biological membranes : Electrochemical and ion-exchange properties of poly(pyrrole) films doped with asparagine and glutamine. *Electrochimica Acta*, 51, 2173-2181.
- [245] **Cakmak, G., Küçükyavuz, Z., & Küçükyavuz, S.** (2005). Conductive copolymers of polyaniline, polypyrrole and poly(dimethylsiloxane). *Synthetic Metals*, 151, 10-18.
- [246] **Hess, E. H., Waryo, T., Sadik, O. A., Iwuoha, E. I., & Baker, P. G. L.** (2014). Constitution of novel polyamic acid/polypyrrole composite films by in-situ eelctropolymerization. *Electrochimica Acta*, 128, 439-448.
- [247] **Hazarika, J. & Kumar, A.** (2013). Controllable synthesis and characterization of polypyrrole nanoparticles in sodium dodecylsulphate (SDS) micellar solutions. *Synthetic Metals*, 175, 155-162.
- [248] **Li, Y.** (1997). Effect of anion concentration on the kinetics of electrochemical polymerization of pyrrole. *Journal of Electroanalytical Chemistry*, 433, 181-186.
- [249] **Andreeva, D. V., Pientka, Z., Brozova, L., Bleha, M., Polotskaya, G. A., and Elyashevich, G. K.** (2002). Effect of polymerization conditions of pyrrole on formation, structure and properties of high gas separation thin polypyrrole films. *Thin Solid Films*, 406, 54-63.
- [250] **Jerome, C., Labaye, D. E., & Jerome, R.** (2004). Electrochemical formation of polypyrrole nanowires. *Synthetic Metals*, 142, 207-216.
- [251] **Ates, M. & Sarac, A.S.** (2009). Electrochemical impedance spectroscopy of poly[carbazole-co-N-p-tolylsulfonylpyrrole) on carbon fiber microelectrodes, equivalent circuits for modelling. *Progress in Organic Coatings*, 65, 281-287.
- [252] **Tuncagil, S., Odaci, D., Varis, S., Timur, S., & Toppare, L.** (2009). Electrochemical polymerization of 1-(4-nitrophenyl)-2,5-di(2-thienyl)-1 H-pyrrole as a novel immobilization platform for microbial sensing. *Bioelectrochemistry*, 76, 169-174.
- [253] **Lu, J., Ma, J., Yi, J., Shen, Z., Zhong, Y., Li, M.** (2014). Electrochemical Polymerization of Pyrrole Containing TEMPO Side

Chain on Pt Electrode and Its Electrochemical Activity. *Electrochimica Acta*, 130, 412-417.

- [254] **Sarac, A. S., Sönmez, G., & Ustamehmetoglu, B.** (1999). Electrochemical polymerization of pyrrole in acrylamide solution. *Synthetic Metals*, 98, 177-182.
- [255] **Pei, Q. & Qian, R.** (1992). Electrochemical polymerization of pyrrole in aqueous buffer solutions. *J. Electroanal. Chem.*, 322, 153-166.
- [256] **Masuda, H. & Kaeriyama, K.** (1995). Electrochemical polymerization of pyrrole with water-soluble polymeric electrolyte. *Synthetic Metals*, 69, 513-514.
- [257] **Yalçinkaya, S., Tüken, T., Yazici, B., & Erbil, M.** (2008). Electrochemical synthesis and characterization of poly(pyrrole-co-o-toluidine). *Progress in Organic Coatings*, 63, 424-433.
- [258] **Li, N., Shan, D., & Huaiguo, X.** (2007). Electrochemical synthesis and characterization of poly(pyrrole-co-tetrahydrofuran) conducting copolymer. *European Polymer Journal*, 43, 2532-2539.
- [259] **Schmeißer, D., Bartl, A., Dunsch, L., Naarmann, H., & Göpel, W.** (1998). Electronic and magnetic properties of polypyrrole films depending on their one-dimensional and two-dimensional microstructures. *Synthetic Metals*, 93, 43-58.
- [260] **Chern, C. S.** (2006). Emulsion polymerization mechanisms and kinetics. *Prog. Polym. Sci.*, 31, 443-486.
- [261] **Thickett, S. C. & Gilbert, R. G.** (2007). Emulsion polymerization: State of art in kinetics and mechanisms. *Polymer*, 48, 6965-6991.
- [262] **Kang, H. C. & Geckeler, K. E.** (2000). Enhanced electrical conductivity of polypyrrole prepared by chemical oxidative polymerization: effect of the preparation technique and polymer additive. *Polymer*, 41, 6931-6934.
- [263] **Vaitkuvienė, A., Kaseta, V., Voronovic, J., Ramanauskaite, G., Biziuleviciene, G., Ramanavicius, A.** (2013). Evaluation of cytotoxicity of polypyrrole nanoparticles synthesized by oxidative polymerization. *Journal of Hazardous Materials*, 250-251, 167-174.
- [264] **Han, M., Chu, Y., Han, D., & Liu, Y.** (2006). Fabrication and characterizations of oligopyrrole doped with dodecylbenzenesulfonic acid in reverse microemulsion. *Journal of Colloid and Interface Science*, 296, 110-117.
- [265] **Tamilavan, V., Song, M., Kang, J., & Hyun, M. H.** (2013). Facile synthesis of 1-(2,6-diisopropylphenyl)-2,5-di(2-thienyl)pyrrole-based narrow band gap small molecules for solar cell applications. *Synthetic Metals*, 176, 96-103.
- [266] **Kızılcan, N., Öz, N. K., Ustamehmetoğlu, B., & Akar, A.** (2006). High conductive copolymers of polypyrrole- α,ω -diamine polydimethylsiloxane. *European Polymer Journal*, 42, 2361-2368.

- [267] **Ma, G., Peng, H., Mu, J., Huang, H., Zhou, X., & Lei, Z.** (2013). In situ intercalative polymerization of pyrrole in grapheme analogue of MoS₂ as advanced electrode material in supercapacitor. *Journal of Power Sources*, 229, 72-78.
- [268] **Papathanassiou, A. N., Grammatikakis, J., Sakkopoulos, S., Vitoratos, E., & Dalas, E.** (2002). Localized and long-distance charge hopping in fresh and thermally aged copolymers of polypyrrole and polyaniline studied by combined TSDC and dc conductivity. *Journal of Physics and Chemistry of Solids*, 63, 1771-1778.
- [269] **Xu, P., Han, X. J., Wang, C., Zhang, B., & Wang, H. L.** (2009). Morphology and physico-electrochemical properties of poly(aniline-co-pyrrole). *Synthetic Metals*, 159, 430-434.
- [270] **Ellis, B. L., Town, K., & Nazar, L. F.** (2012). New composite materials for lithium-ion batteries. *Electrochimica Acta*, 84, 145-154.
- [271] **Verbandt, Y., Thienpont, H., Veretennicoff, I., & Geerlings, P.** (1996). Optical properties of pyrrole oligomers: a coupled quantum oscillator approach. *Chemical Physics Letters*, 251, 47-51.
- [272] **Cheah, K., Forsyth, M., & Truong, V. T.** (1998). Ordering and stability in conducting polypyrrole. *Synthetic Metals*, 94, 215-219.
- [273] **Blinova, N. V., Stejskal, J., Trchova, M., Prokes, J., & Omastova, M.** (2007). Polyaniline and polypyrrole: A comparative study of the preparation. *European Polymer Journal*, 43, 2331-2341.
- [274] **Stejskal, J., Omastova, M., Fedorova, S., Prokes, J., & Trchova, M.** (2003). Polyaniline and polypyrrole prepared in the presence of surfactants: a comparative conductivity study. *Polymer*, 44, 1353-1358.
- [275] **Ermolaev, S. V., Jitariouk, N., & Le Moel, A.** (2001). Polymerization of pyrrole onto "track-etch" membranes. *Nuclear Instruments and Methods in Physics Research B*, 185, 184-191.
- [276] **Adhikari, B. & Samishtha, M.** (2004). Polymers in sensor applications. *Prog. Polym. Sci.*, 29, 699-766.
- [277] **Omastova, M., Mosnackova, K., Trchova, M., Konyushenko, E.N., Stejskal, J., Prokes, J.** (2010). Polypyrrole and polyaniline prepared with cerium(IV) sulfate oxidant. *Synthetic Metals*, 160, 701-707.
- [278] **Lu, G., Li, C., & Shi, G.** (2006). Polypyrrole micro- and nanowires synthesized by electrochemical polymerization of pyrrole in the aqueous solutions of pyrenesulfonic acid. *Polymer*, 47, 1178-1784.
- [279] **Yang, C., Wang, X., Wang, Y., & Liu, P.** (2012). Polypyrrole nanoparticles with high dispersion stability via chemical oxidative polymerization in the presence of an anionic-non-ionic bifunctional polymeric surfactant. *Powder Technology*, 217, 134-139.
- [280] **Jeon, H. J., You, Y., Yoon, M. J., & Youk, J. H.** (2011). Preparation of polyacrylonitrile nanoparticles via dispersion polymerization of acrylonitrile using a poly(N-vinyl pyrrolidone)-cobalt complex in an aqueous system. *Polymer*, 52, 3905-3911.

- [281] **Yavuz, A. G. & Gök, A.** (2007). Preparation of TiO₂/PANI composites in the presence of surfactants and investigation of electrical properties. *Synthetic Metals*, 157, 235-242.
- [282] **Wang, L. X., Li, X. G., & Yang, Y. L.** (2001). Preparation, properties and applications of polypyrroles. *Reactive & Functional Polymers*, 47, 125-139.
- [283] **Percec, S., Howe, L., Li, J., Bagshaw, A., Peacock, S., Brill, D.** (2013). Pyrrole polymerization on polyimide surfaces creates conductive nano-domains. *Polymer*, 54, 5754-5761.
- [284] **Rajesh, Ahuja, T., & Kumar, D.** (2009). Recent progress in the development of nano-structured conducting polymers/nanocomposites for sensor applications. *Sensors and Actuators B*, 136, 275-286.
- [285] **Otero, T. F. & Rodriguez, J.** (1994). Role of protons on the electrochemical polymerization of pyrrole from acetonitrile solutions. *Journal of Electroanalytical Chemistry*, 379, 513-516.
- [286] **Liang, B., Liu, Y., & Xu, Y.** (2014). Silicon-based materials as high capacity anodes for next generation lithium ion batteries. *Journal of Power Sources*, 267, 469-490.
- [287] **Huang, L. M., Liao, W. H., Ling, H. C., & Wen, T. C.** (2009). Simultaneous synthesis of polyaniline nanofibers and metal (Ag and Pt) nanoparticles. *Materials Chemistry and Physics*, 116, 474-478.
- [288] **Otero, T. F. & Rodriguez, J.** (1994). Parallel kinetic studies of the electrogeneration of conducting polymers: mixed materials, composition and properties control. *Electrochimica Acta*, 39, 245-253.
- [289] **Prasanna, A., Somanathan, N., Hong, P. D., & Chuang, W. T.** (2009). Studies on polyaniline-polypyrrole copolymer micro emulsions. *Materials Chemistry and Physics*, 116, 406-414.
- [290] **Boukerma, K., Micusik, M., Mravcakova, M., Omastova, M., Vaulay, M. J., Chenimi, M. M.** (2007). *Colloids and Surfaces A: Physicochem. Eng. Aspects*, 293, 28-38.
- [291] **Gök, A., Omastova, M., & Yavuz, A. G.** (2007). Synthesis and characterization of polythiophenes prepared in the presence of surfactants. *Synthetic Metals*, 157, 23-29.
- [292] **Boukerma, K., Piquemal, J. Y, Chehimi, M. M., Mravcakova, M., Omastova, M., & Beaunier, P.** (2006). Synthesis and interfacial properties of montmorillonite/polypyrrole nanocomposites. *Polymer*, 47, 569-576.
- [293] **Tamilavan, V., Song, M., Agneeswari, R., Kand, J. W., Hwang, D. H., & Hyun, M. H.** (2013). Synthesis and photovoltaic properties of donor-acceptor polymers incorporating a structurally-novel pyrrole-based imide-functionalized electron acceptor moiety. *Polymer*, 54, 6125-6132.
- [294] **Almeida, A. K. A., Monteiro, M. P., Dias, J. M. M., Omena, L., da Silva, A. J. C., de Oliveira, I. N.** (2014). Synthesis and spectroscopic characterization of a fluorescent pyrrole derivative containing electron

acceptor and donor groups. *Spectrochimica Acta Part A: Molecular and Biomolecular Spectroscopy*, 128, 812-818.

- [295] **Omastova, M., Trchova M., Kovarova, J., & Stejskal, J.** (2003). Synthesis and structural study of polypyrroles prepared in the presence of surfactants. *Synthetic Metals*, 138, 447-455.
- [296] **Yoon, C. O., Sung, H. K., Kim, J. H., Barsoukov, E., Kim, J. H., & Lee, H.** (1999). The effect of low-temperature conditions on the electrochemical polymerization of polypyrrole films with high density, high electrical conductivity and high stability. *Synthetic Metals*, 99, 201-212.
- [297] **Pekmez, N. Ö., Cinkılı, K., & Zeybek, B.** (2014). The electrochemical copolymerization of pyrrole and bithiophene on stainless steel in the presence of SDS in aqueous medium and its anticorrosive performance. *Progress in Organic Coatings*, 77, 1277-1287.
- [298] **Appel, G., Schmeißer, D., Bauer, J., Bauer, M., Egelhaaf, H. J., & Oelkrug, D.** (1999). The formation of oligomers in the electrolyte upon polymerization of pyrrole. *Synthetic Metals*, 99, 69-77.
- [299] **Zotti, G. & Schiavon, G.** (1989). The role of water in the electrochemical polymerization of pyrroles. *Electrochimica Acta*, 34 (6), 881-884.
- [300] **Yang, C. & Liu, P.** (2010). Water-dispersed polypyrrole nanoparticles via chemical oxidative polymerization in the presence of a functional polyanion. *Reactive & Functional Polymers*, 70, 726-731.
- [301] **Boguslavsky, L., Baruch, S., & Margel, S.** (2005). Synthesis and characterization of polyacrylonitrile nanoparticles by dispersion/emulsion polymerization process. *Journal of Colloid and Interface Science*, 289, 71-85.
- [302] **Yang, L. C., Shi, Y., Gao, Q. S., Wang, B., Wu, Y. P., & Tang, Y.** (2008). The production of carbon nanospheres by the pyrolysis of polyacrylonitrile. *Carbon*, 46, 1792-1828.
- [303] **Tauer, K., Ramirez, A. G., & Lopez, R. G.** (2003). Effect of the surfactant concentration on the kinetics of oil in water microemulsion polymerization: a case study with butyl acrylate. *C. R. Chimie*, 6, 1245-1266.
- [304] **Zhang, C., Du, Z., Li, H., & Ruckenstein, E.** (2002). High-rate polymerization of acrylonitrile and butyl acrylate based on a concentrated emulsion. *Polymer*, 43, 5391-5396.
- [305] **Wählander, M., Nilsson, F., Larsson, E., Tsai, W. C., Hillborg, H., Malmström, E.** (2014). Polymer-grafted Al₂O₃-nanoparticles for controlled dispersion in poly(ethylene-co-butyl acrylate) nanocomposites. *Polymer*, 55, 2125-2138.
- [306] **Xia, H., Wang, Q., Liao, Y., Xu, X., Baxter, S. M., Westmoreland, D.G.** (2002). Polymerization rate and mechanism of ultrasonically initiated emulsion polymerization of n-butyl acrylate. *Ultrasonics Sonochemistry*, 9, 151-158.

- [307] **Tolue, S., Moghbeli, M. R., & Ghafelebashi, S. M.** (2009). Preparation of ASA (acrylonitrile-styrene-acrylate) structural latexes via seeded emulsion polymerization. *European Polymer Journal*, *45*, 714-720.
- [308] **Miura, Y., Nakamura, N., Taniguchi, I., & Ichikawa, A.** (2003). Radical polymerization of butyl acrylate and random copolymerization of styrene and butyl acrylate and *o*-ethyl methacrylate mediated by monospiro- and dispiropiperidinyl-N-oxyl radicals. *Polymer*, *44*, 3461-3467.
- [309] **Bakhshi, H., Zohuriaan-Nehr, M. J., Bouhendi, H., & Kabiri, K.** (2009). Spectral and chemical determination of copolymer composition of poly(butyl acrylate-co-glycidyl methacrylate) from emulsion polymerization. *Polymer Testing*, *28*, 730-736.
- [310] **Chan-Seng, D., Debuigne, A., & Georges, M. K.** (2009). Stable free radical polymerization of n-butyl acrylate in the presence of high-temperature initiators. *European Polymer Journal*, *45*, 211-216.
- [311] **Ramos-Fernández, J. M., Belena, I., Romero-Sánchez, M. D., Fuensanta, M., Guillem, C., & López-Buendía, A. M.** (2012). Study of the film formation and mechanical properties of the latexes obtained by miniemulsion co-polymerization of butyl acrylate, methyl acrylate and 3-methacryloxypropyltrimethoxysilane. *Progress in Organic Coatings*, *75*, 86-91.
- [312] **Zhao, K., Sun, P., Liu, D., & Dai, G.** (2004). The formation mechanism of poly(vinyl acetate)/poly(butyl acrylate) core/shell latex in two-stage seeded semi-continuous starved emulsion polymerization process. *European Polymer Journal*, *40*, 89-96.
- [313] **Yin, N. & Chen, K.** (2004). Ultrasonically initiated emulsifier-free emulsion copolymerization of n-butyl acrylate and acrylamide, Part I: Polymerization mechanism. *Polymer*, *45*, 3587-3594.
- [314] **Cetiner, S., Karakas, H., Ciobanu, R., Unsal, C., Kalaoglu, F., Sarac, A. S.** (2010). Polymerization of pyrrole derivatives on polyacrylonitrile matrix, FTIR-ATR and dielectric spectroscopic characterization of composite thin films, *Synt. Met.*, *160* (11-12), 1189-1196.
- [315] **Unsal, C., Kalaoglu, F., Karakas, H., & Sarac, A.S.** (2012). Polypyrrole/Poly(acrylonitrile-co-butyl acrylate) Composite. *Advances in Polymer Technology*, *32* (1), 784-792.
- [316] **Yerlikaya, Y., Unsal, C., & Sarac, A. S.** (2014). Nanofibers of Poly(Acrylonitrile-co-Methyl acrylate)/Polypyrrole Core-Shell Nanoparticles. *Advanced Science, Engineering and Medicine*, *6* (3), 301-310.
- [317] **MacDiarmid, A. G.** (2001). Synthetic Metals: A novel role for organic polymers (Nobel lecture). *Angew. Chem. Int. Ed.*, *40*, 2581-2590.
- [318] **Epstein, A. J.** (1999). Electron Transport in Conducting Polymers. In G. Bidan, Patrick Bernier, and S. Lefrant (Eds.), *Advances in Synthetic*

Metals : Twenty Years of Progress in Science and Technology (pp.349-366). Amsterdam, New York : Elsevier.

- [319] **Menon, R., Yoon, C. O., Moses, D., & Heeger, A. J.** (1998). In T. Skotheim, R. Elsenbaumer, and J. Reynolds (Eds.), *Metal-Insulator Transition in Doped Conducting Polymers* (Vol. 2). New York, USA : Marcel Dekker, Inc.
- [320] **Kaiser, A. B.** (2001) Systematic conductivity behavior in conducting polymers: Effects of heterogeneous disorder. *Advanced Materials*, 13 (12-13), 927.
- [321] **Yoon, C. O., Reghu, M., Moses, D., Heeger, A. J., Cao, Y., Rieke, R. D.** (1995). Hopping transport in doped conducting polymers in the insulating regime near the metal-insulator boundary: Polypyrrole, polyaniline and polyalkylthiophenes. *Synthetic Metals*, 75 (3), 229-239.
- [322] **Temmer, R., Maziz, A., Plesse, C., Aabloo, A., Vidal, F., & Tamm, T.** (2013). In search of better electroactive polymer actuator materials: PPy versus PEDOT versus PEDOT-PPy composites. *Smart Mater. Struct.*, 22, 1-16.
- [323] **El-Kady, M. F., Strong, V., Dubin, S., & Kaner, R. B.** (2012). Laser Scribing of High-Performance and Flexible Graphene-Based Electrochemical Capacitors. *Science*, 335 (6074), 1326-1330.

CURRICULUM VITAE



Name Surname : Cem Ünsal

Place and Date of Birth : Bandırma/Balıkesir, 28.05.1980

E-Mail : cemunsal@itu.edu.tr, cemunsal_80@hotmail.com

B.Sc. : Istanbul Technical University, Textile Engineering, 2001

M.Sc. : Istanbul Technical University, Textile Engineering Master Prog., 2004

MBA : Marmara University, Management and Organization Master Prog., 2005

Professional Experience and Rewards:

A senior member of ITU Electropol-Nanotech Research Group, 2008-....

MEBAL Textile Sales and Trading Co., Sales Engineer and Representative, 2007-2008

List of Publications and Patents:

Cetiner, S., Karakas, H., Ciobanu, R., Olariu, M., Kaya, N.U., Unsal, C., Kalaoglu, F., and Sarac, A.S. (2010). Polymerization of pyrrole derivatives on polyacrylonitrile matrix, FTIR-ATR and dielectric spectroscopic characterization of composite thin films. *Synt. Met.*, 160 (11-12), 1189-1196.

Unsal, C., Kalaoglu, F., Karakas, H., and Sarac, A.S. (2012). Polypyrrole/Poly(acrylonitrile-co-butyl acrylate) Composite. *Advances in Polymer Technology*, 32 (1), 784-792.

Yerlikaya, Y., Unsal, C., Sarac, A.S. (2014). Nanofibers of Poly(Acrylonitrile-co-Methyl acrylate)/Polypyrrole Core-Shell Nanoparticles. *Advanced Science, Engineering and Medicine*, 6 (3), 301-310.

